NATIONAL TECHNICAL UNIVERSITY OF ATHENS

SCHOOL OF CIVIL ENGINEERING

DEPARTMENT OF WATER RESOURCES AND ENVIRONMENTAL ENGINEERING

GEOCHEMICAL FATE OF HEXAVALENT CHROMIUM IN OPHIOLITIC SOILS AND GROUNDWATER; QUANTITATIVE ADSORPTION SIMULATION USING SURFACE COMPLEXATION MODELING

DOCTORAL THESIS

ATHANASIOS S. BOURAS

Dipl. Chemical Engineer NTUA, MSc

ATHENS, 2019

NATIONAL TECHNICAL UNIVERSITY OF ATHENS

SCHOOL OF CIVIL ENGINEERING

DEPARTMENT OF WATER RESOURCES AND ENVIRONMENTAL ENGINEERING

"GEOCHEMICAL FATE OF HEXAVALENT CHROMIUM IN OPHIOLITIC SOILS AND GROUNDWATER; QUANTITATIVE ADSORPTION SIMULATION USING SURFACE COMPLEXATION MODELING"

DOCTORAL THESIS

ATHANASIOS S. BOURAS

Advisory Committee

Dermatas Dimitrios,
Professor NTUA (Supervisor)

Papassiopi Nymphodora,
Professor NTUA

Mamais Daniel,
Professor NTUA

Examination Committee

Dermatas Dimitrios,
Professor NTUA

Papassiopi Nymphodora,
Professor NTUA

Mamais Daniel,
Professor NTUA

Chrysochoou Maria,
Associate professor UCONN

Xenidis Anthimos,
Professor NTUA

Argyraki Ariadne,
Associate professor NKUA

Nikolaidis Nikolaos,
Professor TUC

ΕΘΝΙΚΟ ΜΕΤΣΟΒΙΟ ΠΟΛΥΤΕΧΝΕΙΟ

ΣΧΟΛΗ ΠΟΛΙΤΙΚΩΝ ΜΗΧΑΝΙΚΩΝ

ΤΟΜΕΑΣ ΥΔΑΤΙΚΩΝ ΠΟΡΩΝ ΚΑΙ ΠΕΡΙΒΑΛΛΟΝΤΟΣ

"ΓΕΩΧΗΜΙΚΗ ΤΥΧΗ ΤΟΥ ΕΞΑΣΘΕΝΟΥΣ ΧΡΩΜΙΟΥ ΣΕ ΟΦΙΟΛΙΘΙΚΑ ΕΔΑΦΗ ΚΑΙ ΥΠΟΓΕΙΑ ΝΕΡΑ ΚΑΙ ΠΟΣΟΤΙΚΗ ΠΡΟΣΟΜΟΙΩΣΗ ΤΗΣ ΠΡΟΣΡΟΦΗΣΗΣ ΤΟΥ ΜΕΣΩ ΜΟΝΤΕΛΩΝ ΕΠΙΦΑΝΕΙΑΚΗΣ ΣΥΜΠΛΟΚΟΠΟΙΗΣΗΣ"

ΔΙΔΑΚΤΟΡΙΚΗ ΔΙΑΤΡΙΒΗ

ΑΘΑΝΑΣΙΟΣ Σ. ΜΠΟΥΡΑΣ

Συμβουλευτική Επιτροπή

Δερματάς Δημήτριος,
Καθηγητής ΕΜΠ (Επιβλέπων)

Παπασιώπη Νυμφοδώρα,
Καθηγήτρια ΕΜΠ

Μαμάης Δανιήλ,
Καθηγητής ΕΜΠ

Εξεταστική Επιτροπή

Δερματάς Δημήτριος,
Καθηγητής ΕΜΠ

Παπασιώπη Νυμφοδώρα,
Καθηγήτρια ΕΜΠ

Μαμάης Δανιήλ,
Καθηγητής ΕΜΠ

Χρυσοχόου Μαρία,
Αναπληρώτρια καθηγήτρια, Πανεπιστήμιο Κοννέκτικατ

Ξενίδης Άνθιμος,
Καθηγητής ΕΜΠ

Αργυράκη Αριάδνη,
Αναπληρώτρια καθηγήτρια ΕΚΠΑ

Νικολαΐδης Νικόλαος,
Καθηγητής Πολυτεχνείου Κρήτης

To my parents

ACKNOWLEDGEMENTS

The present Doctoral Thesis was performed at the Department of Water Resources and Environmental Engineering of the School of Civil Engineering of the National Technical University of Athens (NTUA). Undertaking this Thesis has been a truly life-changing experience for me and would not have been possible to perform it without the support and guidance that I received from many people.

Firstly, I would like to express my sincere gratitude to my advisor Mr. Dermatas Dimitrios, Professor NTUA, for the continuous support during my PhD study and related research work, for his patience, motivation, and immense knowledge. His guidance and his reliance helped me in all the time of research of this thesis.

Besides my advisor, I would like to thank the rest of my thesis committee Mr. Mamais Daniel, Professor NTUA, and Mrs Papassiopi Nymphodora, Professor NTUA, not only for their insightful comments and encouragement, but also for providing me with the opportunity to join their team as intern, and giving access to the laboratory and research facilities. Without their precious support it would not be possible to conduct this research.

The successful completion of the present dissertation would not have been possible without the scientific guidance and moral support that generously provided me Mrs Chrysochoou Maria, Associate Professor UCONN. This is why I would like to express her, my warmest thanks.

I would also like to thank Mr Xenidi Anthimo, Professor NTUA, Mrs Argyraki Ariadne, Associate Professor NKUA, and Mr Nikolaidi Nikolao, Professor TUC, for their willingness to be members of the Seven-member Examination Committee and for their useful comments on the thesis.

In addition, I would like to thank Dr Panagiotaki Irakli for his advice and cooperation all these years, Mr Kouri Nikolao for his precious comments regarding the performance of lab work and Dr Gkesouli Anthi for sharing our thoughts and problems as PhD candidates for many years.

Undoubtedly, the most heartfelt thanks are to my family, to my parents Stergios and Asimina and to my sister Maria, who always totally supported and encouraged me to chase my dreams.

This research was partially supported by the LIFE+ CHARM project (LIFE10 ENV/GR/000601).

ABSTRACT

In many areas globally, groundwater serves as the sole source of drinking water in rural and urban communities. However, the increased industrial and agricultural activities have resulted in significant contamination of geoenvironment with severe effects on human life and ecosystems. Heavy metals, such as hexavalent chromium [Cr(VI)], and other inorganics, such as phosphate and nitrate, are typically among those contaminants.

Approximately 170,000 tonnes of chromium are released annually to the geoenvironment as a result of anthropogenic activities causing contamination of surface water, groundwater and soils. Nitrate and phosphate are contaminants of major concern on a global scale since they are recognized that controls eutrophication in surface water bodies. Thus their transport and fate in geoenvironment must be well understood to better evaluate their environmental impacts. However, the occurrence of chromium in the geoenvironment can also be related to geogenic origin due to the occurrence of specific geological background like ultramafic rocks and ophiolitic complexes. Thus intensive agricultural activities combined with the presence of ophiolitic complexes can lead to groundwater contamination with hexavalent chromium, and phosphates and nitrates.

The Greek geological background is highly consisted of ultramafic rocks and ophiolitic complexes and thus hexavalent chromium is often detected in groundwater. The aim of this study was to identify such an area in Greece and investigate the geochemistry of hexavalent chromium and simulate its adsorption efficiency on such type of soils. The selected area was close to Vergina town in northern Greece and exhibited such geological background. Agricultural activities were the only anthropogenic pressure in the area. The selection of the study area was based on an extensive groundwater monitoring data base created by the Greek Institute of Geology & Mineral Exploration. In addition, a new well was constructed in order to be used exclusively for research needs. Groundwater and soils sampling was performed along 100 m depth. Soil mineralogical analysis showed that the collected samples exhibited the typical ultramafic origin containing “ultramafic minerals” such as chrysotile and chromite as well as their weathering products (vermiculite), mixed with minerals typical of a mafic assemblage (chlorite, quartz, albite, hematite). Physicochemical analysis of soil samples showed that pH increased with depth probably as a result of the more intensive presence of organic matter and nitrification process in the upper soil layers and due to the effect of weathering processes in greater depths. Elemental analysis showed that the tested soil was poorer in iron and aluminum, richer in silicon and about average in magnesium, compared with serpentine soils of other areas worldwide. However, the relative abundance of magnesium versus aluminum strongly indicated the relative contribution of ultramafic versus mafic materials in the soil sample.

Regarding the presence of chromium the following results were obtained. Total chromium (Cr_{tot}) concentration did not exhibit a uniform trend with depth exhibiting firstly a decrease until the first meters, followed by a slight increase for depths down to 10.5 m and a general increasing trend for depths higher than 43 meters. These results are in accordance with other

presented in the literature mentioning that weathering processes that occur usually in the shallow unsaturated zone favor leaching of elements such as magnesium and accumulation of others like iron, aluminum and chromium while in higher depths the presence of unweathered serpentinitic phases is more intensive. Contrary to Cr_{tot}, Cr(VI) concentration exhibited an almost continuous decrease with increasing depth. Regarding the presence of chromium in groundwater concentrations of Cr_{tot} up to 91 μg/L and hexavalent chromium up to 64 μg/L detected. These values are of the highest reported globally in aquifers with similar geological background. Both Cr_{tot} and Cr(VI) concentrations in groundwater decreased almost linearly with depth. A high correlation between Cr(VI) and Cr_{tot} observed with the Cr(VI)/Cr_{tot} ratio being higher than 83%. In addition, the intense agricultural activities in the tested area resulted in high nitrate concentrations.

Taking into account that the main processes that regulate the fate of hexavalent chromium produced by oxidation of trivalent in aquifers, are sorption and reduction the occurrence of these processes in the case of ophiolitic soil were investigated. In ophiolitic soils there is a mixture of hexavalent and trivalent chromium, both naturally occurring. Hexavalent, but not trivalent chromium, can be leached out of the soil and enter groundwater. As hexavalent chromium is leached from the soil, the remaining trivalent can slowly oxidize to hexavalent in order to reestablish the equilibrium of the soil. The leached hexavalent chromium can be adsorbed or reduced by the solid phase. As regarding reduction minerals that contain divalent iron like magnetite or (magnesio)chromite can act as reductants for hexavalent chromium. Sorption is strongly affected by the occurrence of iron (oxy-hydro)oxides, which are the most common sorbents for Cr(VI). In addition, iron (oxy-hydro)oxides can efficiently act as adsorbents and for other inorganic contaminants like phosphates and nitrates.

In order to determine the processes responsible for hexavalent chromium removal from groundwater batch experiments were performed investigating the effect of several parameters like pH, mineralogy, soil's particle size, initial concentration of hexavalent chromium, ionic strength of the solution and the presence of other inorganic contaminants. The results showed that both adsorption and reduction processes affected hexavalent chromium removal from the soil solution. For both processes removal decreased with increasing pH values but their contribution to the total removal depends on pH. Reduction was attributed to the presence of a magnetic fraction in the soil sample which includes magnetite and magnesio-chromite as primary minerals. Regarding adsorption is probably attributed to the presence of amorphous iron oxy-hydroxides in the soil. Adsorption was found to be semi-reversible since only a fraction of the adsorbed amount was found to be desorbed in the soil solution. This is probably a result of the formation of inner sphere complexes which are sufficiently stable, including exclusively ionic and/or covalent bonds. However, both processes are surface-driven with reduction being influenced by adsorption since partitioning of hexavalent chromium onto the solid surface is required before reduction occurs. In addition, evaluation of sorption as a function of particle size showed that the finer fraction of the soil, which exhibited and the higher value of specific surface area, dominated the adsorption behavior of the soil. The effect of initial concentration of hexavalent chromium was tested for higher concentrations than these occur due to geogenic origin. Langmuir and Freundlich isotherms fitted very well the experimental data, indicating thus the simultaneous

heterogenity of the surface sites on the serpentinitic soils and possibly the formation of a monolayer for hexavalent chromium adsorption. Finally, significant effects observed due to the alteration of ionic strength. Adsorption efficiency was decreased with increasing ionic strength value suggesting thus the formation of outer sphere complexes for the adsorption of hexavalent chromium.

In addition, the adsorption capacity of the ophiolitic soil was tested for the inorganic contaminants phosphates and nitrates that are commonly observed in areas with intense agricultural activities and any possible competitive effects between them and hexavalent chromium. The ophiolitic soil exhibited high adsorption capacity for phosphates with the adsorption process being affected by the pH of the solution. More specifically, the increase of pH decreases the adsorption of phosphates, almost linearly. No competitive effects on phosphates adsorption were observed during the presence of hexavalent chromium. On the other hand hexavalent chromium adsorption was strongly affected by the presence of phosphate in the solution. This is probably due to the formation of exclusively inner sphere complexes between phosphate and the ophiolitic surface, creating competition with chromates which also form inner sphere complexes. Regarding nitrates their adsorption on the ophiolitic soil was very low up and almost zeroed at pH values commonly occur in aquifers. The effect of hexavalent chromium on nitrate adsorption was almost negligible and vice versa. This is probably due to different type of surface complexation of nitrates and chromate, since nitrate form exclusively weak outer sphere complexes contrary to chromate which form both inner and outer sphere complexes.

The following step of this thesis was to compare the adsorption behavior of the ophiolitic soil with that of a pure ferric oxide. The selected ferric oxide was goethite since it is considered as the most abundant iron oxide in the geoenvironment and the most common oxide in ophiolitic soils. Goethite was tested for its adsorption capacity for hexavalent chromium, phosphate and nitrate. The possible competitive effects between the tested anions were also investigated. The experimental results showed that goethite is an efficient adsorbent for chromate and phosphate ions but not for nitrates. The pH increase caused decrease of the adsorption capacity of goethite for hexavalent chromium, phosphates and nitrate ions. For high pH values the goethite surface becomes negatively charged and thus repulsions of chromates and the inorganic anions with the surface occur. In addition, the effect of ionic strength on chromate adsorption was investigated as a way of revealing the type of adsorption. The increase of ionic strength resulted in noticeable decrease of the adsorption of hexavalent chromium, suggesting the formation of outer sphere complexes, which are based on weak electrostatic forces. The investigation of any competitive effects between chromate and phosphate for adsorption on goethite surface showed that phosphates adsorption is not affected by the presence of chromates. On the contrary, an important effect on the adsorption of chromates, was observed in the simultaneous presence of phosphates. This is probably attributed to the fact that chromates, during the presence of phosphates, are mainly adsorbed via outer sphere complexes since phosphate are adsorbed only via inner sphere complexation. Regarding any competition between chromate and nitrate the results showed that adsorption of chromates was decreased under the presence of nitrates. This is probably due to the significant difference on their concentrations. The significant higher concentration of nitrate probably creates

electrostatic repulsions which may affect the complexation of chromates, especially the formation outer sphere complexes. Regarding nitrates the already low adsorption efficiency was not affected by the presence of chromate in the solution.

Taking into account the experimental results obtained from the batch experiments the next aim of this thesis was to simulate the adsorption process applying surface complexation models. The behavior, transport, and generally the fate of heavy metals and inorganic contaminants in the geoenvironment depends largely on their sorption reactions with soil particles and so it is of high importance to investigate such reactions. Different empirical approaches have been used for studying the adsorption behavior of natural soils, but several limitations have been observed since these approaches cannot account for changes in groundwater chemistry. Thus, in the last twenty years extensive studies have been performed using surface complexation models for describing the adsorption of heavy metals and inorganic contaminants with quite promising results. Surface complexation models are generally based on providing a thermodynamic description of the reactions between the surface groups and the adsorbed ions, based on charge and mass balances. However, most of these studies have used pure minerals and especially pure hydrous oxide solid surfaces, and only few studies refer to natural materials and particularly to soils like in the present study. Additionally, since each surface complexation model is based on different specific assumptions regarding the solid–solution interface, which are expressed by different surface complexation reactions and thus different adsorption constants the obtained values cannot be used in different models.

In this study, three of the most common surface complexation models the triple layer model, the diffuse-layer model and the constant capacitance model were used for simulation. Databases with the corresponding surface complexation reactions were created and inserted in the Visual Minteq software. The application of the aforementioned models was based on the general composite approach for adsorption simulation. This approach considers that the soil composition is too complex in order to distinguish and quantify the several individual phases and thus it is assumed that a general type of active sites exists on the soil surface. This assumption creates the need for using stoichiometry and formation constants which are obtained by fitting experimental data. Thus the created databases with the surface complexation reactions can be used only by altering the adsorption constants in order to fit the experimental data. Among the parameters required in each model a general parameter required for all models in order to perform simulation is the concentration of the solid in the solution. Despite in the case of goethite the solid concentration used in the batch experiments was applied for adsorption simulation this was the scenario in the case of using ophiolitic soil. Taking into account that not all the minerals contained in the ophiolitic soil contribute to contaminants adsorption it was assumed that adsorption is mainly controlled by the presence of iron and maybe of the aluminum oxides. Their concentration was calculated using the mass balance as determined by X-Ray fluorescence and via quantitative X-Ray diffraction analysis. Three different scenarios taking into account the contribution of either a) iron and aluminum oxides, b) only iron oxides and c) only the amorphous iron oxides were used for adsorption simulation using each of the three aforementioned surface complexation models.

The application of triple layer model led to satisfactory description of the adsorption process for all the anions tested. The adsorption simulation was effective for any parameters tested like effect of pH, ionic strength and any competitive effects when assuming that adsorption is controlled by either the presence of iron and aluminum oxides or only by the iron oxides. Simulation was not effective when using the concentration of only amorphous iron oxides in the soil sample indicating thus that this solid phase does not correspond to the concentration of the solid phase that contributes to adsorption. Simulating the effect of ionic strength it was revealed that at low ionic strength values adsorption of chromates can be described by the formation of inner sphere, either monodentate or bidentate, and outer sphere complexes. However, the increase of ionic strength showed that adsorption chromate can be efficiently described only by the formation of bidentate complexes. The formation of bidentate complexes of chromates with the soil surface can also describe the competitive effects under the presence of phosphates and nitrates. In addition, satisfactory simulation was achieved for phosphate and nitrate adsorption and their competition with chromates in the soil solution. Thus, Triple Layer Model can in general describe efficiently the adsorption of chromates and the inorganic contaminants on the ophiolitic soil. On the other hand, simulation of experimental data using the diffuse layer model showed that the application of this model is not suitable for describing the adsorption process on the ophiolitic soil. The Diffuse Layer Model was not capable to simulate neither the adsorption of chromates nor of the other inorganic contaminants. A possible explanation is the assumption of monodentate complexes of chromates and phosphates by applying the diffuse layer model and the absence of any outer sphere complexes in the case of chromates and nitrates. Similarly, the constant capacitance model was not capable of simulating the adsorption of neither chromate nor the inorganic contaminants on the ophiolitic soil.

Finally, the application of surface complexation models for describing the adsorption behavior of goethite leads to similar observations as in the case of the ophiolitic soil. The triple layer model described satisfactorily the adsorption of hexavalent chromium and inorganic contaminants, as well as their competition on the goethite surface. Simulation showed that chromates are adsorbed via inner and outer sphere complexation. This fact was verified by the decrease of the adsorption efficiency due to ionic strength increase. Chromates complexation is considered to be governed by the formation of bidentate complexes with the solid surface. The adsorption of phosphate and nitrate was also satisfactorily simulated. The competitive effects occurred between chromates and each inorganic contaminant, were also simulated with high accuracy. On the contrary, simulation of the adsorption of chromates and inorganic contaminants using the diffuse layer model was not effective, as in the case of the ophiolitic soil. As mentioned above, a possible explanation is the assumption of formation exclusively inner sphere monodentate complexes by applying the diffuse layer model and the absence of any outer sphere complexes. In closing, the application of constant capacitance model for simulating adsorption of chromate and phosphate on single anion solutions could efficiently describe the adsorption of chromate and phosphate but not adsorption of nitrate. However, it could not describe the competitive effects created between chromate and inorganic contaminants.

ΠΕΡΙΛΗΨΗ

Σε πολλές περιοχές παγκοσμίως, τα υπόγεια ύδατα λειτουργούν ως μοναδική πηγή πόσιμου νερού για αστικές και αγροτικές κοινότητες. Ωστόσο, οι αυξημένες βιομηχανικές και γεωργικές δραστηριότητες έχουν οδηγήσει σε σημαντική ρύπανση του γεωπεριβάλλοντος με σοβαρές επιπτώσεις στην ανθρώπινη ζωή και στα οικοσυστήματα. Τα βαρέα μέταλλα, όπως το εξασθενές χρώμιο αλλά και άλλοι ανόργανοι ρύποι, όπως τα φωσφορικά και νιτρικά ιόντα, αποτελούν συνήθεις ρύπους των υπόγειων νερών.

Περίπου 170.000 τόνοι χρωμίου απελευθερώνονται ετησίως στο γεωπεριβάλλον ως αποτέλεσμα ανθρωπογενών δραστηριοτήτων προκαλώντας ρύπανση των επιφανειακών και των υπόγειων υδάτων αλλά και των εδαφών. Τα νιτρικά και τα φωσφορικά άλατα αποτελούν ρυπαντικές ουσίες που προκαλούν μεγάλη ανησυχία σε παγκόσμια κλίμακα, δεδομένου ότι έχουν αναγνωριστεί ως ρύποι υπεύθυνοι για τον ευτροφισμό στα συστήματα επιφανειακών υδάτων. Συνεπώς, οι διεργασίες μεταφοράς τους και η γεωχημική τύχη τους στο γεωπεριβάλλον πρέπει να είναι καλά κατανοητές ώστε να αξιολογούν όσο το δυνατόν καλύτερα τις πιθανές περιβαλλοντικές επιπτώσεις που μπορεί να προκαλέσει η παρουσία τους. Στην περίπτωση του χρωμίου η εμφάνισή του στο γεωπεριβάλλον μπορεί επίσης να σχετίζεται με τη γηγενή του προέλευση λόγω της παρουσίας συγκεκριμένου γεωλογικού υποβάθρου όπως τα υπερμαφικά πετρώματα και τα οφιολιθικά συμπλέγματα. Συνεπώς, οι έντονες και εντατικές γεωργικές δραστηριότητες σε συνδυασμό με την παρουσία οφιολιθικών συμπλεγμάτων μπορούν να οδηγήσουν σε ρύπανση υπόγειων υδάτων με ταυτόχρονη παρουσία ρύπων όπως το εξασθενές χρώμιο και τα φωσφορικά και νιτρικά ιόντα.

Στο γεωλογικό υπόβαθρο της Ελλάδας είναι έντονη η παρουσία υπερμαφικών πετρωμάτων και οφιολιθικών συμπλεγμάτων με αποτέλεσμα το εξασθενές χρώμιο να ανιχνεύεται στα υπόγεια ύδατα αρκετών περιοχών. Σκοπός αυτής της διατριβής ήταν ο εντοπισμός μιας τέτοιας περιοχής στην Ελλάδα, η διερεύνηση της γεωχημείας του εξασθενούς χρωμίου και η προσομοίωση της προσρόφησής του σε τέτοιου τύπου εδάφη. Η περιοχή που επιλέχθηκε προς εξέταση βρίσκεται κοντά στην πόλη της Βεργίνας στη βόρεια Ελλάδα και χαρακτηρίζεται από αντίστοιχο γεωλογικό υπόβαθρο. Επίσης, οι γεωργικές δραστηριότητες είναι η μόνη ανθρωπογενής πίεση στην περιοχή. Η επιλογή της περιοχής μελέτης βασίστηκε σε εκτεταμένη βάση δεδομένων παρακολούθησης υπόγειων υδάτων που δημιουργήθηκε από το Ελληνικό Ινστιτούτο Γεωλογικών και Μεταλλευτικών Ερευνών. Στην περιοχή μελέτης, κατασκευάστηκε νέα γεώτρηση συνολικού βάθους 100 μέτρων με σκοπό να χρησιμοποιηθεί αποκλειστικά για την κάλυψη των ερευνητικών αναγκών και συγκεκριμένα για τη δειγματοληψία υπόγειου νερού και εδάφους. Η ορυκτολογική ανάλυση των εδαφικών δειγμάτων που συλλέχθηκαν φανέρωσε τα τυπικά χαρακτηριστικά των υπερμαφικών πετρωμάτων καθώς περιείχαν ορυκτά όπως χρυσοτίλη και χρωμίτη, καθώς και ορυκτά που συνδέονται με αυτά, ως αποτέλεσμα διάβρωσης των πρώτων, όπως ο βερμικουλίτης, αναμεμιγμένα με μαφικά ορυκτά όπως χλωρίτη, χαλαζία, αλβίτη, αιματίτη κ.α. Όσον αφορά στη φυσικοχημική ανάλυση των εδαφικών δειγμάτων διαπιστώθηκε αύξηση των τιμών pH με το βάθος δειγματοληψίας αποτέλεσμα που πιθανώς συνδέεται με την εντατικότερη παρουσία της οργανικής ύλης και των διαδικασιών νιτροποίησης οι οποίες είναι εντονότερες στα ανώτερα εδαφικά στρώματα

σε συνδυασμό με την λιγότερο έντονη παρουσία φαινομένων διάβρωσης σε μεγαλύτερα βάθη. Η στοιχειακή ανάλυση των εδαφικών δειγμάτων έδειξε ότι το εξεταζόμενο έδαφος ήταν φτωχότερο σε σίδηρο και αλουμίνιο, πλουσιότερο σε πυρίτιο και περίπου στο μέσο όρο σε μαγνήσιο, σε σύγκριση με άλλα εδάφη αντίστοιχου τύπου, παγκοσμίως. Ωστόσο, η σχετική αφθονία του μαγνησίου έναντι του αλουμινίου έδειξε έντονα τη συμβολή των υπερμαφικών υλικών έναντι των μαφικών στο εξεταζόμενο έδαφος.

Πιο συγκεκριμένα, αναφορικά με την παρουσία χρωμίου, προέκυψαν τα ακόλουθα αποτελέσματα. Η συγκέντρωση του χρωμίου (ολικού) δεν παρουσίασε ομοιόμορφη κατανομή ως προς το βάθος εμφανίζοντας αρχικά μείωση κατά τα πρώτα μέτρα, ακολουθούμενη από ελαφρά αύξηση για βάθη έως 10,5 μέτρα και γενική τάση αύξησης για βάθη μεγαλύτερα από 43 μέτρα. Τα αποτελέσματα βρίσκονται σε συμφωνία με αντίστοιχα που παρουσιάζονται στη βιβλιογραφία υποδηλώνοντας ότι οι διεργασίες διάβρωσης οι οποίες λαμβάνουν χώρα συνήθως στη ρηχή ακόρεστη ζώνη ευνοούν την έκπλυση στοιχείων όπως το μαγνήσιο, και τη συσσώρευση άλλων όπως ο σίδηρος, το αλουμίνιο και το χρώμιο στα υψηλότερα βάθη ενώ παράλληλα είναι και πιο έντονη η παρουσία μη διαβρωμένων σερπεντινικών φάσεων. Σε αντίθεση με τη συγκέντρωση του ολικού χρωμίου, η συγκέντρωση του εξασθενούς παρουσίασε σχεδόν συνεχή μείωση αυξανομένου του βάθους δειγματοληψίας του εδάφους. Όσον αφορά την παρουσία χρωμίου στο υπόγειο νερό οι συγκεντρώσεις που μετρήθηκαν ανήλθαν μέχρι 91 μg/L ολικό χρώμιο και έως 64 μg/L εξασθενές χρώμιο. Οι τιμές αυτές είναι εκ των υψηλότερων οι οποίες έχουν ανιχνευθεί παγκοσμίως σε υδροφορείς με παρόμοιο γεωλογικό υπόβαθρο. Και στις δυο περιπτώσεις, ολικού και εξασθενούς χρωμίου, οι συγκεντρώσεις στο υπόγειο νερό μειώθηκαν σχεδόν γραμμικά αυξανομένου του βάθους δειγματοληψίας. Επίσης, διαπιστώθηκε υψηλή τιμή συσχέτισης μεγαλύτερη του 83% μεταξύ των συγκεντρώσεων εξασθενούς και ολικού χρωμίου. Επιπλέον, οι έντονες γεωργικές δραστηριότητες στην εξεταζόμενη περιοχή είχαν ως αποτέλεσμα σχετικά υψηλές συγκεντρώσεις νιτρικών ιόντων.

Λαμβάνοντας υπόψη ότι οι κύριες διεργασίες που καθορίζουν την τύχη του εξασθενούς χρωμίου στους υδροφόρους, το οποίο παράγεται ως αποτέλεσμα της οξείδωσης του τρισθενούς, είναι η προσρόφηση και η αναγωγή διερευνήθηκε η παρουσία των διεργασιών αυτών και στην περίπτωση του εξεταζόμενου οφιολιθικού εδάφους. Η διερεύνηση αυτή βασίστηκε στο γεγονός πως στα οφιολιθικά εδάφη εμφανίζεται μια μίξη εξασθενούς και τρισθενούς χρωμίου. Ωστόσο μόνο το εξασθενές μπορεί να εκχυλιστεί από το έδαφος και να εισέλθει στα υπόγεια ύδατα. Καθώς όμως το εξασθενές χρώμιο απομακρύνεται από το έδαφος, το εναπομείνον τρισθενές μπορεί να οξειδωθεί βραδέως σε εξασθενές ώστε να αποκατασταθεί η ισορροπία του εδάφους. Με τη σειρά του το εκχυλισμένο εξασθενές χρώμιο μπορεί να προσροφηθεί ή να αναχθεί ξανά από τη στερεά φάση. Όσον αφορά την αναγωγική διαδικασία ορυκτά που περιέχουν δισθενή σίδηρο, όπως ο μαγνητίτης ή ο (μαγνησιο) χρωμίτης, μπορούν να δρουν ως αναγωγικά μέσα για το εξασθενές χρώμιο. Η διεργασία της προσρόφησης, επηρεάζεται έντονα από την εμφάνιση των (οξυ-υδρο)οξειδίων του σιδήρου, τα οποία είναι οι συνηθέστεροι φυσικοί προσροφητές του εξασθενούς χρωμίου. Επιπροσθέτως, τα οξείδια του σιδήρου δρουν αποτελεσματικά ως προσροφητές και για άλλους ανόργανους ρύπους όπως τα φωσφορικά και τα νιτρικά ιόντα.

Προκειμένου λοιπόν να προσδιοριστούν οι διαδικασίες που είναι υπεύθυνες για την απομάκρυνση του εξασθενούς χρωμίου από τα υπόγεια ύδατα, διεξήχθησαν πειράματα διαλείποντος έργου (παρτίδας) με σκοπό τη διερεύνηση της επίδρασης διαφόρων παραμέτρων όπως το pH, η ορυκτολογία, η κοκκομετρία του εδάφους, η αρχική συγκέντρωση του εξασθενούς χρωμίου, η ιοντική ισχύς του διαλύματος και η παρουσία άλλων ανόργανων ρύπων. Τα αποτελέσματα της παρούσας διατριβής έδειξαν ότι τόσο η προσρόφηση όσο και η αναγωγή επηρέασαν την απομάκρυνση του εξασθενούς χρωμίου από το εδαφικό διάλυμα. Και στις δύο διεργασίες η απομάκρυνση του εξασθενούς χρωμίου μειώθηκε αυξανομένης της τιμής pH. Επίσης, στην περίπτωση της αναγωγής η απομάκρυνση του εξασθενούς χρωμίου αποδόθηκε στην παρουσία ενός εδαφικού κλάσματος με μαγνητικές ιδιότητες το οποίο περιλαμβάνει μαγνητίτη και μαγνησιο-χρωμίτη ως κύρια ορυκτά. Όσον αφορά στην προσρόφηση αυτή πιθανώς αποδίδεται στην παρουσία άμορφων οξυ-υδροξειδίων του σιδήρου στο έδαφος. Η προσρόφηση βρέθηκε να είναι μερικώς αντιστρεπτή αφού μόνο ένα κλάσμα της προσροφημένης ποσότητας βρέθηκε να εκροφάται στο εδαφικό διάλυμα. Το γεγονός αυτό οφείλεται πιθανότατα στο σχηματισμό συμπλόκων εσωτερικής στοιβάδας τα οποία είναι αρκετά σταθερά, συμπεριλαμβανομένων αποκλειστικά ιοντικών ή/και ομοιοπολικών δεσμών. Ωστόσο, καθώς και οι δύο διεργασίες είναι επιφανειακά επηρεαζόμενες, ιδιαίτερα στην περίπτωση της αναγωγής η επίδραση της προσρόφησης είναι σημαντική καθώς προαπαιτείται ως διαδικασία ώστε να πραγματοποιηθεί η αναγωγή του εξασθενούς χρωμίου επί της στερεάς επιφάνειας. Επιπλέον, η αξιολόγηση της προσρόφησης ως συνάρτηση του μεγέθους των σωματιδίων (κοκκομετρίας) έδειξε ότι το λεπτότερο κλάσμα του εδάφους, το οποίο χαρακτηριζόταν και από υψηλότερη τιμή ειδικής επιφάνειας, ήταν το καθοριστικό κλάσμα όσον αφορούσε στην προσρόφηση. Η επίδραση της αρχικής συγκέντρωσης του εξασθενούς χρωμίου διερευνήθηκε και για υψηλότερες συγκεντρώσεις από αυτές που έχουν μετρηθεί ως αποτέλεσμα γηγενούς προέλευσης. Οι ισόθερμες Langmuir και Freundlich προσομοίωσαν με σημαντική ακρίβεια τα πειραματικά δεδομένα, υποδεικνύοντας έτσι την ταυτόχρονη ετερογένεια των επιφανειακών θέσεων των του οφιολιθικού εδάφους και ενδεχομένως τον σχηματισμό μονοστρωματικής προσρόφησης του εξασθενούς χρωμίου. Τέλος, διαπιστώθηκε η σημαντική επίδραση της ιοντικής ισχύος του εδαφικού διαλύματος στην προσρόφηση. Η αποτελεσματικότητα της προσρόφησης μειώθηκε με την αύξηση της τιμής της ιοντικής ισχύος υποδηλώνοντας τον σχηματισμό συμπλόκων εξωτερικής στοιβάδας για την προσρόφηση του εξασθενούς χρωμίου.

Επιπλέον, η προσροφητική ικανότητα του οφιολιθικού εδάφους διερευνήθηκε για τους ανόργανους ρύπους, φωσφορικά και νιτρικά ιόντα, που παρατηρούνται συνήθως σε περιοχές με έντονες γεωργικές δραστηριότητες. Διερευνήθηκαν επίσης και πιθανές ανταγωνιστικές αλληλεπιδράσεις μεταξύ αυτών και του εξασθενούς χρωμίου. Από τα αποτελέσματα προέκυψε πως το οφιολιθικό έδαφος παρουσίασε υψηλή ικανότητα προσρόφησης για τα φωσφορικά ιόντα, με τη διαδικασία της προσρόφησης να επηρεάζεται σημαντικά από το pH του διαλύματος. Ειδικότερα, η αύξηση του pH μειώνει την προσρόφηση των φωσφορικών, σχεδόν γραμμικά. Επίσης, δεν παρατηρήθηκαν ανταγωνιστικές αλληλεπιδράσεις στην προσρόφηση των φωσφορικών ιόντων κατά την ταυτόχρονη παρουσία εξασθενούς χρωμίου στο εδαφικό διάλυμα. Αντιθέτως, η προσρόφηση του εξασθενούς χρωμίου επηρεάστηκε έντονα από την παρουσία φωσφορικών στο διάλυμα. Μια πιθανή εξήγηση είναι ο σχηματισμός αποκλειστικά συμπλόκων εσωτερικής στοιβάδας μεταξύ των φωσφορικών και

της οφιολιθικής επιφάνειας, δημιουργώντας ανταγωνισμό με χρωμικά ιόντα τα οποία σχηματίζουν επίσης σύμπλοκα εσωτερικής στοιβάδας. Για την περίπτωση των νιτρικών ιόντων, η προσρόφηση τους στο οφιολιθικό έδαφος ήταν πολύ χαμηλή και σχεδόν μηδενική σε τιμές pH που συνήθως απαντώνται στους υδροφορείς. Η επίδραση του εξασθενούς χρωμίου στην προσρόφηση νιτρικών, και αντιστρόφως, ήταν σχεδόν αμελητέα. Αυτό πιθανότατα οφείλεται σε διαφορετικό τύπο επιφανειακής συμπλοκοποίησης νιτρικών και χρωμικών ιόντων, καθώς τα νιτρικά σχηματίζουν σύμπλοκα εξωτερικής στοιβάδας σε αντίθεση με τα χρωμικά τα οποία σχηματίζουν τόσο σύμπλοκα εσωτερικής όσο και εξωτερικής στοιβάδας.

Το επόμενο βήμα της παρούσας διατριβής αφορούσε στη σύγκριση της προσροφητικής συμπεριφοράς του οφιολιθικού εδάφους με εκείνη ενός καθαρού οξειδίου του σιδήρου. Το οξείδιο του τρισθενούς σιδήρου που επιλέχτηκε ήταν ο γκαιτίτης αφού θεωρείται από τα πλέον άφθονα οξείδια του σιδήρου στο γεωπεριβάλλον και ένα από το πιο συνηθισμένα στα οφιολιθικά εδάφη. Ο γκαιτίτης εξετάστηκε ως προς την προσροφητική του ικανότητα για εξασθενές χρώμιο, φωσφορικά και νιτρικά ιόντα. Διερευνήθηκαν επίσης οι πιθανές ανταγωνιστικές αλληλεπιδράσεις μεταξύ των εξεταζόμενων ανιόντων. Τα πειραματικά αποτελέσματα έδειξαν ότι ο γκαιτίτης είναι ένας αποτελεσματικός προσροφητής για τα χρωμικά και τα φωσφορικά ιόντα αλλά όχι για τα νιτρικά. Η αύξηση του pH του διαλύματος οδήγησε σε μείωση της προσροφητικής ικανότητας του γκαιτίτη για όλους τους εξεταζόμενους ρύπους ως συνέπεια της αρνητικής φόρτισης της επιφάνειας του γκαιτίτη για υψηλές τιμές pH προκαλώντας απωστικές δυνάμεις μεταξύ των ανιόντων των ρύπων και της επιφάνειας. Επιπλέον, η επίδραση της παραμέτρου της ιοντικής ισχύος στη προσρόφηση του εξασθενούς χρωμίου διερευνήθηκε ως ένας τρόπος αποκάλυψης του είδους της προσρόφησης ως προς τη δημιουργία συμπλόκων. Η αύξηση της ιοντικής ισχύος οδήγησε σε αισθητή μείωση της προσρόφησης του εξασθενούς χρωμίου, υποδεικνύοντας έτσι το σχηματισμό συμπλόκων εξωτερικής στοιβάδας, τα οποία βασίζονται σε ασθενείς ηλεκτροστατικές δυνάμεις. Η διερεύνηση πιθανών ανταγωνιστικών αλληλεπιδράσεων μεταξύ χρωμικών και φωσφορικών ιόντων κατά την προσρόφησή τους στην επιφάνεια του γκαιτίτη έδειξε ότι η προσρόφηση των φωσφορικών δεν επηρεάζεται από την παρουσία χρωμικών. Αντίθετα, παρατηρήθηκε σημαντική επίδραση στη προσρόφηση των χρωμικών υπό την ταυτόχρονη παρουσία φωσφορικών ιόντων στο διάλυμα. Το γεγονός αυτό πιθανώς οφείλεται στο γεγονός ότι τα χρωμικά, προσροφώνται και μέσω συμπλόκων εξωτερικής στοιβάδας ενώ τα φωσφορικά προσροφώνται μόνο μέσω συμπλόκων εσωτερικής στοιβάδας. Όσον αφορά στον ανταγωνισμό μεταξύ χρωμικών και νιτρικών ιόντων, τα αποτελέσματα έδειξαν ότι η προσρόφηση των χρωμικών ελαττώθηκε υπό την παρουσία νιτρικών. Το γεγονός αυτό πιθανώς οφείλεται στη σημαντική διαφορά των συγκεντρώσεων που χρησιμοποιήθηκαν στην παρούσα διατριβή. Η σημαντικά υψηλότερη συγκέντρωση νιτρικών ιόντων δημιουργεί πιθανώς απωστικές ηλεκτροστατικές δυνάμεις οι οποίες μπορεί να επηρεάσουν την συμπλοκοποίηση των χρωμικών, ιδιαίτερα των συμπλόκων εξωτερικής στοιβάδας. Στην περίπτωση των νιτρικών, η ήδη χαμηλή απόδοση προσρόφησης δεν επηρεάστηκε από την παρουσία χρωμικών ιόντων στο διάλυμα.

Λαμβάνοντας υπόψη τα πειραματικά αποτελέσματα που προέκυψαν από τα πειράματα διαλείποντος έργου, ο επόμενος στόχος αυτής της διατριβής ήταν η προσομοίωση της

διαδικασίας της προσρόφησης εφαρμόζοντας μοντέλα επιφανειακής συμπλοκοποίησης. Η συμπεριφορά, η μεταφορά και γενικότερα η τύχη των βαρέων μετάλλων και των ανόργανων ρύπων στο γεωπεριβάλλον, εξαρτάται σε μεγάλο βαθμό από τις αντιδράσεις προσρόφησης με τα εδαφικά συστατικά και επομένως είναι πολύ σημαντικό να διερευνηθούν τέτοιες αντιδράσεις. Παρότι διαφορετικές εμπειρικές προσεγγίσεις έχουν χρησιμοποιηθεί για τη μελέτη της προσροφητικής συμπεριφοράς των εδαφών, έχουν παρατηρηθεί αρκετοί περιορισμοί, καθώς αυτές οι προσεγγίσεις δεν μπορούν να λάβουν υπόψη τις αλλαγές στις φυσικοχημικές ιδιότητες των υπόγειων υδάτων. Τις δυο τελευταίες δεκαετίες διεξήχθησαν εκτεταμένες μελέτες χρησιμοποιώντας μοντέλα επιφανειακής συμπλοκοποίησης για την περιγραφή της προσρόφησης βαρέων μετάλλων και ανόργανων ρύπων με αρκετά υποσχόμενα αποτελέσματα. Τα μοντέλα επιφανειακής συμπλοκοποίησης βασίζονται γενικά στην παροχή μιας θερμοδυναμικής περιγραφής των αντιδράσεων μεταξύ των επιφανειακών ομάδων και των προσροφημένων ιόντων, με βάση ισοζύγια φορτίου και μάζας. Ωστόσο, στις περισσότερες μελέτες έχουν χρησιμοποιηθεί καθαρά ορυκτά και μόνο λίγες εξ αυτών αναφέρονται σε φυσικά υλικά και ιδιαίτερα σε εδάφη όπως στην παρούσα διατριβή. Επιπρόσθετα, ένας ακόμη περιορισμός που υπάρχει έγκειται στο γεγονός πως κάθε μοντέλο επιφανειακής συμπλοκοποίησης βασίζεται σε διαφορετικές συγκεκριμένες παραδοχές σχετικά με τη διεπιφάνεια στερεού-υγρού, οι οποίες εκφράζονται με διαφορετικές αντιδράσεις επιφανειακής συμπλοκοποίησης και συνεπώς διαφορετικές σταθερές προσρόφησης στις αντιδράσεις που χρησιμοποιούνται. Συνεπώς, οι τιμές που λαμβάνονται δεν μπορούν να χρησιμοποιηθούν σε διαφορετικά μοντέλα.

Στην παρούσα διατριβή, τρία από τα πιο κοινά μοντέλα επιφανειακής συμπλοκοποίησης χρησιμοποιήθηκαν για την προσομοίωση των πειραματικών δεδομένων. Αυτά ήταν το μοντέλο τριπλής στοιβάδας (Triple Layer Model, TLM), το μοντέλο στοιβάδας διάχυσης (Diffuse Layer Model, DLM) και το μοντέλο σταθερής χωρητικότητας (Constant Capacitance Model, CCM). Για την εφαρμογή των μοντέλων δημιουργήθηκαν οι αντίστοιχες βάσεις αντιδράσεων επιφανειακής συμπλοκοποίησης οι οποίες εισήχθησαν στο λογισμικό Visual Minteq. Η εφαρμογή των προαναφερθέντων μοντέλων βασίστηκε στην προσέγγιση κατά την οποία η επιφάνεια του εδάφους θεωρείται ενιαία και με ίδια χαρακτηριστικά (general composite approach, GC) παρά την παρουσία διαφορετικών ορυκτών. Πιο συγκεκριμένα η προσέγγιση θεωρεί ότι η σύνθεση του εδάφους είναι ιδιαίτερα περίπλοκη ώστε να καταστεί δυνατή η διάκριση και η ποσοτικοποίηση των μεμονωμένων φάσεων/ορυκτών και συνεπώς αποδέχεται ένα γενικό τύπο ενεργών θέσεων στην επιφάνεια του εδάφους στις οποίες πραγματοποιείται η προσρόφηση. Αυτή η υπόθεση απαιτεί τη χρήση συγκεκριμένων αντιδράσεων με τις αντίστοιχες σταθερές τους (συντελεστές K) οι οποίες θα προκύψουν έμμεσα από την προσομοίωση αποτελεσμάτων τα οποία βασίζονται σε πειραματικά δεδομένα. Έτσι, οι δημιουργούμενες βάσεις αντιδράσεων επιφανειακής συμπλοκοποίησης θα μπορούν να χρησιμοποιηθούν μεταβάλλοντας μόνο τις τιμές των σταθερών των αντιδράσεων συμπλοκοποίησης ώστε για να ταιριάζουν με τα πειραματικά δεδομένα. Επίσης, μεταξύ των παραμέτρων που απαιτούνται σε κάθε μοντέλο, μια παράμετρος που απαιτείται σε όλα τα μοντέλα προκειμένου να πραγματοποιηθεί η προσομοίωση είναι η συγκέντρωση του στερεού στο διάλυμα. Στην περίπτωση που χρησιμοποιήθηκε ο γκαιτίτης ως προσροφητικό υλικό, η τιμή συγκέντρωσης που χρησιμοποιήθηκε ήταν ίδια με την τιμή που χρησιμοποιήθηκε στα πειράματα διαλείποντος έργου. Ωστόσο, στην περίπτωση προσομοίωσης των πειραματικών

αποτελεσμάτων που προέκυψαν από τα πειράματα του οφιολιθικού εδάφους εξετάστηκαν τρεις διαφορετικές περιπτώσεις όσον αφορά την τιμή της συγκέντρωσης του προσροφητή. Με δεδομένο ότι δεν συμμετέχουν όλα τα εδαφικά ορυκτά του οφιολιθικού εδάφους στη διαδικασία της προσρόφησης και με την υπόθεση ότι η προσρόφηση ελέγχεται κυρίως από την παρουσία οξειδίων του σιδήρου και αργιλίου υπολογίστηκαν τρεις διαφορετικές τιμές συγκεντρώσεων προσροφητή. Για τον υπολογισμό τους χρησιμοποιήθηκε το ισοζύγιο μάζας βασισμένο στις μετρήσεις στοιχειακών αναλύσεων με φθορισμό ακτίνων X (XRF) και της ποσοτικής ανάλυσης με περίθλαση ακτίνων X (XRD). Τα τρία διαφορετικά σενάρια συγκεντρώσεων στερεού περιλάμβαναν τη συμβολή στην προσρόφηση είτε α) των οξειδίων σιδήρου και αλουμινίου, είτε β) μόνο των οξειδίων του σιδήρου είτε γ) μόνο των άμορφων οξειδίων του σιδήρου, χρησιμοποιώντας τις τρεις αυτές τιμές συγκεντρώσεων σε καθένα από τα τρία προαναφερθέντα μοντέλα επιφανειακής συμπλοκοποίησης.

Η εφαρμογή του μοντέλου TLM για την περιγραφή της διαδικασίας της προσρόφησης στο οφιολιθικό έδαφος οδήγησε σε ικανοποιητικά αποτελέσματα για όλα τα ανιόντα που εξετάστηκαν. Η προσομοίωση της προσρόφησης ήταν αποτελεσματική κατά τη μεταβολή όλων των εξεταζόμενων παραμέτρων όπως το pH, η ιοντική ισχύς και οι ανταγωνιστικές αλληλεπιδράσεις μεταξύ των ιόντων, στις περιπτώσεις κατά τις οποίες θεωρήθηκε πως η προσρόφηση ελέγχεται είτε από την παρουσία οξειδίων σιδήρου και αργιλίου, είτε μόνο από τα οξείδια του σιδήρου. Αντιθέτως, η προσομοίωση δεν ήταν αποτελεσματική όταν χρησιμοποιήθηκε η συγκέντρωση μόνο των άμορφων οξειδίων του σιδήρου ως τιμή συγκέντρωσης προσροφητή υποδεικνύοντας έτσι ότι αυτή η στερεή φάση δεν αντιστοιχεί στη συγκέντρωση της στερεάς φάσης που συμβάλλει στην προσρόφηση. Προσομοιώντας την επίδραση της ιοντικής ισχύος διαπιστώθηκε ότι σε χαμηλές τιμές η προσρόφηση των χρωμικών ιόντων μπορεί να περιγραφεί με το σχηματισμό συμπλόκων εσωτερικής στοιβάδας, είτε με σύμπλοκα ενός δεσμού (monodentate), είτε δυο δεσμών (bidentate), καθώς και με σύμπλοκα εξωτερικής στοιβάδας. Εντούτοις, η αύξηση της ιοντικής ισχύος έδειξε ότι η προσρόφηση του εξασθενούς χρωμίου μπορεί να περιγραφεί αποτελεσματικά μόνο με το σχηματισμό bidentate συμπλόκων. Ο σχηματισμός bidentate συμπλόκων των χρωμικών ιόντων με την επιφάνεια του εδάφους μπορεί επίσης να περιγράψει τις ανταγωνιστικές αλληλεπιδράσεις υπό την παρουσία φωσφορικών και νιτρικών ιόντων. Επιπρόσθετα, επιτυγχάνεται ικανοποιητική προσομοίωση της προσρόφησης φωσφορικών και νιτρικών ιόντων εξαιτίας του πιθανού ανταγωνισμού τους με χρωμικά ιόντα στο εδαφικό διάλυμα. Συνεπώς, όπως προαναφέρθηκε, το TLM είναι ικανό να περιγράψει αποτελεσματικά την προσρόφηση του εξασθενούς χρωμίου και των ανόργανων ρύπων στο οφιολιθικό έδαφος. Σε αντίθεση με τα αποτελέσματα που προέκυψαν από το TLM, η προσομοίωση πειραματικών δεδομένων χρησιμοποιώντας το μοντέλο DLM έδειξε ότι η εφαρμογή αυτού του μοντέλου δεν είναι κατάλληλη για την ακριβή περιγραφή της διαδικασίας προσρόφησης στο οφιολιθικό έδαφος. Παρά το γεγονός πως το μοντέλο DLM ήταν ικανό να προσομοιώσει την προσρόφηση των χρωμικών και νιτρικών ιόντων, παρατηρήθηκε μικρή ακρίβεια στην περίπτωση προσομοίωσης προσρόφησης των φωσφορικών. Επιπλέον, το DLM δεν μπόρεσε να προβλέψει τον ανταγωνισμό στην προσρόφηση μεταξύ του εξασθενούς χρωμίου και των ανόργανων ρύπων. Μια πιθανή εξήγηση είναι η παραδοχή κατά την εφαρμογή του DLM βάση της οποίας λαμβάνεται υπόψη ο σχηματισμός συμπλόκων μόνο στην εσωτερική στοιβάδα και μόνο monodentate τύπου. Δεν είναι εφικτή λοιπόν η προσομοίωση σχηματισμού συμπλόκων

εξωτερικής στοιβάδας όπως αναμένεται για τις περιπτώσεις των χρωμικών και νιτρικών ιόντων. Αυτό επαληθεύει περαιτέρω τα αποτελέσματα που ελήφθησαν κατά την εφαρμογή του TLM το οποίο περιλαμβάνει τον σχηματισμό συμπλόκων εξωτερικής στοιβάδας. Για την περίπτωση εφαρμογής του μοντέλου CCM διαπιστώθηκε πως είναι ικανό να προσομοιώσει την προσρόφηση του κάθε ρύπου χωριστά ωστόσο εμφάνισε πολύ μικρή ακρίβεια στην περίπτωση ανταγωνιστικής προσρόφησης μεταξύ των χρωμικών και των φωσφορικών ιόντων. Η καλύτερη προσομοίωση της προσρόφησης του εξασθενούς χρωμίου η οποία επετεύχθη σε σύγκριση με το DLM οφείλεται πιθανώς στο σχηματισμό συμπλόκων bidentate αναδεικνύοντας έτσι τη σημασία τους στην προσρόφηση του εξασθενούς χρωμίου.

Τέλος, η εφαρμογή μοντέλων επιφανειακής συμπλοκοποίησης για την περιγραφή της προσροφητικής συμπεριφοράς του γκαιτίτη οδήγησε σε παρόμοιες διαπιστώσεις με αυτές του οφιολιθικού εδάφους. Το μοντέλο TLM περιέγραψε ικανοποιητικά την προσρόφηση του εξασθενούς χρωμίου και των ανόργανων ρύπων, καθώς και τον ανταγωνισμό τους στην επιφάνεια του γκαιτίτη. Η προσομοίωση έδειξε ότι τα χρωμικά ιόντα προσροφώνται μέσω συμπλόκων εσωτερικής και εξωτερικής στοιβάδας. Το γεγονός αυτό επαληθεύτηκε από τη μείωση της αποτελεσματικότητας της προσρόφησης λόγω της αύξησης της ιοντικής ισχύος. Η συμπλοκοποίηση των χρωμικών ιόντων θεωρείται ότι διέπεται από το σχηματισμό bidentate συμπλόκων με τη στερεά επιφάνεια. Η προσρόφηση φωσφορικών και νιτρικών ιόντων αλλά και οι ανταγωνιστικές αλληλεπιδράσεις τους με το εξασθενές χρώμιο προσομοιώνονται επίσης με μεγάλη ακρίβεια. Αντιθέτως, η προσομοίωση της προσρόφησης του εξασθενούς χρωμίου και των ανόργανων ρύπων χρησιμοποιώντας το μοντέλο DLM δεν ήταν εξίσου αποτελεσματική. Μια πιθανή εξήγηση είναι η υπόθεση στην οποία βασίζεται η εφαρμογή του κατά την οποία είναι δυνατός ο αποκλειστικός σχηματισμός monodentate συμπλόκων εσωτερικής στοιβάδας αγνοώντας την πιθανή παρουσία συμπλόκων εξωτερικής στοιβάδας. Κλείνοντας, η εφαρμογή μοντέλου CCM για προσομοίωση προσρόφησης του εξασθενούς χρωμίου και των ανόργανων ρύπων απεδείχθη ικανή να προσομοιώσει αποτελεσματικά την προσρόφηση του έκαστου ρύπου ωστόσο δεν μπορούσε να περιγράψει τις ανταγωνιστικές αλληλεπιδράσεις που δημιουργήθηκαν μεταξύ των εξεταζόμενων ιόντων.

TABLE OF CONTENTS

LIST OF ABBREVIATIONS

BET	Brunauer–Emmett–Teller
CA	Component additivity
CCM	Constant Capacitance Model
Cr(III)	Trivalent chromium
Cr(VI)	Hexavalent chromium
DLM	Diffuse Layer Model
GC	General composite
LOI	Loss of ignition
PZC	Point of zero charge
SCM	Surface complexation model
SSA	Specific Surface Area
TGA	Thermogravimetric analysis
TLM	Triple Layer Model
XANES	X-ray absorption near edge structure
XRD	X-ray Diffraction
XRF	X-ray Fluorescence

LIST OF TABLES

LIST OF FIGURES

1 INTRODUCTION

1.1 Aim of the thesis

Groundwater contamination with heavy metals and inorganic contaminants is one of the most important environmental issues. Chromium [Cr] is a heavy metal that is among the most common contaminants observed in aquifers. The main Cr species in the geoenvironment are the trivalent [Cr(III)] and the hexavalent [Cr(VI)] forms. Under the physicochemical conditions prevailing in geoenvironment, Cr(III) mainly occurs in the minerals of the geological background of the aquifer. Such minerals, rich in chromium are usually found in ultramafic/serpentinitic rocks and ophiolitic complexes. Cr(VI) is generated via the oxidation of geogenic Cr(VI). Therefore, the occurrence of Cr(VI) in aquifers can be either of geogenic or anthropogenic origin. In Greece there are various areas with ophiolitic complexes, located on the Mirdita Sub-Pelagonian and Pelagonian geotectonic zones of the Balkan Peninsula. The ophiolite-rich zone extends from Albania to Northern and Central Greece and into the Anatolides zone of western Turkey. Several studies have been published on the properties of ophiolites and associated metal mobility in Central Greece, where anthropogenic contamination is also of concern. However, there is relatively little data on chromium release from chromium-rich rocks and soils in Northern Greece, where agricultural activity is the main anthropogenic influence.

The present thesis aims at investigating the geochemical behavior of Cr(VI) in ophiolitic soils and quantify those processes (mainly adsorption) able to retard its transport in geoenvironment. Adsorption simulation was performed applying surface complexation modeling. For achieving this goal three general stages were followed. Firstly, the chromium concentration profile in soil and groundwater and its correlation with the geologic background in an ophiolitic aquifer located in the agricultural area of Vergina (Northern Greece) was determined. This was accomplished by employing mineralogical and chemical analyses of soils and groundwater.

At a second stage the physicochemical processes able to affect mobility of Cr(VI) in ophiolitic aquifers was investigated. To this aim, batch experiments were conducted in order to evaluate the removal capacity and distinguish the processes responsible for Cr(VI) removal, mainly sorption and redox reactions. These processes were investigated as a function of pH, mineralogy, soil's particle size and initial concentration of Cr(VI). Langmuir and Freundlich isotherms were fitted in order to extract the necessary distribution factors for transport modeling. In addition, the removal capacity of the ophiolitic soil for common inorganic contaminants related with agricultural contamination, such as phosphates and nitrates, was also investigated. Finally, batch experiments were also conducted in order to assess Cr(VI) leaching from the ophiolitic soil and its interaction with the aforementioned inorganic contaminants. These results aimed at determining the degree of Cr(VI) release in groundwater, while the results of mineralogical analysis were used to determine the minerals that possibly are responsible for contaminants removal. Iron (hydro)oxides and specifically goethite was identified as one of the most important adsorbents. Another series

of batch experiments using pure synthetic goethite were performed in order to compare its removal capacity with that of the real soil.

The third and last step of this thesis aimed at simulating the adsorption capacity of the tested soil and pure mineral (goethite). The adsorption simulation was performed by applying surface complexation models (SCMs), using the geochemical software Visual Minteq. Simulation was based on the batch experimental results obtained at the previous stage. Three surface complexation models were used and evaluated: Triple Layer Model (TLM), Double Layer model (DLM) and Constant Capacitance Model (CCM).

The three stages described above are outlined schematically in Figure 1.1, in order to finally achieve the aim of the present thesis.

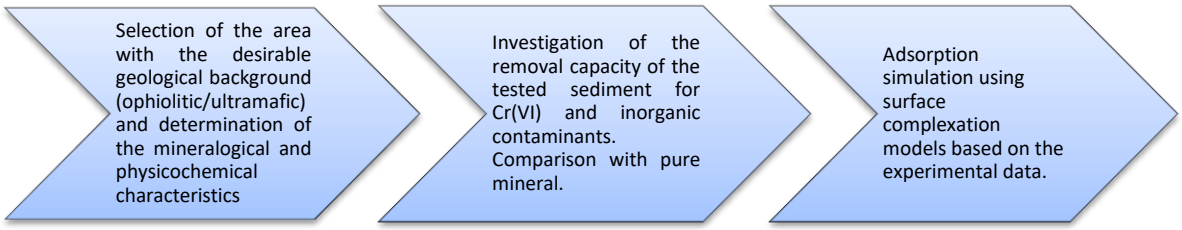

Figure 1.1 Description of the three stages of the thesis

1.2 Contribution in research – Originality

Until recently, high levels of Cr(VI) in the geoenvironment were considered to be a result of anthropogenic contamination. However, over the last two decades some studies [Fantoni et al. (2002); Gonzalez et al. (2005); Robles-Camacho et al. (2000); Oze et al. (2007)] demonstrated that relatively high levels of Cr(VI) may be due to natural geogenic processes, especially in areas where there are relatively high levels of naturally occurring Cr(III) or Cr(VI) in the soils. Such areas are characterized by the presence of ophiolitic complexes and ultramafic rocks in their geological background, and are met in quite a few populated areas in the Pacific [California (USA), Mexico] and in the Mediterranean (Greece, Italy, Albania, France) and other parts of the world. Even though ophiolitic complexes represent only a small percentage of the earth's crust (≈1%), their occurrence in Greece is higher than of other European countries. Typical examples of areas with recorded high concentrations of Cr(VI) in groundwater are the Asopos River basin in Central Greece and Vergina plain at Western Macedonia.

The originality of the present thesis is firstly based on the fact that despite many studies have been referred to the presence of Cr(VI) under the occurrence of ophiolitic complexes and serpentinitic soils, these studies have focused on either characterizing the groundwater or the solid phase (topsoil or deep soil) of the tested cases. In addition, only few of them have analyzed soils from high depths and have tried to correlate the groundwater and soil characteristics. None of them has reported the concentration profile of chromium in high depths. In this study soil and groundwater samples were collected form depths down to

≈100 m, using a new groundwater sampling method (discrete sampling method) able to create more representative sampling data.

The second phase of the thesis aimed at investigating the removal capacity of Cr(VI) by the ophiolitic soil as a function of several parameters. Despite several types of soils have been tested for their sorption capacity, no studies occur reporting the Cr(VI) removal capacity of ophiolitic soils. Furthermore, specifically for ophiolitic soils, the production of Cr(VI) in these geological backgrounds has been extensively investigated in many studies but none of them has been referred to the process that affects its occurrence. Thus the removal capacity of ophiolitic soils was further investigated in order to distinguish the processes that cause its retention, such as sorption and redox reactions. The results of this study are of the first published in the literature. In addition, since several studies have reported the presence of iron (hydr)oxides in serpentinitic soils (Bonifacio et al., 1997; Becquer et al., 2003; Caillaud et al., 2004; Fandeur et al., 2009; Kelepertzis et al., 2013), pure synthetic goethite was selected as the iron hydroxide in order to be compared to the ophiolitic soils for its Cr(VI) and inorganic anions removal capacity. Despite goethite has been extensively investigated as an adsorbent for several contaminants, including Cr(VI), there is no information regarding the possible competitive effects between Cr(VI) and common contaminants, such as nitrates and phosphates.

The results of the experiments performed at the second phase of this thesis were used for developing a more general framework in order to quantify and simulate Cr(VI) adsorption on serpentinitic soils. Adsorption simulation was performed applying advanced surface complexation models. The first attempts to develop such adsorption models took place in the early 1990s. However, the prediction of ion adsorption in natural samples is very challenging due to the difficulty in accounting for any competitive effects between ions and due to the presence of different adsorbing surfaces, like iron (hydr)oxides, aluminum (hydr)oxides and edges of clays. The originality of this thesis lies in the fact that the developed models for simulating the process of adsorption were based on experiments using synthetic rather than real soils, like in this dissertation. In addition, despite the fact that few studies have used real soils none of them has used ophiolitic soils. In order to efficiently simulate the adsorption process specific mineralogical and physicochemical properties were taken into account as an effective way for adsorption simulation.

1.3 Thesis structure

The present thesis consists of seven chapters, the content of which is summarized below:

Chapter 1 – Introduction

Chapter 1 is the introduction of this thesis. The introduction summarizes the subject and the purpose of the dissertation and highlights the originality and its contribution.

Chapter 2 – Literature review

In Chapter 2 a literature review is carried out. In particular, the most important experimental and review papers regarding the geochemistry of Cr(VI) and its occurrence in the geoenvironment are referred. In addition, the presence of other inorganic contaminants like phosphate and nitrate, their occurrence and any possible co-existence with Cr(VI), like in cases of groundwater contamination due to agricultural activities, is investigated. Subsequently, the physicochemical process of adsorption and its affection on the transport of these contaminants is referred. The models used in order to quantitatively predict adsorption of such contaminants by soils are discussed.

Chapter 3 – Experimental methods and protocols

In Chapter 3 a description of the sampling area and the sampling methods applied is provided. The experimental methods and protocols used in the present study for the characterization of the ophiolitic soils and for determining the tested contaminants in the solid or aqueous phases are also presented. Finally, the series of experiments performed in this thesis and the software used for simulating the experimental results are described.

Chapter 4 – Soil and groundwater physicochemical analyses

Chapter 4 includes the results of physicochemical analyses of the collected soils and groundwater samples. In addition, the geotechnical properties and the mineralogy of the soil samples are investigated. This analysis aims at better understanding these properties of soil that can affect the fate and especially the adsorption process of Cr(VI) and the inorganic contaminants that will be tested in the present study.

Chapter 5 – Results of batch experiments

In Chapter 5 the experimental results of this study are presented. Firstly, leaching experiments were performed in order to evaluate the mobility of the tested contaminants. Afterwards, the effect of parameters like pH, soils mineralogy, particle size, contaminants initial concentration and ionic strength of the solid solution on Cr(VI) adsorption by the ophiolitic soil are investigated. In addition, the existence of any adsorption competitive effects due to the occurrence of other inorganic contaminants, in particular nitrates and phosphates, on Cr(VI) adsorption by the ophiolitic soils is also studied. Similar experiments, were performed using as adsorbent pure goethite instead of ophiolitic soil. Goethite is usually the predominant mineral in ophiolitic soils and thus a comparison of the adsorption efficiency is made.

Chapter 6 – Adsorption simulation of Cr(VI) and inorganic contaminants

Chapter 6 includes the simulation of the adsorption process using surface complexation modeling. Adsorption simulation is performed using three different surface complexation models: Triple Layer Model, Diffuse Layer Model and Constant Capacitance Model. Adsorption simulation is performed for two cases using ophiolitic soil and goethite as adsorbents. In the

case of using the ophiolitic soil the determination of specific physicochemical and mineralogical characteristics is performed as a tool for further determining the concentration of adsorbent that will be used in simulation process.

Chapter 7 – Conclusions and recommendations

Chapter 7 summarizes the main points and conclusions of the dissertation and the proposals for future research.

2 LITERATURE REVIEW

2.1 Chemistry of chromium

Chromium is a transition element and belongs to the sixth (6B) group of the periodic table with atomic number equal to 24. It is a very hard, glossy silver-white metal, colorless, tasteless, malleable and extremely anticorrosive. Chromium owes its name to the Greek word "χρώμα" since it forms many colorful compounds that cover the visible spectrum, from violet [Cr(III) salts] to deep red [some Cr(VI)] (Figure 2.1). These compounds are mainly oxygenated and most contain the mineral chromite ($FeCr_2O_3$ or $FeCr_2O_4$). Instead of iron (Fe) other elements like magnesium (Mg), aluminum (Al) or silicon (Si) can occur in such Cr-rich compounds which in general contain 42 - 56% Cr_2O_3.

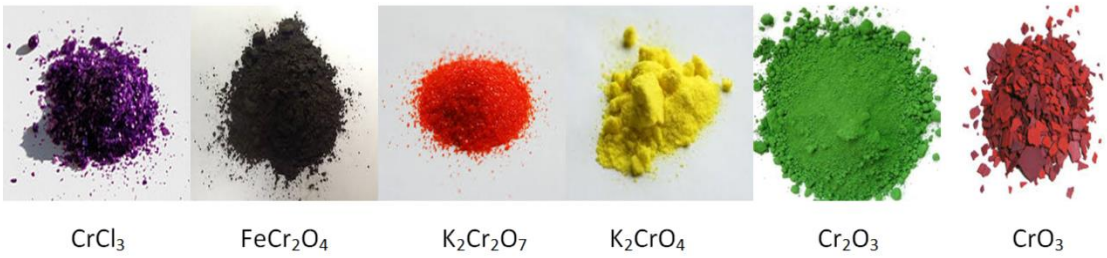

Figure 2.1 Colorful chromium compounds

Chromium compounds have no taste and smell. Elemental chromium has not magnetic properties in room temperature. It has high melting point (1857 °C) and boiling point (2672 °C). Chromium is easily dissolved in non-oxidizing inorganic acids, such as hydrochloric and sulfuric acid. However, it does not react with nitric acid due to passivation phenomena by surface chromium oxides. This is the most important reason for exhibiting anti-corrosive properties against seawater or dry/wet air, in ambient conditions. However, at high temperatures chromium is directly bonded to halogens, sulfur, silicon, boron, oxygen, and carbon forming brightly colored compounds. It also reacts with nitrogen (N) to form nitrides (Jacobs & Testa, 2005).

There are twenty six known chromium isotopes of which only four are stable and non-radioactive in the environment. The natural isotopes of chromium are ^{50}Cr, ^{52}Cr, ^{53}Cr and ^{54}Cr and their percentage abundances are 4.3, 83.8, 9.6 and 2.4%, respectively. Chromium oxidation states range from –2 to +6. Oxidation states −2, −1, 0, and +1 occur only at synthetic organic compounds like chromium- carbonyls, bipyridines, nitrosyls and organometallic complexes. In nature chromium is presented only as [Cr(III)], [Cr(VI)] and very rarely as elemental chromium [Cr(0)] (Jacobs & Testa, 2005).

2.2 Legal framework regarding chromium in water

Cr(III) is generally non-toxic and is an essential nutrient. It is used by the organism in several metabolic actions for the metabolism of fats and sugars. One of the most important actions of Cr(III) is that potentiates the action of insulin in peripheral tissue. However, in high

concentrations Cr(III) can cause adverse effects and it can be considered as toxic and even carcinogenic. In the USA the National Research Council has identified an estimated safe and adequate daily dietary intake for chromium of 50-200 μg/day which corresponds to 0.71 - 2.9 μg/kg-day for a 70 kg adult. The Food and Drug Administration (FDA) has selected a Reference Daily Intake for chromium of 120 μg/day (Anderson, 1989; USEPA, 1998). A recommended intake dose in the range 25-200 μg/day seems to be widely accepted.

On the contrary, Cr(VI) is toxic to plants and animals, and a human carcinogen. Cr(VI) toxicity can result from the generation of reactive intermediates and free radicals during reduction to Cr(V), Cr(IV) and finally to Cr(III) (ATSDR, 2000). Toxic and carcinogenic effects from industrial Cr(VI) pollution have been demonstrated since the 19th century. USEPA classifies chromium among the first seventeen chemicals in groundwater causing the greatest threat to human health, while Canada similarly includes chromium in the group of compounds mentioned as priority pollutants. Since USEPA recognizes chromium as priority pollutant, relevant water quality limits have been set since 1995. Concentration limits for short- and long-term exposure regarding the dissolved chromium have been established for freshwater. These limits refer to the critical maximum (CMC) and critical continuous (CCC) concentrations and are equal to 16 and 11 μg/L Cr(VI), respectively. USEPA has also set an oral RfD for Cr(VI) equal to 0.006 mg/Kg-day or equivalently 210 μg/L. Results of occupational epidemiologic studies of Cr-exposed workers across investigators and study populations consistently demonstrate that Cr(VI) is carcinogenic by the inhalation route of exposure (USEPA, 1998). The Cr(VI) concentration for lifetime cancer risk has been determined to be 0.2 μg/L based on mouse studies (CalEPA OEHHA, 2011). A Tolerable Daily Intake (TDI) for Cr(VI) equal to 5 μg/day was established by the Dutch RIVM in 2001 (Dutch National Institute for Public Health and the Environment). Thus the speciation of chromium is of great significance in terms of risk assessment.

Despite the evidence that Cr(VI) can be even carcinogenic, there has not been established an international standard regarding its concentration in drinking water. The widely adopted limit as proposed by the World Health Organization (WHO) is equal to 50 μg/L and regards Cr_{tot} (WHO, 1993). According to the USEPA there was inadequate data to demonstrate that Cr(VI) has oncogenic potential via ingestion and thus there was not established a separate limit for Cr(VI) in drinking water (USEPA, 1984). The WHO guidelines for drinking water are used as a basis for the standards in the Drinking Water Directive (98/83/EC) of the European Union (EU) and have also been adopted by Greece via the Ministerial Decree (JMD) 67322/2017. However, the California Department of Public Health from 1 July 2014 and the Italian legislation according to the Ministry's Decree of 14 November 2016 (whose entry into force has been extended to December 2018), respectively, have established the concentration of 10 μg/L, as the limit of Cr(VI) in drinking water.

In the case of groundwater the established environmental quality standards for Cr_{tot} and Cr(VI) in the EU are not the same among the Member States. Generally, groundwater protection is governed by the implementation of the general Water Framework Directive (WFD) 2000/60/EC, and its "daughter directive", Directive 2006/118/EC, which aims specifically to groundwater protection. In the framework of the WFD the aim is the achievement of good

chemical status of groundwater based on specific quality factors. These factors are set by each State Member according to the geochemical, hydrogeological etc. background of each State. Most State members, including Greece, have set limits for Cr_{tot} equal to the drinking water standards of 50 μg/L, without separating Cr_{tot} and Cr(VI). Greece has established these fairly strict environmental quality standards by the JMD 1811/2011. In addition, a separate JMD No. 100079/2015 has been enacted in Greece specifically for the area of Asopos River basin, at the region of Central Greece, since the area has been characterized as heavily Cr(VI)-contaminated. Thus, the concentration limits that have been set in the specific area as quality environmental standards are 11 μg/L Cr(VI) and 110 μg/L Cr_{tot}, while the effluent concentrations are 30 μg/L Cr(VI) and 200 μg/L Cr_{tot}.

2.3 Chromium speciation in the geoenvironment

2.3.1 Soils and rocks

Chromium is among the ten most abundant elements in the Earth (Henderson, 1982) and the 21st element in abundance in the earth's crust exhibiting a mean concentration of 100 mg/Kg. As mentioned in paragraph 2.1, chromium can be found in the geoenvironment only with its trivalent [Cr)III)] and hexavalent forms [Cr(VI)] and very rarely as elemental chromium [Cr(0)].

Cr(0) occurs as metallic inclusions in cryptocrystalline diamonds from kimberlite pipes in the Siberian Yakutia diamond deposits of Russia (Gorshkov et al., 1996). Geogenic Cr(0) also has been found in vein deposits from Sichuan, China, in meteorites such as the Agpalilik meteorite fragment from Cape York, Greenland, and as metal alloys in placer deposits (Guisewite, 2001).

Cr(III) is the most common form of chromium occurring as insoluble Cr(III) oxides (Cr_2O_3) and Cr(III) hydroxides [$Cr(OH)_3$] in several minerals. Most of the Cr(III) minerals contain Cr(III) ions in octahedral coordination with oxygen. Since the octahedral radius of Cr(III) is similar to those of Al(III), Fe(III), Ti(IV) and Mg(II) it is possible the formation of several isostructural compounds and minerals, as a result of ion substitutions between Cr(III) and the aforementioned metals in the octahedral sites. Thus the most common minerals containing chromium in their structure are chromite ($FeCr_2O_4$), Cr-magnetite and chromium mixed (Al, Mg, Fe) spinels. $FeCr_2O_4$, also called iron(II)-Cr(III) oxide, is the principal ore of chromium. $FeCr_2O_4$ is a magnetically weak, iron-black, brownish-black to silvery white mineral. $FeCr_2O_4$ is of igneous origin and forms in peridotite of plutonic rocks, occurring exclusively in mafic and ultramafic rocks as a crystal accumulated in the early stages of magmatic crystallization. $FeCr_2O_4$ in the geoenvironment is rarely pure. Theoretically it is composed by 68% Cr_2O_3, and contains 68,4% chromium, and 32% FeO. However, due to substitutions as referred above the chromium content can be reduced down to 35%. Cr-magnetite usually contains less than 15% Cr_2O_3 in its structure. Regarding spinels, the Cr content varies in each case as a function of their origin. High Cr contents reflect origin from subduction zones, while low content is indicative of abyssal origin (Motzer, 2005; Saha et al, 2011; Deschamps et al., 2013; Chrysochoou et al., 2016). In addition, Cr occurs in serpentine minerals. Serpentinite rocks are generally classified as peridotite, common varieties of which are dunite, harzburgite, and lherzolite. The major minerals are olivine, orthopyroxene, clinopyroxene, and chromite. Soils formed from serpentinite contain an

abundance of Fe, Mn, ultramafic rocks form two discontinuous bands along the Cr, Ni, and Mg, and low concentrations of Ca and K (Lee et al., 2001).

Cr(VI) rarely occurs in nature in mineral form. Cr(VI) is typically produced in nature from Cr(III)-bearing minerals as a result of chemical reactions that occur under particular conditions and thus it is usually found in secondary minerals. Chromium was firstly extracted from a rare mineral called crocoite ($PbCrO_4$). Crocoite can be found in the oxidized zones of lead deposits in regions where lead veins have traversed rocks containing chromite. Crocoite occurs only at specific regions such as Australia, Tasmania, and the Urals (Oze et al., 2004; Saha et al., 2011). In addition, Cr(VI) has been observed as chromatite ($CaCrO_4$) and Cr(VI)-ettringite ($Ca_6Al_2(CrO_4)_3(OH)_{12}24H_2O$) in the Judean desert in Israel (Sokol et al., 2011) and as barite-hashemite ($BaSO_4$-$BaCrO_4$) solid solution in the Mazarin Mottled Zone in Jordan (Fourcade et al. 2007). Generally, the presence of Cr(VI) in soils and rocks can be affected by redox reactions and sorption mechanisms rather than by precipitation and other geological reactions.

2.3.2 Groundwater

Contrary to soils and rocks, chromium is rarely found in groundwater and surface waters, except from the areas that chromium bearing deposits or significant industrialization occur. In groundwater Cr(III) occurs only at trace concentrations, since for the pH range of natural waters it forms insoluble compounds. Cr(III) can be present in soluble forms only at extremely low pH values. On the other hand, chromium typically appears with Cr(VI) forms, being soluble compounds and, thus, very mobile in groundwater. The stability of Cr(III) versus Cr(VI) species in aqueous solutions is determined by the pH and redox potential of the aqueous solution. Figure 2.2 presents the valence state and hydrolysis speciation of chromium over a range of pH and Eh values.

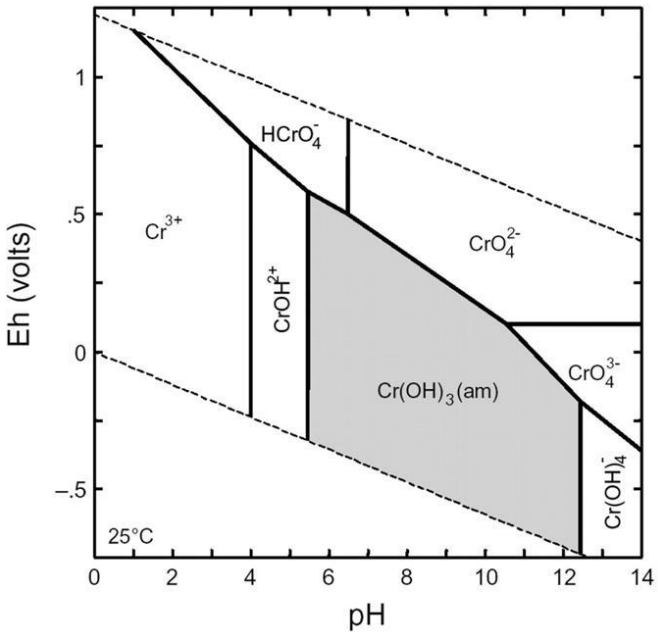

Source: (Motzer et al., 2004)

Figure 2.2 Eh-pH diagram for the chromium–oxygen–water system.

In the chromium–water–oxygen (Cr−H_2O−O) system, under standard conditions, the Cr(III) stability zone occurs over a wide Eh and pH range under both reducing to oxidizing and acid to alkaline conditions. Cr(III) generally forms soluble compounds when pH ranges between 0 and 6 and Eh between −0.3 to 1.2 V. At pH approximately equal to 8, insoluble and amorphous $Cr(OH)_3$ is formed, although small quantities of Cr(III) may be solubilized within this stability zone, while at extreme pH and reducing conditions (pH>12 and Eh<0), soluble chromium hydroxide anions [$Cr(OH)_4^-$] are formed. In aqueous environments under low Eh conditions, the main Cr(III) species are the chromic cations and $CrOH^{2+}$ (Richard and Bourg, 1991). The governing reactions in the chromium–water–oxygen system (Figure 2.2), under standard conditions (predominant in groundwater) are listed in Table 2.1, as a function of the logarithmic value of equilibrium constant (logK). Overall, Cr(III) is weakly mobile in groundwater because of the low solubility of the most common precipitates.

Table 2.1 Governing reactions in the chromium–water–oxygen system.

Reactions	logK
$Cr^{3+} + H_2O \leftrightarrow CrOH^{2+} + H^+$	-3,57
$CrOH^{2+} + H_2O \leftrightarrow Cr(OH)_2^+ + H^+$	-9,84
$Cr(OH)_2^+ + H_2O \leftrightarrow Cr(OH)_3^0 + H^+$	-16,19
$Cr(OH)_3^0 + H_2O \leftrightarrow Cr(OH)_4^- + H^+$	-27,65

Source: (Fendorf et al., 1995)

On the other hand, the Cr(VI) stability zone occurs over a much narrower range than the Cr(III) stability field as shown in the Cr−H_2O−O system (Figure 2.2). Cr(VI) species primarily occur under oxidizing (Eh>0) and alkaline conditions (pH>6). In this field, Cr(VI) generally forms soluble chromate (CrO_4^{2-}) anions from approximately pH 6 to 14 and at an Eh from approximately −0.1 V to +0.9 V (Brookins, 1987). Cr(VI) generally occurs as soluble dichromate ($Cr_2O_7^{2-}$), bichromate ($HCrO_4^-$) and chromate (CrO_4^{2-}) anions. Figure 2.3 shows the predominance diagram for the three species as a function of chromium concentration and pH.

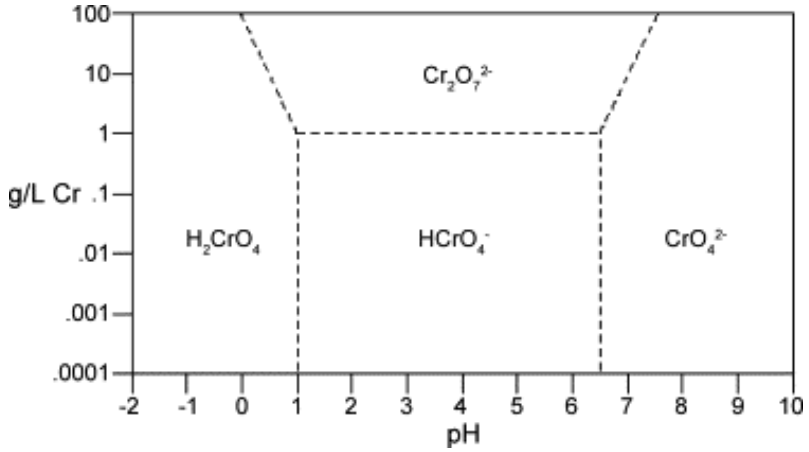

Source: (Dionex, 1996)

Figure 2.3 Predominance diagram for Cr(VI) complexes**.**

2.4 The origin of chromium in the geoenvironment

2.4.1 Anthropogenic chromium

High levels of Cr(VI) in the environment are mainly attributed to various anthropogenic factors, like the wide use of chromium in the chemical industry and inadequate practices of waste management, leading to groundwater contamination (Dermatas et al., 2012). Leakage accidents or inability to properly store highly Cr(VI)-contained wastes may also cause contamination of natural waters (Zazo et al., 2008).

Chromium is used in several industrial processes (Table 2.2) such as chromium plating, leather tanning, metal finishing and paint production. It is also used in the manufacturing of varnishes for wood preservation, of welding materials, of anticorrosion coatings for metallic surfaces and of pigments for paints, inks and plastics. Cr(VI) usage has been also referred at the cement industry as well as an inhibitor of corrosion in refrigerated cooling pipes at power plants (Fendorf, 1995; Saha et al., 2011). In the past, common practice for waste management related with plating operations, and thus containing primarily Cr(VI), was their disposal into dry wells. Nowadays, wastewater containing Cr is either treated on-site or at centralized wastewater treatment plants.

Table 2.2 Anthropogenic Cr(VI) sources.

Applications	Chemical forms
Pigments (paints, inks, plastics)	Lead chromate, zinc chromate, barium chromate, calcium chromate, potassium dichromate, sodium chromate
Anti-corrosion coatings	Chromic trioxide, zinc chromate, barium chromate, calcium chromate, sodium chromate, strontium chromate
Stainless steel	Cr(VI) produced by steel's casting, welding or plasma torch cutting
Textile dyes	Ammonium dichromate, potassium chromate, sodium chromate
Wood preservatives	Chromium trioxide
Leather tanning	Ammonium dichromate

Source: (Saha et al., 2011)

The treatment of Cr-containing wastewater, creates another important potential chromium source, the wastewater sludge. Chromium derived from either domestic or industrial sources can concentrate in the sludge produced at treatment facilities. Although total removal of Cr(III) from wastewater sludge can be achieved in such facilities, this is not the case for Cr(VI) for which the percentage removal ranges between 26 and 48%, since only a part of Cr(VI) is reduced by the organic matter contained in the sludge and the remaining forms compounds with the Cr(VI) species (Saha et al., 2011).

In addition, a significant amount of Cr presented in soils can be related with land surface disposal of coal and fly ash. Disposal of large quantities of such waste can lead to elevated Cr concentrations relatively to these occurring naturally (McGrath and Smith, 1990). Cr can also be found in the drains of landfills (leachates) (Kotaś and Stasicka, 2000). Thus, aquifers contamination with Cr(VI) and other heavy metals can be caused by direct infiltration of landfill

leachate disposal of solid wastes, wastewater, or wastewater sludge. The concentration of Cr(VI) in wastes derived from the human activities described above may be 0.5 - 270,000 mg/L (Chiha et al., 2006).

Apart from industrial origin, anthropogenic chromium may be presented in the geoenvironment as a result of extensive agricultural activities. Fertilizers, limestone and animal manure are extensively applied at several agricultural uses. The presence of chromium in these materials has been of important concern the last decades. Fertilizers can be firstly divided into organic and mineral fertilizers. High concentrations of chromium, and other heavy metals, may be present naturally in mineral fertilizers, which usually come from mine extraction. Organic fertilizers containing Cr originate from a wide range of products such as organic amendments, limestone, sewage and tannery sludge and mineral fertilizers. Among them, tannery sludge fertilizers are widespread used since exhibit good agronomic behavior due to their high content of organic carbon (38% - 50%) and N (8% - 13%). However, the percentage of Cr, and other heavy metals, contained in the fertilizer depends on the origin of fertilizer and the production process (Chaney et al., 1997; Kabata-Pendias and Pendias, 2011; Ciavatta et al., 2012). The highest Cr concentrations have been observed in organic fertilizers with phosphates. The National Research Council of Canada (1976) reported chromium concentrations in phosphate fertilizers ranging at 30 – 3000 mg/kg. This wide range of chromium concentrations contained in fertilizers indicates that the amount contained in such fertilizers is in many cases higher that the concentrations observed in soils (McGrath and Smith, 1990; Ciavatta et al., 2012). As regarding limestone, chromium concentrations have been reported in the range of 1 to 120 mg/kg (average 10 mg/kg), while manure is poor in chromium (Saha et al., 2011).

By legislative terms the effect of Cr-contained fertilizers application is still controversial since in many cases the maximum admissible levels addressed do not take into account any scientific and experimental evidence. The most important issue is that legislation does not distinguish the oxidation state of chromium, considering both Cr(VI) and Cr(III) states as hazardous. In the EU and USA Cr-containing fertilizers are of unlimited use, while in some other countries, in order to prevent any environmental or human health risk, thresholds have been determined in terms of Cr_{tot} concentrations. However, there are no legislations referred to Cr(VI) content and only EU tends to determine limits for several heavy metals concentrations, among them Cr(VI), setting the limit at 2 mg/Kg Cr(VI) on dry matter basis (EC, 2003; EU, 2009; EC, 2010; USEPA, 2010). With respect to the presence of Cr(VI) in Cr-fertilizers, Sager (2005) and Kruger et al (2017) investigated the extractability of Cr(VI) from basic slags used as fertilizers and from soils treated with 20% (dry mass) basic slags. Extraction of the Cr(VI) fraction using as extractants several chemicals, such as NH_4NO_3, phosphate buffer, ammonium sulfate, borate buffer, saturated borax and polyphosphates was performed. The results showed that the basic slag contained appreciable amounts of Cr(VI) and its extraction was a function of the extractant's pH, the extractant's concentration and the liquid to solid ratio used. The extraction efficiency increased depending on the kind of extractant with the following order: borate < sulfate < nitrate < phosphate. In the case of adding the basic slag in the soil, the Cr(VI) amount was much lower indicating possible reduction (Sager, 2005). In another study, Kruger et al (2017) investigated Cr(VI) extraction from several materials used as fertilizers and soil amendments,

such as sludges, sewage sludge ashes, slags and mineral fertilizers by applying a wet extraction method (DIN EN 15192) based on alkaline digestion of Cr(VI). They observed that the Cr(VI) concentrations extracted were lower than the legislation limit of 2 mg/Kg except for the case of using Na_2CO_3-treated sewage sludge ash, which contained 12.3 mg/kg Cr(VI), concluding that no release of Cr(VI) occurs using such materials as fertilizers (Kruger et al., 2017).

Several other studies have tried to determine the possible risk created by the application of Cr-containing fertilizers either by determining the extractability of chromium from fertilizers or by testing the adverse effects on plants due to chromium accumulation in soils. In order to define the levels of heavy metals that may be extracted by biosolids and fertilizers USEPA applied 14 extraction cycles concluding that there are no environmental or health and safety risks by the application of such materials (Sequi et al., 1997). However, Sorensen et al. (2011) investigating the possible risks by the application of mineral fertilizers, reported that no risk exist for short-term applications of fertilizers if the cut-off values for Cr(VI) concentrations in fertilizers is under the proposed limits. In particular no risk observed by using fertilizers with chromium concentration under the limit in annual basis since the chromium concentration measured in soil corresponded to 0.2% of its natural concentration. On the contrary, for long-term use the risks that may occur cannot be ruled out for all the types of soils, since the cut-off value refers only to Cr(VI) concentrations and not to Cr(III), rendering thus impossible the assessment of chromium accumulation effects. Thus the proposed limits might be reconsidered in the case of using mineral fertilizers taking into account not only chromium concentration but also nickel and lead concentrations (Sorensen et al., 2011). Long-term field applications were performed by Watanabe et al (1984) in order to investigate the chromium accumulation in soils and the possible toxicity at plants when using two types of soil amendments: a) Cr-fertilizers containing also N, phosphorus (P) and potassium and b) silicate and liming materials. The chromium content in the untreated soils ranged from 10 to 150 mg/Kg and after the addition of fertilizers an increase of chromium content about 20-50 mg/Kg was observed only in the cases of using calcium silicate and fused magnesium phosphate as soil amendments. Chromium was transferred vertically being extensively distributed in the surface/subsurface soils and less to subsoils. Only in rare cases chromium was detected deeper than subsoils. Regarding toxicity phenomena at plants no effects were observed indicating generally that fertilizers with chromium contents about 0.14% cannot be considered as anthropogenic chromium sources in cultivated soils. Two other studies performed by Ciavatta et al., (1989) and Grubinger et al, (1994) aimed at determining the release of chromium and the possible toxic effects on plants, respectively, by the application of tannery meal fertilizer. In the first study the results showed that chromium was continuously released from the fertilized as a result of the humification process, which decomposed the organic matter but chromium was transformed immediately to the insoluble Cr(III). From the released chromium no Cr(VI) was detectable were measured even after spiking Cr(VI) solution in the tested soil, indicating thus that there is not any important agronomic or environmental effect by the usage of tannery meal fertilizers at low rates as performed in real applications. Similar results were observed by Grubinger et al, (1994) since the presence of chromium in the fertilizer (5900 mg/Kg) containing tannery meal did not affect the growth of plants when used in low rates (adding 5% of the fertilizer in the soil). However, increasing the percentage of fertilizer added to soil at 10 and 15% the increase of chromium amount in the plants was obvious.

As it can be concluded by the above studies, the application of Cr-fertilizers cannot contribute to the increase of Cr(VI) in soils but only to the amounts of Cr(III). Thus any possible risk can be created by the Cr(III) oxidation caused by oxidative factors of soils. The possible oxidative factors for Cr(III) will be discussed in the following paragraphs. However, the oxidation of Cr(III) species contained in such materials has been proved to be a much slower process compared to geologic Cr(III).

2.4.2 Geogenic chromium

As mentioned in paragraph 2.3.1 chromium occurs naturally in the geoenvironment, with the most common minerals containing chromium in their structure being chromite ($FeCr_2O_4$), Cr-magnetite and chromium spinels. In the Earth's crust, chromium is concentrated in ultramafic rocks and serpentinites of ophiolitic complexes, which constitute 1% of the terrestrial landscape. Ultramafic rocks and their serpentine soils occur in several areas globally (Figure 2.4) indicating the presence of high chromium concentrations even in populated areas within the Circum-Pacific margin and the Mediterranean (Brooks, 1987; Coleman and Jove, 1992). Weathering of such rocks is of the main reasons for chromium presence in soils and groundwater as it will be discussed at the following paragraphs.

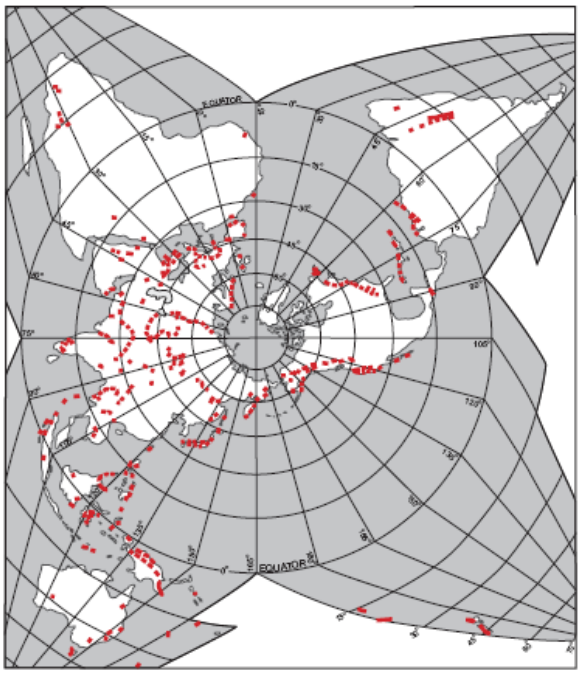

Source: (Oze et al., 2007).

Figure 2.4 Global distribution of serpentinites and ophiolites (red dots) as presented by north polar projection.

2.4.2.1. Natural occurrence of chromium in soils and rocks

The natural occurrence of chromium in the geoenvironment is commonly associated with the presence of ultramafic igneous and metamorphic rocks, like peridotites and serpentinites, and their derived soils, and rarer with the presence of mafic rocks and their weathering products

(Figure 2.5). Granite, carbonates and sandy sediments present the lowest chromium content. Generally, chromium concentration in soils and rocks is influenced by the composition of the parent rock.

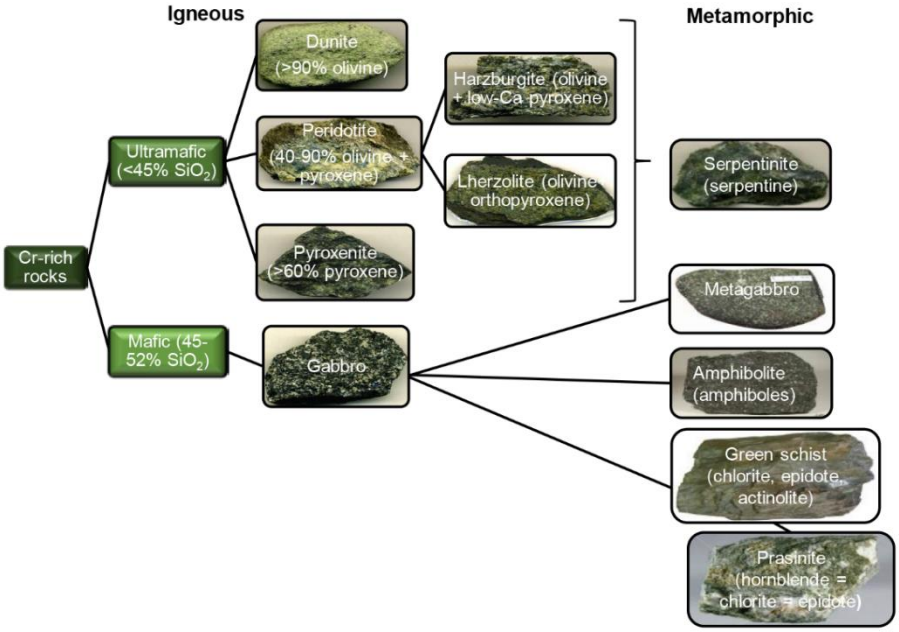

Source: (Chrysochoou et al., 2016)

Figure 2.5 Classification of Cr-rich rocks according to their chemical and mineralogical composition.

The predominance of the Cr-bearing minerals presented in Figure 2.5 depends on the weathering phase of the rock. The average chromium concentration in rocks and soils of ultramafic origin is estimated to 2200 and 2650 mg/kg, respectively (Chrysochoou et al., 2016). Ultramafic rocks have low silica and high magnesium contents, and are composed of olivine and pyroxene (primary minerals). The hydration of such minerals under low temperature and pressure is a process called serpentinization and leads to the formation of metamorphic rocks, the serpentinites. Serpentinites are composed by minerals such as lizardite, antigorite, and chrysotile, which further contribute to the formation of serpentine soils. Such soils are usually characterized by high concentrations of nickel and cobalt, apart from chromium (Roberts and Proctor, 1992; Bulmer et al., 1994). During serpentinization serpentine minerals and also magnetite has been found to incorporate significant amounts of chromium in their structures, usually by isomorphic substitutions. One of the most common substitution is that between Cr(III) and Fe(III) due to the similar size and charge of these species. However, serpentinization is a process that does not affect Cr-spinels, which exhibit high resistance to such metamorphic processes. One of the most common primary spinels in ultramafic (and sometimes in mafic) rocks is chromite, which is the most common chromium mineral, as aforementioned. Though chromite exhibits resistance in serpentinization it is highly affected by the occurrence of isomorphic substitutions. These substitutions usually take place between Al^{3+}, Fe^{3+} and Ti^{4+} in the octahedral sites and Mg^{2+}, Ni^{2+}, Zn^{2+} and Mn^{2+} in the tetrahedral sites. In addition, isomorphic substitutions between Cr(III) and Fe(III) is a common phenomenon during hydrothermal and CO_2 metasomatism of ultramafic rocks, which leads to the formation of Cr-silicate minerals. Substitutions of Al(III) and Cr(III) is preferable since these species exhibit

similarities in charge, octahedral preference and radius with a representative example of mineral that undergoes this substitution being chlorite. Thus, silicate minerals can be thought as chromium sources due to the weathering of serpentinites (Oze et al., 2004). At this point, it must be mentioned that chromium accumulation in minerals formed by serpentinization contain chromium only in its trivalent state. Minerals that contain Cr(VI) in their structure, like crocoites ($PbCrO_4$), are found extremely rare in serpentinites and occur only at specific areas worldwide as mentioned in paragraph 2.3.1.

Contrary to ultramafic rocks, mafic rocks, such as gabbro, are characterized by higher silica and lower magnesium concentrations. However, minerals of mafic origin, such as chlorite and amphiboles, are commonly associated with those originated from ultramafic rocks and are richer in chromium compared to the average chromium content (35 mg/kg) that occurs in the Earth's crust (Alloway, 2013). Chrysochoou et al. (2016) reported that, according to global literature, chromium concentration in such rocks is about 1,100 mg/Kg. This concentration can potentially be increased significantly in cases that mafic rocks are in existence with ophiolitic complexes as has been observed in areas like Italy, Poland and USA (Mojave Desert) (Chrysochoou et al., 2016).

As mentioned above the mean chromium concentration in ultramafic soils is about 2,650 mg/Kg. However, this value can exhibit high variability due to the different geological processes occurring and the different soils mixed with the weathering phases of ultramafic rocks. Thus chromium concentrations of less than 1000 mg/Kg and slightly above 3,000 mg/Kg have been detected globally (Chrysochoou et al., 2016). This variability is strongly related with the weathering rate of ultramafic rocks (Becquer et al., 2006; Caillaud et al., 2009; Fandeur et al., 2009). Except for the accumulation of chromium in soils, the weathering process has also been related with the vertical distribution of chromium in soils. In particular, chromium concentrations exhibit decreasing trend with increasing depth up to 5 m depth, as showed in several cases like soils in USA and Canada (Oze et al., 2004), New Caledonia (Becquer et al., 2006), Brazil (Garnier et al., 2006) and France (Caillaud et al., 2009). This decreasing trend of chromium is attributed to the fact that immobile elements like chromium, iron and aluminum are accumulated near the soil surface. However, this trend is thought not to exist in higher depths where an increase of chromium concentration may occur since other factors like the origin of the parent rock and the weathering stage seem to be predominant (Dzemua et al., 2011). Finally, several studies have tried to interpret the behavior of chromium concentration longitudinally (Bonifacio et al., 1997; Garnier et al., 2006; Cheng et al., 2011) but in this case contradictory results were obtained indicating that chromium concentration in this case is not only affected by the mineralogy and the weathering processes but also from the impact of climate and topography of the tested areas. Table 2.3 presents an overview of the mean concentrations of total chromium in soils and rocks of ultramafic/ophiolitic origin globally, giving also information about the depth and the type of soils that these concentrations were detected.

Table 2.3 Overview of chromium concentrations in soils and rocks of ultramafic/ophiolitic origin globally

A/A	Area	Medium	Depth (m)	Cr_{tot} (mg/Kg)	Analytical method	Reference
1	New Caledonia	Hypermagnesian brown soil	0.2	19,000	DTPA & AAS	Amir and Pineau, 2003
		Ferralitic oxidic soil		124,500		
		Ferrallitic oxidic colluvial soil		30,700		
		Saprolite		2,800		
2	New Caledonia	Highly weathered and strongly desaturated soil on the piedmont	0 – 0.57	20,526 – 21,211	diacid digestion (2:1 HNO_3:HCl ratio) & ICP-AES	Becquer et al., 2003
		Colluvio-alluvial soils with some poorly weathered silicates	0 – 0.51	18,474 – 19,158		
		Alluvial soils subject to temporary water logging on terraces	0 – 0.39	13,684 – 21,895		
3	New Caledonia (soils from the lateritic weathering products of ultrabasic rocks)	Backslope	38 – 57	23,947	digestion with LiBo & ICP-MS	Becquer et al., 2006
		Colluvial	40 – 51	23,947		
		Alluvio-colluvial	26 – 39	26,000		
4	north-western Italy	Soil summit	0 – 0.12+	3,146 – 3,967	HCl-HNO_3 & HF digestion and AAS	Bonifacio et al., 1997
		Soil backslope	0 – 0.18+	3,421 – 4,653		
		Soil footslope	0 – 1.65+	2,326 – 8,552		
		Soil toeslope	0 – 0.75+	958 – 1,095		
5	North-western Italy	Soil (Entisols and inceptisols)	Horizon A	822	HCl-HNO_3 and HF digestion & AAS	Bonifacio et al., 2010
			Horizon AC	1,074		
			Horizon Bw	378		
			Horizon C	745		
6	southwestern British Columbia	Ultramafic soil	0 – 0.70	28 - 209	dithionite-citrate-bicarbonate extraction & ICP-AES	Bulmerl and Lavkulich, 1994
		Ultramafic soil	0 – 0.70	17 – 44	Ammonium oxalate extraction & ICP-AES	

7	Northwestern Spain	chloritized veins in serpentinites	n.a.	137 - 11,837	XRF	Buurman et al., 1998
8	France (serpentinites)	rock	>1.4	2,262	LiBr and HCl & after ICP-MS	Caillaud et al., 2009
		soil	1 – 1.4	5,812 – 8,675		
		Soil	0.6 – 1	6,756 – 7,466		
9	France (Vosges Mountains ultramafic toposequence)	soil (Hypermagnesic Hypereutric Cambisol)	0 – 0.6	2,350 – 2,490	dithionite–citrate–bicarbonate (DCB) extraction & ICP-AES	Chardot et al., 2007
10	eastern Taiwan	soil over serpentine regolith	0 – 1.5	1,060 – 1,663	Sequential extraction & FAAS	Cheng et al., 2011
11	western Alps (Natural Park of Mont Avic, Aosta Valley, Italy)	soil from glacial till composed of serpentinite & metagabbros, amphibolites, prasinites and chlorite schists	0 – 0.5	900 – 2,300	$BaCl_2$ extraction & FAAS	D'Amico et al., 2008
		soil composed of serpentinite with traces of prasinites, amphibolites and chlorite schists		1,700 – 2,800		
		serpentinite till lying on a hard, unweathered serpentinite bedrock		1,400 – 1,900		
12	south-east Cameroon	soil	<10	705 – 6,000	acid digestion & ICP - MS	Dzemua et al., 2011
		soil	10 - 20	8,848 – 10,620		
		soil	>20	16,070		
		serpentinitic rock		1,437		
13	New Caledonia	bedrock (unweathered peridotite)		2,053	alkali fusion with lithium tetraborate & ICP-OES	Fandeur et al., 2009
		soil	1.6	9,578		
		soil	0.8	13,684		
		soil	0.1	15,052		
14	central Eastern Desert, Egypt	rock (serpentinites)		2,463 – 5,337 serpentine	n.a.	Farahat, 2008

				6,883 - 11,084 chlorite		
15	Niquelandia, Brazil	soil	0 - 1.2	5,000 - 8,000	acid digestion & ICP-AES	Garnier et al., 2006
16	(eastern Alps Swiss)	soil	max 0.9	312 – 2,912	XRF	Gasser et al., 1995
		soil	max 0.54	676 – 2,808		
		soil	max 0.6	676 – 3,224		
17	(SW Poland)	rock (serpentine with mesh texture)	n.a.	2,397	XRF	Gunia et al., 2000
18	Taiwan (serpentine mining site)	soil	11 - 27	443 - 894	HF - HNO_3 - $HClO_4$ digestion & FAAS	Ho et al., 2013
19	eastern Taiwan (Tong-An Mountain, comprising serpentinitic rocks)	soil from summit	0 – 0.9	1,550 – 3,100	HF - HNO_3 - $HClO_4$ - H_2SO_4 & FAAS	Hseu, 2006
		soil from shoulder	0 – 2	1,700 – 2,720		
		soil from backslope	0 – 3	200 - 420		
		soil from footslope	0 – 3	440 – 1,180		
20	western Mojave Desert, USA	rock	n.a	1,020	EDXRF	Izbicki et al., 2008
		rock		155	digestion & ICP-OES	
21	Bavaria	soil	n.a	725	Sequential extraction	Kaupenjohann et al., 1995
22	Poland	soil horizon A fine fraction	n.a.	2,805	LiBo digestion & ICP-AES	Kierczak et al., 2007
		soil horizon A coarse fraction		3,147		
		soil horizon A/C fine fraction		3,079		
		soil horizon A/C coarse fraction		3,763		
		rock		3,900		
23	USA (serpentinitic Wetland & Surrounding Landscape)	soil	0 – 0.15	75 – 240	dithionite & ICP-OES	Lee et al., 2001
24	northern California, USA (serpentinitic landslide)	soil	0 - 2	2,100	aqua regia and ICP	Lee et al., 2004
25	northern California, USA	rock	-	2,262	4-acid digestion & ICP-	Morrison et al., 2009

		soil	0.15	4,464	AES	
26	California	soil	0,01 - 0,135	1,725 – 4,760	acid digestion & ICP-AES	Oze et al., 2004
		bedrock serpentinite		580 – 2,280		
27	Northwest Spain	soil over peridotite	0 – 0.20	546	Aqua regia & AAS	Paz-Gonzalez et al., 2000
28	Cuba (moa-baracoa ophiolitic massif)	uvarovite (serpentinized ultrabasic rocks)	n.a.	49,947 – 115,630	Microprobe analyses	Proenza et al., 1999
29	Sources and extractibility of chromium and nickel in soil profiles developed on Czech serpentinites	soil (over ultramafic bedrock)	0 – 0.8	315 – 1,880	sequential extraction & ICP-AES	Quantin et al., 2008
		bedrock	n.a.	1,802 – 3,206	acid digestion & ICP-AES	
30	Pennsylvania (Maryland Soils from serpentinite)	Serpentinitic soil	0 – 1.7	1,000 – 6,000	acid digestion & ICP-AES	Rabenhorst, 1982
31	Leon Valley, Mexico	rock	n.a.	265 – 4,115	acid digestion & FAAS	Robles-Camacho and Armienta, 2000
32	Albania (serpentines)	Serpentinitic soil	0.15	365 – 3,865	HNO_3/H_2O_2 & ICP-AES	Shallari et al., 1998
33	Albania	soil (ophiolite complex consists of a sequence of altered ultramafic formations)	0 – 0.1	843 – 3,385	acid digestion & AAS	Shitza et al., 2005
		litho-serpentinite	-	1,525 – 1,725		
34	East Africa	soil (laterites developed on peridotites)	0 - 12	5,000	fusion at 110^0C with Na metborate and HCl and ICP-AES/ XRF in the residual	Trolard et al., 1995
			12 - 20	16,507		
			20 - 40	4,730		
			33 - 69	7,300		
35	south-east Cameroon (laterite cover on serpentinites)	soil (summit)	16 - 46	5,474 – 13,684	Extraction and ICP-AES	Yongue Fouateu et al., 2006
		soil (top slope)	10 - 22	1,505 – 14,984		
		soil (middle slope)	16 - 23	2,121 – 12,316		
		soil (base slope)	14 - 20	13,889 – 18,953		
36	Sri Lanka (Ussangoda Ultramafic Complex)	soil	n.a	11,352	Aqua regia & AAS	Rajapashka et al., 2012

37	Sri Lanka (Ussangoda ultramafic coast)	soil	n.a.	11,031	XRF	Vithanage et al., 2014
38	Mouriki-Thiva Area, Central Greece	Surface soil samples related to ultrabasic rocks	0.1	277	digestion with hot aqua regia & FAAS	Antibachi et al., 2012
39	Greece (Pindos ophiolite complex)	chromite rock	n.a.	19,773 – 623,687	Electron microprobe	Al-Boghdady and Economou, 2005
40	Asopos basin, Greece	Soil (related to ultramafic rocks)	0.20	67 - 200	aqua regia and ICP-MS	Economou et al., 2011
41	Korinthos, Greece (ultrabasic rocks & Neogene & Quaternary deposits)	soil	0.1	920	digestion, ICP-ES	Kelepertzis et al, 2001
42	Thiva Valley (central Greece)	rock	2	3,100 – 3,200	XRF	Kelepertzis et al, 2013
		soil over rock	0.2 - 2	2,440 – 3,440	XRF	
		topsoil	0.2	max 856 (median 299)	aqua regia & AAS	
43	central Euboea, Greece	soil	0.2	1,300	aqua regia & GFAAS	Megremi, 2010
44	Agia, Thessaly, Greece	Soil (related to ultrabasic rocks)	0.1	40 – 2,500 (300 mean)	acid digestion & ICP-AES	Skordas and Kelepertzis, 2005

n.a.: not available

As it can be observed from Figure 2.4, ophiolitic complexes are extensively presented in Europe and in particular in Balkans. Figure A1.1 presents a better picture of chromium distribution in Europe in both subsoils and topsoils. As shown from this figure, Greece is one of the European countries with high presence of ophiolitic complexes in various areas. Greek ophiolitic complexes are located on the Mirdita Sub-Pelagonian and Pelagonian geotectonic zones of the Balkan Peninsula, extended from Albania to Northern and Central Greece and into the Anatolides zone of western Turkey (Figure 2.6) (Eliopoulos et al., 2012)

Source: (Kaprara et al., 2015)

Figure 2.6 Ophiolites presence in Greece.

More specifically the chromium deposits in Greece occur in ophiolite complexes, within upper mantle rocks (peridotite, dunite). The formation of ophiolitic complexes is attributed to the convergence of two oceanic crusts where the higher part is destroyed and the rest one comes to the surface. The presence of ophiolites in Greece can be distinguished in two parallel lines along Greek geological background oriented from northwest to southeast. The main areas with intensive occurrence of ophiolites and ultramafic rocks are located in Pindos, Vourino, Othris, Euboea, while less extensive occurrence has been reported in Kastoria, Koziakas, Vermio, East Thessaly, Oiti and Argolida (Kaprara et al., 2015 and references therein).

2.4.2.2. Natural occurrence of chromium in groundwater

Despite Cr(III) is the most common chromium state in soils, in natural waters occurs only in traces (unless at extremely low pH). The most common form of chromium in naturals waters and thus in groundwater is Cr(VI). As mentioned in paragraph 2.3.2., in the pH range that

usually occurs in groundwater and under oxidizing conditions, Cr(VI) exists mainly with its anionic form, chromates (CrO_4^{2-}).

The occurrence of Cr(VI) in groundwater, in areas where anthropogenic contamination is excluded, is strongly related with the presence of ultramafic rocks and ophiolitic complexes. Minerals such as peridotites, chromite and serpentinites have been detected in aquifers with important Cr(VI) concentrations, since the process of serpentinization creates an oxidizing environment and leads to alkali pH values in groundwater, conditions that enhance the oxidation of Cr(III) (Fantoni et al., 2002, Oze et al., 2007, Economou-Eliopoulos et al., 2011, Moraetis et al. 2012, Megremi, 2013, Kaprara et al., 2015). The release of Cr(VI) in groundwater is a result of sequential processes at which Cr(III) in host minerals is firstly dissolved, then sorbed on the soil surfaces at which it is oxidized by natural oxidants such as high valence manganese oxides (a more analytical description of natural oxidants for Cr(III) will be given at the following paragraphs) and finally desorbed in groundwater as Cr(VI). Cr(VI) concentrations in the range 0.2 - 180 μg/L in aquifers affected by ultramafic rocks and ophiolitic complexes have been reported in several areas worldwide, exceeding in many cases the limit of 50 μg/L of Cr_{tot} as established by WHO. Table 2.4 presents an overview of the maximum chromium concentrations and the corresponding Cr(VI) concentrations in groundwater, attributed to the presence of ultramafic/ophiolitic geological background in several areas worldwide.

Table 2.4 Overview of Cr_{tot} and Cr(VI) concentrations in groundwater at aquifers related to ultramafic/ophiolitic geological background

A/A	Area	Depth (m)	max (Cr_{tot}) (μg/L)	Analytical method	Cr(VI) (μg/L)	Analytical method	Reference
1	Western Mojave Desert, California	n.a	60	GFAAS	60	FAAS	Ball and Izbicki, 2004
2	Northern California, USA	n.a	50	ICP-MS	50	n.a	Morrisson et al., 2009
3	La spezia Province, Italy)	n.a	73	ICP – OES	73	1,5–DPH	Fantoni et al., 2002
4	Aromas Red Sands, California	76	39	GFAAS	30	GFAAS	Gonzalez et al., 2005
5	Southern Italy	n.a	36	ICP-MS	26	ICP–MS	Margiotta et al., 2012
6	Leon Valley, Mexico	n.a	14.9	FAAS	8	1,5–DPH	Robles-Camacho and Armienta, 2000
7	Calabria National Perk, Sila Piccola, Italy	n.a	10	ICP-MS	<10	1.5-DPH	Apollaro et al., 2011
8	Tuscany, Italy	n.a	49	ICP-OES	49	HPLC/ICP-MS	Lelli et al., 2014
9	Sacramento Valley, California, USA	31-87	46	n.a.	46	n.a	Manning et al., 2015
10	Central California Coast Range Serpentinite Belt	Spring	49	ICP-MS	52	Modified DPH	McClain and Maher, 2016
11	SW Sacramento Valley, California	17-26	n.a.	n.a.	180	ICP-MS	Mills et al., 2011
12*	Thiva, Central Greece	n.a.	29	ICP – OES	25	1,5–DPH	Panagiotakis et al., 2015
13*	Central Euboea, Greece	5 - 180	130	GFAAS	128	1,5–DPH	Megremi, 2010
14*	Asopos basin, Greece	180 - 200	180	GFAAS	180	1.5-DPH	Economou - Eliopoulos et al., 2011
15*	Thiva, Central Greece	n.a	220	GFAAS	212	1.5-DPH	Tziritis et al., 2012

n.a: not available

*: In these cases despite the occurrence of ultramafic geological background the anthropogenic contamination could not be excluded.

As observed from Table 2.4 there are several areas globally at which the presence of ultramafic/ophiolitic is strongly related to Cr(VI) concentrations in groundwater exceeding the WHO maximum contaminant level of 50 μg/L Cr_{tot} in drinking water. Cr(VI) concentrations in such aquifers ranges between 0.2 and 180 μg/L. A more detailed look at these studies proves an interesting correlation between Cr_{tot} and Cr(VI), since Cr(VI) fraction corresponds to a percentage higher than 80% of Cr_{tot}. In addition, Cr(VI) concentrations attributed exclusively to the presence of ultramafic/ophiolitic formations exhibit high variability and as it can be observed from Table 2.4 they do not exceed 100 μg/L regardless the geochemical conditions of the aquifers.

Especially for Greece, the concentrations of Cr(VI) up to 212 μg/L detected are linked with the presence of ultramafic and ophiolitic complexes in the studied areas but the low contribution of anthropogenic activities that could enhance the Cr(VI) presence cannot be excluded either. A more detailed representation of Cr(VI) concentrations distribution in Greek aquifers is given at Figure 2.7.

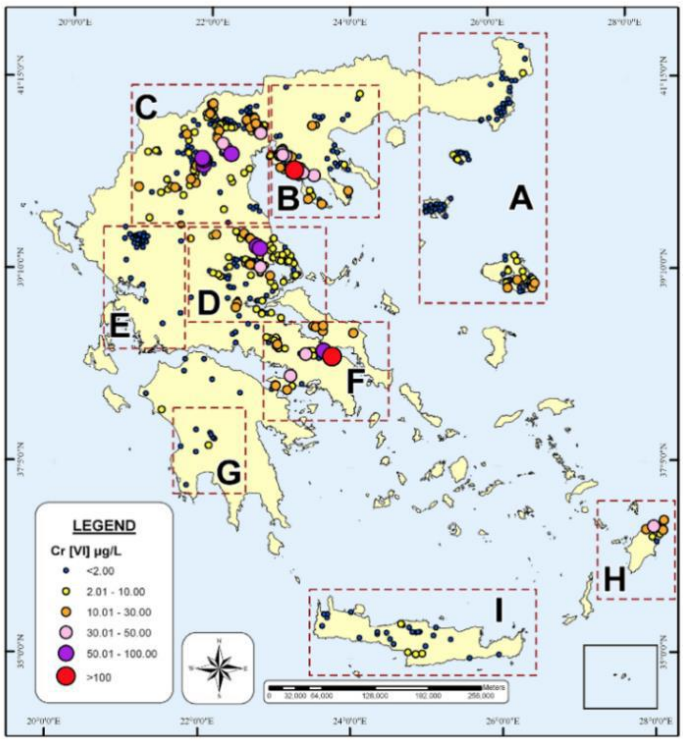

Source: (Kaprara et al., 2015)

Figure 2.7 Cr(VI) concentrations in groundwater in Greece.

As it can be generally concluded, weathering of ultramafic rocks has been linked to the occurrence of elevated concentrations of Cr(VI) in soils and groundwater. The highest chromium contents tend to be associated with finest grain size soils indicating a great variety of chromium concentrations in the geoenvironment (Stanin and Pirnie, 2004). As regarding Cr(VI) in groundwater the distinction between geogenic concentrations and anthropogenic contamination is critical for public health and for applying the appropriate decontamination actions.

2.5 Physicochemical processes affecting chromium transport in geoenvironment

The processes that control Cr(VI) transport in geoenvironment are oxidation/reduction, adsorption/desorption and precipitation/dissolution reactions **(Figure 2.8).** In the following paragraphs these processes will be described in more detail.

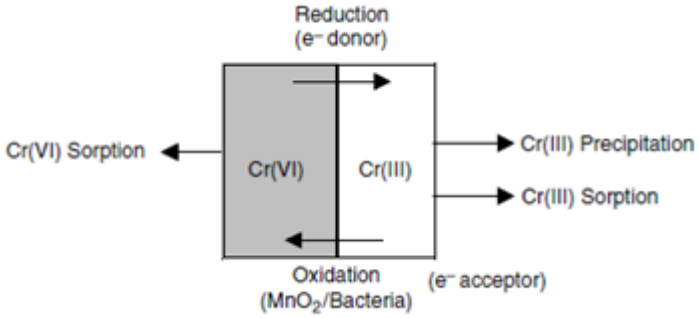

Source: (Hawley et al., 2004)

Figure 2.8 Chromium reactions in the geoenvironment

2.5.1 Redox reactions

Redox reactions is the factor that determines the distribution between Cr(III) and Cr(VI). The oxidation of Cr(III) or the reduction of Cr(VI), can only take place in the presence of another redox couple, able to accept or give, respectively, the three necessary electrons. In natural aquatic environments the main significant redox couples are: a) $H_2O/O_2(aq)$, b) Mn(II)/Mn(IV), c) NO_2/NO_3, d) Fe(II)/Fe(III), e) S^{2-}/SO_4^{2-} and f) CH_4/CO_2 (Richard and Bourg, 1991). In the following sections the various oxidants (electron acceptors) and reductants (electron donors) of Cr(VI) that are encountered in the environment are described.

2.5.1.1. Oxidation of chromium

Oxidation of Cr(III) to Cr(VI) represents a significant environmental hazard, since chromium is transformed from a harmless state into a toxic one. However, due to the fact that the redox potential of the Cr(VI)/Cr(III) couple is very high (0.6 V), only few oxidants are able to oxidize Cr(III) in geoenvironment, as will be described below.

Manganese oxides is the most common and strongest oxidant of Cr(III) in the geoenvironment (Fandeur et al., 2009). Particularly, mixed-high-valence Mn(IV/III)-oxides, such as birnessite (Fendorf and Zasoski, 1992), pyrolusite, and cryptomelane (Eary and Rai, 1987) as well as hausmannite ($Mn^{2+}Mn^{3+}{}_2O_4$) and manganite ($Mn^{3+}OOH$) (Cooper, 2002), which are presented usually as coatings on soil/rock grains, have been referred as potential oxidants for Cr(III). Bartlett and James (1979) were the first who observed that Cr(III) was oxidized to Cr(VI) more readily in soils with high elemental manganese contents than in other soils. The oxidation of Cr(III) by manganese oxides is reported to be a relatively rapid process. The high adsorption capacity of manganese oxides for metal ions provides surface localities at which the coupled

processes of the oxidation of aqueous Cr(III) and the reduction of manganese oxides can potentially occur (Apte et al., 2006). In this way the oxidation reaction would occur in the following four steps proposed (Manceau and Charlet, 1992) and represented schematically in Figure 2.9:

i. Adsorption of Cr(III) onto Mn oxide surface sites,
ii. Diffusion of Cr(III) into Mn(IV) vacancies in the MnO_6 octahedra sheet,
iii. Oxidation of Cr(III) to Cr(VI) by Mn(IV),
iv. Desorption of the reaction products Cr(VI) and Mn(II)

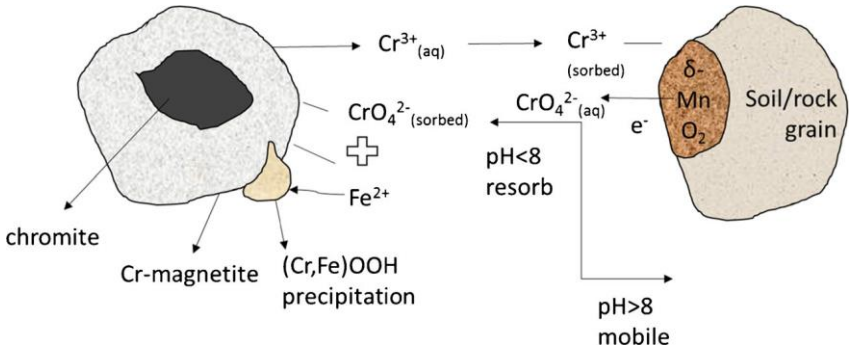

Source: (Chrysochoou et al., 2016)

Figure 2.9 Cr(III) oxidation by manganese oxide considering chromite as the host mineral.

Low solubility of Cr(III) compounds is the limiting factor of the oxidation reaction. Cr(VI) formation is affected by Cr(III) dissolution rate in the presence of manganese oxides. One of the most important parameters able to control the oxidation reaction is the pH values of the soil solution. Chen et al. (1997) suggested that pH affects the oxidation process in two opposite ways. On one hand, the pH increase contributes to the formation of negative charge at the surface of manganese oxides promoting, thus, adsorption and then oxidation of Cr(III). On the other hand, the pH increase enhances complexation and precipitation of Cr(III) with the hydroxyl anions (OH^-), impairing the oxidation efficiency of Cr(III). The alteration of pH of the soil solution can also affect the redox potential between Cr(III) and manganese oxides. Thus, at low pH values manganese oxides can oxidize the more soluble Cr(III) easier due to the higher oxidation potential.

Cr(III) oxidation by several manganese oxides has been reported in the literature. Amacher and Baker (1982) mentioned that Cr(III) oxidation by the common naturally occurring δ-MnO_2 oxide, was observed over a range of Cr(III) concentrations and pH values, with oxidation efficiency being limited as pH and Cr(III) concentrations increased. The increase of pH at values higher than 5 declined significantly the oxidation rate while the high presence of Cr(III) caused surface alterations that prohibited the extension of the oxidation. In addition, they postulated that the formation of Mn(II) and Cr(VI) as reaction products did not inhibit the oxidation process despite the fact that Mn(II) cations formed were strongly adsorbed by the δ-MnO_2 surface. On the contrary, the formation of Cr(VI) anions were repulsed by the oxides surface. Reaction 2.1 represents the overall reaction of Cr(III) oxidation by δ-MnO_2 that occurs in the aquifers as proposed by Amacher and Baker (1982).

$$Cr^{3+} + 1.5\ \delta\text{-}MnO_2 + H_2O \leftrightarrow HCrO_4^- + 1.5Mn^{2+} + H^+ \quad \text{(Reaction 2.1)}$$

As observed from the reaction above, 1.5 mol of Mn(II) is released after the oxidation of each mol of Cr(III). Cr(VI) speciation influences the stoichiometric proportions of H^+ consumed or released by this reaction as also has been reported by Fendorf (1995). Similar results were observed also by Bartlett and James (1983 and 1991) mentioning however that Cr(III) oxidation is not possible in highly reductive soils and in soils developed on natural mineral deposits due to the prevalent anaerobic conditions. More recently, Dai et al. (2009) investigated the oxidation of different Cr(III) compounds [$CrPO_4$, $Cr(OH)_3$ and $Cr,Fe(OH)_6$] by δ-MnO_2 showing that the rate and extent of oxidation of $Cr(OH)_3$ and $Cr,Fe(OH)_6$ decreased with increasing pH, while $CrPO_4$ was not oxidized by δ-MnO_2. Eary and Rai (1987) verified Cr(III) oxidation using β-MnO_2, mentioning that Cr(III) oxidation by soil manganese oxides is also controlled by the surface characteristics of the oxides. Specifically, they reported that soil drying alters the manganese oxide surface, decreasing its oxidative ability. In addition they mentioned the factor of the ionic strength of the solution as a parameter able to affect Cr(III) oxidation. The inhibition of Cr(III) oxidation by β-MnO_2, under anaerobic conditions was also reported by Apte et al. (2006) as mentioned previously by Bartlett and James (1983 and 1991). More evidence about Cr(III) oxidation by γ-MnOOH or manganite have been provided by Johnson and Xyla (1991). γ-MnOOH or manganite is thought as an important type of manganese oxides in the geoenvironment able to oxidize Cr(III). Cr(III) oxidation was found to be a rapid reaction (completed in some minutes), not affected by pH and ionic strength, unlikely to the results published by Bartlett and James (1983 and 1991) and Eary and Rai (1987) who reported that Cr(III) oxidation is more difficult at acidic pH values. The restricted factors for Cr(III) oxidation were found to be the Cr(III) initial concentration and the presence of organic ligands.

Another parameter able to affect Cr(III) oxidation is the concentration of dissolved oxygen (DO) in groundwater. Schroeder and Lee (1975) demonstrated low Cr(III) oxidation rates under the presence of DO in a period of a month using water collected by a lake. Low rates of Cr(III) oxidation by DO were observed by Rai et al. (1986) who found that DO oxidizes Cr(III) into Cr(VI), but the oxidation rate at room temperature is very slow and, thus, enables Cr(III) to be involved in faster concurrent reactions such as sorption or precipitation. Therefore Cr(III) oxidation by DO is unlikely in soils. Similar results reported by Eary and Rai (1987) and Fendorf et al. (1995) observing that only small amounts of Cr(III) were oxidized by DO at highly alkaline pH values, indicating that the oxidation rate is sufficiently slow in the geoenvironment rendering, thus, Cr(III) available to be involved in other reactions mainly sorption before being oxidized by DO.

Cr(III) oxidation may also occur by chemical compounds possibly found in the geoenvironment, such as hydrogen peroxide (H_2O_2) and permanganate (MnO_4^-). Under alkaline conditions H_2O_2 may act as a Cr(III) oxidant either in the presence of oxygen or not (Pettine et al., 2008). In addition, Kilic et al. (2011) using tannery sludge investigated the possible oxidation of Cr(III) by adding H_2O_2 in alkaline environment, by determining the possible formation of chromates proposing the following reaction:

$$Cr^{3+} + 3H_2O_2 + 10OH^- \rightarrow 2CrO_4^{2-} + 8H_2O \quad \text{(Reaction 2.2)}$$

Regarding the effect of MnO_4^- on Cr(III) oxidation, Issa et al. (1955) investigated the oxidation of chromite with alkaline permanganate showing that the reaction efficiency is highly affected by a) the alkalinity, b) the rate of addition of permanganate solution and c) the prevailing gaseous atmosphere. Cr(III) oxidation by permanganate can be quantitatively effected according to the following reactions, which are supposed to take place in alkaline medium:

$$Cr^{3+} + Mn^{7+} \rightarrow Cr^{6+} + Mn^{4+} \quad \text{(Reaction 2.3)}$$

$$Cr^{3+} + 3Mn^{7+} \rightarrow Cr^{6+} + 3Mn^{6+} \quad \text{(Reaction 2.4)}$$

2.5.1.2. Reduction of chromium

Contrary to Cr(III) oxidation, Cr(VI) reduction is a more common reaction with several geoenvironmental agents acting as reductants. Cr(III) is oxidized to Cr(VI) only under the occurrence of high redox potentials and can be easily reduced again to Cr(III) at common environmental conditions. The most important geoenvironmental reductants for Cr(VI) are ferrous iron [Fe(II)], organic matter, sulfides and microorganisms.

Fe(II) can act as an electron donor for the reduction of Cr(VI) even presented in the aqueous or in solid phase (minerals). Fe(II) presence in groundwater can be attributed either to anthropogenic activities (e.g. discharges of industrial wastes) or to geogenic origin such as weathering of Fe(II)-containing minerals (Palmer and Puls, 1994). Table 2.5 presents the most common minerals able to contain Fe(II) in their structure. Cr(VI) reduction by soluble Fe(II) is a much faster process (usually completed in a few/some seconds) contrary to the reduction occurring on the minerals structure (completed in the range of hours or days) (Eary and Rai, 1989).

Table 2.5 Fe(II)-bearing minerals

Class	Group	Mineral	Chemical formula
Silicates		Olivine	$(Mg,Fe^{2+})_2SiO_4$
	Pyroxenes	Augite	$(Ca,Mg,Fe^{2+},Ti,Al)_2(Si,Al)_2O_6$
		Hedenbergite	$CaFe^{2+}Si_2O_6$
	Amphiboles	Hornblende	$Ca_2[Fe^{2+}{}_4(Al,Fe^{3+})]Si_7AlO_{22}(OH)_2$
		Cummingtonite	$(Mg,Fe^{2+})_7Si_8O_{22}(OH)_2$
		Grunerite	$Fe^{2+}{}_7(Si_8O_{22})(OH)_2$
	Micas	Biotite	$K(Mg,Fe^{2+})_3(AlSi_3)O_{10}(OH)_2$
		Phlogopite	$K(Mg,Fe)_3(Si_3Al)O_{10}(F,OH)_2$
		Glauconite	$(K,Na)(Fe^{3+},Al,Mg)_2(Si,Al)_4O_{10}(OH)_2)$
		Chlorites	$(Mg,Fe,Al)_6(Al,Si)_4O_{10}(OH)_8$
Oxides		Magnetite	$Fe^{2+}Fe^{3+}{}_2O_4$
		Ilmenite	$Fe^{2+}TiO_3$
		Wuestite	$Fe^{2+}O$
Sulfides		Pyrite	$Fe^{2+}S_2$

Richard and Bourg (1991) proposed a general reaction (Reaction 2.5) for Cr(Vl) reduction by Fe(II) hosted in hematite or biotite.

$$3Fe(II)O + 6H^{+} + Cr(VI)_{(aq)} \leftrightarrow Cr(III)_{(aq)} + 3Fe(III)_{(aq)} + 3H_2O \quad \text{(Reaction 2.5)}$$

In the case of hematite and biotite, Cr(VI) reduction observed in the aqueous phase as a result of Fe(II) release in small amounts in the solid solution (Eary and Rai, 1989). On the contrary, Cr(VI) reduction by pyrite is thought to mainly occur on the solid surface rather than in the aqueous phase even at slightly alkaline conditions. Magnetite is a ubiquitous magnetic iron oxide that occurs in the lithosphere, pedosphere, and biosphere and is commonly found in ultramafic and ophiolitic soils. Usually contains both ferrous [Fe(II)] and ferric [Fe(III)] iron species. The presence of Fe(II) in the structure of magnetite renders it as an efficient reductant for Cr(VI) as has been mentioned by several studies (Kendelewicz et al., 1999; He and Traina, 2005; Jung et al., 2007; Choi et al., 2008). Apart from the reduction due to the Fe(II) occurring in the minerals presented in Table 2.5, Cr(VI) reduction has been referred due to the presence of small amounts of Fe(II) existing in clay minerals in certain low-pH soils (Eary and Rai, 1989) and by the Fe(II) presented in the Fe(II)-Fe(III) hydroxysalt green rusts leading to the formation of Cr(III)-bearing ferrihydrite (Loyaux-Lawniczak et al., 2001).

Another reductant that is ubiquitous in soils and groundwater and can react with Cr(VI) is organic matter, commonly presented as organic carbon compounds including soil humic (SHA) and fulvic (SFA) acids as well as simple aminoacids (Stanin and Pirnie, 2004). The reaction proposed between soil organic carbon and bichromate can be described by the following Reaction 2.6 (Palmer and Puls, 1994):

$$2Cr_2O_7^{2-} + 3C^{0} + 16H^{+} \rightarrow 4Cr^{3+} + 3CO_2 + 8H_2O \quad \text{(Reaction 2.6)}$$

Several studies have demonstrated the reduction of Cr(VI) by soil humic and fulvic acids (Wittbrodt and Palmer, 1995 and 1996; Stanin and Pirnie, 2004). The conclusions from these studies indicate that Cr(VI) reduction by organic matter is significantly affected by the medium pH, Cr(VI) concentrations, and the organic matter concentration. Specifically, Cr(VI) reduction is favored by acidic conditions, since the reduction rates increased with increasing H^{+} concentration. In addition, Cr(VI) reduction rates have been found to increase with decreasing Cr(VI) concentration and with increasing the organic matter concentrations.

Another primary reductant for Cr(VI) in aquifers are sulfides. Despite naturally occurring sulfides are insoluble, like pyrite mentioned in Table 2.5, their presence in groundwater is usually a result of anthropogenic activities, like industrial waste discharge, organic matter decomposition or sulfate reduction (occurs after adding electron donors for chemicals biodegradation). Cr(VI) reduction by sulfides has been identified as a rapid reaction, which is usually completed within 24 hours (Schroeder and Lee, 1975).

Finally, Cr(VI) reduction by microbial activity has been extensively referred in the literature. Microbial reduction is thought to affect Cr(VI) speciation through direct and indirect mechanisms. Direct mechanisms include chromium removal and/or accumulation by

microorganisms (biosorption and bioaccumulation) and enzymatic reduction. Indirect ones include: 1) pH changes, affecting further the solubility of both Cr(VI) and Cr(III), 2) bacterial production of reductants like Fe(II) (Wielinga et al., 2001) and S^{2-} (Tebo and Obraztsova, 1998) and 3) organic matter degradation to more reactive compounds as a result of microbial fermentation (Deng and Stone 1996). Jeyasingh and Philip (2005) and Desjardin et al. (2002) using sterile and inoculated soils showed that the addition of a carbon source alone has almost no effect on Cr(VI) reduction indicating that biotic activities are leading to Cr(VI) reduction. However, most studies have tested microbial reduction capacity for Cr(VI) in pure cultures, and isolated and controlled systems and only few of them have used real soils (Salunkhe et al., 1998; Tseng and Bielefeldt, 2002; Oliver et al., 2003; Tokunaga et al., 2003a; Freedman et al., 2005; Srivastava and Thakur 2006; Faybishenko et al., 2008; Papasiopi et al., 2009) and fewer have referred to the reduction mechanism that occur in the field, despite bacteria capable of reducing Cr(VI) to Cr(III) are readily isolated from soil (Turick et al., 1996; Camargo et al., 2003).

Concluding, Cr(VI) reduction by Fe(II) exhibits the fastest rates, while under neutral to alkaline pH values and under anaerobic conditions Fe(II) controls primarily Cr(VI) reduction (Pettine et al., 1998; Stanin and Pirnie, 2004). Since Fe(II) and organic matter are ubiquitous in soils and groundwater, Cr(VI) can be reduced to Cr(III) in many natural environments (Rai et al., 1989).

2.5.2 Precipitation and dissolution reactions of chromium

In paragraph 2.3 speciation of chromium in the geoenvironment was discussed, by presenting information regarding the dissolution reactions, the hydrolysis products of chromium and the solubility of chromium as a function of pH-Eh values (Figure 2.2). The precipitation and dissolution reactions of chromium are affected by the solubility of each chromium compound and by the kinetics of dissolution. Parameters such as the pH of the medium, and the presence of organic matter and other ions can strictly affect precipitation/dissolution.

The water soluble Cr(III) species cannot occur in the geoenvironment since under the physicochemical conditions that typically prevailed these species form unstable compounds. Cr(III) reacts in aqueous media with the OH^- forming several chromium hydroxides with varying solubility. Thus, the pH increase leads to the increase of OH^- and thus to higher chromium precipitation, by formation of $Cr(OH)^{2+}$, $Cr(OH)_2^+$, $Cr(OH)_3$, and $Cr(OH)_4^-$. The solid $Cr(OH)_{3(s)}$ equilibrates with the Cr(III) dissolved species (Rai et al., 1987). Amorphous $Cr(OH)_3$ can also crystallize as $Cr(OH)_3 \cdot 3H_2O$ or Cr_2O_3 (eskolaite) depending on the existing conditions (Palmer and Puls, 1994). Cr(III) can also form complexes with inorganic and organic ligands. The most common inorganic ligands are SO_4^{2-}, NH_4^+, and CN^-. Organics can complex with dissolved Cr(III), eliminating its availability for precipitation (Hawley et al., 2004). Another factor that controls significantly Cr(III) precipitation is the presence of ferric iron Fe(III), since Cr(III) can precipitate in the form of mixed hydroxide $Fe_xCr_y(OH)_{3(s)}$ (Eary and Rai, 1988; Richard and Bourg, 1991). The formation of mixed iron-chromium hydroxide enhances the precipitation of Cr(III) in aqueous media with neutral and slightly alkaline pH values. The kinetics of the precipitation reaction with Fe(III) is fast making iron a controlling factor for Cr(III) fate in groundwater (Sass and Rai, 1987). In general, Cr(III) is presented in low dissolved

concentrations in groundwater since the neutral to alkaline pH values that commonly occur in aquifers lead to the formation of Cr(III) compounds of very low solubility.

Regarding Cr(VI), chromate (CrO_4^{2-}), hydrogen-chromate ($HCrO_4^-$) and dichromate ($Cr_2O_7^{2-}$) are soluble in aqueous media, in all pH range. In the typical pH range of groundwater (6.5-8.5), Cr(VI) is mainly presented as chromate. However, chromate can exist as an insoluble salt with a variety of divalent cations, such as Ba^{2+}, Sr^{2+}, Pb^{2+}, Zn^{2+}, and Cu^{2+} (Stanin and Pirnie, 2004). The rates of precipitation/dissolution reactions between chromate, and the aforementioned divalent cations are pH dependent. However, due to low concentrations of such divalent cations in aquifers, Cr(VI) precipitation is not considered as an important reaction. On the contrary, dissolution of such chromate salts in groundwater, usually originating from anthropogenic activities, is thought as a source of chromate anions.

Some Cr(VI) natural precipitates that have been observed are $CaCrO_4$, hashemite ($BaCrO_4$) and crocoite ($PbCrO_4$) (Smith et al., 2003). However, these solids are not much common and are not considered as a removal mechanism for Cr(VI). Contrary to the case of Cr(III), the presence of Fe(III) plays an important role in the immobilization of Cr(VI) only at acidic conditions. As shown at Table 2.6 several solid phases formed under acidic conditions and containing Fe(III) and Cr(VI) have been reported by the research teams of Baron et al and Olazabal et al. The KFe_3-$(CrO_4)_2(OH)_{6(s)}$ and $KFe(CrO_4)_2{\cdot}2H_2O_{(s)}$ phases have been identified in Cr-contaminated soils (Baron et al., 1996; Baron and Palmer, 1996; Baron and Palmer, 1998), while the $FeOHCrO_{4(s)}$ and $FeOHCrO_4{\cdot}2Fe(OH)_{3(s)}$ ones, have been identified as stable in acidic medium, with their stability being strongly affected by the concentration of metal ions (Olazabal et al., 1994, 1997). Additionally to these studies, Lee and Hering (2005) proposed the formation of a chromic hydroxy chromate phase [Cr(VI)-Cr(III) solid phase] under acidic conditions.

Table 2.6 Solid phases incorporating Fe(III) and Cr(VI) ions.

Reaction	log Ksp
$KFe(CrO_4)_2{\cdot}2H_2O_{(s)} = K^+ + Fe^{3+} + 2\ CrO_4^{2-} + 2H_2O$	-19.4
$KFe_3(CrO_4)_2(OH)_{6(s)} + 6H^+ = K^+ + 3Fe^{3+} + 2CrO_4^{2-} + 6H_2O$	-18.4
$FeOHCrO_{4(s)} = Fe^{3+} + CrO_4^{2-} + OH^-$	-22.5
$FeOHCrO_4{\cdot}2Fe(OH)_{3(s)} = 3Fe^{3+} + CrO_4^{2-} + 7OH^-$	-99.8

As it can be observed natural precipitation of Cr(VI) cannot be considered as an important process for Cr(VI) immobilization, contrary to Cr(III), which is not only easily precipitated under the physicochemical conditions that usually occur in aquifers but also can indirectly affect Cr(VI) presence since its precipitation increases the reaction rates of Cr(VI) to Cr(III) according to Le Chatelier's Principle (Hawley et al., 2004).

2.5.3 Sorption and desorption reactions of chromium

The general term of "sorption" comprises two processes: "adsorption", which is the process by which a solute clings to a solid surface, and "absorption", which is the process by which the solute diffuses into a porous solid and clings to interior surfaces. Adsorption occurs due to the attraction of dissolved ionic species to the mineral surfaces that exhibit a net electrical charge.

The presence of electrical charge is attributed to imperfections or substitutions in the crystal lattice or chemical dissociation reactions at the particle surface. The electrical charge varies significantly with pH (Stanin and Pirnie, 2004; Sposito, 2008). Sorption significance to the fate and transport of contaminants in groundwater is related to the retardation that can cause to the contaminants transport with respect to the groundwater velocity, reducing, thus, its concentration in the aqueous media. However, sorption is a reversible process and so the sorbed contaminants can be released back into the aqueous medium (desorption), causing increase in contaminants concentration

Cr(III) behaves like a cation when adsorbed onto surfaces and thus sorption is enhanced as pH increases. The pH increase causes surface deprotonation as the OH^- concentration increases, a fact that enhances the attraction between Cr(III) and the surface. Cr(III) can be rapidly, strongly and specifically sorbed onto soil by iron and manganese oxides and by clay minerals (Hawley et al., 2004; Motzer, 2004; Stanin and Pirnie, 2004). The Mn oxides typically accumulate on the surface of Fe oxides and clay minerals in aquifers (Bartlett and James, 1979). Several experimental data have shown that Cr(III) sorption on iron oxides and clays is a fast process that is completed in one day. One more factor able to strongly enhance Cr(III) adsorption is the presence of organic matter in soils, while the presence of dissolved ligands, organic or inorganic, and other heavy metal cations can act competitively to Cr(III) adsorption (Sposito, 2008).

On the contrary, Cr(VI) is presented in anionic forms $H_xCrO_4^{2-x}$ (mainly as CrO_4^{2-} and $HCrO_4^-$) under the physicochemical conditions occurring in the geoenvironment. The ratio of $HCrO_4^-$ to CrO_4^{2-} is a function of pH. Thus Cr(VI) sorption efficiency decreases with increasing pH, due to the increase of negative surface charge of the natural sorbents (Sposito, 2008). In the neutral to alkaline pH values that occur in groundwater it is expected that Cr(VI) anions would not be retarded by adsorption mechanisms, since Cr(VI) sorption by clays, soil and natural materials is low to moderate. However, contrary to clays, sandy materials have exhibited greater sorption affinity for Cr(VI). This is possibly due to their higher preponderance of positively charged surfaces able to adsorb the Cr(VI) anions over the pH range (5 – 7.5) possibly measured in groundwater (Stanin and Pirnie, 2004). These positively charged surfaces presented in alluvium aquifer materials are attributed to the presence of Fe, Al and Mn (oxy-hydro)oxides that have been mentioned as important adsorbents for Cr(VI) and other anions. These minerals are usually presented as coatings at aquifer materials and due to their structure and surface properties can remain positively charged even at neutral to alkaline pH values causing thus charge attractions with anions. Among them amorphous Fe is the mineral phase found at predominant concentrations in most aquifer materials (James and Bartlett, 1983; Rai et al., 1986; Zachara et al., 1987; Rai et al., 1988; Hawley et al., 2004).

Richard and Bourg (1991) investigated the sorption efficiency of Cr(III) and Cr(VI) on Fe_2O_3 surfaces, as a function of pH. The results verified that Cr(III) adsorption increases with increasing pH, but decreases when competing cations are present, whereas Cr(VI) adsorption decreases with increasing pH and when competing dissolved anions are present. Competing anions have drastic effects on Cr(VI) adsorption, with their extent depending on several parameters such as their concentration in the soil solution, their relative affinities for the solid

surface and the surface site concentration (Rai et al., 1986). The presence of chloride and nitrates have little effect on Cr(VI) sorption, whereas sulfates and phosphates tend not only to inhibit its sorption but also to replace them even when they are already sorbed. Additionally, sorption of chromates in the presence of a mixture of ions is lower when $H_2SiO_4^{2-}$ is present. On the contrary, chromates either increase or have no effect on the sorption of heavy metals (e.g. Cd^{2+}, Co^{2+}, Zn^{2+}) since competition for surface sites is relatively minor. Sorption of Cr(VI) becomes less important as the concentration of competing anions sorbed to solid surfaces increases (Rai and Zachara, 1988; Richard and Bourg, 1991; Fendorf, 1995; Ball and Nordstrom, 1998; Oze et al., 2004; Stanin and Pirnie, 2004). Thus, in groundwater, especially in contaminated one, Cr(VI) adsorption is usually negligible.

Sorption of chromates can be a reversible process, which depends on the chemistry of the extractant and of the soil (Baron et al., 1996). It can be concluded that sorption reactions, as with redox and precipitation reactions, are highly influenced by the complex environmental conditions inherent in the subsurface and can affect the transport and fate of Cr(VI) in aquifers. Cr(VI) adsorption will be more extensively discussed in the following paragraphs.

2.6 Groundwater inorganic contamination due to agricultural activities – Fate and transport of nitrates and phosphates

As mentioned in paragraph 2.4.1, the extensive use of fertilizers and other materials (liming materials, agrochemicals, and sewage sludge) used as soil amendments can increase the content of heavy metals, such as chromium, in soil and groundwater. The intensive applications of such materials in combination with organic materials like manure, fungicides or other pesticides can lead to higher extractability of heavy metals from soil. However, the mobility of such metals depends not only on the metals concentration but also on the soil properties (Han et al., 2000; Covelo et al., 2007).

However, the intense use of manure and synthetic fertilizer, and irrigation with wastewater have been shown to directly contaminate water bodies (surface water and groundwater). In the early 1960s, elevated P and N concentrations in groundwater have been observed globally as a result of intensive agricultural activities. This is also the case in Greece where extensive agricultural activities occur in several areas. The Greek legislation incorporated the Directive 91/676/EEC, establishing the law with No. 16190/1335/1997 (Government Gazette 519), according to which each Member State shall establish one or more codes of good agricultural practice. These are optionally applied by the farmers and include environmentally-friendly rules for agriculture activities and livestock farming, both aiming at ensuring the protection of surface and groundwater from nitrate pollution linked to agricultural origin. Such practices include the use of certain fertilizers and irrigation treatment, avoiding the application of fertilizers or manure at short distances from water sources, proper handling of livestock waste and manure disposal, etc. However, no legislation occurs regarding the treatment of phosphates. Thus although a limit for NO_3^- concentration (50 mg/L) in groundwater has been established this does not happen regarding P concentrations. The possible sources of these two contaminants in groundwater and their fate and transport after their addition in aquifers will be described below.

2.6.1 Nitrates in the geoenvironment

2.6.1.1. General

The total content of nitrogen (TN) is divided into Total Inorganic Nitrogen (TIN), including nitrates (NO_3^-) and nitrites (NO_2^-), as well as Total Organic Nitrogen (TON). Organic nitrogen consists of truly dissolved organic nitrogen (DON) and particulate organic nitrogen (PON). NO_2^- and NO_3^- ions are the oxidized forms of N. These N compounds are dissolved in the aquatic environment and are usually the product of oxidation of ammonia by aerobic bacteria, according to the following reaction (Reaction 2.7):

$$NH_4^+ + 3/2O_2 \rightarrow NO_2^- + 2H^+ + H_2O \quad \text{(Reaction 2.7)}$$

Nitrites in the aquatic environment are found at very low concentrations, as they are rapidly oxidized to nitrate, according to the following reaction (Reaction 2.8):

$$NO_2^- + 1/2O_2 \rightarrow NO_3^- \quad \text{(Reaction 2.8)}$$

Nitrates and nitrites are particularly soluble compounds, resulting in easily reaching surface water or groundwater. Due to their high solubility in aqueous media, they are possibly the most widespread groundwater contaminants globally imposing an important threat to drinking water supplies and eutrophication. The presence of elevated nitrates concentrations in drinking water has gain great concern in the recent decades. Humans ingest nitrate in food and water. Little is known about the adverse effects may be caused in adults even at chronic consumption of high amounts of nitrates. Only in the case of nitrates consumption by infants there have been detected health risk effects like methemoglobinemia (blue-baby syndrome) (Mahler et al., 2007). In order to prevent adverse health effects by nitrates consumption the European Union enacted the Drinking Water Directive (98/83/EC) setting a maximum allowable concentration for nitrate of 50 mg/L. Since in many countries groundwater is a very important source of drinking water and it is often used untreated, groundwater protection by nitrate contamination was prevented by the Nitrates Directive (91/676/EEC). This Directive aims to control N pollution and requires Member States to identify groundwater that contain more than 50 mg/L nitrate or could contain more than 50 mg/L nitrate if preventative measures are not taken. It must be noted that by this directive not only the nitrates but also phosphates are considered as target contaminants mainly due to application of fertilizers. In addition, the EU promotes the adoption of rules on good agricultural practices since nitrate concentrations higher than the 50 mg/L limit are mainly recorded in private and small communal supplies from shallow aquifers, and in areas with intensive agricultural and livestock production (https://www.eea.europa.eu/themes/water/status-and-monitoring/state-of-groundwater/water-quality-and-pollution-by-nutrients**).**

Finally, the Groundwater Directive 2006/118/EC (12 December 2006) of the European Parliament and of the Council of the European Union which refers to the protection of groundwater against pollution and deterioration established the limit of 50 mg/L for nitrates concentration in groundwater.

2.6.1.2. Origin of nitrate in groundwater

Natural occurrence

Nitrogen concentration in cultivated soils usually ranges between 0.17 and 0.45 Kg/m^2 of N bounded in living and dead plants and organisms (Mahler et al., 2007). Natural nitrate levels in groundwater are generally very low, typically less than 10 mg/L (http://www.lenntech.com/groundwater/nitrates.htm#ixzz4hWzL8IKY, Mahler et al., 2007). Natural contamination of groundwater with nitrates is usually rare and can be attributed to loss of N from the soil zone, which will cause under specific climate conditions groundwater enrichment with high levels of nitrates. However, several factors can affect natural groundwater contamination such as the nature and thickness of surface deposits, the rainfall quantity and distribution, the groundwater level, the distribution of vegetation types and presence of N-fixing vegetation. Usually, in order to identify high levels of nitrates contamination, all or most of the aforementioned parameters must occur. For example, droughts and fires can affect the N cycle by disturbing the plant cover, which can lead to nitrate leaching under the root zone, especially after the occurrence of great rainfalls (Tredoux et al., 2009).

Some examples of natural groundwater contamination with nitrates have been reported by Tredoux et al. (2009) like in the semi-arid to arid regions of the Northern Cape Province and Namibia, where anthropogenic influences are excluded, since the population density is very low. Similarly in the Australian arid zone and the Sahel area nitrate contamination was attributed to biological N fixation or to a combination of N fixation and termite activity, and to leguminous vegetation and leaching of nitrate due to varying climatic cycles, respectively (Tredoux et al., 2009)

Anthropogenic sources

Groundwater contamination by nitrates can be attributed to a wide range of anthropogenic activities, such as agricultural activities, industrial activities, domestic effluents and emissions from combustion engines. The most common anthropogenic sources of nitrates are the following (European Environmental Agency, 1999):

- over fertilization of crops
- cultivation in areas where soils exhibit high thickness of their layer or have poor nutrient buffering capacity or they are subjected to alterations of land use
- cultivation of seasonal crops (soil is bare for high period annually, especially in winter) which require high amounts of fertilizes
- intensive agricultural rotation cycles involving frequent ploughing
- drainage systems which lead to drainage of fertilizers
- organic fertilizers form animal waste/by-products
- increased urbanization

As it can be observed, agriculture is the largest contributor of groundwater contamination with nitrates. Agricultural contamination includes non-point and point sources. Non-point sources can be manure and fertilizer application to land, tilling of the soil, deforestation and land clearing, while as point sources can be considered on-site sanitation, kraals, and other places

where livestock congregate, especially at stock watering points, and feedlots (Tredoux et al., 2009). As regarding fertilizers application the most common inorganic N fertilizers contain nitrates and/or ammonium (NH_4). Plants do not necessarily use all the nitrates contained in fertilizers or produced by organic matter decomposition (Mahler et al., 2007). In addition, the continuous cultivation causes a depletion of nutrients from soils, which secondly is tried to be replenished by adding more and more N-based fertilizer on the land in an attempt to keep the productivity constant (Behm, 1989). The kind of crops, the frequency of irrigation and the type of soil are important parameters able to affect groundwater contamination (Burkart and Kolpin, 1993).

2.6.1.3. Processes that affect fate and transport of nitrates

The excess of N from fertilizers percolates through the soil and can be detected as nitrates or ammonium, under aerobic or anaerobic conditions, respectively. Nitrates can be accumulated in soils or be infiltrated by them, when the input amounts are higher from what the system can use. The rate of infiltration is relatively slow and usually a lag time of 20 up to 40 years between the pollution phenomena and the presence of the contaminant in groundwater, depending on the hydro-geological conditions. However, if the anthropogenic activities are intensive, nitrates transport to the saturation zone can be rapid. The high risk of nitrates presented in groundwater is that usually have similar electric charge with soil colloids, resulting thus in increased mobility within the water bodies (Mahler et al., 2007; https://www.eea.europa.eu/themes/water/status-and-monitoring/state-of-groundwater/water-quality-and-pollution-by-nutrients**)**.

In aquifers nitrates can be involved in redox reaction undergone by biological or chemical factors. Nitrates can be reduced by microbial action into nitrite or other forms. Since nitrites are unstable under the physicochemical conditions in aquifers chemical and biological processes can further reduce them to N compounds or oxidize them back to nitrates (Bhatnagar and Sillanpää, 2011). The chemical reduction of nitrates demands the presence of chemical factors able to act as electron donors. Table 2.7 presents some inorganic chemical factors that can potentially act as nitrates reductants since their oxidation potentials are lower or similar to that of the NO_3^-/N_2 (0.75 V) redox pair (Zhu and Getting, 2012).

Table 2.7 Inorganic chemical factors possibly able to reduce nitrates.

Half reaction	Standard potential (V)
$Fe^{3+} + e^- \rightarrow Fe^{2+}$	0.77
$NO_3^- + e^- \rightarrow N_2$	0.75
$I_2 + 2e^- \rightarrow 2I^-$	0.54
$Cu^{2+} + 2e^- \rightarrow Cu$	0.34
$Cu^{2+}_{(aq)} + e^- \rightarrow Cu^{+}_{(aq)}$	0.13
$2H^+ + 2e^- \rightarrow H_2$	0.00
$Pb^{2+} + 2e^- \rightarrow Pb$	-0.13
$2SO_4^{2-} + 19H^+ + 16e^- \rightarrow H_2S + HS^- + 8H_2O$	-0.22
$SO_4^{2-} + 8H^+ + 6e^- \rightarrow S^0 + 4H_2O$	-0.33

$Fe^{2+} + 2e^- \rightarrow Fe^0$	-0.44
$Zn^{2+} + 2e^- \rightarrow Zn$	-0.76
$Al^{3+} + 3e^- \rightarrow Al$	-1.66
$Mg^{2+} + 2e^- \rightarrow Mg$	-2.37
$Na^{+} + e^- \rightarrow Na$	-2.71
$Ca^{2+} + 2e^- \rightarrow Ca$	-2.87
$K^{+} + e^- \rightarrow K$	-2.93

Source: (Zhu and Getting, 2012)

Another factor able to affect nitrate transport is the sorption process. The ability of soils to adsorb nitrates so that can be used for plants growth, causes retardation to their movement to deeper horizons and thus to groundwater. Several studies have reported nitrates sorption by soil (Reynolds-Vargas et al., 1994; Qafoku et al., 2000; Tani et al., 2004; Hamdi et al., 2013). However, the presence of nitrates in concentrations higher than the soils adsorption capacity renders them susceptible to leaching (Bhatnagar and Sillanpää, 2011). Several soil properties such as iron and aluminum oxide concentrations (Wong and Wittwer, 2009), organic matter content (Panuccio et al., 2001), pH (Donn and Menzies, 2005), and soil texture and clay mineralogy (Schrothez-Villegas et al., 2004) have been reported to control nitrates mobility. In addition, the presence of other anions, such as chlorides, are able to cause adsorption competitive effects on nitrates (Feder and Findeling, 2007), while Qafoku et al. (2000) reported that nitrates sorption is strongly related to their concentration. Thus nitrate concentration in groundwater can vary over a very wide range depending on the aquifer's geochemistry.

2.6.2 Phosphates in the geoenvironment

2.6.3.1. General

P in the geoenvironment can be found in soil, rocks, plants and groundwater. It is an essential nutrient for plant growth but at high concentrations can cause water quality problems, especially in surface waters by promoting eutrophication. Phosphates exist in three forms: orthophosphates ($H_xPO_4^{3-}$, x=0-2), metaphosphate (or polyphosphate) and organically bound phosphate. The main difference among them is the chemical arrangement of P. These forms of phosphate occur in living and decaying plant and animal remains, as free ions or weakly chemically bounded in aqueous systems, chemically bonded to soils, or as mineralized compounds in soil and rocks (USEPA, 2005; Oram, 2014). The most common form of P in aqueous media is orthophosphates. Orthophosphates are strongly affected by the pH values of the aqueous media occurring with several anionic species. Species derived from orthophosphoric acid (H_3PO_4), such as $H_2PO_4^-$ and HPO_4^{2}, exist under acidic and slightly alkaline pH values, respectively, and both are preferentially absorbed by plants. In alkaline pH values the predominant specie is PO_4^{3-} (Hinsinger, 2001; Fink et al., 2016).

Except for eutrophication, which is the main environmental problem created by phosphates, extremely high levels of phosphates can cause digestive problems in humans. The WHO, in 1980 concluded that there is no nutritional basis for the regulation of P levels in the US drinking water supplies. In EU the most important Directives related to phosphorus are the

Water Framework Directive 2000/60/EC and the Groundwater Directive (daughter directive of Water Framework Directive) 2006/118/EC and the Nitrates Directive 91/676/EEC. However, at none of them a specific concentration limit of P is referred. The main environmental objectives at these Directives are to achieve and maintain a good status for all surface waters and ground waters and to prevent deterioration and ensure the conservation of high water quality where it still exists.

The primary concern with P is discharge to surface waters in order to prevent/control eutrophication. Thus USEPA makes the following recommendations regarding the P concentrations (Murphy, 2005; Oram, 2005):

- total PO_4–P ≤ 0.05 mg/L in a stream at a point where it discharges into a lake or reservoirs,
- total PO_4–P ≤ 0.1 mg/L in streams that do not discharge directly into lakes or reservoirs,
- total PO_4–P ≤ 0.025 mg/L for reservoirs.

For the purpose of monitoring and water rating the following are the useful requisite levels of total PO_4–P (Oram, 2005; Fadiran et al., 2008):

- <0.03 mg/L: level in uncontaminated lakes;
- 0.025 – 0.1 mg/L: levels at which plant growth is stimulated;
- 0.1 mg/L: maximum acceptable for avoidance of rapid eutrophication;
- > 0.10 mg/L: high level resulting in accelerated algal growth problems.

2.6.3.2. Origin of phosphate in groundwater

Natural occurrence

Natural sources of P in groundwater include atmospheric deposition, natural decomposition of rocks and minerals, weathering of soluble inorganic materials, decaying biomass, runoff, and sedimentation (Fadiran et al., 2008). Concentrations of P in rocks may be as high as 1,000 mg/kg (MPCA, 1999). P in soil parent materials is primarily in mineral form and especially as apatite, a mineral that is also commercially available, and consisted by calcium phosphate. Generally, apatite is a family of phosphates containing calcium, iron, chlorine and several other elements in varying quantities (Oram, 2014). When calcium phosphate is crystalized with fluoride or calcium chloride it is formed the chloro-apatite $Ca_5(PO_4)_3(OH,F,Cl)$. Another source of P can be considered to be the phosphorite, which is in fact a product of apatite's weathering. During the soil synthesis/weathering the P contained in apatite is released and can be either taken up by the plants or incorporated into the organic matter of the soil or bound by different soil components. Other P minerals are monazite $[(Ce,La,Pr,Nd,Th,Y)PO_4]$, a rare earth metal phosphate and vivianite $[Fe^{2+}{}_3(PO_4)_2 \cdot 8H_2O]$ that contains ferrous iron. Generally, several factors, such as the type of the parent material, the climate, the slope of the area, the presence of organisms and the geological processes that lead to soil formation, can affect the release of P in the soil solution. However, these amounts of P are immediately used by plants and organisms. Naturally occurring levels of phosphates in surface and groundwater bodies are not harmful to human health, animals or the

environment. The form of P presented in groundwater due to natural processes is that of orthophosphates (Fink et al., 2016).

Anthropogenic sources

Anthropogenic sources of P include fertilizers, wastewater and septic system effluents, animal wastes, industrial discharges, phosphate mining, forest fires. In these cases phosphates are presented as orthophosphates. Small amounts of certain condensed phosphates, usually poly forms, are added to some water supplies during treatment to prevent corrosion and this chemical is used extensively in the treatment of boiler waters. Larger quantities of these compounds can be found in laundering and commercial cleaning agents (Fadiran et al., 2008; Oram, 2014).

In several areas P concentrations in soils is likely to be considerably higher compared to background levels. Agricultural activities are considered as one of the most important sources for phosphates presence in soils and groundwater since considerable amounts of P are tied up in vegetation. Huge quantities of sulfuric acid are used in the conversion of the phosphate rock into a fertilizer product called "super phosphate" (Oram, 2014). In agriculture activities, in order to achieve efficient use of fertilizers, P aqueous concentrations higher than 3 mg/L are required. In such areas with intensive agricultural activities, P concentrations as high as 30 mg/L have been found in soil runoffs. These values are much higher than the limit for P concentrations (<0.1 mg/L) in surface water that USEPA suggests (Withers et al., 2000; Weng et al., 2012). As a result, the importance of P release from agricultural areas has increased in recent years (Sharpley et al., 1994; Barberis et al., 1996; Koopmans et al., 2007). The main form of P occurs in groundwater/soil is that of orthophosphates, since this form occurs in fertilizers, in order to be readily available for plants. In addition, the poly-forms are transformed into orthophosphate and are available for plant uptake in the conditions of groundwater, while organic phosphates that are usually bound or tied up in plant tissues, waste solids or other organic material, after their decomposition, are converted to orthophosphates (Oram, 2014).

2.6.3.3. Processes that affect transport of phosphates

P in soils can be divided into two categories; 1) the P portion that is available to be used by plants and thus is presented in pore water; usually referred as “environmentally available” and it is measured in order to determine the need of crops but also used as a method for predicting the amount of P adsorbed to the soil, 2) the rest of P that remains in the subsurface (Figure 2.10). The second portion of P, which is applied as orthophosphates to agricultural or residential lands as fertilizers, can be carried into the surface water during storm events or snow melt. Storm events can also cause the vertical migration of the phosphates into the groundwater system. However, since most soils exhibit affinity for phosphates, the soil mantle acts as storage media (Oram, 2014). The main processes by which phosphates can be immobilized in soils are precipitation/mineralization and adsorption. Regarding precipitation/mineralization process, phosphates have the ability to form several highly insoluble secondary minerals. The most common minerals formed are calcium phosphate

minerals, such as hydroxyapatite ($Ca_5(PO_4)3OH$) and others like strengite ($FePO_4 \cdot 2H_2O$), vivianite ($Fe_3(PO_4)_2 \cdot 8H_2O$) and variscite ($AlPO_4 \cdot 2H_2O$) (Nriagu and Dell, 1974; Nriagu and Moore, 1984; Zanini et al., 1998; Robertson, 2003). Tunesi et al (1999) reported that P precipitation was dominant for P concentrations higher than 15.5 mg/L in calcareous soil solutions. Except for P concentration, experimental results showed that precipitation is also affected by the concentration of Ca^{2+} ions, the reaction time, the concentration of the background electrolyte and the pH values.

Though orthophosphates are soluble in groundwater, they can also bind or adsorb onto soil particles. Thus, adsorption is a crucial process that can affect the availability of phosphates to the biosphere and their mobility in groundwater. Phosphates adsorption on soils depends on several parameters, such as the pH of the medium and their concentration in groundwater, as well as on the geochemical soil characteristics, such as the specific surface area (SSA), the crystallinity, and the configuration and density of hydroxyl groups on the iron oxides surface. These parameters are further affected by the geological background including the processes occurring for the soil formation, the extent of weathering processes, the drainage conditions and the pH (Fink et al., 2016). Sorption of phosphates is thought to be a two-step process at which the first step involves rapid adsorption at high affinity mineral surface sites (Parfitt, 1978; 1989) and the second one involves the slower diffusion into micropores (Barrow, 1985; Torrent et al., 1992; Slomp et al., 1998; Mikutta et al., 2006) or precipitation of metal phosphate phases (Van Riemsdijk et al., 1984). The most important adsorbents for orthophosphates in soils are colloids such as clays, metal oxides (iron and aluminum), natural organic matter and biocolloids (microorganisms) (Pang et al., 2016). Especially, the fine-grained iron oxides are considered as the main adsorbents for orthophosphates in the subsurface. The pH of the medium and the concentration of DO are crucial factors that may affect the adsorption capacity of such minerals. Iron oxides exhibit higher adsorption capacity below neutral pH values and in the presence of DO, while in the case of anoxic and alkaline environments they become saturated much faster. In addition, in rare cases anaerobic conditions may cause the release of phosphates back to the soil solution due to the dissolution of the iron oxides, under the occurrence of specific bacteria. In addition, the effect of iron and aluminum sesquioxide species on soil adsorption–desorption phenomena is affected by the presence of natural organic matter (NOM) (Brennan et al., 1994; Zhang, 2008; U.S.G.S., 2012; Bortoluzzi et al., 2015). So far, little quantitative information is available on the relative roles of fast and slow sorption and mineral precipitation in determining P mobility in groundwater (Spiteri et al., 2007).

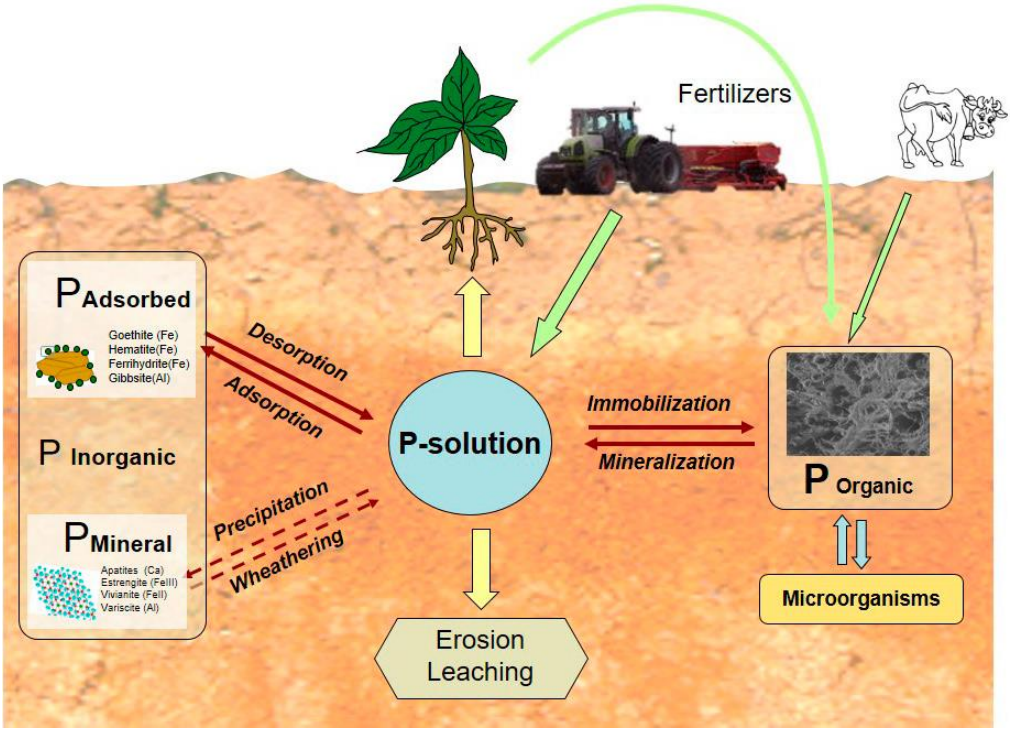

Source: (Fink et al., 2016)

Figure 2.10 P cycle in the environment

Since the soil reaches its adsorption capacity the excess of phosphates remains in the soluble phase and thus phosphates are transported deeper in the unsaturated zone and finally into the underlying aquifer according to the vertical water movement. However, this pathway has received little attention since in most studies/cases the basic assumption made is that it is retained by the soil due to its high adsorption capacity (Correll, 1998). There are several cases at which significant concentrations have been observed in groundwater and this fact is a result of soil's attenuation capacity or preferential transport of P-containing wastes through the soil to groundwater (MPCA, 1999). Several studies have investigated the behavior and trend of nutrients concentrations, like P in groundwater associated with anthropogenic activities (Carlyle & Hill, 2001; Burkart et al., 2004; Abraham & Hanson, 2008; Holman et al., 2010; Heeren et al., 2011; Mittelstet et al., 2011; Gray et al, 2015). A first indication of the possible presence of phosphates transport from subsurface to groundwater is the type of subsurface and the depth of groundwater table, with shallow aquifers being most likely to be affected by human activities. For instance, alluvial gravel subsurfaces, with low organic matter content, due to their high permeability are more sensitive to leaching phenomena. The formation of significant preferential flow paths allows the easy vertical transport of contaminants (MPCA, 1999; Pang et al., 2016). Such an example was reported by McDowell et al. (2015) who detected elevated P concentrations in groundwater associated with sandy and gravel aquifer. The site was used for dairying for a period of about 10 years. Finally, even if soils exhibit high amounts of colloids able to bind phosphates this cannot be sufficient to retard phosphates transport. The presence of mobile colloids (e.g. iron oxides), which can be transported through the soil pores enhances phosphates transport (de Jonge et al., 2004; Schelde et al., 2006; Walshe et al., 2010).

2.7 Principles and modeling of adsorption process

2.7.1 General

Adsorption is the process by which a chemical substance reacts at the interface of two different phases. In the case that the phases are a solid and a liquid one, as occurs in aquifers, the solid phase is termed as "adsorbent" and the substances that are adsorbed as "adsorbate". During adsorption, ion accumulation occurs at the solid/liquid interface forming a 2D structure. In the case that this 2D accumulation continues with the formation of a 3D structure then the precipitation process takes place. These two processes belong to a more general process, which refers to the loss of substances from a fluid phase to a solid surface, called "sorption" (Goldberg et al., 2004).

Adsorption can be affected by several parameters, the main of which are listed below (Al-Anber, 2011):

- *Surface area of adsorbent*. The higher the surface of the adsorbent the higher the adsorption capacity.
- *Particle size of adsorbent*. Particle size affects adsorption efficiency since particles with smaller size increase internal diffusion and can be transferred deeper in the solid porous, utilizing all the available sites for adsorption. By this way equilibrium is achieved faster, the adsorption rates are higher and adsorption capacity is maximized.
- *Contact/residence time*. High contact time indicate that possibly adsorption is completed since equilibrium has been achieved. By this way it can be found the minimum time required for equilibrium and possibly information about the diffusion mechanism.
- *Affinity of the solute for the adsorbent*. Surface polarity attributes to the higher adsorption of polar compounds compared to non-polar ones.
- *Molecule size with respect to size of the pores*. The molecule size may cause adsorption effects since its size can affect the entrance in the solid porous.
- *Ionization degree of the adsorbate molecule*. Neutral molecules are more efficiently adsorbed than highly ionized ones.
- *pH.* The pH of the aqueous solution can affect adsorption by two ways. Either by affecting the surface charge of the solid surface, due to the presence of OH^-/H^+ or by affecting the ion speciation, since the degree of ionization of a species is affected by the pH. The pH value at which the surface charge is zeroed under constant temperature, pressure and soil solution composition is called point of zero charge (PZC).
- *Effect of initial concentration*. The higher ion concentrations create their excess taking into account the constant amount of the adsorbent and the available surface sites. Thus, the adsorption efficiency decreases. The decrease is also related to the diffusion process and the possible competitive effects. This competition prevents the ion passing inside the solid pores with the adsorption occurring only on the solid surface. This phenomenon creates less favorable adsorption sites (from an energy point of view) since ions concentration increases.

- *Effect of solid concentration*. Adsorption efficiency generally increases with increasing the concentration of the adsorbent (dosage effect), since more mass and, thus, surface area is available for adsorption.

Adsorption can be divided into two main categories: chemisorption and physisorption processes. In the case of chemisorption (chemical adsorption) the adsorbate is bounded at the solid surface via the formation of chemical bonds. Thus chemisorption can be either an endothermic or exothermic process. In order to be achieved a high activation energy is usually required and thus the process is favored at high temperatures. It is generally a slow process and thus increased time is needed for achieving equilibrium. In addition, chemisorption is strongly affected by the size of surface area, since high surface area provides higher capacity for adsorption due to the formation of more valence bonds. The adsorbed molecules create a layer that covers the surface with thickness equal to the size of the adsorbed molecule, since each site adsorbs only one molecule which cannot be transported to other site (specific adsorption). Thus a monomolecular layer is formed, which also controls the adsorption capacity of the adsorbent since, up to its formation on the whole surface area, the capacity is exhausted. On the other hand, physisorption, is a process based on the occurrence of intermolecular attractions (e.g. Van der Waals forces), not including any important alterations at the electronic orbitals of the species. In this case, no activation energy is required and low temperatures favor this kind of adsorption. Physisorption can be characterized as multilayer adsorption and as non-specific due to the formation of weak forces between molecules, which allow to the molecule to move freely near the solid surface (Al-Anber, 2011).

The physicochemical conditions of the aquifers under which adsorption process occurs, such as pH, surface area and density of active sites (affected by the type of minerals) can influence the time required for sorption equilibrium. As a result, in some cases the adsorption reactions can be fast, completed in some minutes or hours, or exhibit higher duration upon their completion in the timescale of days or weeks. Experimental data have proved that adsorption reactions in soils are commonly rapid. This characteristic is attributed to the presence of readily exchangeable ions. Exchangeable ions are adsorbed/desorbed very fast since the predominant adsorption mechanism is the film diffusion. However, adsorbed ions in soils exhibit a more complicated behavior affected by multiple mechanisms, which require different time periods to be completed. These mechanisms also affect the desorption rates of the ions (Stanin and Pirnie, 2004; Sposito, 2008).

As regarding desorption process, one of the main characteristics of adsorption is its reversibility. The reversibility is determined by the desorption efficiency of an adsorbate, described by the ability of an ion to be released back to the solution. In the geoenvironment desorption is an important process since it can be used for determining contaminant mobility and evaluating soil decontamination/remediation. However, in some cases the strongly bounded ions cannot be desorbed immediately in the aqueous solution. A hysteresis at desorption is observed since much more time is needed for total desorption, compared with the time required for reaching equilibrium. Hysteresis is an apparent indication of sorption irreversibility (Davis and Kent, 1990). Usually, chemisorption is thought as an irreversible (or partially reversible) process since for desorption of the adsorbed species extreme conditions

are required like high temperature and/or pressure, or application of chemical treatment. This may cause the alteration of the surface nature/properties or the alteration of the adsorbate species. Contrary, physisorption, is considered as fully reversible since the adsorbate can be desorbed back to the solution in the same extent and chemical nature at which it was adsorbed. However, in many cases both types of adsorption may occur at the same surface with a layer of physically adsorbed molecules occurring over a chemisorbed layer (Al-Anber, 2011). Hingston (1981) and Padmanabham (1983b) were of the first researchers who studied desorption of anions (phosphates) and cations using goethite mineral as adsorbent. They observed that the rate and extent of desorption was a function of pH and the time allowed for adsorption. These two parameters affected the formation of different surface complexes. More extreme pH values and more time for adsorption led to the formation of bidentate complexes, which are characterized by higher activation energies for dissociation. In addition, hysteresis can be attributed to ion diffusion in the porous media, precipitation after adsorption on the solid surface or chemical/biological transformations; processes that can cause slow release back to the aqueous solution (Davis et al., 1987; Fuller and Davis, 1989). From experimental aspect the presence of hysteresis may be due to inadequate time provided in order to achieve equilibrium.

2.7.2 Adsorption isotherms

Adsorption isotherms, also referred as equilibrium data, are fundamental for the description of adsorption process. Using adsorption isotherms is possible to determine the adsorption capacity of an adsorbent. The isotherm is obtained when equilibrium is achieved under constant temperature and pressure. Thus equilibrium is referred to the conditions at which the adsorbents exhibit their maximum adsorption capacity and the rate of adsorption equalizes that of desorption. Graphically, adsorption isotherm represents the adsorption capacity of the adsorbent in each case of adsorbate's concentration, keeping constant parameters such as pH and ionic strength. The adsorption isotherm diagram presents the relation between the adsorbed amount of the contaminant and its corresponding concentration in equilibrium in the aqueous phase (Sposito, 2008; Al-Anber, 2011). There are several types of isotherms as will be discussed below.

Linear isotherm

Linear isotherms are described by the coefficient factor (K_d). However, since soils are dynamic systems it is very rare to achieve equilibrium conditions. Thus linear isotherms cannot describe efficiently the adsorption processes. In addition, it has been found that heavy metals, like chromium, exhibit linear correlation very seldom. Thus mathematical equations with more than to two parameters able to be changed are needed (Stanin and Pirnie, 2004).

Langmuir isotherm

Langmuir is one of the simplest non-linear isotherms which is used for quantitative description of adsorption, based on the following assumptions (Al-Anber, 2011):

- Adsorption occurs on a homogenous surface forming a monolayer between the adsorbate and the outer surface of adsorbent.
- Adsorption sites are identical and equivalent from thermodynamic aspect.

- No interactions occur between the adsorbed molecules

The mathematical expression of the Langmuir isotherm is given by Equation 2.1:

$$\frac{C_e}{q_e} = \frac{1}{Q*b} + \frac{1}{Q}C_e \quad \text{(Equation 2.1)}$$

Where C_e (mg/L) is the concentration of adsorbate remaining in the solution at equilibrium, q_e (mg/g) is the amount of adsorbate per unit mass of adsorbent, Q (mg/kg) is the maximum adsorption representing completion of the covering of the monolayer, and b (L/mg) is the Langmuir bonding energy coefficient representing the degree of adsorption affinity of the adsorbate. The higher the b value, the stronger the affinity of the adsorbate.

Freundlich isotherm

Contrary to Langmuir, Freundlich isotherm is usually used for describing adsorption on heterogeneous surfaces. Freundlich approach indicates that adsorption is a surface phenomenon initially, followed by strong adsorbate - adsorbate interactions. The Freundlich curve exhibits an exponential trend. Thermodynamically, the meaning of this trend is that the adsorption heat may decrease with increasing the adsorption extent, with the adsorption sites being expanded exponentially in respect of adsorption energy. The mathematical logarithmic expression of the Freundlich isotherm is given by Equation 2.2 (Al-Anber, 2011):

$$logq_e = logK + \frac{1}{n}logC_e \quad \text{(Equation 2.2)}$$

Where C_e (mg/L) is the concentration of adsorbate remaining in the solution at equilibrium and q_e (mg/g) is the amount of adsorbate per unit mass of adsorbent. K (mg/kg) and n (L/mg) are Freundlich parameters characteristic of the system, which are determined empirically and indicate the adsorption capacity and adsorption intensity, respectively. The value of K factor depends on temperature. The n factor is indicative of the surface heterogeneity and the higher the n factor, the more the expected heterogeneity of the available sorption sites.

Despite Langmuir and Freundlich equations are the most commonly used nonlinear isotherms for describing adsorption of heavy metals on soils, in many cases the assumptions made using these isotherms are not representative of the real conditions that occur in soil (Stanin and Pirnie, 2004). Some other isotherms used for describing adsorption on soils are presented below.

The S-curve isotherm exhibits a small slope initially, which afterwards increases with increasing the concentration of the adsorbate. This trend indicates that the soil particles affinity for the adsorbate is lower than the affinity of the aqueous solution for the adsorbent. The formation of the S-curve isotherm is attributed to synergistic interactions among the adsorbed substances, which are further responsible for the formation of multinuclear surface complexes on the solid surface. This results on enhanced affinity for the adsorbate with increasing the surface coverage.

The L-curve isotherm exhibits a slope initially, as in the case of the S-curve, which however is not affected by the concentration of the adsorbate in the soil solution. This trend indicates the occurrence of high affinity of soil for the adsorbate at low surface coverage. However, the affinity is affected by the decreasing amount of adsorbing surface, which remains available as the surface excess increases. The L-curve isotherm is expressed mathematically by the Langmuir equation.

The H-curve isotherm is characterized by a great initial slope indicating the great affinity of the soil for the adsorbate and is considered as an extreme case of the L-curve. Its trend is attributed to the formation of either inner-sphere surface complexes or strong van der Waals interactions.

Finally, the C-curve isotherm exhibits an initial slope, which is not affected by the adsorbate concentration unless the maximum adsorption capacity is accomplished. The C-curve trend is attributed either to a constant distribution of the adsorbate between the interfacial area and the bulk solution, or by a proportional trend between the amount of the available for adsorption surface and the surface excess. The C-curve isotherm is expressed mathematically by a linear equation (Sposito, 2008).

2.7.3 Adsorption under the view of surface complexation

The molecular units standing out of the solid surface and into the soil solution are called surface functional groups. In soils the most common functional groups are the reactive hydroxyl groups on oxide/clay minerals and carboxyl/phenol groups on organic matter. The reaction between the functional groups and the ion of the soil solution is called “surface complexation” and the product “surface complex”. Two general categories of surface complexes are considered; the inner-sphere and the outer-sphere surface complexes. As inner-sphere complexes considered those complexes that formed between the functional group and the ion, in the absence of water molecule between them. On the other hand, outer sphere complexes are formed when during the binding of the functional group and the adsorbed ion at least one molecule of water exists between them. Generally, inner sphere complexes are based on ionic or covalent or both of them bonds, while outer sphere complexes are formed as a result of electrostatic attractions. Therefore, inner sphere complexes are based on stronger bonds and thus are more stable compared to outer sphere complexes (Sposito, 2008; Goldberg et al., 2013).

As mentioned in the previous paragraph, adsorption process can be characterized as specific or non-specific. Specific adsorption is attributed to the occurrence of inner sphere complexes, which are formed as a result of high affinity of the ions for the solid surface. Contrary, non-specific adsorption is governed by the occurrence of electrostatic attractions between the ions and surface functional groups (outer sphere complexes) or by adsorption in the diffuse ion swarm. Adsorption via diffusion in the ion swarm indicates that the ion is not bounded with any functional group but occurs in the aqueous solution very closely to the solid surface, causing the neutralization of the surface charge. These types of ions are called readily exchangeable ions and can be easily replaced by leaching with an electrolyte solution of

prescribed composition, concentration and pH value. Usually, the fully solvated ions adsorbed on soils are considered as readily exchangeable ions, since their adsorption is based on the diffuse-ion swarm and outer-sphere complex mechanisms. However, the formation of functional groups on soils surface as a result of protonation or/and dissociation reactions undergone by the pH alterations can lead to the occurrence of ligand exchange reactions. At such reactions the hydroxyl of functional groups is replaced by the adsorbed ion, causing the occurrence of specific adsorption and further the formation of an inner-sphere complex (Sposito, 2008; Goldberg et al., 2013). In addition, surface complexes can be distinguished as monodentate or bidentate. Monodentate complexes are created by the formation of one bond between the adsorbing ion and the functional group, while bidentate ones by the formation of two bonds between the adsorbing ion and two surface functional groups (Goldberg et al., 2013).

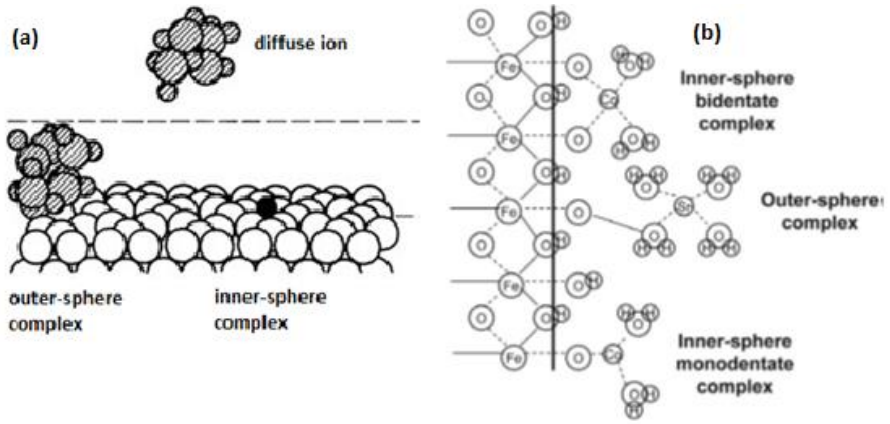

Source: a) (Sposito, 2008), b) (Goldberg et al., 2007).

Figure 2.11 Representation of a) inner- and outer-sphere complexes and diffuse ions and b) mono- and bi-dentate complexes.

In soils the electrical surface charge can be developed by two ways. As a result of isomorphic substitutions of ions with difference valence in soil minerals or due to reactions of surface functional groups with ions of the aqueous soil solution. As mentioned above, the pH value at which the surface charge is zeroed under constant conditions (temperature, pressure, solution composition) is called PZC (Sposito, 2008). In soils iron and aluminum oxides have high PZC values in the range 5 to 10, contrary to silicate clays which have low PZC in the range 2 to 5. The high PZC means that the net positive charge exists in high pH values, like these occurring in groundwater, and thus anion adsorption is enhanced.

Common soil anions can be adsorbed from soils by different ways. Chlorides (Cl^-) and nitrates (NO_3^-) are adsorbed as diffused ions or by forming outer-sphere surface complexes. On the contrary, oxyanions, and mainly phosphates (PO_4^{3-}), arsenates (AsO_4^{3-}), selenate (SeO_3^{2-}) etc. are usually adsorbed as inner-sphere surface complexes. Two important indications of the formation of inner-sphere complexes are the irreversibility of their adsorption and the adsorption strength despite pH alterations. Two examples of these indications are: a) the difficulty of anions like phosphates to be leached by anions like chlorides and b) the persistence of borate adsorption contrary to chloride adsorption for pH values higher than the PZC of the solid surface. In addition, spectroscopic evidence have shown that ions like

phosphate, selenite, silicate etc., are adsorbed via ligand exchange by soil minerals. Ligand exchange is a mechanism favored by pH < PZC in the case of anions (Sposito, 2008).

2.7.4 Surface complexation models

The term "model" refers to a representation of real conditions, taking into account those characteristics of the tested system that are related with the "problem" that must be solved. More specifically, chemical models are used for describing chemical systems and their properties as simpler and chemically correct, as possible. A chemical model, in order to be considered as "correct" and useful, must be set up as realistic and comprehensive, and its application to produce effective and predictive information. In terms of realism the model must be based on general chemical theories, in terms of efficiency must be able to describe experimental results, in terms of comprehension must be able to be applied in several experimental cases without modifications and finally in terms of prediction must be able to be applied under different chemical conditions (Goldberg et al., 2013).

In particular, surface complexation models (SCMs) are chemical models applied for describing adsorption phenomena on molecular basis and considering an equilibrium approach. SCMs contrary to empirical models adopt a more mechanistic approach to adsorption taking into account system's characteristics such as the properties of adsorbate and adsorbent, the pH values, the ionic strength and the component compositions. SCMs incorporate surface species, chemical reactions with their equilibrium constants and mass and charge balances. Thus they require a larger number of parameters to accommodate their increasing complexity. Most SCMs exhibit common characteristics and adjustable parameters. Their basic differences are attributed to structural representations of the solid – solution interface, such as the placement and configuration of the adsorbates. The main advantages of applying the surface complexation concept to describe adsorption are the following (Bethke and Brady, 2000; Koretsky, 2000; Goldberg et al., 2007; Alessi and Fein, 2010; Goldberg et al., 2013):

- Surface complexation modeling provides a thermodynamic framework for determining the adsorption reactions of contaminants.
- A plethora of chemical reactions that occur in the geochemical equilibrium can be used with their corresponding constants combined also with thermodynamic data of the species in the equilibrium.
- SCM modeling provides the ability for predictions over a range of chemical conditions keeping constant the values of the applied parameters despite chemical conditions can vary in space or time.
- The results of SCM modeling can be efficiently applied in transport modeling, which take into account chemical processes.
- SCMs may require less parameters determined compared with multiple empirical approaches, in order to incorporate physicochemical heterogeneities.

In order to retain the importance of SCMs on ion adsorption, the adsorption mechanisms must be determined using either direct or indirect experimental data. These data must be suitable to describe ion adsorption mechanisms, such as the PZC shifts, the ionic strength dependence and the calorimetry (Goldberg, 2007). Several researchers have applied SCMs adsorption

modeling in environmental engineering to investigate issues about the adsorption of heavy metal and inorganic ions on pure minerals, in most cases successfully. However, SCMs have rarely been applied for adsorption modeling on natural materials, like soils. Mouvet and Bourg (1983) were of the first researchers having used chemical equilibrium models in order to quantitatively simulate adsorption of metals to sediment. The difficulties on applying SCM models for describing adsorption is usually due to lack of data regarding parameters necessary for modeling and due to lack of information about surface solid properties (Wen et al., 1998). Three of the most common SCMs used for adsorption modelling on soils are the Constant Capacitance Model (CCM), the Double Layer Model (DLM), and the Triple Layer Model (TLM), which will be described below. However, it's not clear which of the three model can best simulate adsorption of contaminants on real soils. Wen et al. (1998) were of the first researchers having investigated the ability of these models on simulating adsorption of heavy metals on natural soilt.

The CCM, DLM and TLM models are two-pK models. This means that at all of these models the surface functional groups (mentioned as SOH) can undergo both protonation and dissociation reactions as shown at Table 2.8, contrary to one-pK models at which each functional group undergoes only one protonation reaction. In all these models the charges on the surface complexes are designated using formal charges.

Table 2.8 Protonation and dissociation reactions

A/A	Reaction	Constant
1	$SOH + H^+ \leftrightarrow SOH_2^+$	$K_+ = \frac{[SOH_2^+]}{[SOH]\{H^+\}} \exp[\frac{F\psi}{RT}]$
2	$SOH \leftrightarrow SO^- + H^+$	$K_- = \frac{[SO^-]\{H^+\}}{[SOH]} \exp[\frac{-F\psi}{RT}]$

where F: the Faraday constant, ψ: the surface potential, R: the molar gas constant and T: the absolute temperature. Square and curly brackets represent concentrations and activities, respectively. A schematic representation of the interfaces at these models is provided at Figure 2.12.

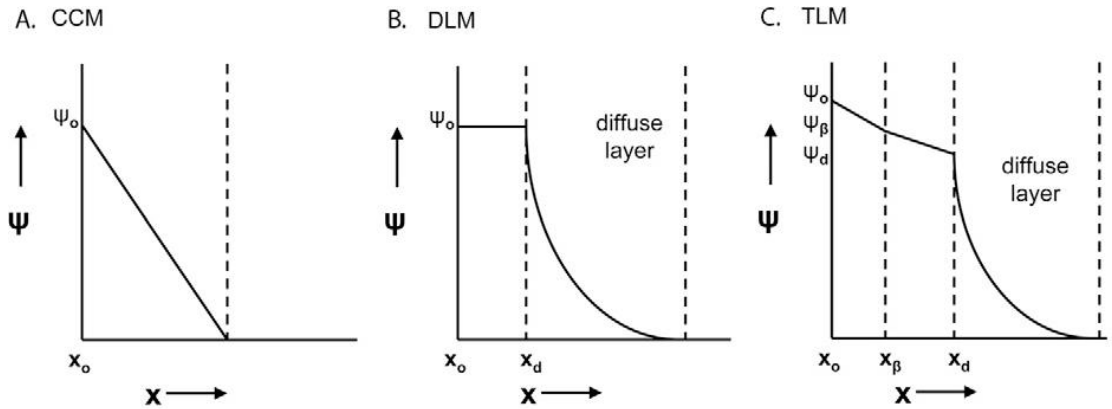

Figure 2.12 Schematic representation of the solid–solution interface for the surface complexation models (SCMs)

2.7.4.1. Constant capacitance model (CCM)

The CCM model was of the first models developed in order to describe the adsorption on the oxide mineral surface-aqueous solution interface. The CCM model is based on the following assumptions:

- all surface complexes are inner-sphere complexes and located in a single surface o-plane, with anion adsorption occurring via a ligand exchange mechanism,
- the constant ionic medium reference state determines the activity coefficients of the aqueous species in the conditional equilibrium constants and therefore no complexes are formed with ions in the background electrolyte,
- a linear relationship exists between surface charge and surface potential.

Surface complexes can be either monodentate or bidentate. Table 2.9 presents the reactions and their corresponding equilibrium constants used for modeling with the CCM model.

Table 2.9 Reactions and their corresponding equilibrium constants used at the CCM model.

No.	Reaction	Constant
1	$SOH + M^{m+} \leftrightarrow SOM^{(m-1)} + H^+$	$K_M = \frac{[SOM^{(m-1)}]\{H^+\}}{[SOH]\{M^{m+}\}} \exp[\frac{(m-1)F\psi}{RT}]$
2	$2SOH + M^{m+} \leftrightarrow (SO)_2M^{(m-2)} + 2H^+$	$K_M = \frac{(SO)_2M^{(m-2)}]\{H^+\}^2}{[SOH]^2\{M^{m+}\}} \exp[\frac{(m-2)F\psi}{RT}]$
3	$SOH + L^{l-} + H^+ \leftrightarrow SL^{(l-1)-} + H_2O$	$K_L = \frac{[SL^{(l-1)-}]}{[SOH]\{L^{l-}\}\{H^+\}} \exp[\frac{-(l-1)F\psi}{RT}]$
4	$2SOH + L^{l-} + 2H^+ \leftrightarrow S_2L^{(l-2)-} + 2H_2O$	$K_L = \frac{S_2L^{(l-2)-}]}{[SOH]^2\{L^{l-}\}\{H^+\}^2} \exp[\frac{-(l-2)F\psi}{RT}]$

where, M represents a metal cation with charge m+, and L an anionic ligand of charge l–.

2.7.4.2. Double layer model (DLM)

In the diffuse layer models, as in the case of CCM, all surface complexes are inner-sphere and are located in a single surface o-plane. However, the DLM also includes a "diffuse" layer, where counter ions are attracted to the charged mineral surface but remain in the bulk fluid phase. This difference between CCM and DLM models is represented by the modification of reaction 4 of Table 2.9 with the fourth reaction representing the complexes at the diffuse layer. In the DLM, metal–anion pairs are thought to be placed in the surface plane.

Table 2.10 Reactions and their corresponding equilibrium constants used at the DLM model.

No.	Reaction	Constant
1	$SOH + M^{m+} \leftrightarrow SOM^{(m-1)} + H^+$	$K_M = \frac{[SOM^{(m-1)}]\{H^+\}}{[SOH]\{M^{m+}\}} \exp[\frac{(m-1)F\psi}{RT}]$
2	$2SOH + M^{m+} \leftrightarrow (SO)_2M^{(m-2)} + 2H^+$	$K_M = \frac{(SO)_2M^{(m-2)}]\{H^+\}^2}{[SOH]^2\{M^{m+}\}} \exp[\frac{(m-2)F\psi}{RT}]$
3	$SOH + L^{l-} + H^+ \leftrightarrow SL^{(l-1)-} + H_2O$	$K_L = \frac{[SL^{(l-1)-}]}{[SOH]\{L^{l-}\}\{H^+\}} \exp[\frac{-(l-1)F\psi}{RT}]$

4	$SOH + L^{l-} + 2H^+ \leftrightarrow SHL^{(l-2)-} + H_2O$	$K_L = \frac{SHL^{(l-2)-}]}{[SOH]\{L^{l-}\}\{H^+\}^2}\exp[\frac{-(l-2)F\psi}{RT}]$

2.7.4.3. Triple layer model (TLM)

In the TLM model adsorbed ions are able to form both inner-sphere complexes to the o-plane surface and outer-sphere complexes to the outer β-plane, located between the surface plane and the diffuse layer (Figure 2.12). However, Sverjensky (2001) proposed that in some cases that the adsorbent has high dielectric constant inner-sphere complexes may reside in the β-plane. Thus, in the TLM, metal–anion pairs may occur either on the o-plane, or on the β-plane, or between the two planes. The following chemical reactions (Table 2.11) are defined in the TLM model. Reactions 1-4 represent the reactions of inner-sphere complexes while reactions 5-10 those of outer-sphere complexes.

Table 2.11 Reactions and their corresponding equilibrium constants used at the TLM model.

No.	Reaction	Constant
1	$SOH + M^{m+} \leftrightarrow SOM^{(m-1)} + H^+$	$K_M = \frac{[SOM^{(m-1)}]\{H^+\}}{[SOH]\{M^{m+}\}}\exp[\frac{(m-1)F\psi}{RT}]$
2	$2SOH + M^{m+} \leftrightarrow (SO)_2M^{(m-2)} + 2H^+$	$K_M = \frac{(SO)_2M^{(m-2)}]\{H^+\}^2}{[SOH]^2\{M^{m+}\}}\exp[\frac{(m-2)F\psi}{RT}]$
3	$SOH + L^{l-} + H^+ \leftrightarrow SL^{(l-1)-} + H_2O$	$K_L = \frac{[SL^{(l-1)-}]}{[SOH]\{L^{l-}\}\{H^+\}}\exp[\frac{-(l-1)F\psi}{RT}]$
4	$2SOH + L^{l-} + 2H^+ \leftrightarrow S_2L^{(l-2)-} + 2H_2O$	$K_L = \frac{S_2L^{(l-2)-}]}{[SOH]^2\{L^{l-}\}\{H^+\}^2}\exp[\frac{-(l-2)F\psi}{RT}]$
5	$SOH + M^{m+} \leftrightarrow SO^-–M^{m+} + H^+$	$K_M = \frac{[SO^- - M^{m+}]\{H^+\}}{[SOH]\{M^{m+}\}}\exp[\frac{F(m\psi_\beta - \psi_{0)}}{RT}]$
6	$SOH + M^{m+} + H_2O \leftrightarrow SO^-–MOH^{(m-1)} + 2H^+$	$K_M = \frac{[SO^- - MOH^{(m-1)}]\{H^+\}^2}{[SOH]\{M^{m+}\}}\exp[\frac{F[(m-1)\psi_\beta - \psi_0]}{RT}]$
7	$SOH + L^{l-} + H^+ \leftrightarrow SOH_2^+–L^{l-}$	$K_L = \frac{SOH_2^+ - L^{l-}]}{[SOH]\{L^{l-}\}\{H^+\}}\exp[\frac{F(\psi_0 - l\psi_\beta)}{RT}]$
8	$SOH + L^{l-} + 2H^+ \leftrightarrow SOH_2^+–LH^{(l-1)-}$	$K_L = \frac{SOH_2^+ - LH^{(l-1)-}]}{[SOH]\{L^{l-}\}\{H^+\}^2}\exp[\frac{F(\psi_0 - (l-1)\psi_\beta)}{RT}]$
9	$SOH + C^+ \leftrightarrow SO^-–C^+ + H^+$	$K_C = \frac{[SO^- - C^+]\{H^+\}}{[SOH]\{C^+\}}\exp[\frac{F(\psi_\beta - \psi_{0)}}{RT}]$
10	$SOH + A^- + H^+ \leftrightarrow SOH_2^+–A^-$	$K_A = \frac{SOH_2^+ - A^-]}{[SOH]\{A^-\}\{H^+\}}\exp[\frac{F(\psi_0 - \psi_\beta)}{RT}]$

where C^+ is the cation and A^- is the anion of the background electrolyte.

2.7.5 Approaches of SCMs application on natural materials

Adsorption modeling of heavy metals and inorganic ions on multi-component systems like soils is generally difficult and complicated, despite the advantages that SCMs offer compared to empirical methods. The main approaches that are used in order to quantitatively determine the adsorption process using SCMs are two:

- the component additivity (CA) approach and
- the general composite (GC) approach.

The CA approach aims at predicting adsorption in multi-sorbent systems taking into account the adsorption affinities of each component (adsorbent) – contaminant (adsorbate). These affinities are determined experimentally using single binary systems at which the relative concentrations of the adsorbent (the available sorption sites) are used. In order to be successful the application of an SCM model according to the CA approach three main hypotheses must be achieved/satisfied; a) no interactions occur between adsorbents, b) all the ions able to be adsorbed have the equivalent possibilities to access all the available surfaces and c) the formed surface complexes are the same with that formed at the binary (single adsorbent, single ion) experiments. Despite several applications of SCMs based on the CA approach have been made, the degree of success varied significantly (Alessi and Fein, 2010).

Contrary to the CA approach, the GC approach considers that the soil composition is too complex in order to distinguish and quantify the several individual phases. Thus, it is assumed that a general type of active sites exists on the soil surface. This assumption creates the need for using stoichiometry and formation constants obtained by fitting experimental data. A simplification of the approach includes the fitting of adsorption efficiency as a function of pH, even with no explicit determination of electrostatic energies. This fact means that the GC approach is less predictive compared to CA since it can be applied to cases for which experimental data exist, that will be further used for model calibration (Davis et al., 1998; Goldberg, 2007; Alessi and Fein, 2010).

Table 2.12 Main differences between CA and GC approaches used for adsorption by soils

CA approach	GC approach
Used for adsorption prediction.	Used for adsorption simulation.
Surface sites are unique since attributed to different adsorbents included in soils.	The assumption for generic surface sites at the tested material is made.
Site densities are quantified according to the presence of each surface in the soil.	Site densities are quantified by measuring the surface area and by fitting the experimental data for the soil.
Reactions' constants and stoichiometry are obtained from studies with single minerals.	Reactions' constants and stoichiometry are obtained by fitting to the experimental data of the tested soil.
Adsorption is considered to be the sum of adsorption efficiency of each individual adsorbent.	The site types and the constant values used are those that best simulate experimental data at each model used.

One of the first studies compared the two aforementioned approaches using the same SCM model, a two site-one proton DLM, was that of Davis et al. (1998). They aimed to simulate Zn(II) adsorption on a natural well-characterized soil. The CA approach under-predicted Zn(II) adsorption. The main reason for the unsuccessful application of the CA approach was thought to be the incomplete determination of site concentrations of each component of the soil. On the contrary, the application of the GC approach was more successful.

Concluding the application of the CA approach to geoenvironmental sorbents like soils demands very good and accurate characterization of the soil's composition, while the GC approach can be considered as more practical for modeling since requires less information (Davis et al., 1998).

3 METHODS AND PROTOCOLS

In order to achieve the aim of the thesis for investigating the geochemical behavior of Cr(VI) in ophiolitic soils and quantify those processes (mainly adsorption) able to affect its transport in geoenvironment the experimental steps described at Figure 3.1 were performed. The characterization/verification of the ophiolitic origin of the tested aquifer was performed via soil and groundwater physicochemical analysis. Soil analysis included also mineralogical analysis.

The second experimental step aimed at investigating the removal capacity of the tested soil for Cr(VI) and inorganic contaminants related to agricultural activities, like phosphates and nitrates. Batch experiments were carried out in order to determine the leachability of Cr(VI) and thus its desorption efficiency. The next series of batch experiments aimed at evaluating the Cr(VI) adsorption capacity of the tested ophiolitic soil as a function of pH and:

i. Soil mineralogy,
ii. Soil's particle size,
iii. Ionic strength of the soil solution
iv. Cr(VI) initial concentration
v. Nitrates concentration
vi. Phosphates concentration

In addition, the adsorption capacity of the ophiolitic soil for the inorganic contaminants was investigated. Most of the above mentioned series of batch experiments, and specifically series iii – v, were also carried out for the case of using pure synthetic goethite as adsorbent. Goethite was selected as an adsorbent to be compared with the ophiolitic soil since goethite is of the most common iron oxides in ophiolitic soils. A more detailed description of the series of batch experiments performed at the present thesis is given at Table 3.1.

In the third step, simulation of the adsorption capacity of the ophiolitic soil and goethite was performed applying the following three SCMs:

i. the Triple Layer Model (TLM),
ii. the Double Layer model (DLM) and
iii. the Constant Capacitance Model (CCM).

The corresponding reactions' databases for each model were developed and applied at the visual Minteq geochemical software. In the case of ophiolitic soil three different cases of solid concentration were used in order to simulate the effect of different minerals on the adsorption efficiency of the soil.

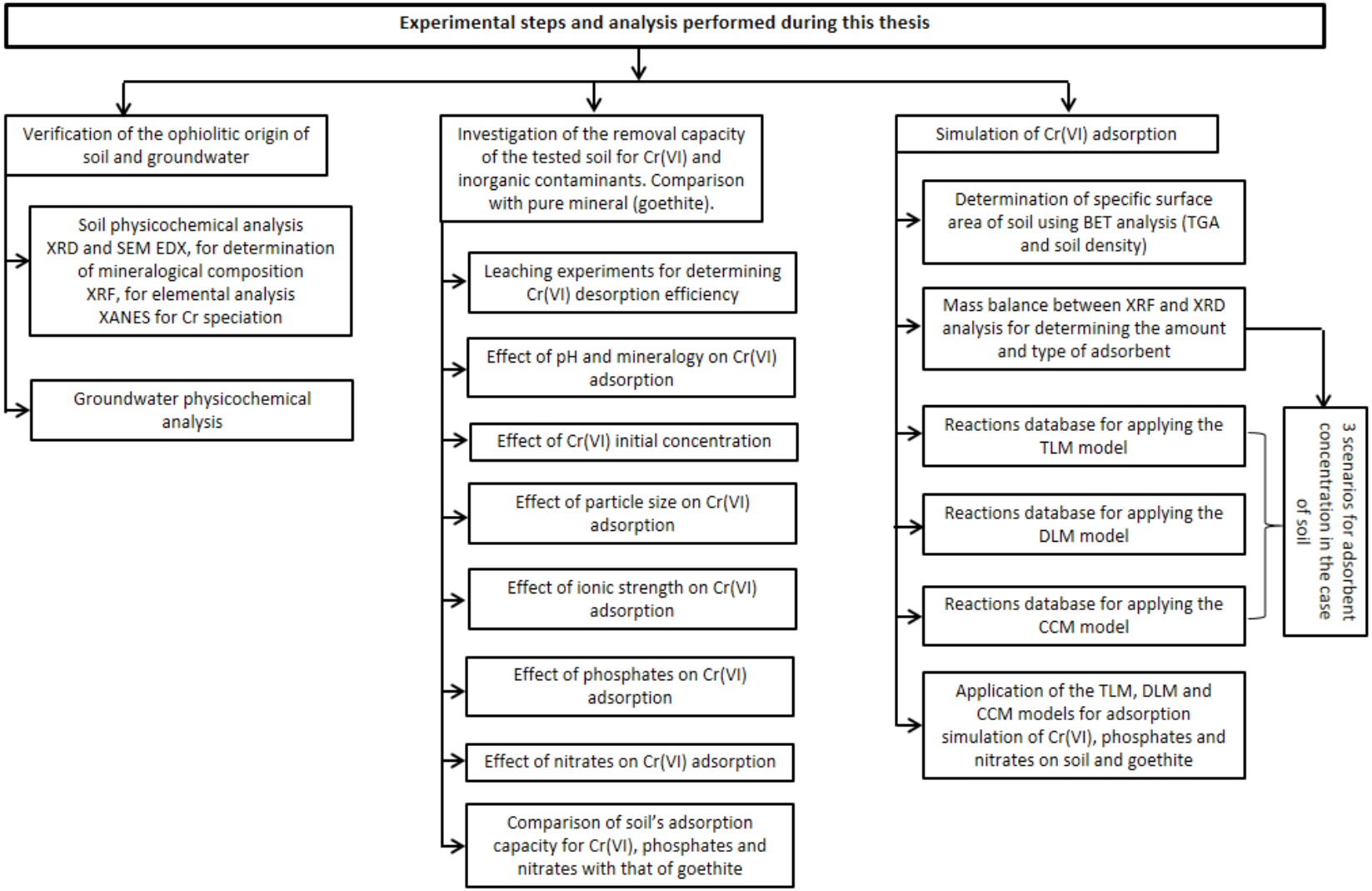

Figure 3.1 Schematic representation of the steps followed in this thesis

Table 3.1 Series and aim of batch experiments carried out

Adsorbent	Parameter		Contaminant			Aim
	pH	Ionic strength as NaCl (M)	Cr(VI)	PO_4	NO_3	
Soil	3 - 9	0.01	250 μg/L	-	-	The effect of soil particle size on Cr(VI) adsorption (4 fractions used)
		0.01	250 μg/L	-	-	The effect of soil mineralogy on Cr(VI) adsorption
		0.01	10 - 70 mg/L	-	-	The effect of Cr(VI) initial concentration (adsorption isotherms)
		0.01 & 0.1	250 μg/L	-	-	The effect of ionic strength on Cr(VI) adsorption
		0.01	-	8 mg/L	-	Adsorption of phosphates
		0.01	250 μg/L	8 mg/L	-	Competitive adsorption of Cr(VI) and phosphate
		0.01	-	-	5 mg/L	Adsorption of nitrate
		0.01	-	-	50 mg/L	
		0.01	250 μg/L	-	5 mg/L	Competitive adsorption of Cr(VI) and nitrate
		0.01	250 μg/L	-	50 mg/L	
Goethite	3 - 9	0.01 & 0.1	250 μg/L	-	-	The effect of ionic strength on Cr(VI) adsorption
		0.01	-	250 μg/L	-	Adsorption of phosphate
		0.01	-	8 mg/L	-	
		0.01	250 μg/L	250 μg/L	-	Competitive adsorption of Cr(VI) and phosphate
		0.01	250 μg/L	8 mg/L	-	
		0.01	-	-	50 mg/L	Adsorption of nitrate
		0.01	250 μg/L	-	50 mg/L	Competitive adsorption of Cr(VI) and nitrate

3.1 Selection and description of the study area

The selection of the study area was based on an extensive groundwater monitoring data base created by the Greek Institute of Geology & Mineral Exploration (Siemos, 2010) and the application of the following criteria: (a) significant and consistent Cr_{tot} groundwater concentrations, (b) presence of ophiolitic formations and (c) large distance from anthropogenic activities (Panagiotakis et al., 2012). The selected study area is located in northern Greece, near the town of Vergina and lies between latitudes 40◦28 and 40◦29 and longitudes 22◦18 and 22◦19, with the altitude ranging from 56 to 135 m (Figure 3.2). Vergina lies on a plateau at the southwestern edge of the Central Macedonia plain, where Mt. Vermio is located, and at the northern foot of the Pierian Mountains, which consist mainly of ophiolites with limestone lenses. The area geology comprises Quaternary deposits, although the wider area consists of the Almopia and Pelagonian geological formations (Figure A1.2). The stratigraphic column of the study area consists of the following formations from top to bottom (Latsoudas and Sonis, 1991; Papanikolaou, 2009).

1. Quaternary deposits: unconsolidated, unsorted rubbles and cobbles of carbonate and schist rocks and alluvial sediments.
2. Neogene fluviolacustrine deposits: clays, marls, sandstones and sands with banks of arenitic limestones or intercalations of conglomerates, with cobbles of quartz, metamorphic and volcanic rocks of ophiolitic composition.
3. Upper cretaceous limestones: unconformably emplaced over the underlying formations.
4. Flysch-phyllitic series: composed of metapelites, metasand-stones, shales and phyllites, as well as quartzites andschists-gneiss with marble fragments, limestone lenses and ophiolitc olistoliths.
5. Ophiolites: composed of strongly serpentinized and weath-ered ultrabasic and basic rocks, mainly pyroxenic and dunitic serpentinites with chromite crystals. Also, diabases, diorites, microgabbros and rodingites in form of veins occur.
6. Marbles and Schists of Pelagonian zone.

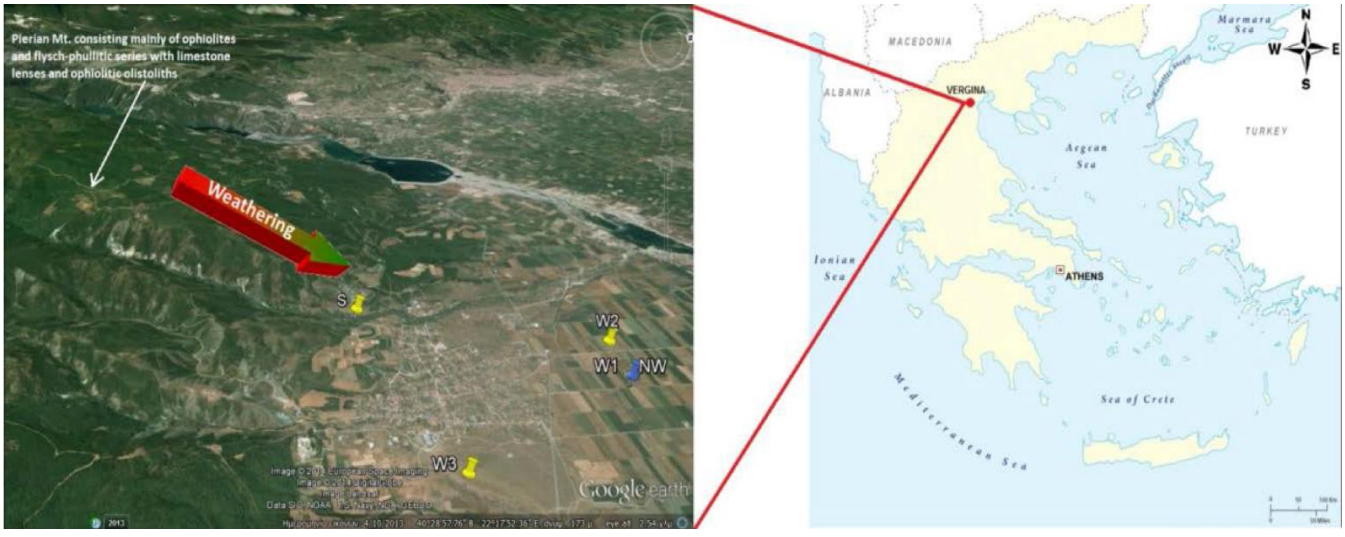

Figure 3.2 Location and topography of the study area

3.2 Soil and groundwater sampling

The sampling campaign consisted of four different stages regarding soil and groundwater sampling as mentioned below:

(a) the preliminary conventional groundwater sampling campaign from totally four sampling points; three existing irrigation wells (W1, W2 and W3) and a spring (S),
(b) the discrete groundwater sampling from the new well (NW),
(c) the topsoil sampling and
(d) the drillcore continuous sampling during the construction of the new well (NW).

3.2.1 Groundwater sampling

Firstly, the preliminary conventional groundwater sampling campaign was executed in order to verify the presence of Cr(VI) in the Vergina aquifer. Subsequently, a new well (NW) was drilled near the existing irrigation well (W1) with the highest measured Cr(VI) concentration. Upon completion of the drilling, Ø 75 mm diameter PVC pipes were installed at 93 m depth and screens were distributed along the different aquifers that were encountered: 41 – 49 m, 54 – 60 m, 74 – 86 m and 91 – 94 m. The annulus between borehole walls and casing was filled in with suitable gravel pack and a protective well head was installed to complete the construction of the groundwater monitoring well. Groundwater samples were also obtained from the NW with four different screens (41 – 49 m, 54 – 60 m,74 – 86 m and 91 – 94 m) using a discrete interval sampler (Solinst Model 425 Sampler) to assess groundwater quality.

The discrete sampling method employs a low-flow sampling technique at discrete aquifer locations within the water column that targets groundwater concentrations at specific depths rather than the mixed column concentrations obtained by conventional groundwater sampling. Although the installation of a multilevel well would probably give more reliable samples, this new groundwater well (NW) with discrete screens was chosen instead. This decision was mainly based on the two following reasons: (a) groundwater sampling using a single well with discrete screens is generally a widely applied (EPA, 2005; Nielsen, 2005) and reliable practice (Parker and Clark, 2004) with significantly lower capital cost compared to multi-level well and (b) this sampling method may be widely employed to determine background natural levels using existing wells (e.g., abandoned irrigation wells), without the need for new expensive installations.

At this point it should be noted that groundwater samples taken from the open borehole may not be representative of that specific depth, due to the possible cross contamination effect produced by the borehole itself, that hydraulically connects different aquifer units of different hydraulic heads. In this study, in order to minimize cross-contamination and remove standing water during sampling, all groundwater samples were obtained when 3 – 5 casing volumes had been purged using low-flow pumping that did not disturb the well.

3.2.2 Soil sampling

Solid samples were collected from NW well during drilling. Drillcore samples were collected every 20 – 50 cm along the whole NW depth. Topsoil samples were also collected covering an area of 34 m^2 around the NW. Soil samples for performing the analysis which will be described at the following paragraphs were obtained by applying the quadrants method at the collected soil samples. At this point should be mentioned that with the term "soil" we refer to all the soil/sediment samples collected by the new borehole.

3.3 Soil geotechnical properties

3.3.1 Determination of particle size distribution

Particle size distribution of the tested soil was performed according to the ASTM 2487-06 Standard Practice for Classification of Soils for Engineering Purposes. This practice describes a system for classifying mineral and organo-mineral soils for engineering purposes based on laboratory determination of particle-size characteristics, liquid limit, and plasticity index and was used when precise classification is required. This standard is the ASTM version of the Unified Soil Classification System. The group symbol portion of this system is based on laboratory tests performed on the portion of a soil sample passing the 3 in. (75 mm) sieve. This standard is used for qualitative application only and is limited to naturally occurring soils (ASTM 2487-06).

3.3.2 Determination of particle size distribution of the finer fraction

Bouyoukos method (Bouyoukos, 1936) aims at distinguish the particle size distribution of the fine soil fraction -2 mm by determining the following fractions:

- Sand (0.02 mm < d < 2 mm)
- Silt (0.002 mm < d < 0.02 mm)
- Clay (d < 0.002 mm)

The method is based on the application of Stoke's law, regarding the sedimentation velocity of the spherical granules (Equation 3.1):

$$\nu = \frac{\gamma s - \gamma w}{18\mu} D^2 \quad \text{(Equation 3.1)}$$

where:
γs the specific weight of soil
γw the specific weight of water
D the diameter of the spherical granule
μ the viscosity of the liquid.

The parameters determined by Stoke's law are not the real diameters of the granules but equivalent diameters of the spherical particles. By sedimentation due to gravity particles with

grain size 0.2 μm to 0,2 mm can be determined. The upper limit is referred to particles at which the flow around the granule is laminar, while the lower limit represents the granules at which the Brownian movement keeps the granules suspended infinitely (Mitchell, 1993). More details about the exact experimental procedure followed is provided at Appendix II.

3.3.3 Determination of particle size distribution using laser

The technique of laser diffraction is based on the fact that the particles that pass through a laser beam will scatter the light at an angle that is directly related to their size. The size range is directly related to the range scattering angle, but also with its intensity. The laser beam diffraction method is used to determine the particle size gradient of the fine fraction, with grain size less than 75 μm. A Mastersizer Microplus ver 2.19 laser instrument used in this study.

3.3.4 Atterberg limits

The limits of moisture and plasticity have been proposed by Atterberg et al. and describe the transition of soil from liquid to plastic state and then in the semi-solid and solid state, according to the percentages of the humidity. These limits indicate the soil's sensitivity at humidity alterations (Geotechnical engineering bureau of New York, 2007).

Liquid Limit (LL)

The Liquid Limit (LL) is the lowest water content at which the fine grained soil behaves like a viscous mud, flowing under its own weight. It represents the percentage of moisture content (Equation 3.2) by separating the plastic from the watery state. If the percentage moisture is higher than the moisture limit, the soil behaves more as a fluid mass while for percentage lower than this limit the soil behaves as a pliable material.

$$Moisture\ content = \frac{weight\ of\ water}{weight\ of\ oven\ dry\ soil} x100 \quad \text{(Equation 3.2)}$$

Then the LL is calculated using the following formula, in which the moisture content (W) expressed as a percent is multiplied by $(N/25)^{0.12}$ calculated for specific number of drops (Equation 3.3):

$$LL = Wx(N/25)^{0.12} \quad \text{(Equation 3.3)}$$

where:

N = the number of drops of the cup required to close the groove at the moisture content

W=moisture content

Values of $(N/25)^{0.12}$ have been calculated and presented in the literature.

Plastic Limit (PL)

The Plastic Limit (PL) is the lowest water content at which the soil exhibits plastic characteristics. It is expressed as the percentage value of the moisture content that separates the plastic state from a weak state. If the moisture content is between the plastic limit and the

liquid limit, the soil will behave as a pliable material. Below this limit, the soil, saturated or not, tends to be fragile. The plastic limit is calculated as show below (Equation 3.4):

$$\text{Plastic limit} = \frac{\text{weight of water}}{\text{weight of oven dried soil}} * 100 \quad \text{(Equation 3.4)}$$

Plasticity index

The range of water content, over which the soil remains plastic is called the plasticity index (PI). The soil plasticity index is calculated as the difference between the moisture limit and the plasticity limit (Equation 3.5), and is a dimensionless number. Both the liquid and plastic limits are moisture contents.

$$\text{Plasticity index} = \text{Liquid limit} - \text{Plasticity limit} \quad \text{(Equation 3.5)}$$

The plasticity index gives an indication of the reduction in moisture content required to convert a soil from a liquid to a semisolid state. It gives the range in moisture at which a soil is in a plastic state. The plasticity index may be considered as a measure of the cohesion possessed by soil. The plastic limit and the plasticity index are presented rounded to the nearest integer. For materials with plasticity index of less than 10, the index is expressed with accuracy of 0.1. Silts are non-plastic and thus PI ≈ 0

3.4 Physicochemical and geochemical characterization

3.4.1 Physicochemical analysis

Soil characterization included pH measurements according to method SW-846 (US EPA 9045C). The total organic carbon (TOC) was measured using the Walkley-Black method. Elemental soil analysis, including major and trace elements, performed by X-ray fluorescence spectrometry (XRF) using a Spectro Xepos instrument. Soil Analysis via XRF is a widely used and accepted method for site investigation, assessment, remediation, and monitoring. Sample preparation involved drying at 103 ^{0}C for 24 h and crushing to −100 μm. The total Cr(VI) concentration naturally occurring in the soil was determined using the USEPA method 3060A (alkaline digestion).

3.4.2 Mineralogical analysis

X-Ray Diffraction (XRD) technique provides detailed information about the atomic structure of crystalline substances. It is a powerful tool for the identification of minerals in rocks and soils. Using XRD technique it is able to determine the clay fraction of soils that is crystalline and which cannot be identified by other crystallographic methods. It can also be applied to coarser soil fractions. Its application can be performed by single crystals or powders. The most commonly used technique to soil mineralogy is XRD which was also used in this study (Harris and White, 2008). For XRD measurements a Brucker D8 Focus instrument was used. XRD patterns were collected between 5◦ and 65◦ with a 0.02◦ step size. Data were processed by the Jade software (Materials Data, Inc.) with reference to the International Center for Diffraction

Data database. Quantitative XRD analysis was based on the Rietveld method using the Whole Pattern Fitting method of Jade, suing structural data from the American Mineralogist Crystal Structure database.

The Rietveld method provides a relative quantification of the phases that are used in the model; thus, the presence of phases that are too disordered or too low in amount to observe by XRD is not captured and leads to an overestimation of all the observed phases in the model. To estimate the amorphicity of a specimen and obtain true phase quantification, the XRD powder sample is spiked with a known mass of a substance of very high crystallinity (an internal standard) (Jones et al. 2000; De La Torre et al. 2001; Whitfield and Mitchell 2003). The amorphous content is

$$A = \frac{W_{s,o} - W_s}{W_{s,o}(1 - W_s)}$$

Where:
Ws,o is the amount of the spike calculated by the Rietveld model and
Ws, the actual amount.
All phases can then be normalized using the amorphous content to obtain true weight percentages.

3.4.3 Scanning electron microscopy analysis

Scanning electron microscopy (SEM) analysis has a variety of applications in a number of scientific and industry-related fields, especially where characterizations of solid materials is required. The high-resolution, three-dimensional images produced by SEM providing topographical, morphological and compositional information makes them valuable for several science and industry applications. In addition, SEM can detect and analyze surface fractures, provide information in microstructures, examine surface contaminations, reveal spatial variations in chemical compositions, provide qualitative chemical analyses and identify crystalline structures. In this study SEM analysis was performed using a JEOL JSM5600 microscope equipped with an energy dispersive spectrometer (EDS) (Oxford ISIS 300).

3.4.4 Determination of specific surface area

The determination of the SSA of the soils was performed by applying the Brunauer, Emmett and Teller (BET) method. The BET method is based on gas adsorption by the external and porous surface of a solid matrix assuming an integrated monolayer. The gas is adsorbed with weak bonds to the solid surface (Van der Waals bonds) and can be desorbed by increasing the pressure at the same temperature. N was used as gas at boiling point (77.3 K). The monolayer capacity is measured by the adsorption isotherm. In this study a NOVA-1200 Ver. 5.01 instrument used.

3.4.5 Determination of soil density

Soil density was determined using a pycnometer flask. The protocol was applied as follows. The flask was weighted and then filled with deionized water at 20 ^{0}C temperature. The flask is

fully completed with water and then the lid is placed until overflow. Care should be taken to ensure that there are no bubbles and the flask is weighted. In a second step the soil sample is added in the flask and filled again with deionized water. The final weight is determined. The density is calculated according the following equation (Equation 3.6):

$$Density = \frac{Weight\ of\ soil}{\text{Weight of soil +Weight of flask filled with water} - \text{Weight of flask filled with water and soil}} \quad \text{(Equation 3.6)}$$

3.4.6 Thermogravimetric analysis (TGA)

Thermogravimetric analysis or thermal gravimetric analysis (TGA) is a method of thermal analysis in which the mass of a sample is measured over time as the temperature changes. The aim of this analysis was to verify that the soil matrix would not be altered/corrupted at temperature higher than 250 ^{0}C which is required for applying the BET method for SSA determination. TGA analysis was performed using a Setsoft 2000 instrument.

3.4.7 Determination of amorphous oxides content

The determination of amorphous iron oxides in the soil sample was performed by applying the Chao and Zhou (1983) method. According to this method, 1 g of soil is added to 20 mL of combined solution of $NH_2OH{\cdot}HCl$ (0.25M) and HCl (0.25M). The solution was placed at a waterbath at 50 ^{o}C for 30 min. The extraction was analyzed for iron content by applying Flame Atomic Absorption Spectroscopy (FAAS) using an Optima 2100 DV (Perkin Elmer Inc) instrument. This method was chosen since it is a fast method and minor dissolution of crystalline iron oxides (< 1% of the total iron) occurs.

3.4.8 Determination of divalent iron content

The determination of divalent iron or ferrous iron [Fe(II)] was performed by applying the acid digestion method. 1 g of pulverized soil with grain size less than 0.5 mm was added in a flask containing 100 ml of HCl 0.1 N. The flask with the soil solution was placed in an orbital shaker for 24 h in room temperature. Then the phenanthroline method was applied for the determination of ferrous iron. This method is based on the reaction of Fe(II) ions with 1,10-phenanthroline ($C_{12}H_8N$) forming a deep red solution which becomes darker as the concentration of iron increases. The method is suitable for solutions with Fe(II) concentration up to 5 mg/L. The complex is generally very stable and exhibits maximum absorption at 510 nm wave length. The extraction was measured for Fe(II) using a Hitachi U-1100 spectrophotometer. Soil pulverization is required since the method cannot be applied at solutions that contain chemical complexes due to interferences created, not allowing sufficient (or no) coloring of the solution.

3.4.9 X-ray Absorption Near Edge Spectroscopy

Three soil samples (a topsoil and two samples from 44 and 56.5 m depth), were analyzed at the Cr and Mn K-edge using X-ray Absorption Near Edge Spectroscopy (XANES). Samples were dried and pulverized prior to analysis. XANES analysis was performed on beamline X23A2 operated by the National Institute of Standards and Technology, at the National Synchrotron Light Source (Brookhaven National Laboratory, Upton, NY). Incident X-ray energy was scanned across the XANES region of the Cr K-edge (E = 5989 eV) and the Mn K-edge (E = 6539 eV) using a Si(3 1 1) mono-chromator and a single-bounce harmonic rejection mirror. The mono-chromator was calibrated using Cr and Mn foil. Fluorescent X-rays were collected using a Stern-Heald fluorescence detector. Data processing for alignment and normalization was carried out using the Athena software (Ravel and Newville, 2005). The final spectra was obtained as the result of three averaged scans.

3.5 Analytical methods

3.5.1 Groundwater analysis

Groundwater samples were analyzed in the field for indicator parameters such as pH, temperature, redox potential (with Ag/AgCl (3M KCl) reference electrode) and specific conductance.

Elemental analysis was performed using an Atomic Absorption Spectrophotometer (PERKIN ELMER 2100; using flame) for Ca, K, Na, Mg, Si analysis and an Inductively Coupled Plasma-Mass Spectrometry (ICP-MS) (Thermo X SERIER II) for Cr analysis. Cr(VI), was determined colorimetrically applying the diphenylcarbazide method (US EPA method 7196A) as it is described at the following paragraph (paragraph 3.5.2).

Nitrites (NO_2^-) were determined spectrometrically according to 4500-NO2−B standard method. The US EPA 375.4 turbidimetric method applied for determination of sulfates (SO_4^{2-}). Ammonium was determined according to the La Motte salicylate method. Phosphates, nitrates and chlorides were determined as mentioned at the following paragraphs (3.5.3 – 3.5.5)

Total alkalinity measurements (expressed as mg $CaCO_3$/L) were performed by titration with H_2SO4 (0.01 – 0.1 N) to pH equal to 4.5. The HCO_3^- concentration was then calculated assuming it was the only base contributing to the alkalinity.

The QA/QC measures included analysis of blanks and duplicate measurements every 10 samples for each parameter. The sum of negative and positive equivalents was also calculated to check the accuracy of chemical analyses. In the majority of groundwater samples the deviation was less than 5%.

3.5.2 Determination of Cr(VI)

Cr(VI) determination in groundwater and soil solutions was performed according to the 7196-A USEPA method. This method is used to determine the concentration of dissolved Cr(VI) in EP/TCLP characteristic extracts and groundwater and may also be applicable to certain domestic and industrial wastes, provided that no interfering substances are present. It is based on the reaction of Cr(VI) ions with 1,5-diphenylcarbazide ($C_6H_5NHNHCONHNHC_6H_5$) under acidic conditions (Equation 3.7). After this reaction the solution is colored as red-violet regarding Cr(VI) concentration.

$$Cr_2O_7^{2-} + 3\ H_4L + 6H^+ \rightarrow [Cr(III)(HL)_2] + Cr^{3+} + H_2L + 7H_2 \quad \text{(Equation 3.7)}$$

Where:
(H_4L) = 1,5 diphenylcarbazide & (H_2L) = 1,5 diphenylcarbazone

More details about the exact experimental procedure followed is provided at Appendix II.

3.5.3 Determination of phosphates concentration

The determination of phosphates, as orthophosphates ions (PO_4^{-3}, HPO_4^{-2}, $H_2PO_4^-$), was performed using the ascorbic acid method (Standard Methods for the Examination of Water and Wastewater, 2012). According to this method ammonium molybdate and antimony potassium tartrate react in acid medium with orthophosphate to form a heterpoly acid – phosphomolybdic aid – (Equation 3.8) that is reduced to intensely colored molybdenum blue by ascorbic acid.

$$PO_4^{3-} + 12(NH_4)_2MoO_4 + 24H^+ \rightarrow (NH_4)_3PO_4*12MoO_3 + 21NH_4^+ + 12H_2O \quad \text{(Equation 3.8)}$$

Then in the presence of ascorbic acid, molybdate that is contained in the ammonium phosphomolybdate is reduced to free molybdate coloring as blue the solution. Color intensity is analogous of phosphates concentration. Phosphates determination is performed colorimetrically at 880 nm wave length. The minimum detectable concentration is approximately 10 μg P/L. More details about the exact experimental procedure followed is provided at Appendix II.

3.5.4 Determination of nitrates concentration

The determination of nitrate ions was performed using the LCK 339 reagents of Hach-Lange. The method is based on the reaction of nitrate ions with 2.6-dimethylphenol in solutions containing sulphuric and phosphoric acids to form 4-nitro-2.6-dimethylphenol. This method is sufficient for nitrates determination in wastewater, drinking water, raw water, surface water, soils, substrates and nutrient solutions. The pH of the sample must be in the range 3-10 and the temperature of sample/reagents in the range 20 – 24°C. The measurement using a HACH spectrophotometer performed at 345 nm wave length. More details about the exact experimental procedure followed is provided at Appendix II.

3.5.5 Determination of chlorides concentration

The determination of chlorides was performed using the Iron(III)-Thiocyanate method (LCK 311, Hach-Lange). According to this method, during the reaction of chloride ions with mercury thiocyanate the slightly dissociated mercury(II) chloride is formed. Simultaneously an equivalent amount of thiocyanate ions are set free, which react with iron(III) salts to form iron(III) thiocyanate. The pH of the sample must be in the range 3-10 and the temperature of sample/reagents in the range 15 – 25°C. The measurement using a HACH spectrophotometer performed at 468 nm wave length. More details about the exact experimental procedure followed is provided at Appendix II.

3.6 Batch sorption - desorption experiments

Adsorption experiments that involve solid particles are generally carried out based on three stages:

i. Reaction of the adsorbent with the adsorptive included in an aqueous phase with constant composition, under constant temperature and pressure for a prescribed period until steady concentration of the adsorptive in the aqueous phase will be achieved (equilibration time) or lower in order to achieve the adsorption kinetics,
ii. Separation of the adsorbent from the aqueous phase using centrifugation, filtration, or gravitational settling,
iii. Quantification of the adsorbed chemical substance in both the aqueous and the solid phase.

In this study the soil fraction with grain size less than 0.5 mm was used as adsorbent in batch experiments. It is expected that the fine soil fraction determines the adsorption process in the aquifers and since the finer the fraction, the greater the adsorption effects, the soil fraction with grain size <0.5 mm was used in all the series of experiments at a concentration of 20 g/L. Soil samples were sterilized prior to the experiments in order to prevent microbial reduction of Cr(VI). The effect of pH on adsorption was tested using initial Cr(VI) concentration equal to 250 μg/L. This concentration was chosen as the upper limit of Cr(VI) concentration in an aquifer with ophiolitic background and low contribution of anthropogenic activities.

The experiments were carried out at room temperature (24±0.5 °C), in a 0.01 M NaCl solution, in the pH range from 3 to 9. The pH adjustment was performed using HCl/NaOH solutions of 1 M. Erlenmeyer flasks containing 50 mL of the suspension were placed in an orbital shaker at 150 rpm for 24 h. For Cr(VI) determination soil solutions were filtered using 0.45 μm pore filters and Cr(VI) was then determined using EPA method 7196A. The batch experiments were carried out in duplicates. The accepted error percentage between the experimental results was 10%. The removal of Cr(VI) was determined by the difference between the initial and the final concentration in the equilibrium solution of Cr(VI), according the following equation (Equation 3.9):

$$\%\text{removal} = \frac{C_0 - C_f}{C_0} x100 \quad \text{(Equation 3.9)}$$

Where:
C_0 (μg/L) is the initial concentration of Cr(VI)
C_f (μg/L) the final concentration of Cr(VI) in the equilibrium solution

After removal of the supernatant and filtration, the recovered soil was added again to a 0.01 M NaCl solution and the pH was raised to 11 in order to desorb the adsorbed amount of Cr(VI). This pH value was selected in order to prevent dissolution of the solid phases. The suspension was shaken for another 24 h to facilitate complete Cr(VI) desorption into solution. The recovered Cr(VI) in this solution was measured using the same filtration and analysis process. Thus, the following concentrations of Cr(VI) may be defined at each pH value tested at the batch experiments (Equations. 3.10 - 3.12):

$Cr(VI)_{removed} = Cr(VI)_{added\ (250\ \mu g/L)} - Cr(VI)_{remaining\ in\ solution\ at\ the\ given\ pH}$ (Equation 3.10)

$Cr(VI)_{adsorbed} = Cr(VI)_{released\ in\ solution\ at\ pH\ 11} - Cr(VI)_{naturally\ occurring\ in\ soil}$ (Equation 3.11)

$Cr(VI)_{reduced} = Cr(VI)_{removed} - Cr(VI)_{adsorbed}$ (Equation 3.12)

3.6.1 Soil properties that affect Cr(VI) adsorption

The aim of this first series of batch experiments was to investigate the processes that affect Cr(VI) removal in serpentine soils and study these processes as a function of a) pH, b) mineralogy, c) soil's particle size and d) Cr(VI) initial concentration.

3.6.1.1. Effect of mineralogy

During the series of batch experiments for determining the effect of pH, the presence of black grains with magnetic properties was observed upon addition of the soil in the NaCl solution. This magnetic fraction was easily removed using a magnetic bar. Three series of experiments were carried out using the initial soil sample (bulk soil), the residual soil fraction after the removal of the magnetic fraction (non-magnetic fraction) and the isolated magnetic fraction.

3.6.1.2. Effect of particle size

The effect of particle size was tested using the non-magnetic soil fraction. The non-magnetic sample with grain size -0.5 mm was further sieved in order to obtain the three following fractions: a) 0.5 mm > d > 0.25 mm, b) 0.25 mm > d > 0.075 mm and c) d < 0.075 mm. Sampling from the obtained fractions was performed using the quadrant method at each fraction.

3.6.1.3. Effect of initial Cr(VI) concentration

A $K_2Cr_2O_7$ stock solution of 100 mg/L was used for achieving initial concentrations of Cr(VI) between 10 to 100 mg/L. The non-magnetic soil sample with grain size -0.5 mm was used. Four series of experiments were carried out, keeping constant the pH value at 4.5, 5.5, 6.5 and 7.5. In addition, Langmuir (Equation 2.1) and Freundlich (Equation 2.2) isotherms were fitted in order to extract the necessary distribution factors for transport modeling.

3.6.2 Other contaminants effects on Cr(VI) adsorption

In this second series of batch experiments the effect of inorganic major anions like phosphates and nitrates that are usually presented in groundwater was investigated.

Phosphates (PO_4^{3-}) concentration used in the batch experiments was equal to 8 mg/L. PO_4^{3-} were added using a 100 mg/L stock solution of sodium phosphate monobasic (NaH_2PO_4).

Nitrates (NO_3^-) were added using a 500 mg/L stock solution of $NaNO_3$, at two different concentrations:
a) 5 mg/L, representing the case of a non-contaminated aquifer and
b) 50 mg/L, this value is the maximum allowable concentration of nitrates in groundwater according to Greek legislation and is usually detected in groundwater affected by intensive agricultural activities.

In addition the effect of ionic strength of the soil solution was tested. The effect of ionic strength of the solution was tested by using two different concentrations of NaCl solution 0.01 and 0.1 M, as background electrolyte.

3.7 Goethite

3.7.1 Goethite characterization

The goethite used in this study was a commercial powder purchased by Sigma–Aldrich (purity equal to 30-63% Fe). The pH of goethite and the total SSA were determined by the method SW-846 (US EPA 9045C) and the N_2/BET adsorption method, respectively.

3.7.2 Adsorption of Cr(VI) on goethite

Batch experiments were performed for investigating the adsorption capacity of goethite for Cr(VI), phosphates and nitrates. In addition, binary systems of these chemicals were used in order to determine the effect of phosphates and nitrates on Cr(VI) adsorption. The concentration of goethite and temperature kept constant in all series of experiments at 10 g/L and 25 ^oC, respectively. Goethite suspensions were created by adding 0.01 M NaCl solution in order to simulate the ionic strength that usually occur in groundwater. In order to achieve equilibrium, Erlenmeyer flasks containing 20 mL of the suspension were placed in an orbital shaker at 200 rpm for 24 hours. All the experiments were carried out in a pH range from 4 to 9.

The pH adjustment was performed using HCl/NaOH solutions of 0.01 M. In order to investigate the adsorption of phosphates and nitrates on goethite similar experiments as in the case of soil, were performed.

3.8 Adsorption simulation

Adsorption simulation was performed using the Visual Minteq v.3.1 software (Gustafsson, 2013). This is a freeware chemical equilibrium model for the calculation of metal speciation, solubility equilibrium, sorption and other chemical processes for natural waters. It combines state-of-the-art descriptions of sorption and complexation reactions. In this software adsorption can be described using: a) adsorption isotherms, b) ion exchange mechanisms and/or c) surface complexation models.

In the Visual MINTEQ, the surface complexation models included can simulate the distribution of ions between adsorbed and dissolved phases in a colloidal suspension. These models are primarily used for oxides and clay mineral edges. Surface complexation calculations are the most advanced features of MINTEQ. Such models, address adsorption reactions for inorganic constituents in which there is a significant chemical contribution to the adsorption process ("surface complexation reactions"). This is done in a thermodynamically more correct way compared to the isotherms, usually taking into account both chemical and electrostatic contributions to adsorption. The following six surface complexation models can be used applying Visual MINTEQ:

- Constant Capacitance Model (CCM)
- Diffuse Layer Model (DLM)
- Triple Layer Model (TLM)
- Basic Stern Model (BSM)
- Three Plane Model (TPM)
- Non-Electrostatic Model (NEM)

These six models are closely related in many ways. Each treats adsorption as a surface complexation reaction and each accounts for the electrostatic potentials at the charged surface. Their primary difference lies on the way electrostatics are included. In this study the Constant Capacitance Model (CCM), the Diffuse Layer Model (DLM) and the Triple Layer Model (TLM) were used.

4 SOIL AND GROUNDWATER PHYSICOCHEMICAL ANALYSIS

4.1 Stratigraphy of sampling well

Figure 4.1 shows a simplified geological cross section of the borehole constructed in Vergina area (see Chapter 3) and used herein for soil sampling down to 98 m depth. The unsaturated zone extended to 43 m depth, after which a succession of 3 aquifers and aquicludes was encountered. The unsaturated zone consisted of alternating layers of clayey sand with gravel that predominated at the top 10 m, followed by a dense clay-sand mixture that present some variation in the relative contents of each with depth. Rock fragments with the characteristic green color of serpentinites were observed throughout the soil column, confirming the clear presence of ophiolites. The aquifers consisted of gravelly particles mixed with sand and clay, while the impermeable layers had predominantly clay, also mixed with some sand and gravel. Thus, the cross-section does not fully capture the complexity of the material, in the sense that the layers were not as clearly defined as in the illustration but rather continuously changing in proportions. Overall, the layers of the cross section were reflective of the first two formations of the stratigraphic column in the area (Section 3.1).

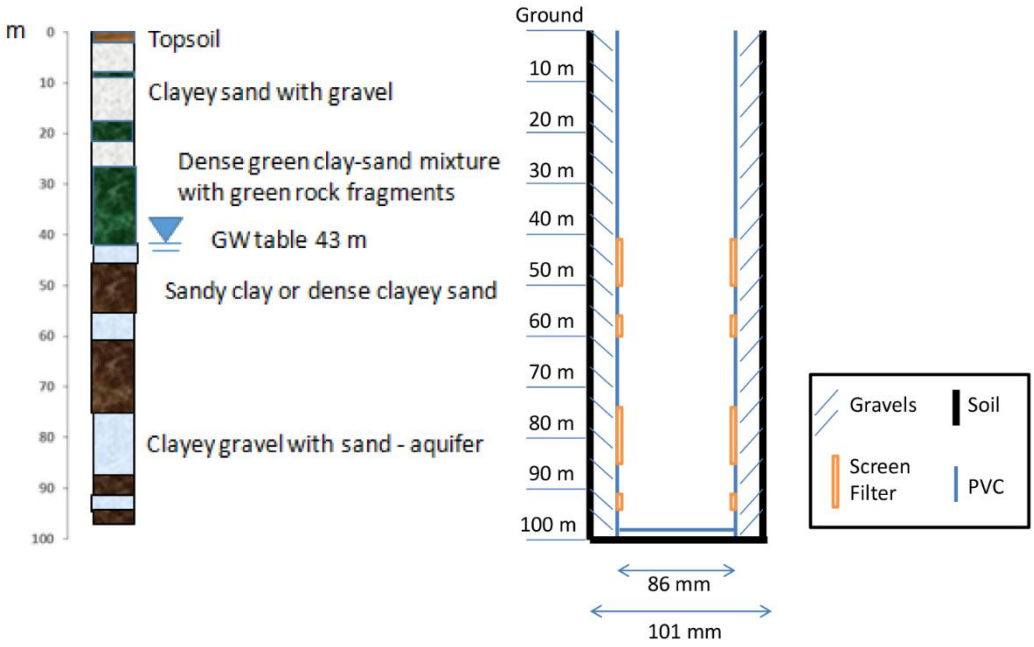

Figure 4.1 Statigraphy and well design of the sampling well

4.2 Soil classification according to geotechnical properties

The grain size distribution of the tested soil is usually determined through sieve analysis. The results of this analysis are shown at Figure 4.2, presenting the grain size distribution curve by calculating the percentages of weight passing different sieve sizes. The total weight of the soil used was 648.45 g and the loss of weight after sieving was 1.1%. Results showed that the collected soil was consisted of gravels at 25.2%, sand at 69.8% and clays at 5.0% indicating that the soil is classified as a coarse grained soil.

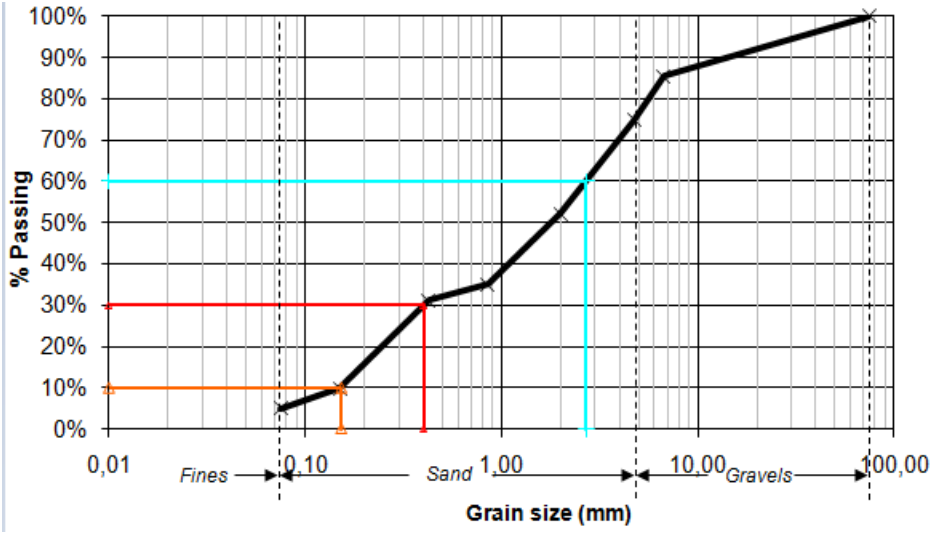

Figure 4.2 Grain size distribution curve of the collected soil.

The grain size distribution curve is a way of giving a complete and quantitative picture of the relative proportions of the different grain sizes within the soil mass and can be used for estimating several parameters regarding the tested soil. Such a parameter is the D_{10}, called as effective grain size, and is defined as the maximum value of sieve diameter that the 10% of soil weight passes through. This parameter is an indication of soil permeability characteristics. Similarly, the D_{30} and D_{60} values are commonly used for soil characterization and represent the maximum diameter of the sieve pores that is necessary in order to pass through the 30% and 60% of the soil weight, respectively. The values of the active sizes are presented at Table 4.1.

Table 4.1 Values of D_{10}, D_{30} and D_{60} active sizes.

Active size	D_{10}	D_{30}	D_{60}
Value	0.151	0.401	2.703

Based on these values further information regarding the shape of the grain size distribution curve can be described through the parameters, of a) coefficient of uniformity (C_u) (Equation 4.1) and b) coefficient of curvature (C_c) (Equation 4.2). They are defined as:

$$C_u = \frac{D_{10}}{D_{60}} \qquad \text{(Equation 4.1)}$$

$$C_c = \frac{D_{30}^2}{D_{10} D_{60}} \qquad \text{(Equation 4.2)}$$

The C_u and C_c parameters of the tested soil are equal to 17.88 and 0.39, respectively. Using these values we can draw conclusions about the occurrence of a well or not graded soil. A well graded soil is thought when a good distribution of sizes in a wide range occurs and the smaller grains fill the voids created by the larger grains, producing a dense packing. Such soils exhibit smooth and concave curves. Sands with $C_u > 6$ and $C_c = 1 - 3$ values are well graded, while the corresponding values for gravels are $C_u > 4$ and $C_c = 1 - 3$. Otherwise the soil is not well graded and called poorly graded. Poorly graded soils are further distinguished to uniform at which the grains are about the same size, and gap-graded soils when there are smaller and larger grains,

but none in an intermediate size range. Thus the soil tested in this study can be classified as uniform poorly graded soil (Sivakugan, 2000).

Commonly, for soils that contain both coarse and fine grains a further analysis of the finer fraction is needed, since the sieve analysis has been carried out firstly. In order to verify the classification as coarse grained soil the grain size distribution of the -2 mm fraction was investigated using the Bouyoucos method. The results of this analysis showed that the sample is consisted of 58.74% fine sand (0.063 mm < d < 2 mm), 27.74% silt (0.002 mm < d < 0.063 mm) and 13.52% clay (d < 0.002 mm)

A third analysis was also carried out using the extra fine fraction (d<0.075 mm) of the tested soil using a Laser instrument (Figure 4.3). Two samples of the -0.075 mm fraction used in order to achieve repetition of the analysis. The results showed that this fraction was consisted of 78.07% silt (0.002 mm < d < 0.075 mm) and 18.62% clay (d < 0.002 mm).

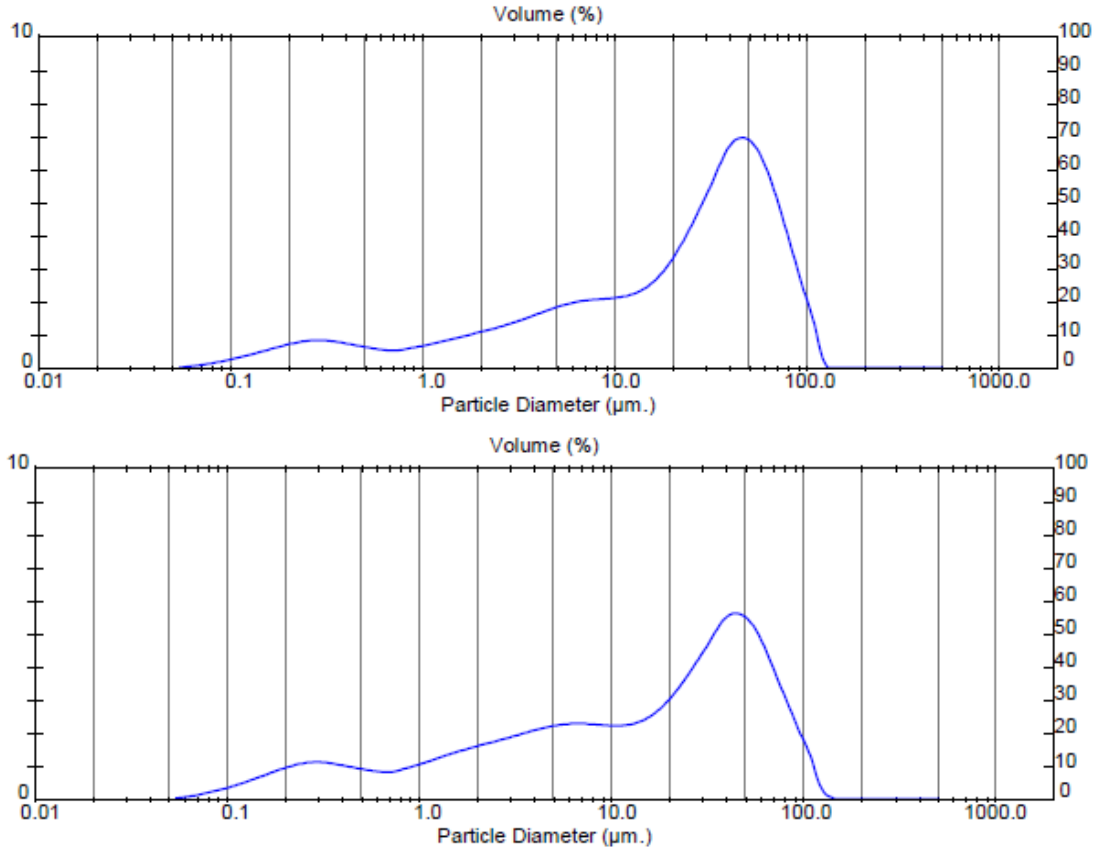

Figure 4.3 Grain size distribution of two samples with grain size –0.075 mm.

Despite the indications that our soil is classified as a coarse grained soil the Atterberg limits were also determined. The Atterberg limits are of empirical nature. However, they had been correlated very well with the geotechnical characteristics of fine grained soils and are therefore very valuable in soil classification. The LL and PL limits of the tested soil calculated as 41.75% and 20.90%, respectively. Thus the PI limit is equal to 20.85%. High PI value means higher range of humidity for which ths soil keeps its plasticity. According to Cassagrande's chart (Figure 4.4) the soil is characterized as clay with low plasticity (CL).

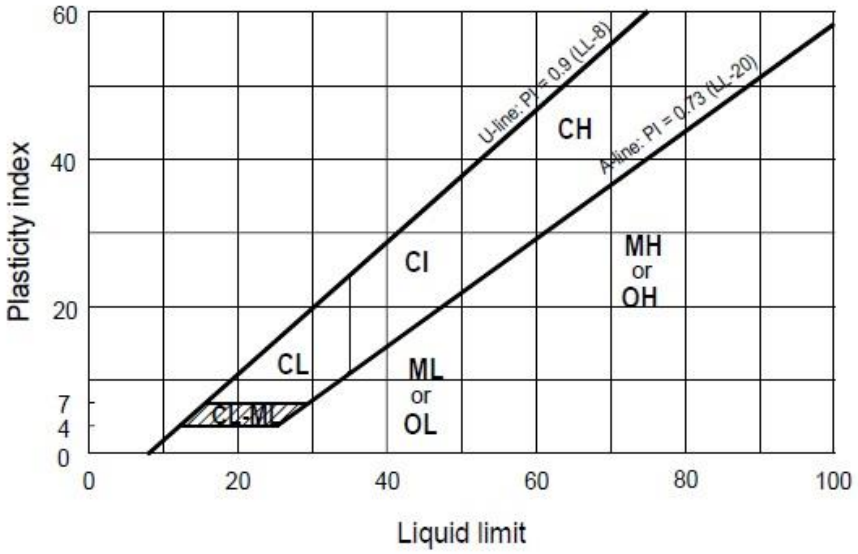

Figure 4.4 Casagrande's PI-LL chart

Overall, according to ASTM 2487-06 unified soil classification system (ASTM, 2006) the soil is characterized as poorly graded sand with silty clay and gravel (SP-SC) since more of the 50% retained the 0.075 mm sieve, the percentage of sand was higher than gravels, the percentage passed the 0.075 mm sieve was 5 - 10%, the Cc value was lower than 1 and the gravels percentage higher than 15%.

4.3 Soil mineralogy

Four soil samples from different horizons (topsoil, 3, 44 and 58 m depth) and two rock fragments from 44 m depth were analyzed with XRD in order to verify the ophiolitic origin of the soil. All soil samples showed similar mineral assemblage shown in Figure 4.5, with the exception of vermiculite, which was only identified in samples from the saturated zone. In soil, vermiculite is a clay mineral that is known as a weathering product of serpentines (Hseu et al., 2007; Chrysochoou et al., 2016). Generally, serpentinitic soils exhibit magnesic mineralogy (except for the fragments presented in such soils) since a percentage higher than 40% w/w of magnesium-silicate occur in their geological composition. Magnesium and silicate minerals, like serpentine minerals (antigorite, chrysotile, lizardite) as well as talc, olivines, Mg-rich pyroxenes and amphiboles, occur predominantly in the fine -2 mm fraction. In addition, serpentines exhibit low substitutions of iron for magnesium but high incorporation rates of Fe occurs in peridotite to minerals like magnetite and hematite (Covelo et al., 2007). The tested soils were a mixture of relicts and weathering products of both ultramafic and mafic rocks, with serpentine minerals being typically the predominant phase and indicating that the ultramafic contribution is more pronounced.

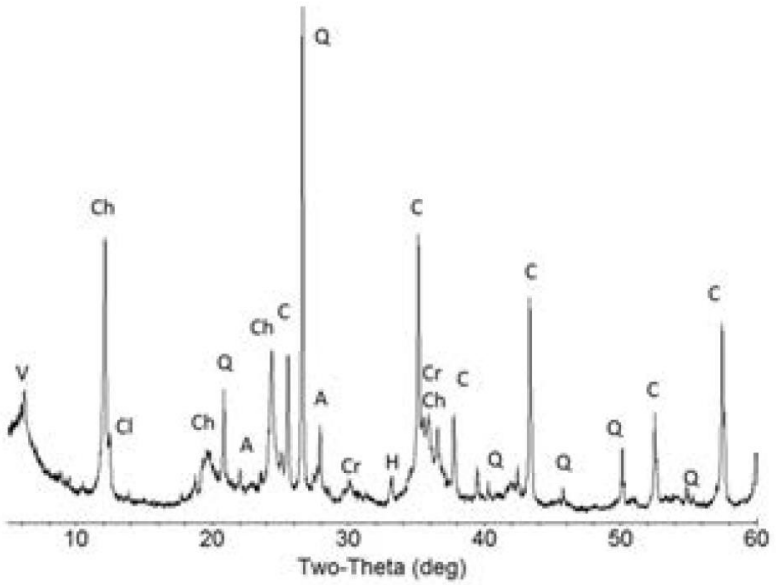

Figure 4.5 XRD pattern of soil sample recovered at 44 m depth (A: Albite, C: Corundum, Ch: Chrysotile, Cl: Chlorite, Cr: Chromite, Q: Quartz, V: Vermiculite).

Table 4.2 provides the quantitative mineralogy of a representative soil sample, obtained by applying the quadrants method, from 44 m depth as observed by the XRD pattern at Figure 4.5. Applying the Rietveld method Corundum was used to back-calculate the amorphous content using the estimated amount versus the known amount (section 3.4.2). The results showed that chrysotile was the mineral with the highest content in the soil sample, while important was also the content of the amorphous phase.

Table 4.2 Quantitative mineralogy of a representative soil sample with grain size -0.5 mm (44 m depth).

Mineral Name	Chemical Formula	Wt. (%)
Albite	$NaAlSi_3O_8$	6.8
Chlorite	$(Mg,Fe)_6(Si,Al)_4O_{10}(OH)_4$	8.8
(Magnesio)Chromite	$(Fe,Mg)Cr_2O_4$	3.5
Chrysotile	$Mg_3Si_2O_9H_4$	35.3
Hematite	Fe_2O_3	1.6
Quartz	SiO_2	12.6
Vermiculite	$Mg_{3.41}Si_{2.86}Al_{1.14}O_{10}(OH)_2(H_2O)_{3.72}$	4.4
Amorphous		27.0

The XRD patterns of the rock fragments are provided in Figure 4.6. Two types of rocks were identified; one containing chrysotile, diopside ($Ca(Mg,Al)(Si,Al)_2O_6$) and chromite, and another one containing albite, quartz and chlorite. Chrysotile, diopside and chromite are typical minerals occur in ultramafic rocks. Chrysotile is the main mineral of serpentinized ultramafic rocks, diopside belongs to the pyroxene mineral group, while chromite is a mineral of ultramafic rocks, which exhibits persistence during serpentinization and weathering processes (Oze et al., 2004). Regarding the minerals of the second type of rocks, albite and quartz are not related to the ultramafic background of the area but their occurrence and association with

chlorite as well as muscovite ($KAl_2(AlSi_3)O_{10}(OH)_2$) and hematite, is indicative of the presence of gabbro or greenschist, which are igneous and metamorphic mafic rocks, respectively (www.britannica.com). However, the observed minerals in soil and rocks are in accordance with the general geological background of the area.

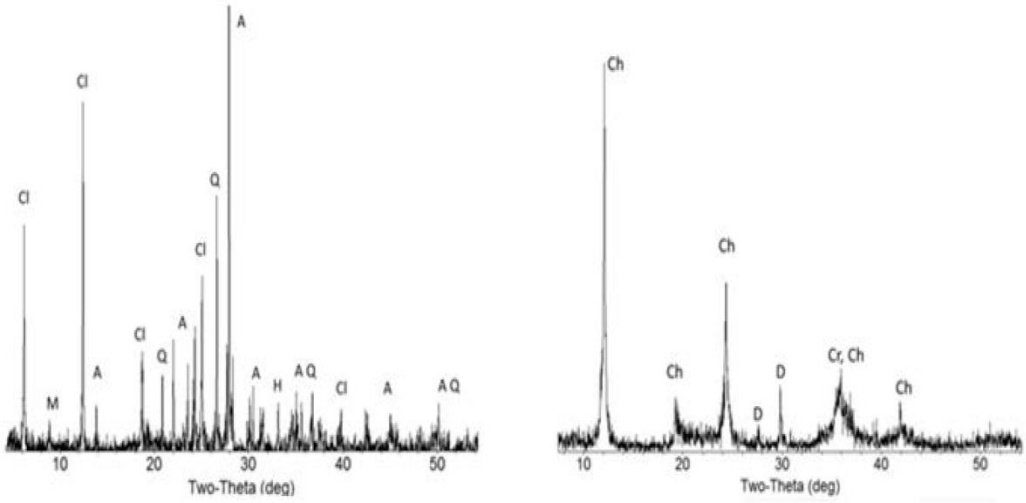

Figure 4.6 XRD patterns of rock fragments recovered from 44 m depth (A: Albite, Ch: Chrysotile, Cl: Chlorite, Cr: Chromite, D: Diopside, H: Hematite, M: Muschovite, Q: Quartz).

After the addition of soil in the aqueous solution the presence of a discrete solid phase presented as black grains was obvious. This phase exhibited magnetic properties and could be isolated from the bulk sample using a magnetic bar as mentioned in section 3.4.1.1, and so on will be called “magnetic fraction”. Figure 4.7 presents the two XRD patterns of the soil sample with grain size -0.5 mm and the isolated magnetic fraction. Both patterns contain the typical minerals of serpentine origin, like chromite/magnetite and chrysotile, as well as quartz and albite as observed in the bulk sample and discussed above (Figure 4.5). However, the relative intensity of chromite and chrysotile in the magnetic fraction is higher, while the content of alumino-silicates is very low. This fact, is in agreement with the accumulation of Fe and Cr in the magnetic fraction, and the lower concentration of Si as it will be discussed below.

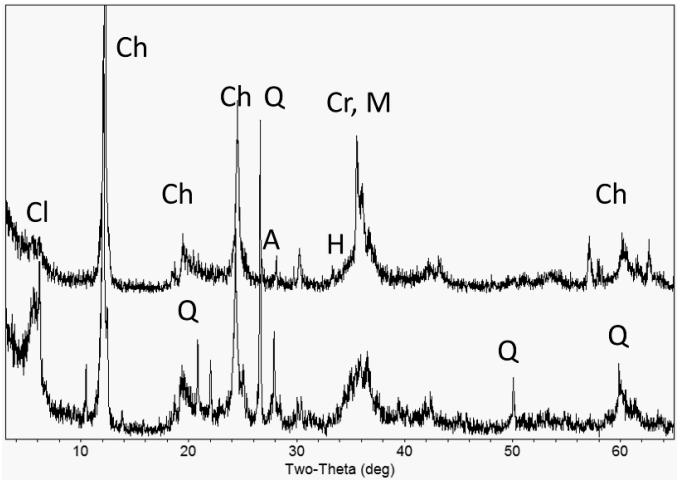

Figure 4.7 Comparison of the XRD patterns of the bulk soil (bottom) and the magnetic fraction (top) (A: Albite, Ch: Chrysotile, Cl: Chlorite, Cr: Chromite, H: Hematite, M: Magnetite, Q: Quartz).

The presence of chromite ($Fe^{2+}Cr_2O_4$) and Cr-magnetite ($Cr\text{-}Fe^{2+}F^{3+}{}_2O_4$) as observed by the XRD analysis was also verified by SEM-EDS analysis (Figure 4.8; Table A3.1 Appendix III). SEM analysis showed the occurrence of a spinel mainly covered by bulk serpentinized mass (black area).

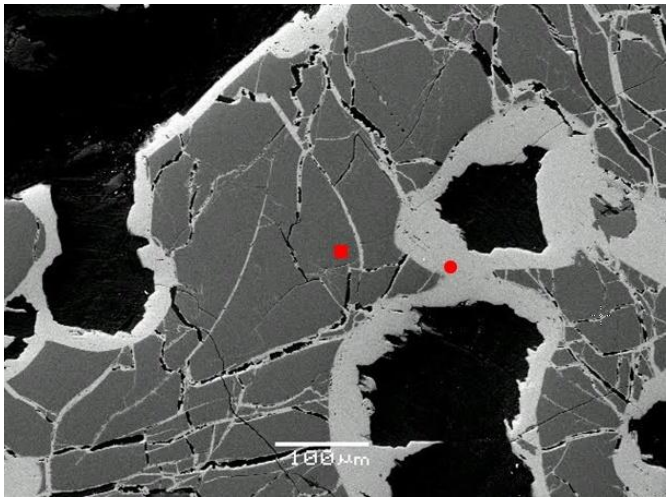

Figure 4.8 SEM image of a soil sample with grain size -0.5 mm (circle: Cr-magnetite ($Fe^{2+}Fe^{3+}{}_2O_4$); rectangular: chromite ($Fe^{2+}Cr_2O_4$)).

The presence of chromite and magnetite with isomorphic substitutions between Mg with Fe^{2+} and Cr with Fe^{3+} is typical for serpentine soils (Barnes and Roeder, 2001; Farahat, 2008). Economou-Eliopoulos (2003) mentioned that apart from grained magnetite in a soil matrix, magnetite can be associated with chromite since magnetite is the final product of sequential transformations of chromite to ferrian-chromite and finally to magnetite. Another option is the occurrence of magnetite as rims on chromite.

4.4 Physicochemical analysis

Table 4.3 presents the physicochemical analysis results of the topsoil and soil samples as a function of depth. Soil pH values ranged from 7.2 to 8.8, with values increasing steadily with depth. Most serpentine soils present slightly acidic to neutral pH values (Oze et al., 2004), and a literature review indicated that the observed values are amongst the highest observed globally (pH = 5 – 7.5 according to references presented in Table 2.3). These high pH values can be justified by two possible reasons. At first, the high Mg content of pure serpentinite has an equilibrium pH of 8.3, due to the presence of Mg(II), a strong base-forming cation (Mizuno et al., 1979). Thus, relatively un-weathered serpentine soil with low organic matter is expected to have higher pH values. Secondly, the presence of limestone that dominates the geological background of the area provides an alkaline environment (Latsoudas and Sonis, 1991). Despite the low content of calcium in the tested samples, the soil solution may be affected by the occurrence of limestone up-gradient of the sampling area.

Apart from the relatively high pH values of the tested samples, an increase of pH with depth was also observed. Topsoil samples (0.05 m) exhibited the lowest pH values about 7.3. For depths higher than 0.6 m pH values increased in the range 8.0 to 8.6 (Table 4.3). Similar results

in serpentine soils have been observed by Oze et al. (2004). This trend is probably attributed to the absence of organic matter and weathering/leaching processes in higher depths, which result in increasing pH (Rabenhorst et al., 1982; Gasser et al., 1995; Shallari et al., 1998). Topsoils are mostly influenced by organic matter and especially in agricultural areas by acidification due to the use of ammonium fertilizers (Mills et al., 2011). Vergina area is characterized by intensive agricultural activities and thus both parameters mentioned are able to play an important role in the case of soils near the surface. Acidification of deeper samples is possibly attributed to the presence of weathering processes, which cause the substantial leaching of base-forming cations [Mg(II)] and accumulation of acid-forming cations [Al(III) and Fe(III)] (Oze et al., 2004; Caillaud et al., 2011). However, the effect of weathering as described above has been investigated at soil samples obtained from some meters depth (e.g. <5 m depth). In such depths the weathering processes occur in higher extend than in higher depths, such as 100 m in our case, where weathering may not be so extensive. A further investigation of the elemental distribution along the depth profile could verify the discussion above about weathering.

Table 4.3 Chemical analysis results of soil samples

Layer	Depth	pH	LOI	C	Mg	Si	Fe	Al	K	Ca	Cr	Mn	Co	Ni	Cr(VI)
	(m)		(g/Kg)					(mg/Kg)							
GSC	0.05	7.3	165	14.0	159	192	84	11,488	4,232	5,643	2,805	1,549	244	>3,143	4.5
	0.05	7.4	179	19.7	162	191	80	10,641	830	5,286	2,471	1,472	181	>3,222	7.5
	0.05	7.2	168	13.5	194	213	62	15,512	5,394	3,929	2,585	930	157	1,965	4.0
GSC	0.6	8.0	155	9.9	159	201	77	12,971	4,647	10,571	2,274	1,394	220	2828	2.9
GSC	2.8	8.3	130	1.1	161	194	79	11,224	4,398	4,929	2,203	1,394	197	>2,357	2.7
CL	5.2	8.2	138	0.6	214	200	60	1,112	830	2,071	1,410	1,085	189	>2,357	4.2
GSC	7.8	8.1	130	0.9	219	199	57	1,853	1,328	2,571	1,919	852	149	>2,357	5.2
CL	10.4	8.1	134	2.7	167	204	74	14,029	4,398	3,571	2,257	1,162	189	>2,357	3.2
GSC	43.1	8.5	98	0.8	163	225	60	20,647	2,738	8,000	3,944	1,085	142	>2,357	1.7
CL	45.0	8.4	107	0.8	147	224	69	23,612	5,062	6,429	4,393	1,085	157	1807	1.4
CL	46.5	8.3	132	0.7	170	212	69	16,518	4,730	3,429	2,091	1,085	173	>2,357	1.9
GSC	48.1	8.2	131	0.6	230	206	65	265	581	3,500	4,057	930	157	>2,357	2.1
GSC	56.6	8.1	110	0.4	226	204	72	8,735	3,153	5,214	12,137	1,317	173	2121	1.5
GSC	59.0	8.6	140	0.6	154	208	72	20,965	3,734	6,214	5,199	1,162	157	2043	1.1
CL	75.0	8.6	151	2.1	124	225	63	30,706	8,879	7,429	2,919	1,007	173	>2,357	1.0
GCL	79.0	8.6	140	0.5	226	210	66	3,547	1,577	4,357	5,455	930	118	>2,357	0.8
GSC	82.6	8.7	109	0.8	185	221	64	10,959	<83	7,214	6,187	1,085	165	1885	0.8
GSC	83.6	8.8	122	0.9	197	212	56	9,265	2,821	5,357	3,073	1,007	142	1964	2.5
GCL	92.4	8.5	154	0.6	190	210	66	6,247	2,821	4,643	5,357	930	165	>2,357	0.7
GCL	93.1	8.6	152	0.5	195	206	74	4,871	2,489	6,357	9,880	1,007	157	>2,357	1.3

GSC: Gravelly sand with clay, CL: sandy clay, GCL: sandy clay with gravel

Elemental analysis results (Table 4.3) showed that soil samples have low Si (191 – 225 g/kg) and high Mg (159 - 230 g/kg) contents compared to the average concentrations of the elements globally, which is 330 and 5 g/Kg, respectively (Sparks, 2003). However, the observed elemental distribution is typical of serpentine soils (Fandeur et al., 2009). Cr_{tot} concentration decreased in the first 5 m with concentrations ranging between 1,410 and 2,805 mg/Kg (Table 4.3). This decrease is a result of the weathering processes to the upper layers, which cause substantial leaching of mobile elements like Mg and accumulation of immobile ones like Fe, Al, Mn and Cr near the surface (Bulmer and Lavkulich, 1994). Moving deeper, in the depth range from 5.2 to 7.8 m, it is clear that concentrations of Fe, Al, Mn and Cr decrease, while Mg increases, contrary to the shallower depths (0.6 - 2.8 m), where its concentration remains almost constant (average conc. ≈198 g/Kg) (Table 4.3). These results confirmed the presence of weathering processes in the unsaturated zone, a phenomenon that has been observed in several areas with serpentinitic soils in the geological background. For depths higher than 43 m (saturated zone) an overall increase of Cr_{tot} concentrations was observed compared to the concentrations of the unsaturated zone (Figure 4.9). Similar results were observed by several studies showing that chromium concentration presented a decreasing trend for depths down to 5 m (Oze et al., 2004; Caillaud et al., 2009; Fandeur et al., 2009; Dzemua et al., 2011) followed by an increase at higher depths (Dzemua et al., 2011). In all these studies the trend was attributed to the effect of weathering processes, which resulted in accumulation of immobile elements near the surface. In addition, among the concentrations measured in the saturated zone, two extremely high Cr_{tot} concentrations observed about 10,000 and 12,000 mg/Kg, at 93 and 57 m depth, respectively. Such values are usually identified in lateritic soils areas with tropical climate like New Caledonia, Sri Lanka, Brazil and Africa as mentioned in Table 2.3. In temperate climate areas only in France a similar concentration at about 8,000 mg/Kg, at shallow soil layers (≈1 m), has been observed (Caillaud et al., 2009). These heterogeneities in chromium concentrations can be attributed to factors such as heterogeneity in the mineralogical and chemical composition of the parent rocks and different characteristics of weathering processes (e.g. weathering stage, age).

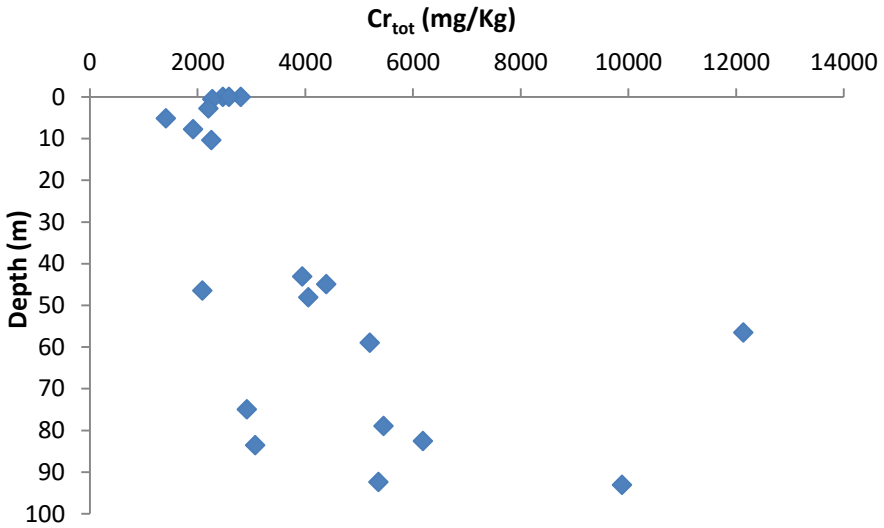

Figure 4.9 Cr_{tot} concentration profile along 100 m depth.

On the contrary, Cr(VI) exhibited the opposite trend compared to Cr_{tot}, with almost continuous decrease with increasing depth (Figure 4.10). Three clusters of Cr(VI) concentrations can be distinguished. Firstly the three topsoil samples, with the highest Cr(VI) concentrations ranging between 4 and 7.5 mg/Kg. The second cluster including samples collected down to 10.5 m depth with concentrations ranging between 2.7 and 5.2 mg/kg and finally the samples collected from the saturated zone with lower concentrations ranging between 0.7 mg/kg and 2.5 mg/kg. The samples of the saturated zone showed a decrease of Cr(VI) concentration with depth, despite the increase of Cr_{tot} in the soil. This observation may be related to factors that influence Cr(III) oxidation like the decrease of weathering at higher depths, rendering Cr(III) less available for oxidation.

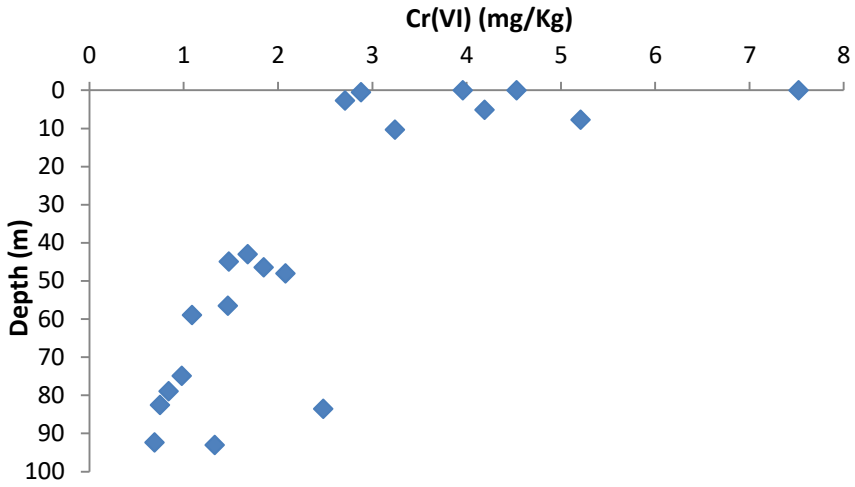

Figure 4.10 Cr(VI) concentration profile along 100 m depth.

In general, for depths higher than 43 m, where the first aquifer is encountered the concentrations of the elements discussed above seem to change overall. The indication for this observation is the value of LOI, which represents the volatile materials lost from the soils sample during heating. Such materials are usually "combined water" like hydrates and labile hydroxy-compounds and carbon dioxide from carbonates. LOI values are shown to be lower at samples collected from the saturated zone compared to those of the unsaturated zone. This is likely due to the greater weathering and the earlier hydration stage in shallower depths. It is obvious that the very deep layers (>80 m) are richer in un-weathered serpentine materials.

The MgO - SiO_2 – (Fe_2O_3 + Al_2O_3) ternary plot (Figure 4.11) presents a comparison between the soil chemistry data of this study and selected literature data related to ultramafic soils and rocks. The Vergina's samples were overall poorer in Fe and Al (10 – 20%), about average in Mg content (30 – 40%) and on the high end of Si content (80 – 90%). The higher Si content was related to the presence of non-ophiolitic materials origin, like mafic rocks, as it has also been observed by XRD analysis (quartz and albite minerals). The lower Al content can verify the higher pH of the Vergina soil, given that Al contributes significantly in the soil acidity. Al contributes indirectly to soil acidity since pH decrease leads to Al solubilization through hydrolysis.

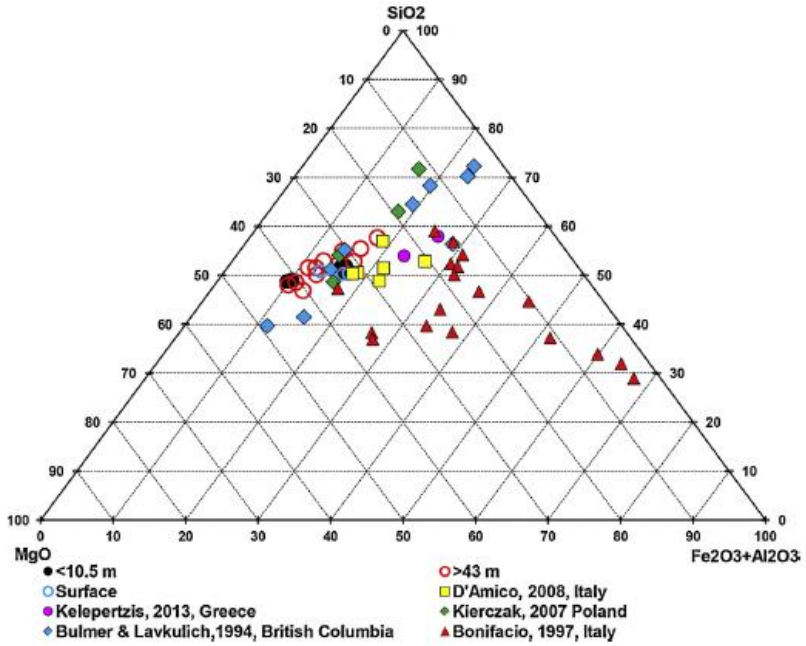

Figure 4.11 Ternary SiO_2 – MgO – (Fe_2O_3 + Al_2O_3) plot for Vergina's soil and other ultramafic soils globally.

Table 4.4 shows the values of Pearson correlation factors (r) between the values of elements concentration, pH and depth. From this analysis the three topsoil samples were excluded since they exhibited different chemical properties such as the higher carbon content and the lower pH. Correlation was considered as significant when r>0.7. Thus, the most significant correlation observed were between depth/pH (proportional, r=0.79), depth/Cr(VI) (inversely proportional, r=-0.79), Mg/K and Mg/Al (inversely proportional, r=-0.86 and r=-0.91, respectively) and Fe/Mn and K/Al (proportional, r=0.72 and r=0.86, respectively). Regarding the correlation of K/Al it may be attributed to the presence of these elements in non-ultramafic minerals, contrary to Mg, which is the main element in soils with ultramafic origin. Thus their correlation factor value provides an indication of their distribution across the geological section, giving information about the presence of ultramafic and non-ultramafic background. The most contrasting values of Al and Mg concentration were observed at 43, 45, 59 and 75 m depth (Figure 4.1), indicating the occurrence of non-ultramafic minerals there. A similar observation is made for Ca exhibiting its higher concentrations at the three upper aquifers (43.1 – 45 m, 59 m and 75 m). Only the deepest aquifer (92 m) exhibited a clear ophiolitic origin. According to these observations, it may be expected that Mg and Si concentrations could be correlated with pH and Cr as well. However, this fact was not verified by these data. The reason may that silicon exhibits higher concentrations in non-ultramafic minerals and so its contribution between ultramafic and non-ultramafic minerals could not be distinguished. Regarding Mg, its high mobility as a result of weathering processes, renders the creation of vertical profile difficult. This fact further verifies that Cr concentration increasing trend in the saturated zone is strongly related to the ultramafic geological background especially in very high depths (>80 m) and in the zones of aquicludes.

Table 4.4 Correlation factors, excluding topsoil samples.

	Depth	pH	Mg	Al	Si	K	Ca	Mn	Fe	Co	Cr_{tot}	Cr(VI)
Depth	1											
pH	0.79	1										
Mg	0.08	-0.17	1									
Al	0.07	0.23	-0.91	1								
Si	0.54	0.56	-0.44	0.65	1							
K	0.05	0.12	-0.86	0.87	0.45	1						
Ca	0.16	0.23	-0.57	0.55	0.42	0.51	1					
Mn	-0.47	-0.38	-0.35	0.27	-0.31	0.34	0.42	1				
Fe	-0.22	-0.34	-0.29	0.12	-0.38	0.30	0.27	0.72	1			
Co	-0.60	-0.60	-0.35	0.12	-0.43	0.37	0.21	0.72	0.57	1		
Cr_{tot}	0.58	0.18	0.32	-0.14	0.10	-0.14	0.18	0.06	0.24	-0.26	1	
Cr(VI)	-0.79	-0.58	0.24	-0.38	-0.61	-0.33	-0.43	0.03	-0.20	0.32	-0.55	1

At a next step fractionation of a soil sample, used as working sample in this study, collected from 44 m depth was conducted. This aimed at determining the distribution of Cr_{tot}, Cr(VI) and other elements collected from 44 m depth. Fractionation included six fractions as mentioned in Table 4.5. The fraction with grain size - 0.5 mm (4^{th} fraction), which will be used for the experimental needs of this study and will be called as “bulk sample”, was further divided in two more fractions the “non magnetic” and the “magnetic” fractions.

Fe and Cr_{tot} exhibited their highest concentrations in the fraction with grain size between 0.5 and 2 mm, without any important variations among the six analyzed fractions. However, these elements concentrations in the isolated magnetic fraction, which weighs about 10% of the bulk sample, were significantly higher compared to the non-magnetic fraction. In particular, Fe and Cr concentrations in the magnetic fraction were two and seven times higher compared to the non-magnetic fraction. The mass balance for these two elements in the magnetic and the non-magnetic fractions coincides satisfactorily with the mass measured in the bulk sample. Another observation from this analysis is that magnesium, manganese and cobalt concentrations were slightly higher in the magnetic fraction, contrary to aluminum and silicon concentrations which were significantly lower. These observations verify the mineralogy of this fraction as discussed above (Figure 4.8; Table A3.1 Appendix III).

Table 4.5 XRF analysis for the tested soil fractions using a bulk sample of 44 m depth.

Soil sample	Grain size (mm)	Elements (mg/Kg)							
		Fe	Al	Cr	Mg	Si	Mn	Co	Cr(VI)
1st fraction	d>4.75	52,563	19,170	1,724	152,220	226,240	830	117	n.q.
2nd fraction	2<d<4.75	64,323	13,511	3,632	173,820	210,700	1,032	156	n.q.
3rd fraction	0.5<d<2	67,179	12,515	4,767	171,000	207,386	1,092	162	n.q.
4th fraction	0.25<d<0.5	61,062	n.q.	2,148	n.q.	n.q.	1,175	n.q.	0.67
5th fraction	0.075<d<0.25	63,800	n.q.	1,658	n.q.	n.q.	1,248	n.q.	0.76
6th fraction	d<0.075	69,786	n.q.	1,522	n.q.	n.q.	1,458	n.q.	0.81
"Bulk" soil	d<0.5	74,270	17,350	3,754	150,720	209,766	1,215	153	1.47
"Non-magnetic" fraction	d<0.5	61,278	18,281	2,361	144,480	207,386	1,164	149	0.87
"Magnetic" fraction	d<0.5	129,290	3,857	14,197	153,240	148,820	1,264	263	0.94

n.q. not quantified

In order to verify the possible presence of the tested elements (Fe, Cr, Mg, Si, Al) in the amorphous phase the mass balance was applied at the -0.5 mm bulk fraction based on the concentration results as calculated through quantitative XRD (Table 4.2) and measured by XRF (Table 4.5). The SEM-EDX analysis was used in order to better identify the composition of the (magnesio)chromite mineral referred at Table 4.2. The results are presented in Table 4.6 and indicate that the amorphous phase consisted mainly of Fe, Mg and Si, while Al and Cr occured in the crystalline phases. The presence of iron in the amorphous phase indicated the presence of iron (oxy)hydroxides. Poorly crystallized goethite is thought as the predominant amorphous iron hydroxide in serpentine soils, without excluding the presence of other amorphous iron oxides (Chardot et al., 2007). Goethite, as well as hematite, has been identified in serpentine soils in Greece (Kelepertzis et al., 2013). The presence of silicon and magnesium can be attributed to the occurrence of amorphous silicon oxides or cryptocrystalline and amorphous magnesite, respectively. These minerals are commonly presented as alteration products of serpentinized ultramafic rocks (Peterson, 1984; Zachmann and Johannes, 1989).

Table 4.6 Mass balance determined by XRF and XRD.

Element	Fe (g/Kg)	Mg (g/Kg)	Si (g/Kg)	Al (g/Kg)	Cr (mg/Kg)
Total XRD	41.1	111.7	163.8	19.2	4.6
XRF	74.3	150.7	209.8	17.4	3.8
Amorphous (XRF - XRD)	33.2	39	46	-1.8	-0.8
XRD/XRF (%)	55	74	78	111	121

At a next step, XANES analyses were conducted to investigate chromium speciation. Since a) chromium speciation is affected by the presence of oxidants and b) the main oxidants in soils are the Mn oxides, XANES analysis was performed for both chromium and manganese. As it can be observed from Figure 4.12a, which depicts the chromium spectra, there is no Cr(VI) feature at the characteristic energy of 5993 eV. This is attributed to the very low Cr(VI) concentrations, which cannot be detected by XANES. Regarding the Cr(III) spectra its edge is placed in the 6070 eV resembling the presence of pure chromite ($FeCr_2O_4$), including low

content of Cr(III) oxyhydroxides. Similar analyses performed by Fandeur et al. (2009), who mentioned that Cr(III) derived from serpentinitic soils was bound in chromite in 25-30% and the rest was bound in two iron oxides, goethite and hematite. These data are quite in accordance with the results of this study. Less amounts can be observed in other serpentine minerals. In the case of manganese the XANES spectra proved the presence of all the three oxidation states, Mn(III) (peak at 6558 eV), Mn(IV) (peak at 6561 eV) and Mn(II) (peak at 6553 eV) (Figure 4.12b) indicating the presence of chromium oxidants. Fandeur et al. (2009) showed that in lateritic soils the Mn(III) and Mn(IV) species occurred in shallower depths, while deeper the Mn(II) occurred predominantly.

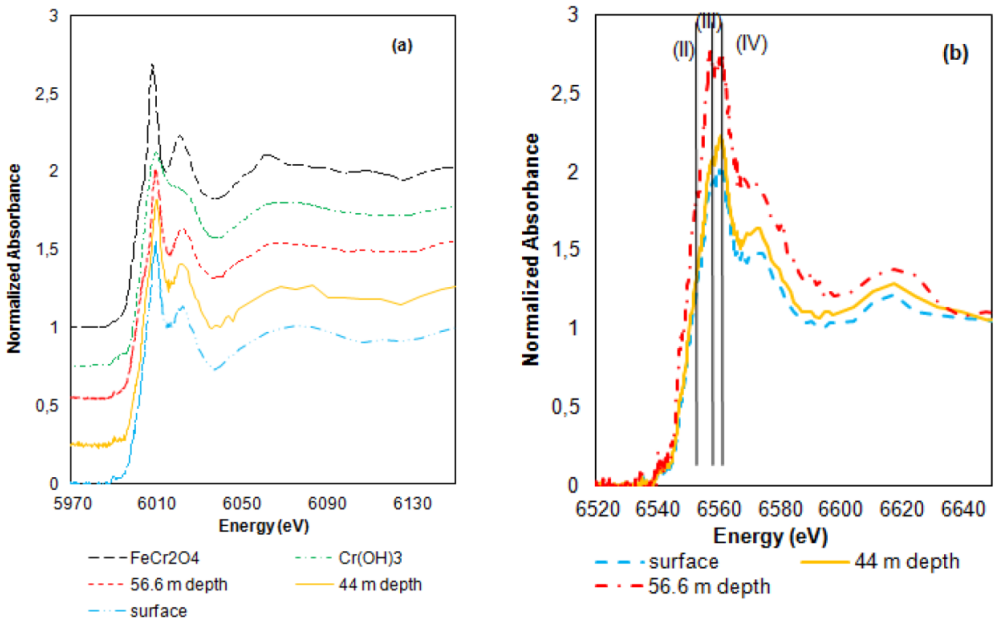

Figure 4.12 Cr K-edge (a) and Mn K-edge (b) XANES spectra of a topsoil sample and two samples obtained from 44 and 56.6 m depth – Cr reference spectra courtesy of P. Nico.

Finally, the SSA of the bulk sample was determined by BET method and was found equal to 55.95 m^2/g. For the calculation of surface area, soil density was measured equal to 2.3 g/mL. An important factor parameter that may affect soil adsorption capacity is the degree of mineral crystallinity and especially of clay minerals and iron oxides. The degree of crystallinity is reflected by the surface area with the best crystallized solids exhibiting the lowest SSA values (Strauss et al., 1997). The chemical and physical properties of soil iron oxides are thought to be a function of their surface area rather than of their mineralogical form (Borggaard, 1983). The low degree of crystallinity implies the non-stoichiometric incorporation of various elements in the crystal lattice. Serpentine type minerals usually show low crystallinity at the surface, where the degree of weathering is predominant. The presence of silica able to migrate in the soil solution prevents crystal growth leading in low crystallinity of minerals like goethite. In this case, elements such as nickel, chromium and aluminum can be incorporated in goethite. Another important characteristic of poorly crystalline minerals is their high water content. The charge imbalance that is created as a result of the disordered structures with large surface area is compensated in the areas of broken edges by the $-OH_2$ molecules. The presence of high water content can be effectively determined by applying thermal gravimetric analyses. In

addition, for the case of serpentine minerals, the degree of crystallinity is affected by more factors like the different genetic types and changes during weathering (Kuhnel et al., 1975).

The application of the BET method for determining the SSA value presupposed the absence of any alterations of the solid surface due to the high temperatures established during the measurement. Thus, a thermogravimetric analysis (TGA) was also performed (Figure 4.13). This analysis could eliminate any overestimation of the SSA value. Indeed, no surface alterations occurred by applying the BET method since the weight loss observed, about 12% (green axis), for temperatures between 50 and 150 ^{0}C (red horizontal axis) was attributed to soil's humidity and hard-bound water.

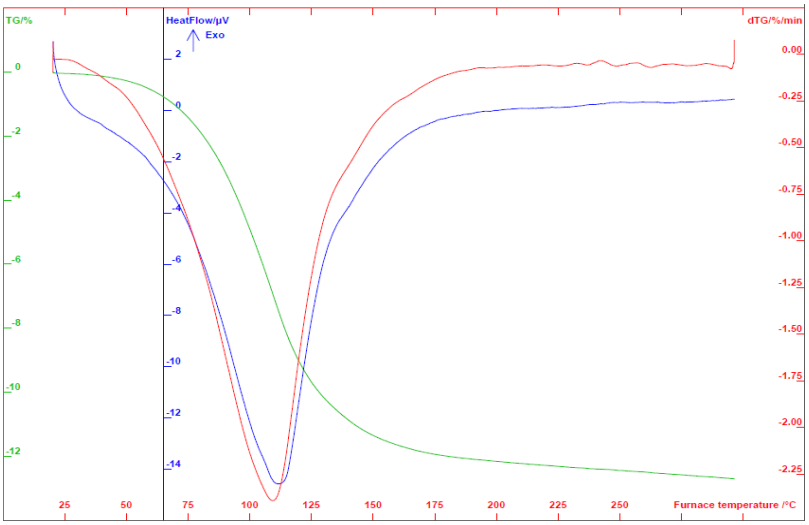

Figure 4.13 TGA diagram of soil sample with grain size -0.5 mm.

4.5 Groundwater chemistry

The ophiolitic origin of the tested aquifer was also verified by performing groundwater physicochemical analysis. In order to better investigate the ophiolitic origin groundwater samples were collected not only from the tested well but also from existing sampling points (3 wells and 1 spring) in very close proximity. Table 4.7 presents the chemical analysis data of the groundwater samples collected from the existing wells and the newly constructed well.

Table 4.7 Results of physicochemical analysis of groundwater samples.

	Unit	LOD[(1)]	W1	W2	W3	S	NW			
Depth	(m)		n.a.[(2)]	n.a.	n.a.	n.a.	44	57	78	92
Cr_{tot}	(µg/L)	0.1	91	44	34	33	71	55	42	35
Cr(VI)	(µg/L)	10	64	35	18	20	61	49	38	29
pH			8.06	7.99	8.28	8.20	8.49	8.47	8.52	8.54
ORP	(mV)		145	161	167	203	154	153	204	176
EC	(µS/cm)		798	694	664	516	650	628	633	631
T	(^{0}C)		22.1	19.8	18.7	18.8	19.8	20.0	19.6	19.1
HCO_3^-	(mg/L)		471.1	380.8	433.2	342.9	695.2	673.5	543.2	521.4
Cl^-	(mg/L)	5	17	<5	7	<5	8	9	12	25

SO_4^{2-}	(mg/L)	5	23	6	7	7	<5	<5	<5	7
NO_3^-	(mg/L)	2.2	40.1	15.9	9.0	2.5	54.8	78.3	79.6	69.9
NO_2^-	(mg/L)	0.007	0.095	0.088	0.082	0.076	0.032	0.026	0.045	0.035
PO_4^{3-}	(mg/L)	1.5	<1.5	<1.5	<1.5	<1.5	<1.5	<1.5	<1.5	<1.5
NH_4^+	(mg/L)		0.12	0.23	0.14	0.12	n.a.	n.a.	n.a.	n.a.
Na^+	(mg/L)	0.05	11.6	3.6	3.6	3.0	3.6	5.8	4.0	3.6
K^+	(mg/L)	0.05	2.5	2.0	1.5	1.2	2.5	2.5	2.5	2.5
Ca^{2+}	(mg/L)	0.1	26.0	41.4	15.5	11.4	72.3	73.0	119.0	118.8
Mg^{2+}	(mg/L)	0.01	105	64	94	77	86	86	86	87
Si	(mg/L)	2.5	14.4	18.7	11.1	12.9	11.1	11.2	11.5	11.3

[(1)]Limit of Detection, [(2)]Not available

As observed from Table 4.7, pH values range between 7.99 and 8.54. Such pH values are typical of groundwater derived from serpentinized ultramafic rocks, since values ranging from 8 to 12 have been reported (Barnes et al., 1972; Oze et al., 2004). In addition, all samples exhibit high concentrations of both Crtot (max 91 μg/L) and Cr(VI) (max 64 μg/L). These concentrations are of the highest measured globally attributed exclusively to geogenic origin and in particular to the presence of ultramafic/ophiolitic geological background, as it is shown at Table 2.4. Especially in Greece, in several areas have been detected considerably higher Cr(VI) concentrations (Table 2.4) than in Vergina aquifers but the origin cannot be considered as exclusively geogenic due to the presence of industrial activities at these areas (e.g., Inofyta, Central Greece). In Vergina area the only anthropogenic pressure is related to agricultural activities. Agricultural activities can affect groundwater quality due to the extensive use of fertilizers, which may cause increased naturally occurring Cr(VI) concentration in groundwater by increasing its mobility due to the presence of phosphates (Becquer et al., 2003) and to a less extent due to the presence of nitrates (Mills et al., 2011; Mills and Goldhaber, 2012). Chemical analysis of the collected groundwater samples showed low concentrations of phosphates (<1.5 mg/L) but high concentrations of nitrates (80 mg/L max) even at high depths, down to 92 m. The lateral and vertical distribution of nitrates in the tested area indicated both the extensive use of fertilizers and the typical high mobility of nitrates.

A more detailed assessment of the chromium concentration results led to the observation that both Cr_{tot} and Cr(VI) decreased, almost linearly as shown in Figure 4.14, with increasing depth. Regarding Cr_{tot} its concentration decreased from 71 to 35 mg/L with increasing depth from 44 to 92 m. As far as Cr(VI) concentration is concerned during increasing the sampling depth from 44 to 92 m, Cr(VI) concentration decreased from 61 to 29 mg/L. A possible explanation is that Cr(VI) in soils was also decreased with depth (Figure 4.10) and thus less Cr(VI) was available for mobilization. Regarding the decreasing trend of alkalinity this can be linked with the increasing concentrations of calcium cations, since HCO_3^- anions are consumed in order to maintain equilibrium with respect to calcite. One more important observation was the high correlation between Cr(VI) and Cr_{tot}, especially in the samples obtained from the new well, since the ratio of Cr(VI)/Crtot is higher than 83%. Similar results have been reported in cases that Cr(VI) presence in groundwater is due to geogenic origin (Fantoni et al., 2002; Sparks, 2003). This high correlation is a result of the Cr(VI) predominance over Cr(III), which is highly insoluble.

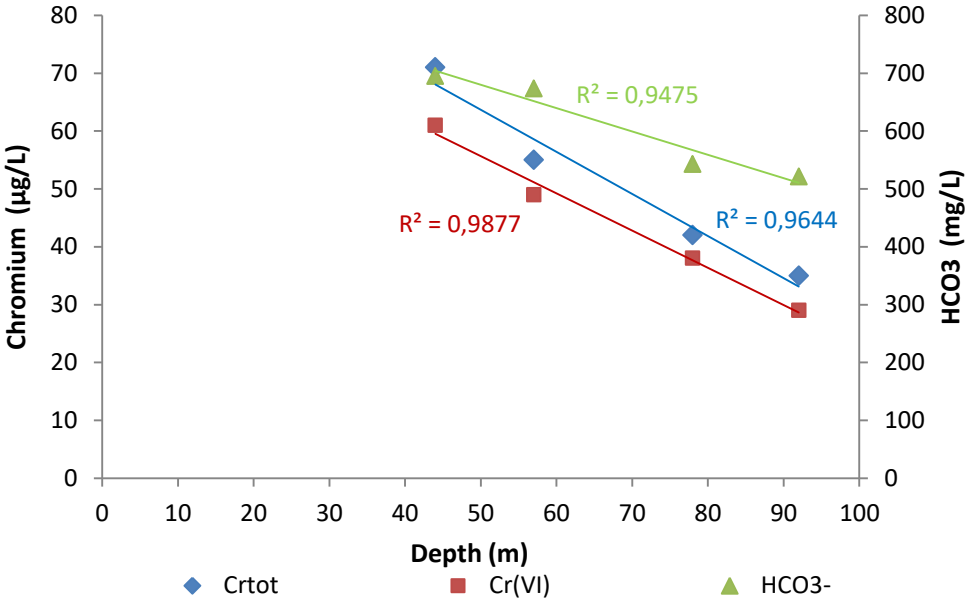

Figure 4.14 Cr(VI), Cr_{tot} and HCO_3^- concentration trends with depth.

In order to determine the geological origin of groundwater in the tested area the results of physicochemical analyses were used after being divided in two groups; those obtained from the existing sampling points and those of the new well. The Piper diagram (Figure 4.15) indicates that the groundwater is of the Ca-Mg-HCO_3 type.

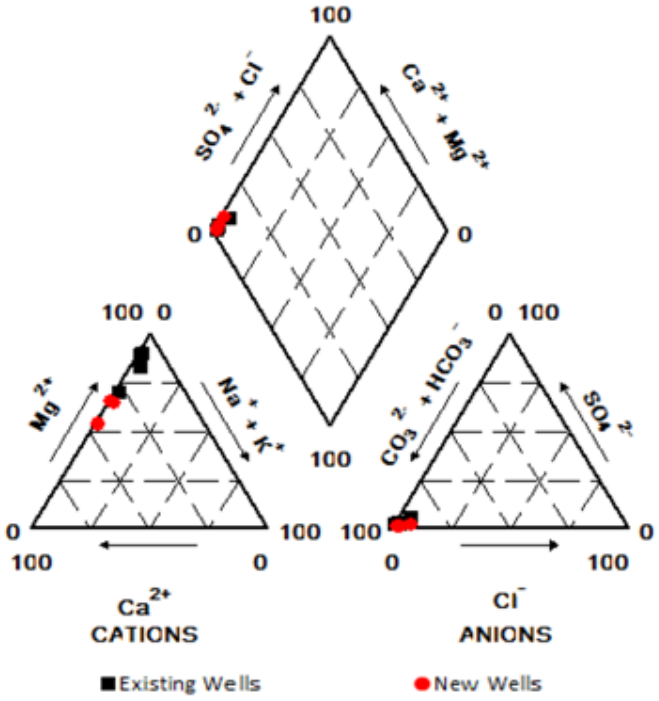

Figure 4.15 Piper diagram of Vergina groundwater samples.

Groundwater from Vergina area related to geological background affected by serpentinization processes can be divided in two types: the magnesium bicarbonate type (Mg-HCO_3) and Ca hydroxide (Ca-OH^-) type. The Mg-HCO_3 type exhibits pH values at about 8 and it is characteristic of surface waters or shallow groundwater affected by serpentinites and

ultramafic rocks. Regarding Ca-OH^- type with pH values ranging from 10 to 11, it originates from incompletely serpentinized peridotites or serpentinization of Cr-rich pyroxenes (Barnes et al., 1972; Oze et al., 2004). Further analysis of the existing data showed that the tested groundwater is of Mg-HCO_3 type (Figure 4.16a). In addition, the Mg-Si-HCO_3 plot (Figure 4.16b) indicates that the groundwater composition is very close to equilibrium with chlorite or serpentine minerals. Such minerals were identified by the XRD analysis as mentioned at section 4.3.

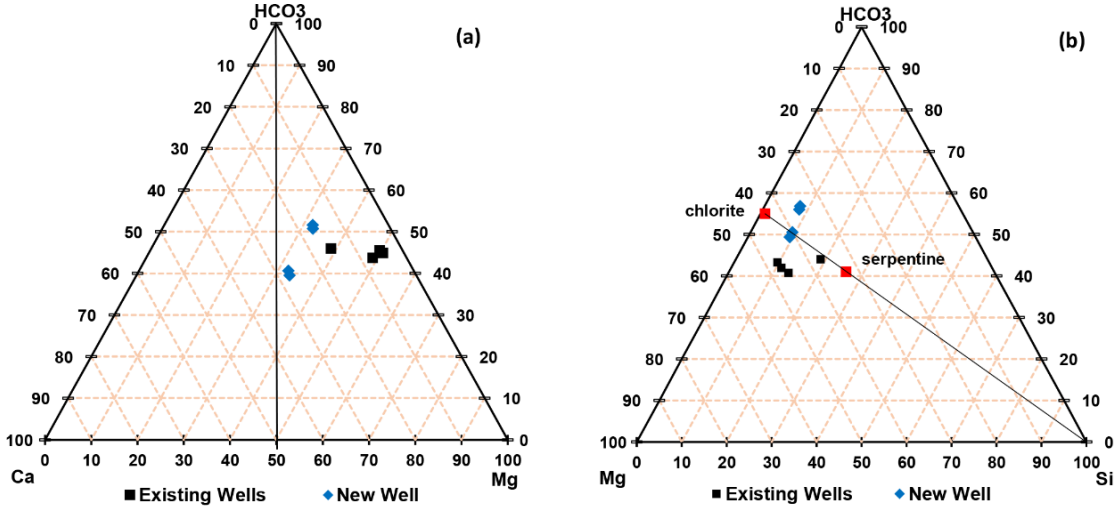

Figure 4.16 Ternary Mg–Ca–HCO_3 (a) and Mg–Si–HCO_3 (b) plots of the Vergina groundwater samples.

Possible differences between the groundwater samples collected from the existing and the new well were investigated by examining the Ca-Mg and Mg-HCO_3^- molar ratios. Groundwater of Mg-HCO_3 type with HCO_3/Mg ratios close to 2 originate from pure serpentinites. In this case Mg derives from the incongruent dissolution of the rock. Higher ratios are linked to the presence of carbonate rocks resulting in higher concentrations of calcium ions for balancing the HCO_3^- anions (Fantoni et al., 2002). The groundwater samples collected from the new well exhibited HCO_3/Mg ratio about 0.9, while higher values ranging between 1.2 and 1.6 were observed for the samples collected from existing sampling points (Fig. 4.17a). The lower values observed in the samples of the new well indicate that non-ophiolitic impurities decrease the HCO_3/Mg ratio. The Ca/Mg ratio provides information about the influence of rocks rich in calcium and magnesium on groundwater chemistry. Mg-HCO_3 waters related to serpentinites exhibit Ca/Mg ratios lower than 1/3 contrary to Ca-HCO_3 waters, which exhibit ratios greater than 1. Intermediate values indicate groundwater as a mixture of the two types (Margiotta et al., 2012). As presented at Figure 4.17b most of the samples obtained from existing sampling points are pure Mg-HCO_3 waters, while groundwater from the new well is possibly a mixture of the two types. Maybe this difference is attributed to the effect of different soil horizons that contribute to groundwater quality in the case of sampling from the existing sampling points. Groundwater samples from existing sampling points are richer in magnesium, while samples from the new well are richer in alkalinity indicating the influence of Ca-HCO_3 waters on the groundwater composition. All these observations confirm the ultramafic origin of groundwater in Vergina area.

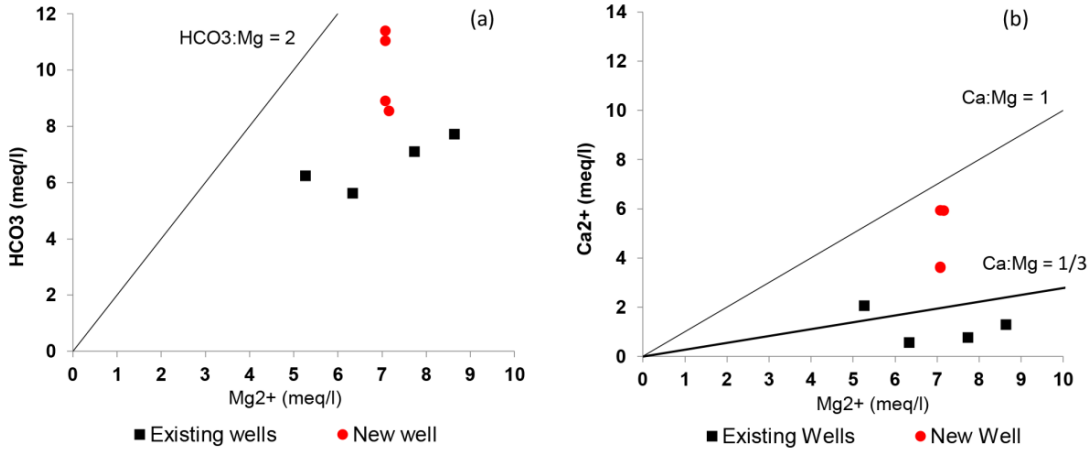

Figure 4.17 HCO_3^- - Mg^{2+} (a) and Ca^{2+} - Mg^{2+} (b) plots for Vergina groundwater samples.

5 BATCH EXPERIMENTAL RESULTS USING OPHIOLITIC SOIL AND GOETHITE

5.1 Adsorption of Cr(VI) and inorganic contaminants on ophiolitic soil

5.1.1 Leaching experiments

Leaching experiments were performed in order to determine the desorption efficiency of Cr(VI) from the tested ophiolitic soil collected from Vergina area. Several series of leaching experiments were carried out as shown at Table 5.1. Firstly, Cr(VI) leaching was determined by elevating pH of the aqueous soil solution at 11. As mentioned in Section 3.6 the elevation of pH to 11 aimed at determining the Cr(VI) that could be possibly leached as a result of Cr(VI) desorption without causing dissolution of solid phases. This amount of Cr(VI) was used at the calculations performed using the results of batch experiments for determining Cr(VI) desorption efficiency, as mentioned at Equations 3.10 - 3.12 at paragraph 3.6. Similarly Izbicki et al. (2008) observed Cr(VI) concentrations higher than 5 μg/L, when the pH of a mafic soil solution increased above 8, as a result of desorption.

Regarding the addition of nitrates, as $NaNO_3$ salt solution, the results showed that almost no desorption of chromates caused, either using the lower nitrates concentration (620 mg/L NO_3^-, $NaNO_3$ = 0.01 M) or the higher one (6.2 g/L, $NaNO_3$ = 0.1 M). This fact indicates that nitrates do not compete for the same adsorption sites with chromates.

At the next series of leaching experiments the effect of phosphate on Cr(VI) desorption was tested. Aqueous soil solutions containing 0.01 M $NaNO_3$ (620 mg/L NO_3^-) and two different concentrations of phosphates, added as $NaH_2PO_4 \bullet H_2O$ 0.01 M (940 mg/L PO_4^{3-}) and 0.1 M (9.4 g/L PO_4^{3-}), were used. The results showed that the presence of phosphates caused significant desorption of Cr(VI), higher than in the cases of elevating pH of the solution or in the presence of nitrates. However, no alterations were observed when using different phosphate concentrations. The effect of phosphate on Cr(VI) desorption has also been reported by several studies. The presence of phosphate in the solution improved the Cr(VI) desorption rate significantly due to specific anion competition. The weakly adsorbed chromates form highly labile complexes that can be readily displaced by ions such as phosphate and sulfate (Bartllet and Kimble, 1976; Burden, 1989; Schroth, 1990; Fendorf, 1995; Oze et al., 2004). In addition, P adsorption depends on the nature of the iron (hydr)oxides, with the P amount adsorbed by ferrihydrite and hematite being higher than that adsorbed by goethite, since ferrihydrite exhibits poor crystallinity and high micropore volume. This leads to low phosphate desorption (Wang et al., 2013; Bortoluzzi et al., 2015).

Table 5.1 Cr(VI) leaching using different types of extractants related to inorganic contaminants usually occur in groundwater (nitrates and phosphates).

Extractant	Liquid/Solid (L/g)	pH	Cr(VI) (μg/L)	Cr(VI) (mg/Kg)
NaOH (0.1 M)	0.05	11.04	15	0.75
$NaNO_3$ (0.01 M)	0.01	7.78	5	0.05
$NaNO_3$ (0.1 M)	0.01	7.71	5	0.05
$NaNO_3$ (0.01 M) and $NaH_2PO_4 \bullet H_2O$ (0.1 M)	0.01	8.66	32	0.32
$NaNO_3$ (0.1M) and $NaH_2PO_4 \bullet H_2O$ (0.1 M)	0.01	8.52	33	0.33

5.1.2 Effect of pH and mineralogy

The effect of pH on Cr(VI) removal was investigated using at first the bulk soil sample and then the two fractions of the magnetic and non-magnetic, which obtained by its division (Section 3.6.1.1). A series of experiments carried out as described in Section 3.6 and the results are shown at Figure 5.1.

In particular, Figure 5.1a shows the experimental data obtained using the bulk soil sample. The results showed a decreasing trend in Cr(VI) removal with increasing pH. Removal maximized at acidic pH values (<4), exhibiting a percentage of almost 80%. The desorption experiments showed that Cr(VI) removal from the aqueous phase was not completely reversible. The irreversibility of adsorption can be attributed to two processes:

i. Reduction of Cr(VI) to Cr(III) by soil constituents able to act as reductants such as divalent iron, which leads to strong retention due to Cr(III) immobilization, and is characterized by lack of reversibility.
ii. Irreversible adsorption, which is a result of surface complexation reactions which lead to the formation of inner-sphere complexes. Inner-sphere complexes are quite stable, since include exclusively ionic or covalent bonds, or a combination of both (Sposito, 1989). This type of adsorption is not reversible, even when raising the pH at values higher than PZC.

The presence of black grains which were analyzed using the SEM-EDX proved the occurrence of mineral phases such as (magnesio)chromite or magnetite. Such minerals can act a source of divalent iron able to reduce Cr(VI). Thus it can be assumed that at least a part of the irreversible amount is attributed to reduction phenomena. For simplicity reasons the amount of Cr(VI) that was not desorbed back to the soil solution will be called as the reduced fraction and is calculated by the difference between removal and adsorption and will be discussed below. The relative contribution of adsorption and reduction was also a function of pH. Cr(VI) adsorption was approximately constant and corresponded to 50% of the removed Cr(VI) in the pH range 4 - 7. The Cr(VI) adsorption capacity in this pH range is equal 2 mg of Cr(VI) per kilogram of soil. For pH values greater than 7, adsorption decreased, but its relative contribution increased, being the predominant process since contributed almost 100% to the total removal. On the other hand, reduction was more significant at acidic pH values (3 to 4),

decreased to about 50% of removal in the pH range 5 - 7 and finally almost zeroed at pH values higher than 7.5.

The inversely proportional trend of reduction with pH has been reported by several studies investigating Cr(VI) reduction in the geoenvironment (Henderson, 1994; Rai et al., 1988). The main reductant of Cr(VI) in the Vergina soil is considered to be ferrous iron, since the organic matter content is very low, about 0.8 g/Kg as carbon (Table 4.4), and possible microbial reduction was prevented by sterilization of the soil sample. The macroscopic identification of the black grains in the bulk sample (magnetic fraction) and the presence of (magnesio)chromite and Cr-magnetite identified by the SEM analysis further verify this assumption.

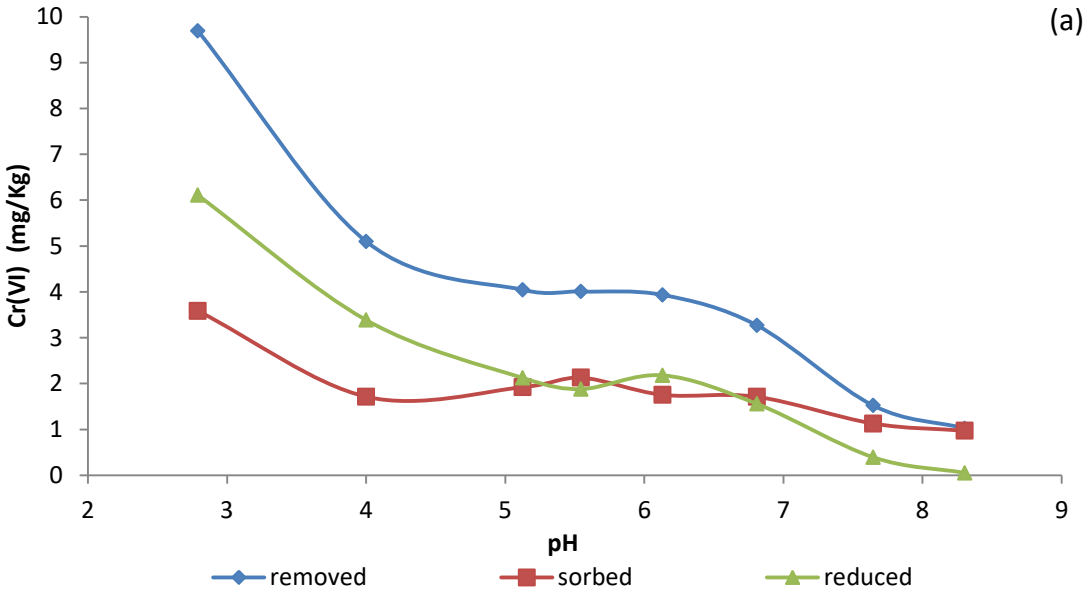

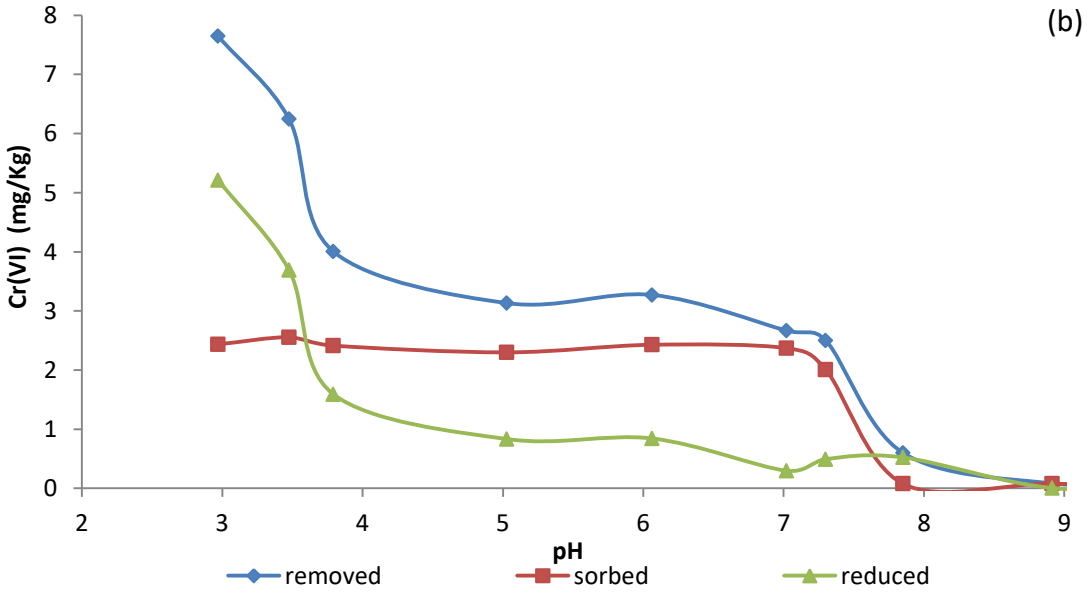

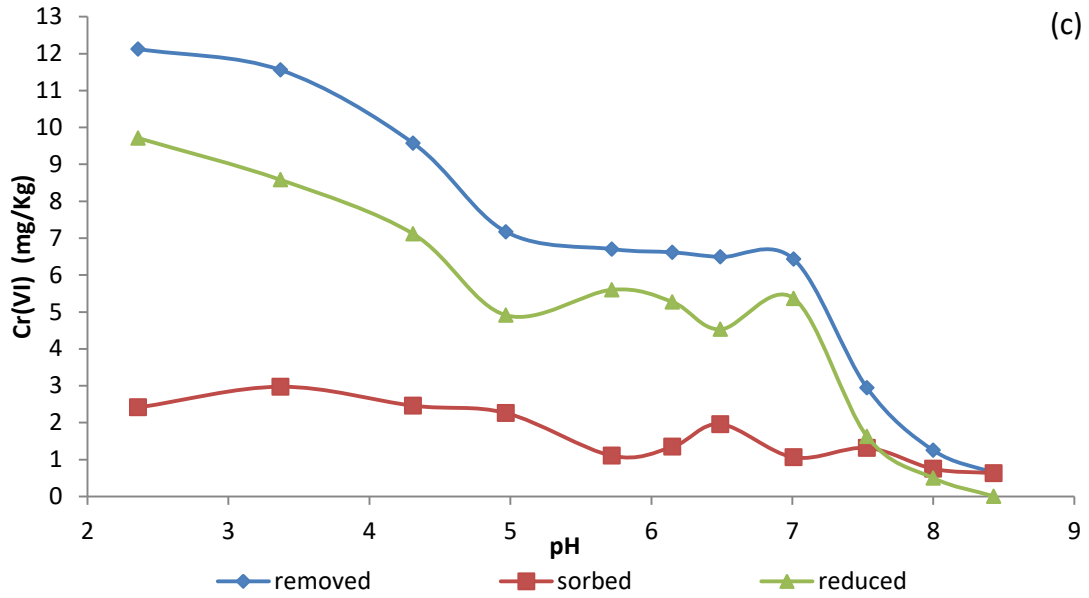

Figure 5.1 Adsorption of Cr(VI) ($[Cr(VI)]_0$ = 250 μg/L) on a) the bulk soil, b) the non magnetic fraction and c) the magnetic fraction (diamonds: removal; squares: adsorption; triangles: reduction).

In order to further determine the contribution and investigate the role of the magnetic fraction on adsorption, two more series of batch experiments were carried out, testing Cr(VI) removal in the non-magnetic (Figure 5.1b) and magnetic (Figure 5.1c) fractions. The non-magnetic fraction presented a similar trend of Cr(VI) removal with pH. However, an overall lower removal capacity compared to the bulk soil was displayed. The removal was maximized again at acidic conditions, at pH values about 3, and was approximately 8 mg/kg, corresponding to 60% of total Cr(VI) removal. This value is significantly lower compared with the 80% achieved in the case of using the bulk soil sample. The 20% difference was mainly observed in acidic values and thus probably stems from the lower reduction capacity, especially at pH>4, indicating that the reducing compounds are depleted in the non-magnetic fraction. The contribution of adsorption was similar for both the bulk and non-magnetic fractions, at about 2 mg/kg, indicating that the sorptive surfaces are similar in the bulk and in the non-magnetic fraction. Regarding Cr(VI) removal by the magnetic fraction, the results verified the assumption that the high removal efficiency is mainly attributed to reduction. As shown at **Figure 5.1c**, the maximum Cr(VI) removal was about 90% and achieved at pH values about 3. For higher pH values in the range of 5 - 7, removal efficiency decreased at 50%, about 6.5 mg/kg, but even this decrease still remains almost 1.5 times higher compared to the decrease for bulk soil. The adsorption capacity of the magnetic fraction was found to be constant at 2 mg/kg, verifying further that the increase in total removal was exclusively due to enhanced reduction.

Among the minerals identified by XRD analysis, potential minerals with magnetic properties able to present reduction capacity, are primarily magnetite and to a lesser extent chromite. It has been reported that the reduction rate of Cr(VI) by magnetite is relatively faster at acidic conditions than at neutral and alkaline pH values (Kendelewicz et al., 1999; He and Traina, 2005). Choi et al. (2008) mentioned that Cr(VI) reduction rate decreases for pH values higher than the PZC of magnetite (pH_{PZC}≈7.5). Their results at adsorption equilibrium are in good

accordance with the results of this study, mentioning that the mechanism for Cr(VI) removal is a combination of adsorption and reduction processes. However, even considering reduction as Cr(VI) removal mechanism, the contribution of adsorption still remains important. Cr(VI) is initially adsorbed on the surface of magnetite and then is reduced by the surface reactive sites (Jung et al., 2007). Thus, the ferrous iron content on the magnetite surface is a factor able to control Cr(VI) reduction (Choi et al., 2008). In addition, possible release of ferrous iron in very lower amounts by serpentine minerals has been observed since their dissolution is much easier than that of spinels (Apollaro et al., 2019).

Finally, applying the mass balance equation for the adsorbed amount of Cr(VI) by the bulk sample and the weighted average of the magnetic and non-magnetic fractions it is proved that the adsorption capacity of the bulk soil is almost equal with that of the other two fractions. Applying the mass balance for the case of removal capacity a deviation of about 10% is observed with the weighted sum of the two fractions being higher than that of the bulk soil. This can be explained by the fact that the magnetite surface when presented in the bulk soil is not entirely available for reaction with the liquid phase comparing to the case of isolating and suspending the magnetic fraction in the aqueous solution.

5.1.3 Effect of particle size

Another parameter able to affect the adsorption efficiency is the soil particle size. The effect of particle size at Cr(VI) removal was tested using three fractions of the non-magnetic fraction: a) 0.25 mm < d < 0.5 mm, b) 0.075 mm < d < 0.25 mm and c) d < 0.075mm. The removal of magnetic fraction aimed at minimizing the effect of reduction and isolating the adsorption process. As shown in Table 5.2, the mass of the magnetic fraction decreased with decreasing grain size. This trend is possibly attributed to the fact that chromite and its alteration products, such as magnetite, which were observed in higher concentration in the magnetic fraction (SEM results, Figure 4.8), belong to the spinels group exhibiting weathering resistance and accumulation in the coarser fractions.

Table 5.2 Properties of various particle size fractions.

Sample	SSA (m^2/g)	Fraction percentage (%)	Mass of magnetic fraction per mass of "bulk" soil (g/g)
"non-magnetic" fraction	55.95	100%	0.10
0.25 mm < d < 0.5 mm	45.84	44%	0.19
0.075 mm < d < 0.25 mm	52.49	36%	0.09
d < 0.075 mm	57.67	20%	0.02

The experimental results (Figure 5.2) showed that Cr(VI) removal decreased with increasing soil particle size. Keeping constant the pH value at 3, the maximum removal presented a continuous decrease from 10 mg/kg in the -0.075 mm fraction, to 8.5 mg/kg in the intermediate and 7.8 mg/kg in the 0.25 mm < d < 0.5 mm fraction. The weighted average adsorption capacity of the three fractions is calculated to 8.5 mg/kg, while the corresponding maximum removal in the non-magnetic fraction in the same pH (3) was 7.6 mg/kg (Figure 5.1b). This deviation, about 10%, of the mass balance indicates that separating the soil

fractions increases removal efficiency. Similar results obtained when comparing the bulk soil with the individual magnetic and non-magnetic fractions. More specifically, both the coarser and the intermediate fractions exhibited zero reduction capacity for pH > 4, while the contribution of reduction at pH < 4 corresponded approximately to the 50% of the total Cr(VI) removal. Thus, for pH > 4, adsorption was the only mechanism for Cr(VI) removal in the two coarser fractions. The adsorbed amount was about 2 mg/kg in the pH range 4.5 - 7.5. For pH > 7.5, adsorption was decreased and finally almost zeroed at pH>8. The finest fraction maintained a similar adsorption capacity in the tested pH range, but had substantially higher reduction capacity at pH < 5, which increased continuously with decreasing pH.

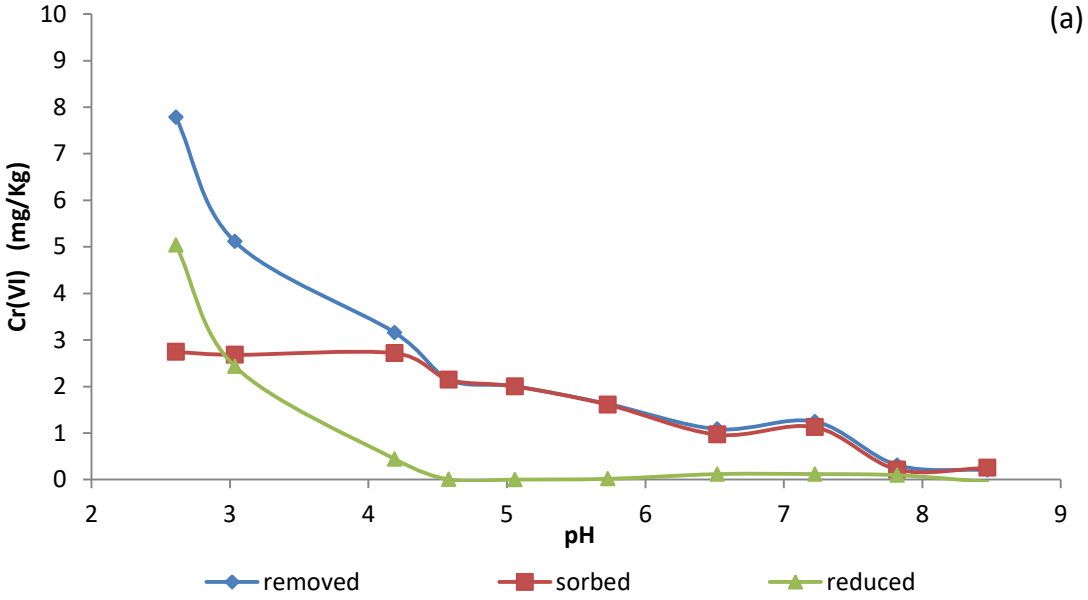

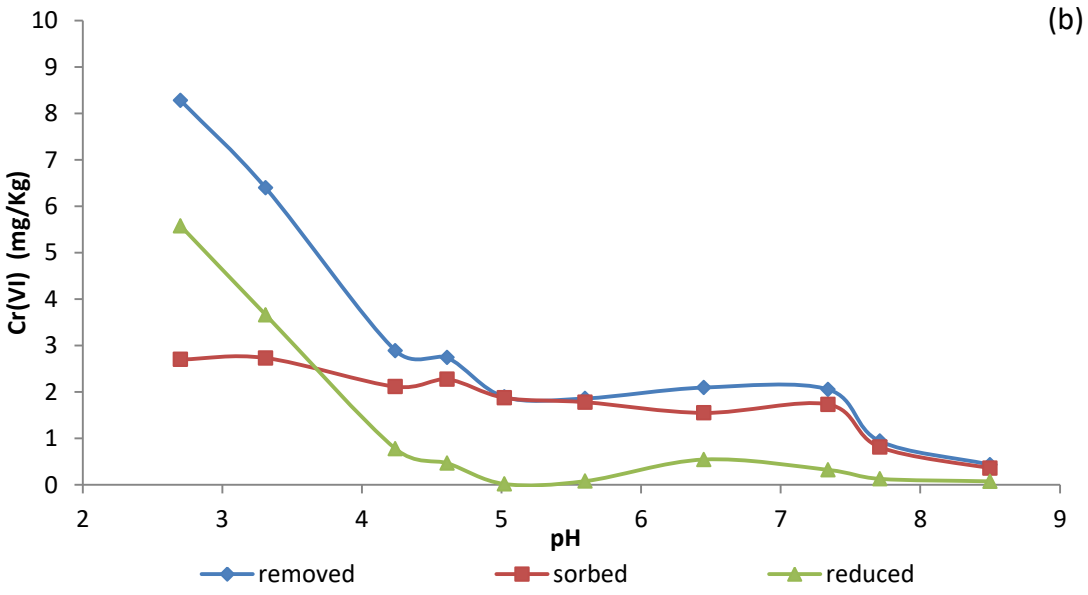

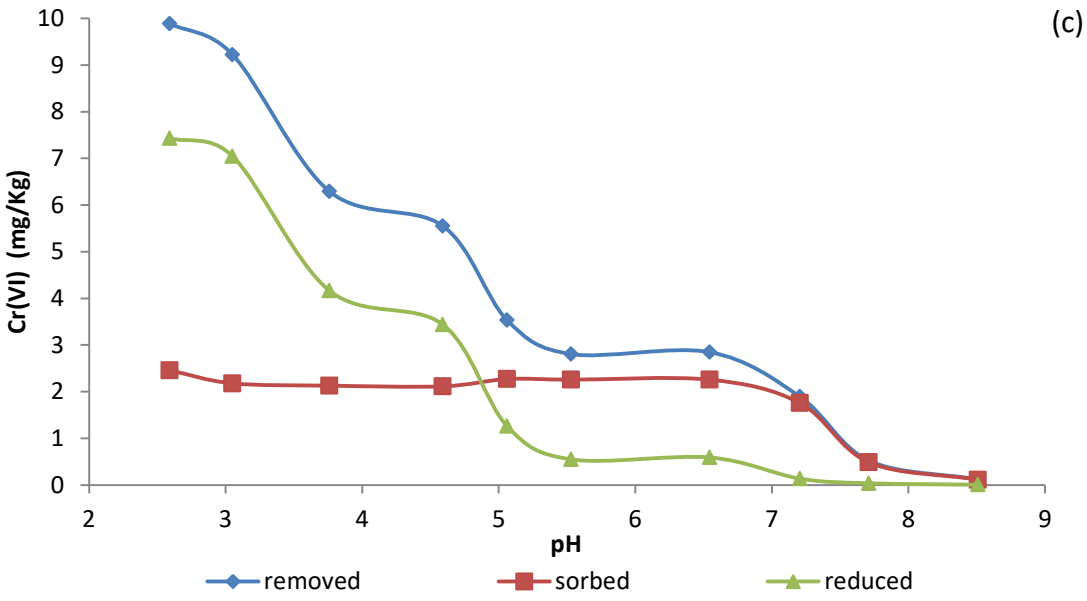

Figure 5.2 Removal of Cr(VI) ($[Cr(VI)]_0$ = 250 μg/L) on a) the 0.25 mm < d < 0.5 mm soil fraction, b) the 0.075 mm < d < 0.25 mm soil fraction and c) the d < 0.075 mm soil fraction (diamonds: removal; squares: adsorption; triangles: reduction).

In order to better evaluate the experimental results for both adsorption and reduction the SSA was determined. Since adsorption is generally a surface-driven process, as well as Cr(VI) reduction by magnetite, SSA is an important parameter that accounts for the observed differences between the tested fractions. The decreasing adsorption of metal ions with increasing the particle size is strongly related to the fact that the larger particles are characterized by lower SSA values leading to less active sites per unit of adsorbent mass (Aravanakumar and Umar, 2011; Krishna and Swamy, 2012; Choudhury et al., 2014). The BET-measured SSA values (Section 3.4.4) for the bulk non-magnetic fraction as well for the tested fractions are presented above at Table 5.2. The determined SSA values are all very high, with respect to SSA values measured generally at soils, especially for the coarser fractions that are not expected to include substantial amounts of minerals with high SSA values, like vermiculite or chlorite. According to the XRD analysis (Table 4.2) those that can contribute to the high SSA values from the identified minerals are goethite, which has SSA values in the range of 25 - 90 m^2/g (Villalobos and Perez-Gallegos, 2008) and chlorite with SSA values in the range of 25 - 150 m^2/g (Sparks, 2003). Quartz and generally serpentine minerals exhibit low SSA values, 1-2 and about 7 m^2/g, respectively (Meloni et al. 2012; Daval et al. 2013). Thus, according to the observed mineralogical composition of the tested soil (Table 4.2), it is possible that the soil fabric has significantly high surface porosity, which dominates the effect of particle size. For this reason the adsorption results will be further treated by normalizing reduction and adsorption according to the measured SSA values.

The molar mass of the reduced and adsorbed Cr(VI) per m^2 for the three tested fractions, for their weighted average and for the non-magnetic fraction is presented in Figure 5.3. As it can be observed only small differences occur between the fractions for both reduction and adsorption processes. Regarding adsorption (Figure 5.3a), the non-magnetic fraction shows identical behavior as the finer fraction. The fact that the finest fraction governs adsorption is a

common phenomenon in soils. The coarser fractions exhibit increased adsorption capacity at acidic pH values and decreased capacity at neutral values. This phenomenon of increasing adsorption with increasing particle size is a contradictory fact which cannot be explained only by taking into account the SSA parameter. Thus, the observed differences are probably attributed to other chemical or surficial properties of the soil like differences in the protonation behavior. For constant pH and SSA values equal to 7 and 50 m^2/g, respectively, the adsorption capacity of the ophiolitic soil was equal to 0.4 $nmol/m^2$. In addition, the maximum adsorption capacity of the non-magnetic fraction is equal to 0.8 $nmol/m^2$, indicating the presence of additional sorption sites for Cr(VI) in the amorphous iron fraction. These different surface sites can be attributed to minerals like hematite, chlorite and chrysotile, which were identified by the XRD analysis and can potentially contribute to Cr(VI) adsorption due to their high PZC points.

The trend of reduction curve of the non-magnetic fraction follows more closely the intermediate fraction and the weighted average of all fractions (Figure 5.3b). The fine fraction presents the greatest reduction potential and seems to play a more significant role for pH values higher than 5, since the non-magnetic fraction maintains higher reduction capacity than the weighted average of the individual fractions. Thus, SSA affects positively the reduction curves, since the reduction potential is increased with reduced particle size, confirming the hypothesis that any reduction phenomena occur in this soil are affected by the solid surface.

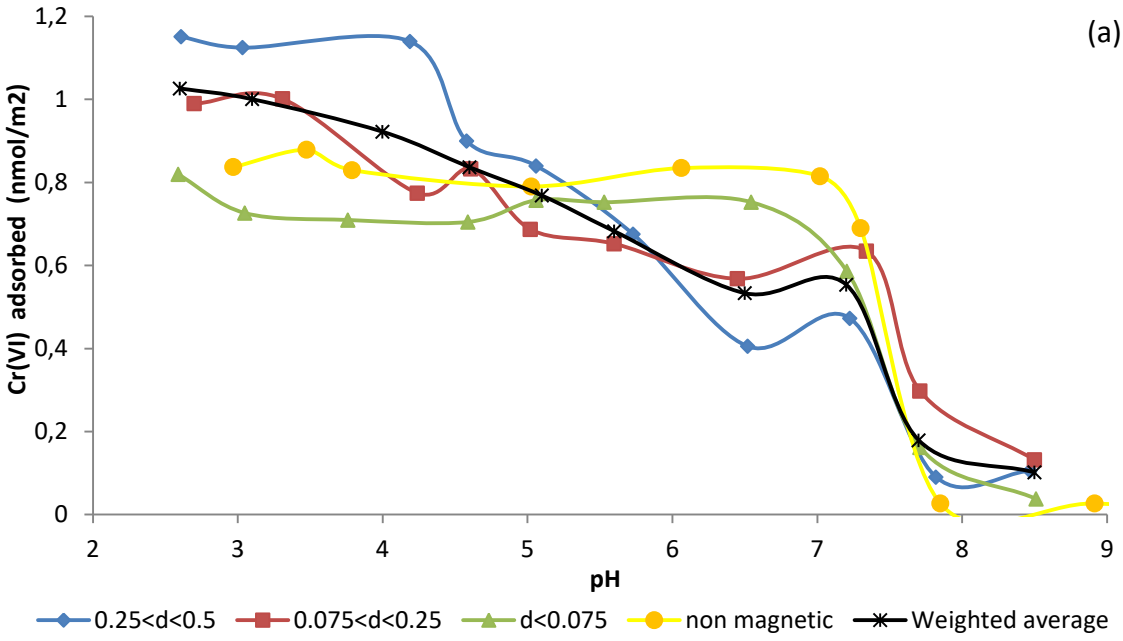

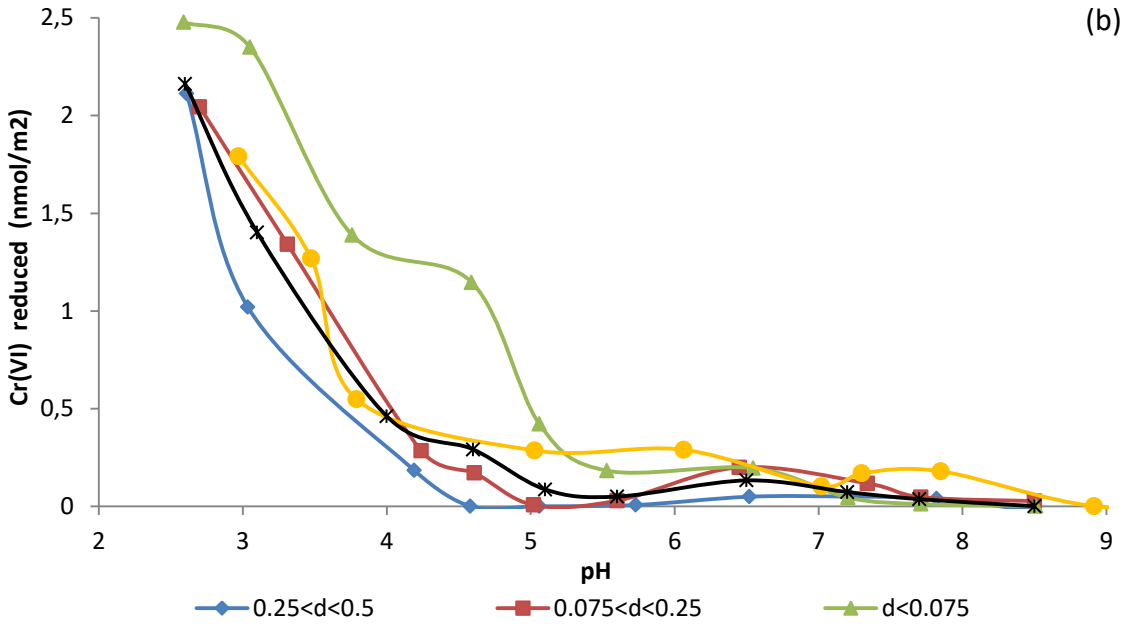

Figure 5.3 Mass of Cr(VI) a) adsorbed and b) reduced, per m^2 for the three tested fractions and the non magnetic fraction.

5.1.4 Effect of initial concentration

The effect of Cr(VI) initial concentration on adsorption and reduction was tested on the non-magnetic fraction in the range of 10 - 100 mg/L Cr(VI), using four different pH values (4.5, 5.5, 6.5 and 7.5). The considerably higher concentrations used in this series of experiments aimed to reach a plateau in the isotherms, maintaining the L/S ratio constant, while these concentrations can also be observed in heavily contaminated groundwater. Figure 5.4 presents the effect of initial Cr(VI) concentration on its adsorption and reduction by the non-magnetic soil fraction. As it can be observed by Figure 5.4, the soil possesses greater removal capacity compared to the values measured in the non-magnetic fraction in the case of using initial concentration equal to 250 μg/L. This fact also demonstrates that reduction is a surface-driven process, strongly affected by adsorption since requires Cr(VI) partitioning onto the surface in order to occur. In other words, reduction is partially driven by adsorption equilibria as well. Similar observations have been reported by Kendelewicz et al. (2000) and He and Traina (2005) using pure magnetite.

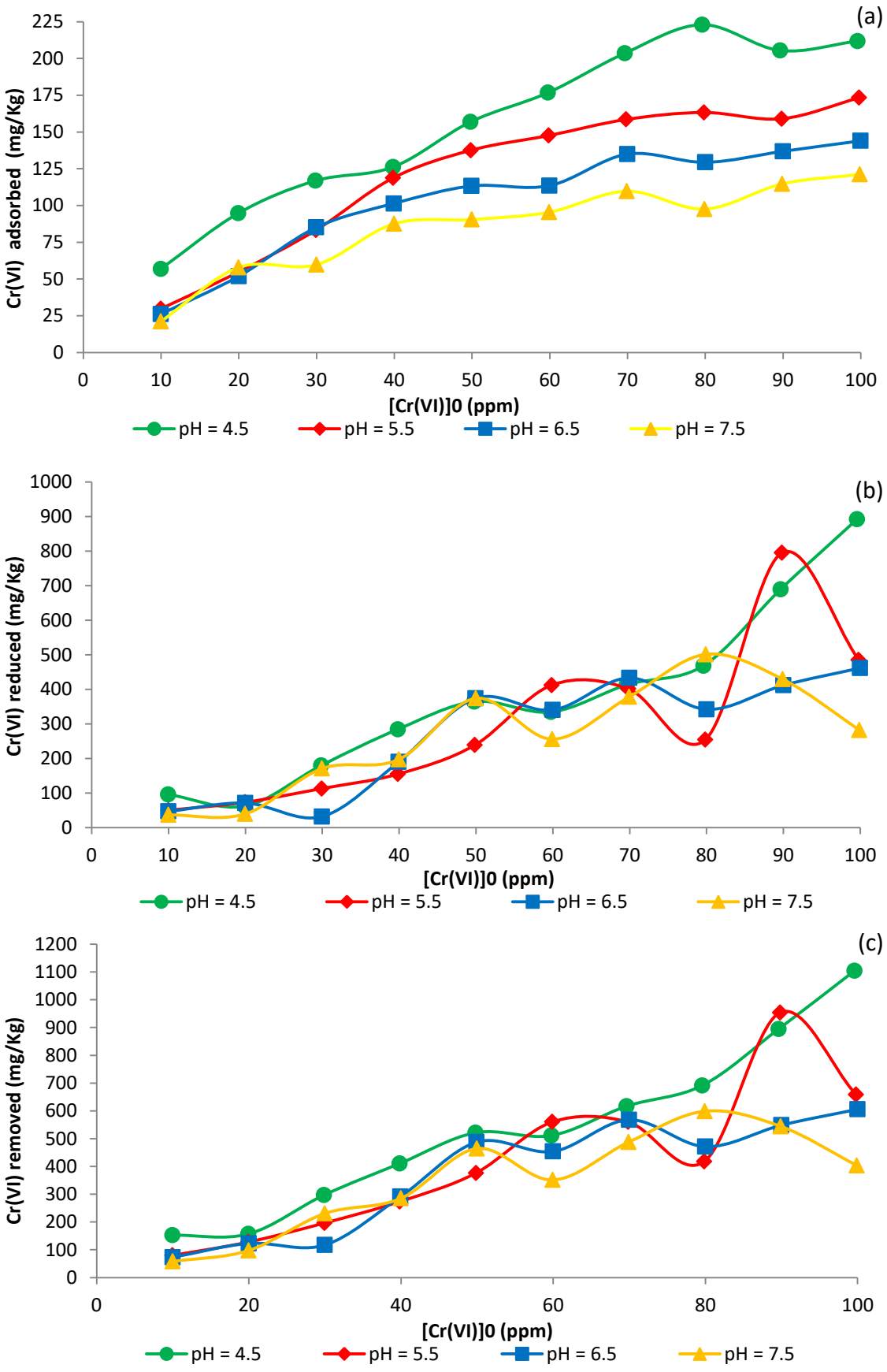

Figure 5.4 Effect of Cr(VI) initial concentration on (a) adsorption, (b) reduction and (c) total removal for four different pH values (4.5, 5.5, 6.5 and 7.5) at room temperature (25^{0}C).

Comparing the adsorption curves (Figure 5.4a) with those of reduction (Figure 5.4b) it is concluded that a main difference between adsorption and reduction curves is the greater variability that the last ones exhibit, especially at high Cr(VI) initial concentrations. At the acidic pH value the reduction curve did not exhibit a plateau and the reduction capacity at the maximum initial concentration tested [100 mg/L Cr(VI)] was equal to 900 mg/kg. For higher pH values, a plateau seemed to be reached in the range of 400-500 mg/kg, but the high variability does not allow making a reliable quantitative distinction between the different pH values. It can be concluded that for pH values higher than 5, Cr(VI) reduction is limited by the decrease of H^+. Similar observation was made in the case of using much lower Cr(VI) concentration (250 μg/L). Assuming that the 400 mg/kg Cr(VI) (≈7.7 mmol/kg) is the maximum removal capacity of the soil and that magnetite is the main mineral for Cr(VI) reduction the following reaction (Reaction 5.1) can be written (Peterson et al. 1997):

$$6Fe^{2+}Fe^{3+}O_4 + 2CrO_4^{2-} + 4H^+ \rightarrow 9\gamma Fe_2O_3 + 2CrOOH + H_2O \qquad \text{(Reaction 5.1)}$$

According to stoichiometry of Reaction 5.1, 3 mol of ferrous iron, or equivalently 3 mol of magnetite, are required per mol of Cr(VI) reduction. Considering that 350 mg/Kg of chromates are reduced at pH = 7.5, it can be calculated that for their reduction, 506 mg of Fe(II) per kg of soil are required or correspondingly ≈1.6 g of pure magnetite. Applying a mild acid extraction, as mentioned in Section 3.4.8, the concentration of ferrous iron in the non-magnetic bulk soil was equal to 220 mg Fe(II)/Kg of soil. This Fe(II) concentration corresponds to about 0.7 g of magnetite per Kg of soil. Thus it can be concluded that Cr(VI) reduction by the tested soil fraction is feasible but cannot be totally explained in terms of mass by applying this Fe(II) extraction method.

The adsorption curves (Figure 5.4a) follow the trends of traditional isotherms. As it can be observed, the increase in Cr(VI) concentration leads to increase of Cr(VI) adsorption up to 70 mg/L, above which it reaches a plateau for all pH values tested. This phenomenon is, most likely, attributed to the saturation of the available surface sites. In addition, decrease of pH values causes increase in Cr(VI) adsorption, for the same values of initial concentration. The decrease of pH from 7.5 to 4.5 doubled Cr(VI) adsorption, from a maximum of 100 to 200 mg/kg, or approximately 25% of the total removal, for initial concentrations higher than 70 mg/L. The contribution of adsorption process to the total Cr(VI) removal was lower in the concentration range 10 to 70 mg/L compared to the batch experiments with 250 μg/L Cr(VI) initial concentration, in which it ranged between 35% at pH 3 and 95% at pH 8. The maximum adsorption capacity follows a logarithmic trend with pH (R^2 = 0.99) (Figure A1.3). The logarithmic trend generally indicates that the rate of change in the data increases or decreases quickly and then levels out. This means that the maximum adsorption capacity strongly affected by the increase in H^+, which increases the positively charged surface sites and thus anion surface complexation (Sposito, 1989).

The adsorption and removal data presented in Figure 5.4 were also used to fit Langmuir and Freundlich isotherms and to determine distribution factors that can be employed in transport modeling (Figure A1.4). Generally, adsorption isotherms are significant since they show the distribution of adsorbate molecules between the solution and the solid surface at equilibrium

conditions (Al-Anber, 2011). In this study, while removal includes reduction, which is not traditionally modeled through isotherms, it is more practical to determine a single distribution factor to describe both processes, since they occur simultaneously as mentioned above. The linearized Langmuir (Equation 2.1) and Freundlich (Equation 2.2) isotherms and their associated constants are included in Table 5.3. The correlation coefficient (R^2) values (Table 5.3) indicate that the Freundlich isotherm describes better the experimental data in both cases, indicating the presence of heterogeneous surface sites on the solid surface. The values of K Freundlich parameter were very close for pH>5 for both adsorption and removal and increased substantially at pH 4.5. The natural pH of these soils is in the range of 7.5 - 8.5, so that acidic pH is unlikely to occur and the K values should not vary much in natural conditions. In addition, the values of n parameter are greater than 1 and thus are indicative of the favorable nature of adsorption. On the contrary, the Langmuir isotherm could only describe the adsorption data and not those regarding the removal. In this case, according to the literature, it can be excluded that a slight formation of a Cr(VI) monolayer on the soil surface is possible (Ajouyed et al., 2011; Vázquez et al., 2007).

Table 5.3 Langmuir and Freundlich isotherms constants for Cr(VI) adsorption and removal at four different pH values (4.5, 5.5, 6.5 and 7.5) at room temperature (25 ^{0}C).

pH	Langmuir						Freundlich					
	Adsorption			Removal			Adsorption			Removal		
	Q	b	R^2	Q	b	R^2	K	n	R^2	K	n	R^2
4.5	0.33	2.29E-03	0.94	6.07	8.11E-02	0.05	17.08	1.74	0.98	22.33	1.19	0.91
5.5	0.35	1.46E-03	0.85	33.00	2.83E-01	0.001	6.10	1.30	0.95	8.16	0.98	0.90
6.5	0.25	9.50E-04	0.91	0	0	0.001	6.58	1.42	0.93	7.62	1.00	0.87
7.5	0.19	6.26E-04	0.87	2.37	1.95E-02	0.08	6.28	1.50	0.90	7.62	1.01	0.87

* Q (mg/Kg); b (L/mg); K (mg/Kg); n (L/mg)

5.1.5 Effect of ionic strength on Cr(VI) adsorption

The effect of ionic strength on Cr(VI) adsorption was tested using NaCl solutions of 0.01 and 0.1 M concentration (Figure 5.5). In both cases, Cr(VI) removal decreased with increasing pH, indicating the significance of pH on the adsorption process regardless the value of ionic strength. In addition, adsorption was maximized for pH<5. In the case of using 0.1 M NaCl adsorption efficiency was significantly decreased compared to that of 0.01 M NaCl. In particular at pH about 7 that usually occur in groundwater, the removal is decreased almost 79%. According to Richard and Bourg (1991) adsorption efficiency decrease with increasing ionic strength which is a result of reducing chromates activity, which is based on the Coulomb forces that draws them on the solid surface. In this study the significant decrease is probably attributed to the presence of chloride anions able to affect Cr(VI) adsorption either by reducing the available surface sites for adsorption or by electrostatic repulsions with chromates.

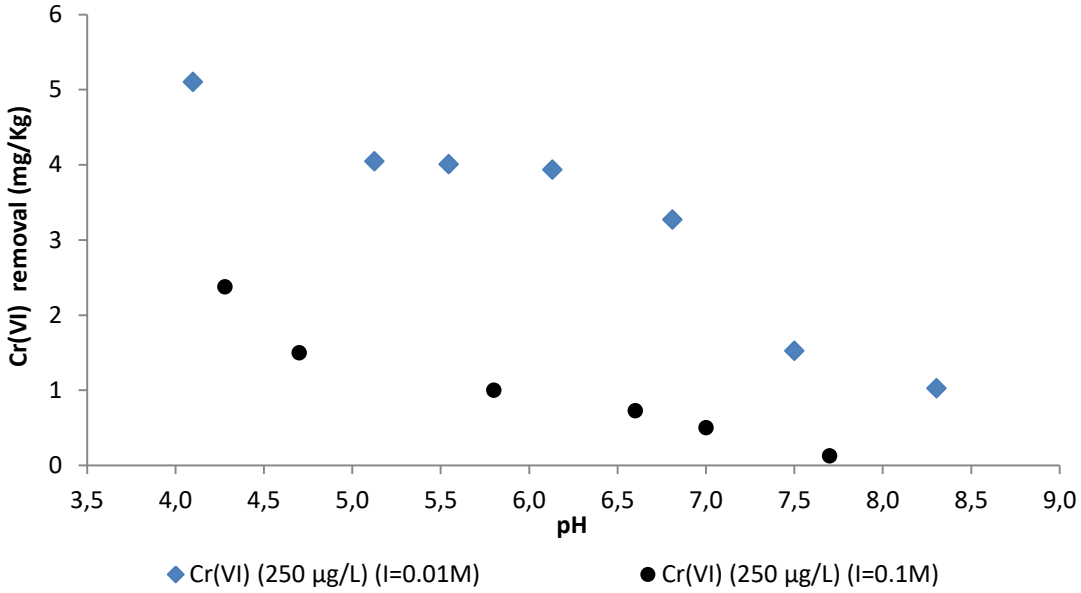

Figure 5.5 Effect of ionic strength on Cr(VI) adsorption versus pH ($[Cr(VI)]_0$=250 µg/L)

Similar results were obtained in several studies that investigated the effect of ionic strength on Cr(VI) adsorption by soils. The most recent of them performed by Kwikima and Lema (2017) showed that Cr(VI) adsorption decreased with increasing ionic strength, due to the addition of KCl electrolyte solutions. Two possible facts were mentioned as reasons for the adsorption decrease. Firstly, the direct competition of chloride anions with Cr(VI) for the soil's oxyhydroxide surface sites and secondly the decrease in the electrostatic potential near the surface sites, which further affects the Cr(VI) surface complexation reactions (Kwikima and Lema, 2017). Azizian (1993) also reported the decrease of Cr(VI) adsorption with increasing pH using NaCl as background electrolyte. Finally, Zachara et al. (1989) using $NaNO_3$ solutions observed the increase of Cr(VI) adsorption with decreasing ionic strength, implying the effect of ionic strength on surface charge and the aqueous activity coefficient of chromates. Thus, it can be concluded that independently of the kind of background electrolyte Cr(VI) adsorption is expected to decrease with increasing ionic strength. Only in one study performed by Tzou et al. (1998) the increase of ionic strength, using $Ca(NO_3)_2$ as electrolyte, caused increase of Cr(VI) adsorption efficiency using real soil as sorbent. The effect of sorbent type on Cr(VI) adsorption at different ionic strength values was investigated at another study by Veselská et al. (2016) using as sorbents natural clays (illite and kaolinite) and synthetic minerals (birnessite and ferrihydrite). Ionic strength was determined using KNO_3 as background electrolyte and the results showed that Cr(VI) adsorption is strongly dependent on ionic strength for all solid phases tested.

5.1.6 Effect of phosphates on Cr(VI) adsorption

In general, non-crystalline or short-range ordered iron and aluminum hydroxides, poorly crystalline alumino-silicates and organo-mineral complexes are mainly responsible for phosphate retention in the geoenvironment. Among them iron and aluminum (hydr)oxides surfaces and specific edges of clay minerals thought to be the most important adsorbents in soils. Aluminum and iron oxides usually exist as coatings on soil particles or as amorphous

aluminum or iron hydroxyl compounds. The high affinity of iron oxides for phosphate has been extensively studied (Fontes and Weed, 1996; Violante et al., 2002; Fink et al., 2014; Bortoluzzi et al., 2015; Fink et al., 2016). More recent studies have noticed the importance of clays on phosphates adsorption (Spiteri et al., 2008; Cui and Weng, 2013; Gérard, 2016). Clays, which are characterized by high values of SSA, contain iron in their structure and varying amounts of iron oxides. The high adsorption capacity of clays for phosphates cannot exclusively be explained by their great SSA. Their content of iron oxides is a parameter that strongly affects their adsorption capacity, since only little evidence proves that the structural iron contributes to the adsorption capacity. In addition, the presence of well or poorly crystallized iron oxides contributes to the increase of SSA, enhancing thus the adsorption efficiency (Sei et al., 2002). Weng et al. (2011) mentioned that phosphate binding capacity of clay minerals is more than 100 times lower than that of pure iron oxides. This phenomenon was also noticed by Pinto et al. (2013) who stated that taking into account only the clay content in a soil for interpreting the sorption phenomena of P may lead to misunderstandings. As a consequence, even in the case of clays the occurrence of iron oxides is the crucial factor for phosphates adsorption.

Bache et al. (1964) were of the first that studied phosphates adsorption on natural soils mentioning the effect of aluminum and iron oxides. They reported that the removal of phosphates is a three stage process, which involves both the mechanisms of adsorption and precipitation as described below:

1. a high energy chemisorption of small amounts of phosphate in a wide pH range.
2. precipitation of a separate phase of phosphates in case of higher amounts of phosphates with the general type of precipitate being $(Al,Fe)(H_2PO_4)_n(OH)_{3-n}$, where $n < 1$ at high pH values.
3. a low energy adsorption of phosphate onto the precipitate.

The important effect of iron and aluminum oxides was also determined by Fontes and Weed (1996) reporting that phosphate adsorption is strongly related to goethite, gibbsite, the sum of iron and aluminum oxides and amorphous aluminum oxides, as well. More specifically, they depicted that the variations in the iron oxide mineralogy of the clay samples caused alterations on the SSA of the soil and, thus, altered the adsorption capacity of soil for phosphates. Fink et al. (2014; 2016) carried out long term experiments in order to quantify the maximum P adsorption capacity and the effect of mineralogical composition and tillage on Brazilian tropical soils. The results showed that adsorption capacity was strongly correlated with the iron oxides content such as goethite and ferrihydrite, the gibbsite/(gibbsite + kaolinite) ratio and the SSA. Amongst them goethite was the iron oxide that exhibited the strongest effect on P adsorption. The soil management due to agricultural activities showed that did not affect the P retention. Similar results obtained by Bortoluzzi et al. (2015) who reported that P adsorption was explained by the sesquioxides concentration and especially by goethite concentration contained in the clay fraction.

Apart from adsorption, another important process that affects phosphates removal is the precipitation. Generally, in soils with high amounts of extractable cations that are able to react with P and form insoluble P-phases, precipitation is considered as a dominant mechanism for P immobilization. Since iron and aluminum are not commonly extractable in soil solutions,

adsorption rather than precipitation is usually related with such elements. However, the presence of calcium ions is thought to be the predominant force for P precipitation. Thus, precipitation is significant at calcareous soils with two pathways being proposed for phosphates removal. The first refers to partitioning on soil surfaces and the second to the precipitation induced by soluble Ca^{2+} ions, which leads to the formation of insoluble Ca-P phases. In such soils, P removal through precipitation is thought to be comparable to the removal attributed to the adsorption (Razaq et al., 1989; Tunesi et al., 1999; Rietra et al., 2001). In this study, the total removal of phosphates was determined without trying to distinguish the effect of either adsorption or precipitation.

Apart from single anion adsorption on the ophiolitic soil, the simultaneous effects of chromates and phosphates were tested (Figure 5.6). The presence of competitive interactions between anions is able to cause decrease of their adsorption efficiency leading to higher mobility of contaminants in aquifers. Firstly, the adsorption capacity of the ophiolitic soil for phosphates, either with the presence of Cr(VI) or not, was tested in the pH range 3 – 9 (Figure 5.6). Adsorption efficiency was not affected by the presence of Cr(VI) ions in the solution. This is probably due to either the significant difference of the concentration of the two kinds of ions or the selective adsorption of phosphates instead of chromates on the ophiolitic surface (Antelo et al., 2007). Moreover, it is known that ions with higher valence state, like phosphates in this specific case, are more strongly adsorbed on the solid surface than those of lower valence state like chromates. Generally, phosphates adsorption to mineral surfaces can be attributed to either non-specific electrostatic interactions or to chemical interactions leading to the formation of aqueous and surface complexes (Spiteri et al., 2008). However, the main way of phosphates adsorption is through inner sphere complexes, indicating the formation of strong bonds, ionic or/and covalent, with the surface (Sposito, 1989). Contrary to chromates, sulfates and arsenates are anions capable of strongly competing with phosphates (Violante et al., 2002).

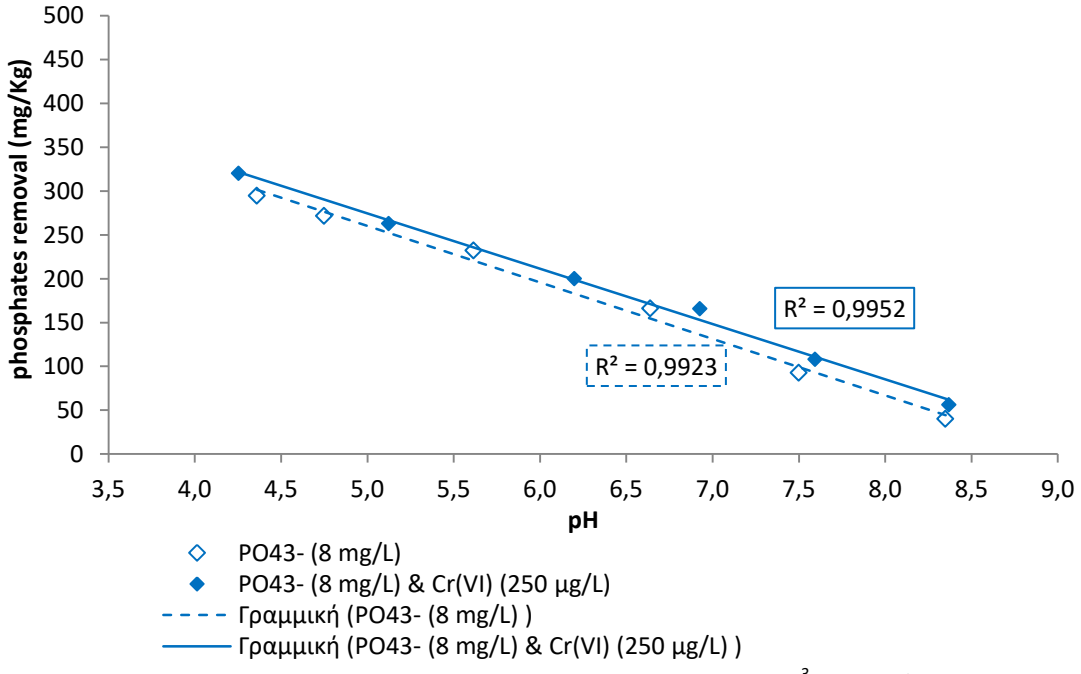

Figure 5.6 Effect of Cr(VI) on phosphates adsorption ($[PO_4^{3-}]_0$=8 mg/L)

As it is shown in Figure 5.6, the effect of pH was significant in both cases tested (with or without PO_4^{3-}). More specifically, phosphates adsorption decreased with increasing pH exhibiting a linear trend (R^2=0.99). The maximum adsorption capacity of soil was about 320 mg/Kg (pH=3) and the minimum in the range of 56 - 166 mg/Kg (pH = 7 - 8.5). Similar adsorption capacity values have been reported by Sibanda and Young (1986) who used tropical soils as adsorbents. The pH of the soil solution is one of the most important parameters that can control P adsorption. pH values affect the phosphates speciation ($H_2PO_4^-$, HPO_4^{2-}, PO_4^{3-}), which further affects the phosphates reactivity towards soil surfaces. The HPO_4^{2-} and PO_4^{3-} ionic forms occur for pH values higher than 7 and, consequently, are the most important species in the geoenvironment. The HPO_4^{2-} and PO_4^{3-} anions present higher affinity for soil surfaces than $H_2PO_4^-$ ones. As pH increases, the concentration of divalent phosphate ions increases 10 times for each pH unit. In parallel, the pH increase causes the negative charging of the surface, resulting in greater electrostatic repulsions. Especially in soils containing variable charge colloids, the pH may also influence the net charge in the adsorption plane. However, the increase of the HPO_4^{2-} concentration counterbalances the decrease of electrostatic potential with increasing pH (Razaq et al, 1989). Thus, the decreasing adsorption trend with increasing pH can be attributed to the presence of H^+ or OH^- in the solution in acidic and alkaline pH values, respectively. The presence of H^+ enhances the adsorption of phosphate anions on the soil surface through electrostatic attractions, while the presence of OH^- enhances the electrostatic repulsions between the anions and the surface.

The decreased adsorption trend of phosphates with increasing pH observed in this study is one of the two trends that have been observed using natural soils as adsorbents. The other approach suggests that phosphates adsorption can be described by a graphic depiction, which exhibits minimal at pH values usually within the range of 5 - 7 (Razaq et al, 1989); this trend was not observed in the experimental results of this study. The first adsorption behavior of soils suggests that the adsorption increase at acidic values is related to the increase of net positive surface charge with decreasing pH. However, even in this approach some contradictory observations have been made. Experimental findings showed that adsorption efficiency can be maximized either at pH values slightly below 4 or at exactly 4. This behavior is attributed to the high activity of iron and aluminum presented in soil matrix and the development of positive charge in soil colloids. On the contrary, the pH increase leads to low retention of P due to the decrease of iron and aluminum activities and the decrease of positive charges on colloidal surfaces. Especially for pH values closely to the PZC values of the soil constituents, adsorption occurred very difficult.

Figure 5.7 depicts the effect of phosphates on Cr(VI) adsorption by the ophiolitic soil. Cr(VI) adsorption is strongly affected by the presence of phosphates. For pH<7 the effect of phosphates is maximized since Cr(VI) adsorption efficiency is depressed exhibiting a difference about 3 mg/Kg. Phosphates compete chromates for the active surface sites of soil, being finally more efficiently adsorbed. The much higher concentration of phosphates and their higher valence state can cause stronger electrostatic repulsions with chromates eliminating their adsorption. Thus, the presence of phosphates in groundwater can act as a competitive factor for Cr(VI) retardation by the adsorption process. However, it is obvious that the pH has an

important effect on adsorption since the adsorption efficiency significantly decreases with increasing pH, regardless the presence or the absence of phosphate ions. More specifically, Cr(VI) adsorption is zeroed for pH values higher than 7.5 in the presence of phosphates, while it is maximized in both cases for pH values lower than 4.

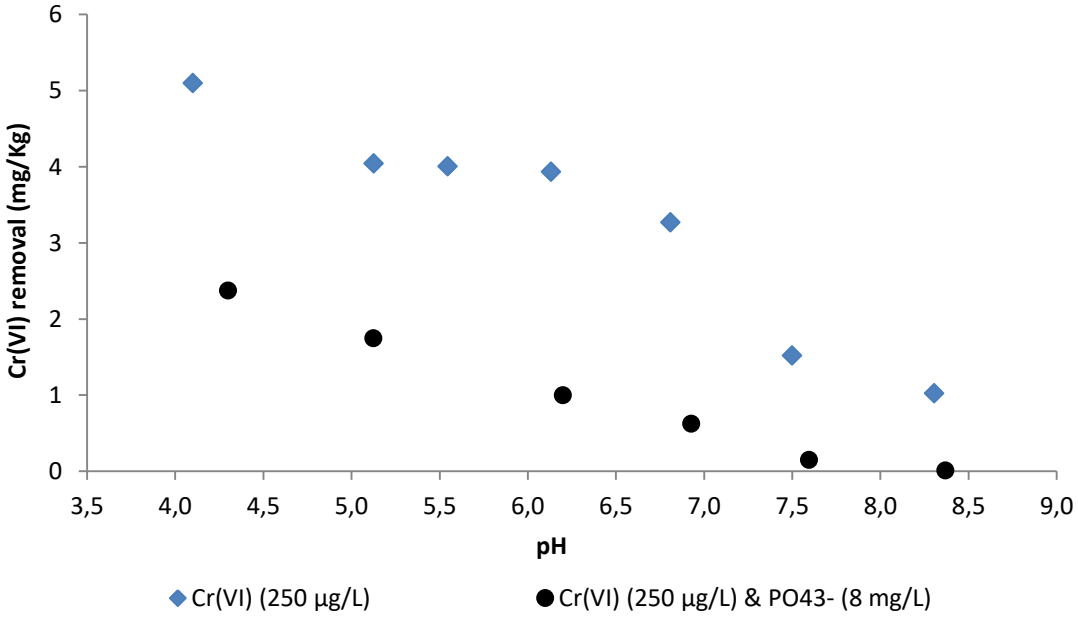

Figure 5.7 Effect of phosphates ($[PO_4^{3-}]_0$ = 8 mg/L) on Cr(VI) adsorption

Adsorption of chromates in the presence of other anions has also been widely studied. The results indicate that chromates are usually affected by competitive adsorption phenomena due to the presence of other inorganic anions like PO_4^{3-}, SO_4^{2-}, $H_2SiO_4^-$, etc. The effects of competitive adsorption strongly depend on the concentration of the dissolved anions. A common observation regarding chromates adsorption during the simultaneous presence of other anions in the aqueous solution is the shift of the edge of the pH-adsorption curve to lower values. The presence of more than one kind of anions decreases chromates adsorption with the phenomenon being additive regarding the number of different anions presented in the solution (Zachara et al., 1987).

Tzou et al. (1998) is one of the very few studies investigated the possible competition of phosphates and chromates during their adsorption by soils. The results of their study showed that the presence of phosphates inhibited chromates adsorption due to the weaker adsorption of chromates by soils compared to phosphates adsorption and the competition of the anions for the sorption sites (Tzou et al., 1998; 2003). Similarly to the results of Tzou et al. (1998), the research team of Jiang et al. (2004), who used hydroxy-Fe-montmorillonite complex as adsorbent, showed that phosphates were strong competitors for chromates probably due to the greater sorption affinity for the surface than chromates.

5.1.7 Effect of nitrates on Cr(VI) adsorption

Nitrate leaching from agricultural lands is one of the most serious problems related to both environmental quality and human health. Nitrates mobility in the geoenvironment is affected

by a number of factors, such as the concentration of iron and clay oxides, the concentration of organic material, pH and ionic strength of the soil solution and the soil composition and mineralogy. In addition, competition with other anions, such as chlorides, plays a critical role in nitrate adsorption (Qafoku et al., 2005). Nitrate ions are thought to be adsorbed on iron and aluminum hydroxides, which subsequently are precipitated resulting, thus, in decrease of nitrates concentration. Soils with low iron and aluminum hydroxide content may have very low adsorption capacity (Sposito, 1989). In this study, nitrates adsorption on the ophiolitic soil was investigated using two concentrations of 5 and 50 mg/L, in the pH range of 4-9. The effect of chromates on nitrates adsorption was also investigated.

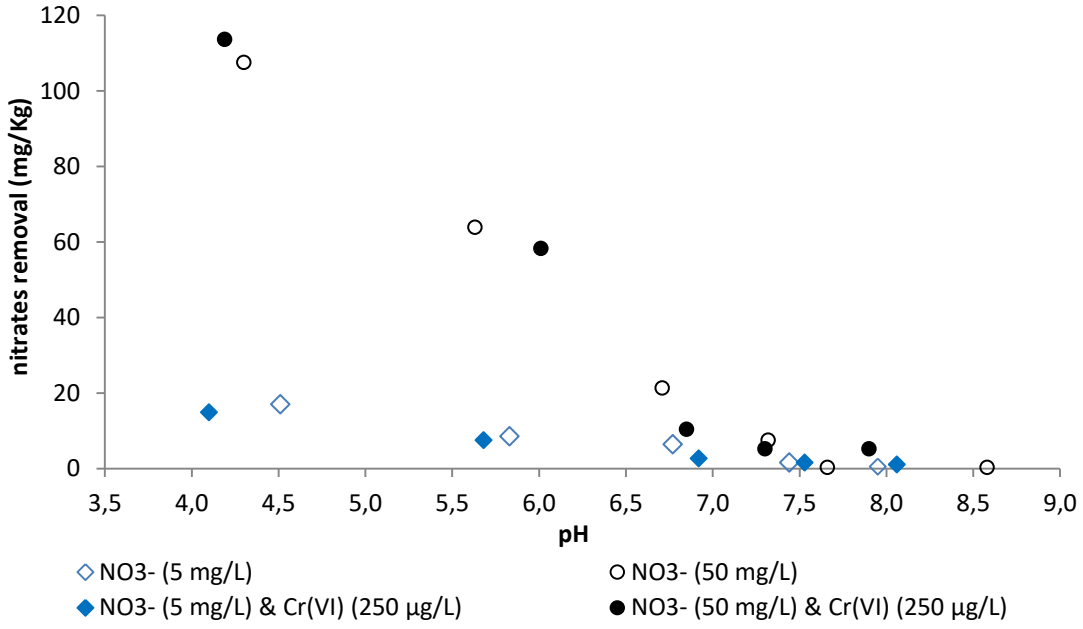

Figure 5.8 Effect of Cr(VI) on nitrates adsorption

As observed from Figure 5.8 the presence of chromates did not affect the nitrates adsorption neither in the case of using 5 mg/L nor using 50 mg/L of nitrates. However, the effect of pH on nitrates adsorption was significant, as in the case of phosphates adsorption, since nitrates adsorption decreased with increasing pH independently the presence of chromates. In both cases of using 5 and 50 mg/L nitrates, the adsorption efficiency was very low since the maximum percentages observed were 6% and 4%, respectively. In addition, for pH > 7, nitrates adsorption was minimized and almost zeroed. The effect of pH on nitrate adsorption is mainly attributed to the change in neutral proton charge (σ_H) in soil particles. Increasing the pH, the σ_H decreases, even to negative values, resulting in increase in the repulsions from the soil particles. These repulsions are dominant for pH > PZNC (Sposito, 1989).

Numerous studies have investigated nitrates adsorption by different types of soils. A literature review of these studies is presented below. Kinjo and Pratt (1971) were of the first studied nitrates adsorption by subsoils of Andepts, Oxisols, and Alfisols from Mexico and South America using batch experiments. The results showed that nitrates adsorption was maximized at pH about 3.5, while the adsorption efficiency was significantly correlated with the content of amorphous inorganic materials extractable with 0.5 N NaOH. Using similar types of soils (Oxisols and Entisols), Dynia (2008) showed that nitrates adsorption was

attributed to the presence of positive electrical charges in these types of soils. In addition, nitrate retention capacity was ranged between 120 and 370 mg/Kg at pH value about 6, and was strongly affected by the soil depth since subsoils exhibited larger capacity for nitrate retention than surface ones.

The study of Wang et al. (1987) mentioned the effect of different factors on nitrates adsorption, such as the iron oxide content, the pH of the soil solution, the concentration of other anions and the kind of cations present in the solution. More specifically, they investigated the effect of chlorides on soil adsorption of nitrates, observing that the affinity of the soil for chlorides was higher than for nitrates.

The adsorption capacity of acidic soils for nitrates was investigated by Eick et al (1999) and Strahm and Harrison (2006). High adsorption capacity of acidic soils for nitrates was determined by Eick et al (1999), who, using 5 and 50 mg/L initial concentration of nitrates, estimated that the soil adsorption capacity for nitrates is 62 and 310 mg/Kg respectively, demonstrating that acidic soils, high in variable charge minerals, may have the potential to decrease nitrates mobility to groundwater. On the contrary, significantly lower adsorption capacity of acidic soils (pH≈4.5) was reported by Strahm and Harrison (2006) who used acidic soils from the Pacific Northwest. The tested soils were rich in iron and aluminum non-crystalline forms. However, their adsorption capacity for nitrates was in the same range with the adsorption capacity of the ophiolitic soil used in this study, exhibiting also a concentration dependent adsorption trend. More specifically, for initial nitrate concentration of 5 and 50 mg/L the adsorbed amounts of nitrates ranged between 2 to 7 mg/Kg and 5 to 60 mg/Kg, respectively.

More recently, Mise and Bashetty (2013) investigated the adsorption capacity of red soils for nitrates as a function of pH, contact time and adsorbent dosage. Adsorption equilibrium reached in about 2 hours with adsorption capacity determined at 5.4 mg/Kg for initial concentration of 10 mg/L nitrates at pH equal to 6. These values of adsorption capacity are also close to the tested ophiolitic soil.

Contrary to the aforementioned studies, Hamdi et al. (2013) reported that nitrates were weakly retained by a Tunisian soil sample, despite adsorption experimental results showed that adsorption capacity was affected by the soil sampling depth (samples collected down to 1 m depth), the contact time, nitrates initial concentration and adsorbent concentration. Comparing with the results of the present study for pH value about 8.1, soil concentration equal to 20 g/L and nitrate initial concentration of 50 mg/L, the adsorption capacity of nitrates was about 0.02 mg/kg, two orders of magnitude lower than the capacity of the ophiolitic soil used in the present study. The phenomenon of very low adsorption of nitrates was investigated by Brousseau (2012) using forest soils (pH ≈ 5, Fe = 26.4 – 40.2 mg/Kg, Mn = 15.1 – 101.4 mg/Kg). They reported that nitrates are not immediately adsorbed by soil and usually a minimum concentration is required in order to be adsorbed. This threshold is attributed to the lower affinity of nitrates for the solid surface due to the presence of organic matter or other contaminants in the soil solution that act competitively. Thus in deeper horizons, where biologically mediated processes and inorganic compounds, such as

phosphates and sulfates that can inhibit nitrates sorption are decreased, highest potential for nitrates adsorption exists. In addition, the adsorption of nitrates is affected by the ionic strength of the soil solution, with adsorption increasing with decreasing ionic strength. As a result, nitrates adsorption may be a spatially and temporally variable mechanism.

Finally the effect of aluminum oxides concentration apart from iron oxides was mentioned by Tani et al. (2004). Studying the nitrates adsorption on allophanic Andisols mentioned that the presence of allophanes is an important factor able to control nitrates adsorption. The tested soils displayed low total carbon concentration and high allophane content, which was responsible for nitrates adsorption. These soils, with high amorphous aluminum content, showed similar and, in some cases, higher adsorption capacities compared to soils rich in iron oxides such as Ultisols (quite acidic soils with pH < 5, lack of organic matter, red and yellow colored due to the accumulation of iron oxides, major nutrients calcium and potassium, they have less than 10% weatherable minerals) and Oxisols (quite alkaline soils with pH > 7, red or yellowish colored, due to the high concentration of iron(III) and aluminium oxides and hydroxides, also they contain quartz and kaolin and small amounts of other clay minerals and organic matter).

Regarding the effect of nitrates on Cr(VI) adsorption (Figure 5.9) the results showed that Cr(VI) adsorption was not affected by the presence of nitrate anions in the solution, despite the high difference in concentrations between chromates and nitrates, 20 and 200 times, respectively. Only a very slight decrease seems to occur in the case of using 50 mg/L of nitrates in the pH range 7 - 8. Thus, it can be concluded that the presence of nitrates cannot act competitively for Cr(VI) adsorption, at least for nitrates concentrations that are typically met in groundwater. This can be a result of surface selectivity for chromates towards nitrates. In addition, the electrostatic repulsions that may occur between nitrates occur in the aqueous phase could not inhibit Cr(VI) adsorption. Chromates are thought to form stronger bonds with the solid surface since they can form inner sphere complexes, which include covalent and/or ionic bonds contrary to nitrates, which form exclusively outer sphere complexes, which are based solely on electrostatic interactions (Sposito, 1989; Komárek et al., 2015). These results are of the first being published regarding any competition between chromates and nitrates in real soils.

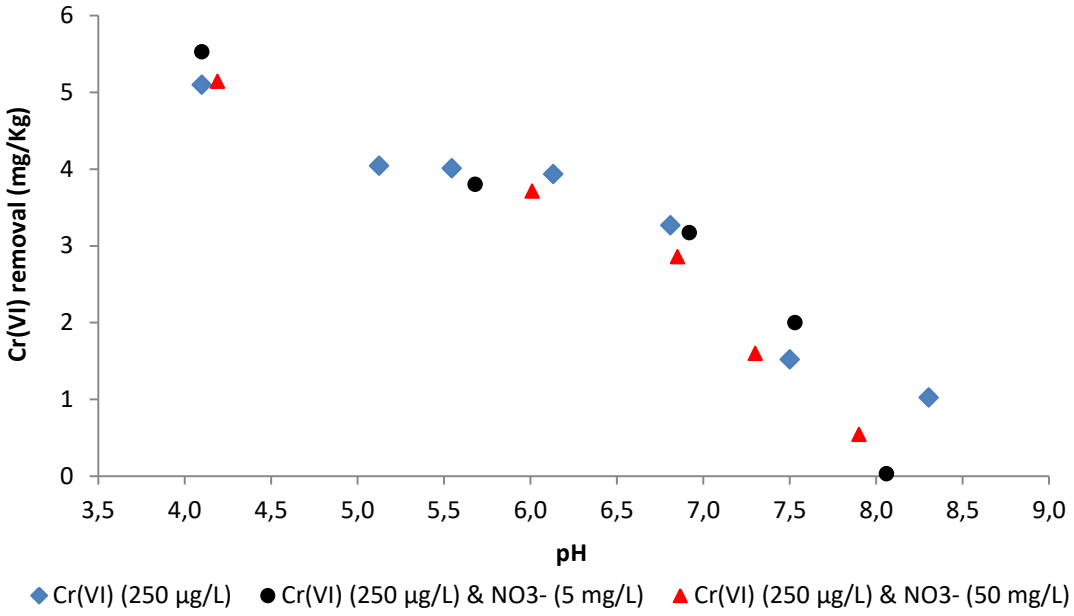

Figure 5.9 Effect of nitrates on Cr(VI) adsorption

5.2 Adsorption of Cr(VI) on goethite

Among ferric (hydr)oxides that occur in the geoenvironment, goethite is the most abundant. Goethite and hematite are the predominant pedogenic iron oxides, followed by maghemite and ferrihydrite. The concentrations of these minerals in the soil and their characteristics, such as crystallinity and SSA, vary depending on the parent material, the intensity of weathering, the composition of the soil solution and drainage conditions (Cornell and Schwertmann, 2006; Fink et al., 2014). Goethite was selected as an adsorpbent in this study since it is a common iron oxide presented in ophiolitic soils. The high pH_{PZC} values that have been reported for goethite, usually in the range 7.5–9, render α-FeOOH a highly potential adsorbent for metal anions in groundwater (Li and Stanforth, 2000). In this study the pH of the goethite solution measured equal to 7.4 and the goethite total surface area equal to 9.09 m^2/g.

The value of SSA is strongly correlated with another important factor parameter in soil science able to affect adsorption efficiency; the degree of crystallinity of goethite. As mentioned in Chapter 4.4, the degree of crystallinity is reflected by the surface area with the best crystallized solids exhibiting the lowest SSA (Strauss et al., 1997). Thus, the low SSA value of the goethite sample used in this study can be attributed to the high degree of crystallinity. In the geoenvironment goethite crystallinity is affected by a number of factors and in natural profiles it may vary laterally as well as vertically. Considering that higher values of surface area are attributed to greater weathering and taking into account that the soil samples in our study obtained from deep horizons with low weathering, the usage of a low surface area goethite will possibly better simulate the adsorption phenomena of the real soil. In addition, the value of surface area is correlated with the required time for the completion of the adsorption process. Low surface area of goethite need only some hours until adsorption is completed, indicating that the time of 24 h given in the present study for achieving adsorption equilibrium is sufficient (Torrent et al., 1990; Strauss et al., 1997).

5.2.1 Effect of pH and ionic strength on Cr(VI) adsorption

The effect of pH and ionic strength of the goethite solution on Cr(VI) adsorption was tested in the first series of experiments. The results showed that Cr(VI) adsorption decreased by increasing the pH, regardless of the ionic strength of the solution (Figure 5.10). Cr(VI) adsorption is almost 100% at acidic conditions and decreases with increasing pH values exhibiting the typical adsorption behavior of anions. This phenomenon is attributed to the alteration of surface charge, which becomes less positively charge, as pH increases and finally negatively charged for pH values higher than the pH_{PZC} value. This leads to the occurrence of electrostatic repulsions between the hydroxyl groups at the goethite surface and chromates (Sposito, 2008; Ajouyed et al., 2010).

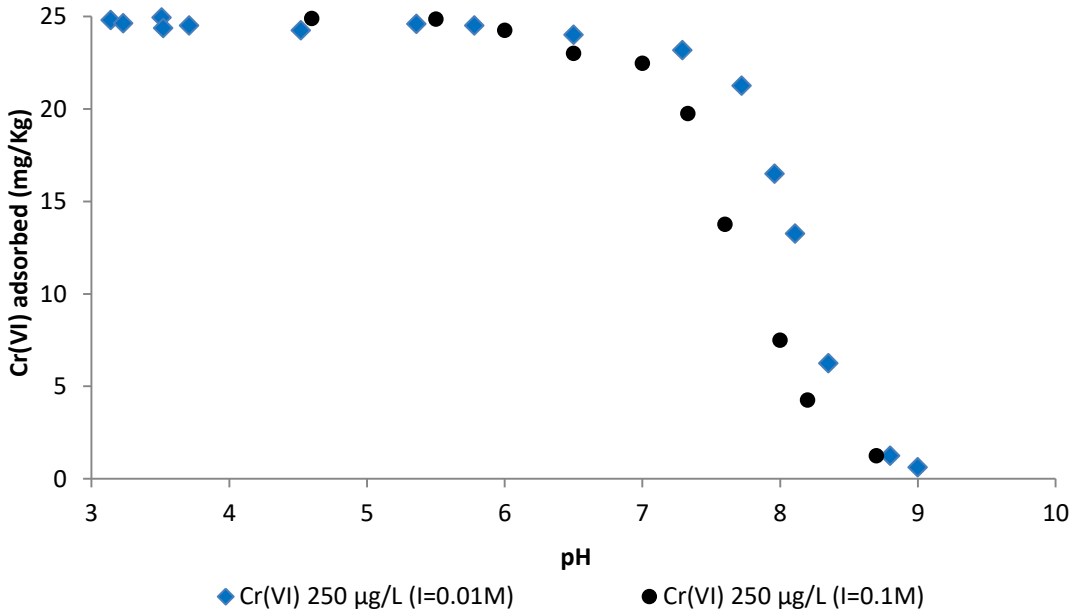

Figure 5.10 Effect of ionic strength on Cr(VI) adsorption at goethite

Ionic strength, besides pH, is another important factor influencing Cr(VI) adsorption. In this study, the effect of ionic strength was tested by using two different NaCl concentrations as background electrolyte differing one order of magnitude, i.e., 0.01 and 0.1 M. Different adsorption efficiency of chromates was observed (Figure 5.10). Specifically, adsorption is maximized for pH values lower than 6.5 and 7.5, in the case of using 0.1 and 0.01 M NaCl, respectively. However, in the pH range of 7.5 - 8.5, the effect of ionic strength was important. The ionic strength can affect the thickness of the double layer and the interface potential, influencing thus the binding of the adsorbed species. Adsorption efficiency for pH < PZC point can be attributed to the fact that ionic strength reduces the adsorption of chromates by decreasing the activity of chromates for adsorption and by decreasing the positive charge of the solid surface. Thus, the electrostatic attractions between the chromate anions and the more negatively charged surface are decreased. Several studies have investigated the effect of ionic strength on Cr(VI) adsorption using synthetic goethite as sorbent, with the results showing that Cr(VI) adsorption was not or only slightly affected by ionic strength and slightly affected by the type of background electrolyte (Burden 1989; Measure and Fish, 1992; Weerasooriya and Tobschall, 2000; Ajouyed et al., 2010; Xie et al., 2015).

5.2.2 Effect of phosphates on Cr(VI) adsorption

The crystalline iron oxides, goethite and hematite, and the crystalline aluminum oxide gibbsite, as well the amorphous aluminum oxides are important minerals in phosphate adsorption. In clay samples the iron oxides are the main adsorbents for P and among iron oxides goethite exhibits higher adsorption capacity than hematite. Gibbsite and amorphous Al-oxides are more likely to be related to phosphate adsorption, mostly based on their relative abundance in the samples contrary to iron oxides, which exhibit specific characteristics additionally to their content that influence P adsorption (Fontes and Weed, 1996; Fink et al., 2016). Thus, goethite, which is one of the most common and stable crystalline iron (hydr)oxides in natural systems, is considered of the main adsorbents for phosphates. The significant contribution of goethite on phosphates adsorption has been determined several years ago using electron microscope analysis (Fordham and Norrish, 1979; Razaq et al., 1989).

The determination of removal process of phosphates from goethite, either adsorption or precipitation, is usually difficult and cannot be achieved by calculating the mass difference between the initial phosphates concentration and the loss of phosphates from the aqueous phase. Li and Stanforth (2000) reported that no discernible alterations between adsorption and precipitation observed in the adsorption isotherms of phosphates on goethite, proposing a methodology based on the alteration of zeta potential with increasing adsorption. This alteration is attributed to the increase of the negative surface charge due to the adsorption of the more acidic phosphate ions, which replace the less acidic hydroxyl groups. However, in the case of phosphates precipitation, the increase of the negative charge is much smaller, since there are no changes in the characteristics of the surface. A complication is created in the case that adsorption is followed by precipitation (Li and Stanforth, 2000). In general, even with other methodologies it has been reported that the distinction between adsorption and precipitation of phosphates is very difficult. Regarding adsorption of phosphates on goethite, the process of ligand exchange is considered involving the replacement of phosphate for one or more surface hydroxyl groups. Two discrete stages have been proposed, an initial fast stage followed by a slow one usually more pronounced, in the case of well crystalline solids, which is related with the diffusion into the micropores or aggregates of the solid particles. More specifically phosphates are thought to be preferentially exchanged with two groups of Fe-$OH_2^{1/2+}$ and Fe-$OH^{1/2-}$, releasing surface structural H_2O or OH^- in the solution. Thus, the affinity of phosphates for goethite surface depends, on both the anions' capacity for surface complexation through ligand exchange, as well as on the attractive or repulsive electrostatic interactions with the charged surfaces (Wang et al., 2013).

In this study the removal of phosphates by goethite will be called as "adsorption", without excluding the possibility of some precipitation occurring. The results of phosphates adsorption and the effect of Cr(VI) presence on their adsorption efficiency by goethite used in this study are presented at Figure 5.11. Phosphates adsorption exhibited the typical adsorption behavior of anions as a function of pH values. Specifically, adsorption was maximized for pH values lower than 7.5 for both concentrations tested. Similar results have been reported by other studies indicating that phosphates are strongly adsorbed on goethite even at high pH values. It is considered that phosphates adsorption on goethite is based on ligand exchange mechanism

rather than electrostatic attractions. Thus, the increase of the solution pH would cause lower phosphate adsorption due to the increasing concentration of hydroxyl (OH^-) ions in the solution, which consequently cause negatively charged surface of goethite (Li and Stanforth, 2000; Rietra et al., 2001; Antelo et al., 2005; Chitrakar et al., 2006). Adsorption efficiency is minimized at pH values higher than 9, where strong repulsions between the phosphate anions and the negatively charged surface occur. However, goethite can be considered as an important adsorbent, able to decrease the mobility of phosphate ions even at alkaline pH values. The efficient adsorption of goethite even at alkaline pH values where the solid surface is negatively charged have also been referred by Hiemstra et al. (1996) and Strauss et al. (1997).

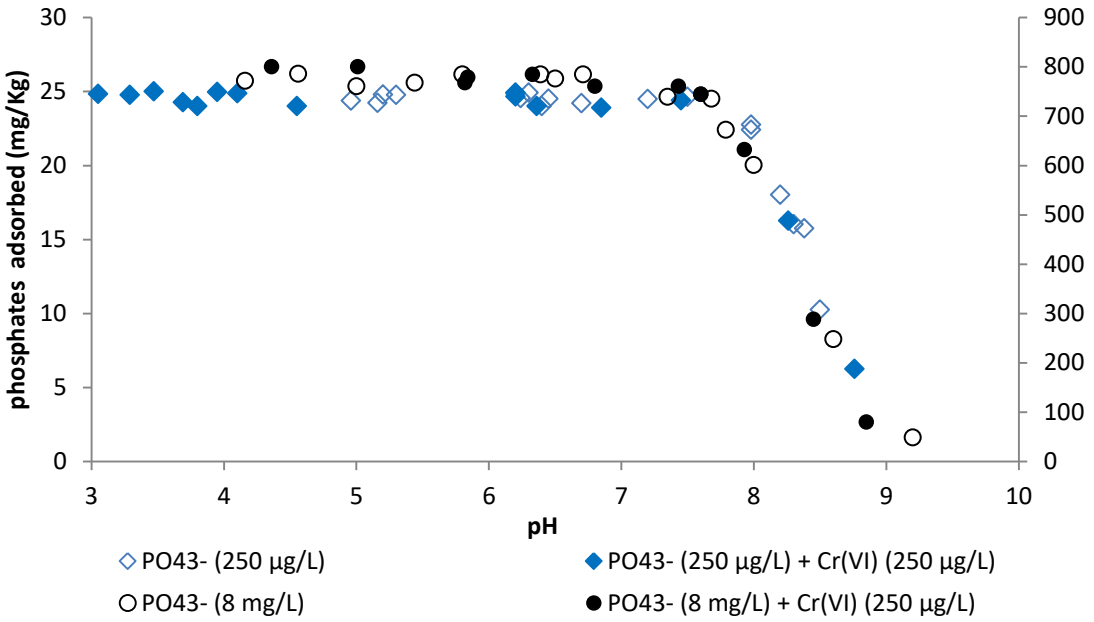

Figure 5.11 Adsorption of phosphates (250 µg/L and 8 mg/L) on goethite, in the presence (250 µg/L) and absence of Cr(VI).

The decreasing trend of phosphates adsorption curve with increasing pH values has been also observed from several studies (Madrid and Posner, 1979; Razaq et al., 1989; Geelhoed et al., 1997; Antelo et al., 2005; Luengo et al., 2006; Tzou et al., 2010; Boukemara and Boukhalfa, 2012; Wang et al., 2013). Razaq et al. (1989) were of the first group of researchers investigating the effect of pH on phosphates adsorption on goethite, reporting that phosphates adsorption decreases slowly with increasing pH values due to the following factors. Firstly, the pH increase leads to the increase of HPO_4^{2-} concentration in the aqueous phase about 10-fold for each pH unit and the surface becomes negatively charged resulting in greater electrostatic repulsions. However, the increase in HPO_4^{2-} concentration offsets the decrease in electrostatic potential with the pH increase. As a result, phosphate adsorption decreases slowly until the pK_2 of H_3PO_4 is reached at 7. For higher pH values the concentration of phosphate divalent ions decreases, while the surface charge becomes more negative resulting in greater repulsions decreasing the adsorption efficiency. Thus, at pH values that H_3PO_4 is fully dissociated (pK_2), specific adsorption occurs only due to the impact of the positive surface charge. The effect of pH due to the presence of OH^- groups affecting the surface charge and due to the phosphates aqueous chemistry was mentioned by Boukemara and Boukhalfa

(2012). The reported results showed that adsorption was maximized at acidic conditions and started decrease at pH values about 6. The presence of hydroxyls on the solid surface act by attracting or dissociating protons depending on the pH solution, rendering, thus, the surface either positively or negatively charged. Since the pH_{PZC} value is the threshold pH value for the alteration of the surface charge, for pH values lower than the PZC point non-specific adsorption of phosphates is favorable due to the action of electrostatic attractions, while for pH values higher than the PZC the $Fe(OH)_2^+$ sites are fewer reflecting the adsorption decrease. In addition, the pH values affect the protonation of phosphates. In the pH range 3-6, $H_2PO_4^-$ are the predominant species which are strongly adsorbed on the positively charged surface as also mentioned by Razaq et al. (1989).

The effect of chromates on phosphates adsorption is also presented at Figure 5.11. For both cases of phosphates concentration tested (8 mg/L and 250 μg/L as PO_4^{3-}), adsorption was not influenced by the presence of Cr(VI) in the goethite solution, indicating that phosphates are preferably adsorbed on the goethite surface compared to chromates. The higher affinity of phosphates for the goethite surface compared to other anions, such as sulfates, arsenates, molybdate, organic compounds etc., has also been reported by several studies. However, only few of them have investigated the possible competition with chromates. Burden (1989) was of the first researchers reporting the affinity of several inorganic contaminants for the goethite surface, since the relative affinity of an anion for the specific adsorption sites is a crucial factor for determining the possible preferential adsorption. The results showed that P exhibits higher affinity than chromium for the goethite surface, and thus phosphates are preferably adsorbed on goethite compared to chromates. Boukemara and Boukhalfa (2012) also mentioned that phosphates removal is not affected by the presence of chromates but influences the retention mechanism. The results of the Infrared Spectroscopy analysis showed that in the presence of chromates the predominant mechanism is the formation of inner sphere complexes with the solid surface.

The higher affinity of phosphates for the goethite surface compared to other anions, such as sulfates, arsenates, molybdate, organic compounds etc., has also been reported by several studies. However, only few of them investigated the possible competition with chromates. The effect of chromates on phosphates adsorption is also presented at Figure 5.11. For both cases of phosphates concentration tested, their adsorption was not influenced by the presence of Cr(VI) in the goethite solution, indicating that phosphates are preferably adsorbed on the goethite surface compared with chromates. Burden (1989) was of the first researchers reporting the affinity of several inorganic contaminants for the goethite surface, since the relative affinity of an anion for the specific adsorption sites is a crucial factor for determining the possible preferential adsorption of anions. The results showed that P exhibits higher affinity than chromium for the goethite surface, and thus phosphates are preferably adsorbed on goethite compared to chromates. Boukemara and Boukhalfa (2012) also mentioned that phosphates removal is not affected by the presence of chromates but influences the retention mechanism. The results of the IR analysis showed that in the presence of chromates the predominant mechanism is the formation of inner sphere complexes with the solid surface.

Despite the absence of any competitive effects of chromates on adsorption of phosphates in the reverse case namely the impact of phosphates on chromates adsorption was significant, as it can be observed from Figure 5.12. The effect of phosphates on Cr(VI) adsorption was tested for both concentrations of phosphates 250 μg/L and 8 mg/L. In both cases Cr(VI) adsorption decreased with increasing pH. For pH<7 Cr(VI) adsorption was maximized and not influenced by the presence of phosphates. This is possibly attributed to the fact that the available sites for Cr(VI) adsorption are not limited, despite the presence of the phosphate ions. For pH>7, the presence of phosphates affected Cr(VI) only in the case of using the higher concentration of phosphates. The fact that the presence of phosphate ions at low concentration (250 μg/L) did not affect Cr(VI) adsorption is probably attributed to the excess of surface active sites, even at high pH values, able to adsorb both anions. This can be supported by the fact that by increasing phosphate concentration to 8 mg/L, Cr(VI) adsorption decreased in the pH range 7.5 - 8.3, where the adsorption sites eliminated due to the alteration of the surface charge.

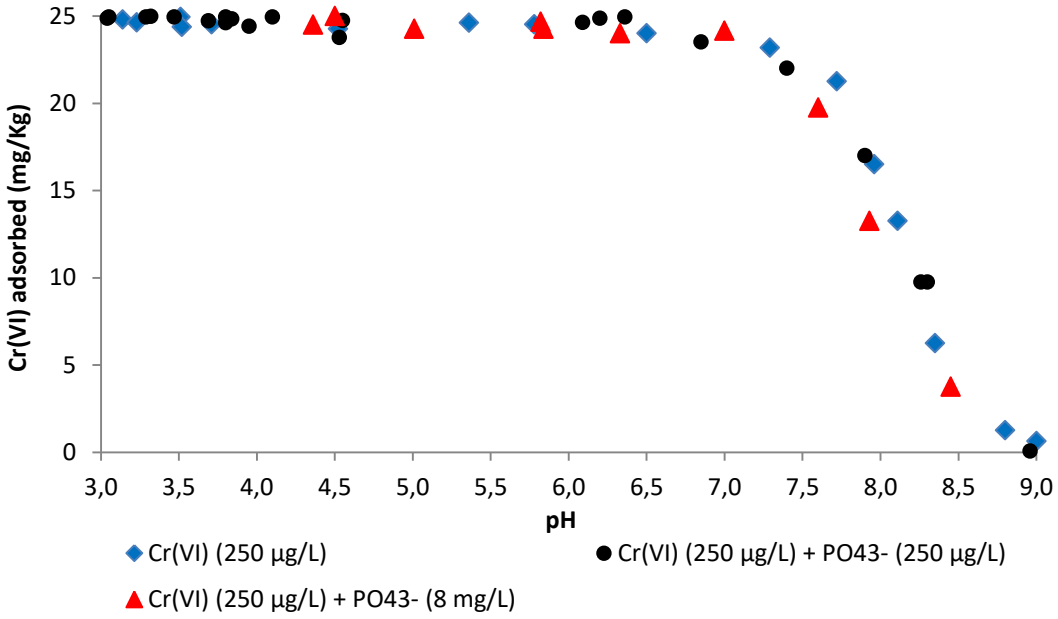

Figure 5.12 Effect of phosphates on Cr(VI) adsorption on goethite.

As mentioned above, the extent of the interaction depends on the affinity of the anions for the surface. Phosphates exhibit higher affinity than chromates and, thus are preferably adsorbed, inhibiting the adsorption of chromates (Geelhoed et al., 1997; Chitrakar et al., 2006). However, only one recent work has extensively studied the possible competition between chromates and phosphates on goethite (Xie et al., 2015). The results were in accordance with these of the present study, since the presence of phosphates inhibited the adsoprtion of chromates, while no effects observed for the opposite case.

5.2.3 Effect of nitrates on Cr(VI) adsorption

Despite that several studies have reported the adsorption efficiency of different materials towards nitrates, the adsorption behavior of nitrates on minerals that present in their structure exclusively ferric iron has not been reported yet (Bhatnagar and Sillanpää, 2011). Adsorbents that occur in the aquifers like clays have been reported for their adsorption

capacity but only at low pH values (Mohsenipour et al., 2015), while the presence of ferrous iron in soil minerals like magnetite is able to reduce nitrates to nitrites and other N forms (Dhakal, 2013; Cho et al., 2015). Nitrate anions are considered to be adsorbed on goethite surface through electrostatic attractions (Chitrakar et al., 2006). Adsorption of nitrates (Figure 5.13), and the effect of Cr(VI) presence on their adsorption efficiency by goethite was tested herein. The nitrates found not to be effectively adsorbed on goethite neither in the absence nor in the presence of Cr(VI). Adsorption efficiency reached the level of 10% at acidic pH values, while it was diminished in the pH range 7 – 8.5 that usually occurs in groundwater. Thus, goethite cannot be considered as an effective natural adsorbent for nitrates in the geoenvironment. In general the low adsorption capacity of soils for nitrates has been reported by Hamdi et al (2013) and several factors can be responsible for this low affinity of nitrates. One of the first studies investigated the nitrates adsorption on hydrous ferric oxides was that of Harrison et al. (1982). Using IR spectroscopy they stated that monovalent oxyanions, such as nitrates, are adsorbed primarily via electrostatic interactions with the hydrated surface and thus are not strongly retented. In addition, the presence of divalent ions, such as chromates, are directly coordinated to two surface iron cations and, thus, inhibit further the nitrates adsorption as it is verified by the results of this study (Figure 5.13). Furthermore, the low adsorption affinity of nitrates on the goethite surface can also be attributed to the fact that chlorides presented in the solution, as anions of the background electrolyte, are preferably adsorbed on the solid surface compared to nitrate anions. Regarding the presence of Na^+ is considered to exhibit low affinity for the goethite surface (Rietra et al., 2000). It seems that adsorption of nitrates by minerals consisted exclusively by ferric iron cannot be the main mechanism for nitrates immobilization in aquifers. Therefore, possibly redox reactions and microbial degradation are the mechanisms that control their transport in the geoenvironment.

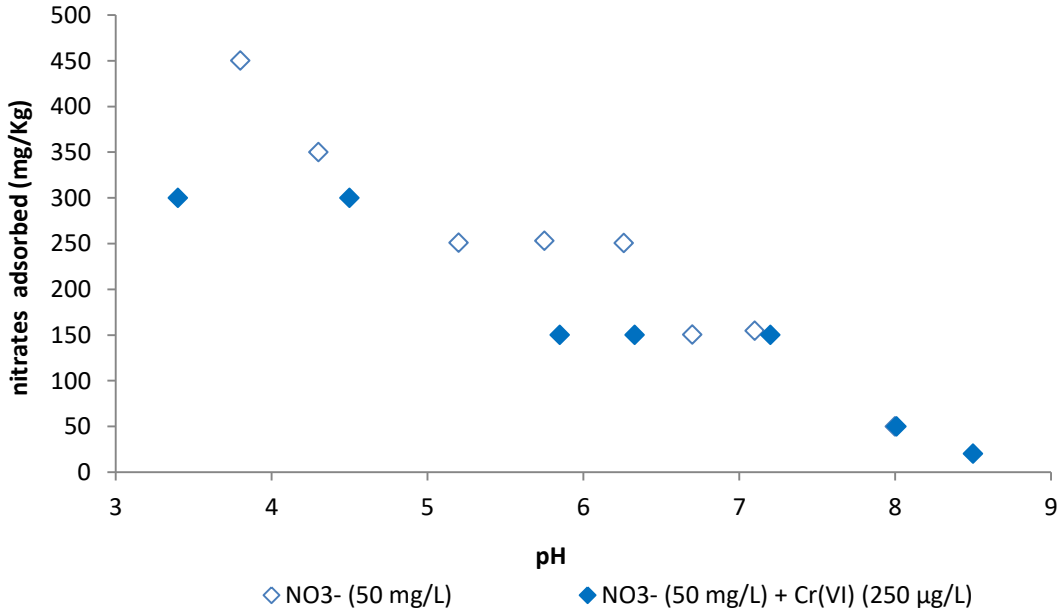

Figure 5.13 Adsorption of nitrates (50 mg/L) on goethite in the presence (250 µg/L) and the absence of Cr(VI).

The effect of nitrates on Cr(VI) adsorption was tested using 50 mg/L of nitrates (Figure 5.14), since this concentration is considered as typical in aquifers affected by agricultural activities

and is also the maximum allowable concentration in groundwater according to the European and the Greek legislation. Based on the results shown at Figure 5.14, Cr(VI) adsorption decreased with increasing pH. For pH values lower than 7, Cr(VI) adsorption was maximized and not influenced by the presence of nitrates. This is possibly attributed to fact that the available sites for Cr(VI) adsorption are not limited despite the presence of nitrate ions. For pH values higher than 7 the presence of nitrates (50 mg/L), with concentration 200 times higher than that of chromates (0.25 mg/L), possibly caused electrostatic repulsions, able to decrease the adsorption efficiency, since no Cr(VI) reduction is considered to occur (Vilardi et al., 2017). The results of this study are of the of the first being published for describing any competitive interactions between nitrates and chromates on goethite.

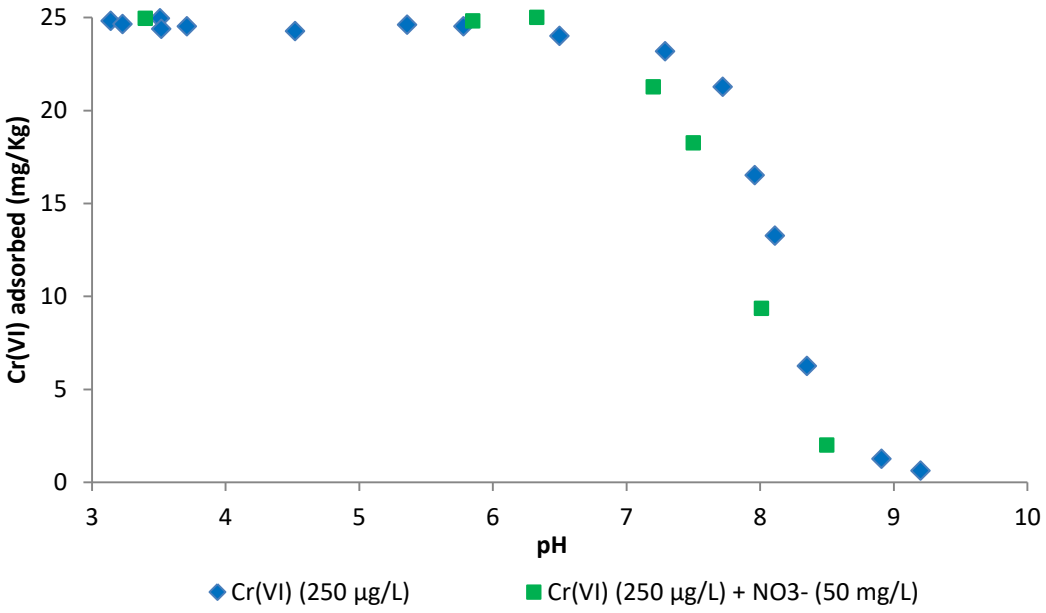

Figure 5.14 Effect of nitrates on Cr(VI) adsorption on goethite

6 ADSORPTION SIMULATION OF Cr(VI) AND INORGANIC CONTAMINANTS

6.1 Adsorption simulation on ophiolitic soil

The results obtained from the batch experiments (chapter 5) and the physicochemical analysis (chapter 4) of the ophiolitic soil were used in order to simulate adsorption of Cr(VI) and the rest inorganic contaminants by applying SCMs via the visual Minteq software. For adsorption simulation the results of Cr(VI) total removal were used, including possible reduction of Cr(VI) by soil, based on the three following assumptions:

i. Adsorption based on the formation of inner sphere complexes is thought as an irreversible process. Thus, a percentage of the non-desorbed mass can be attributed to the formation of inner-sphere complexes.
ii. Reduction implies the occurrence of Cr(VI) adsorption on the soil surface.
iii. In most models that describe contaminants transport, the retardation factor due to geochemical process does not distinguish the process that causes the retardation and thus the total contribution of each process is taken into account.

Three adsorption models used for simulation of experimental data of this study are based on surface complexation reactions; the Triple Layer Model (TLM), the Diffuse Layer Model (DLM) and the Constant Capacitance Model (CCM). Despite the fact that these three surface complexation models are of the most frequently used it is not clear which of the three models better describes adsorption in natural systems like soils. Thus a comparison of the efficiency of these models was performed in this study. The main parameters used for adsorption simulation were the following:

- Solid concentration (g/L)
- Specific surface area (m^2/g)
- Site density (#sites/nm^2)
- Inner capacitance (C_1) (F/m^2)
- Outer capacitance (C_2) (F/m^2)

The acceptable deviation between the experimental data and the modeling results, in order to qualify simulation as satisfactory and, thus, to accept the values of surface complexation constants, was determined to ±5%.

6.1.1 Determination of solid concentration

Neither the identification nor the quantification of iron oxides using XRD analysis are easy and efficient in soil samples, especially in the case that other minerals, like quartz, are in abundance (Schwertmann et al., 1982; Bortoluzzi et al., 2015). The contribution of iron oxides on the binding of several contaminants is due to the reactive groups presented on their surface. The chemical reactions that occur on their surface lead to the formation of a complex system rendering, thus, the prediction of the interactions with several compounds very difficult (Weng et al., 2012). According to the mineralogical analysis performed in the tested soil and taking into account the PZC values (Table 6.1) of the identified minerals, Cr(VI) adsorption can mainly be attributed to several minerals that have high PZCs: Iron

oxides such as hematite (Singh et al., 1993), and amorphous goethite (Fendorf, 1995) that have also been previously identified in serpentine soils in Greece (Kelepertzis et al., 2013) are possibly the main adsorbents. In addition, chlorite (Brigatti et al., 2000) and magnetite (Jung et al., 2007) can contribute to Cr(VI) removal via both reduction and adsorption. Chromite and chrysotile also have PZCs that can justify Cr(VI) adsorption; however there is no information in the literature with respect of the sorption behavior of these minerals.

Table 6.1 Range of PZC values of the identified minerals (RES^{3}T).

Mineral	Medium	PZC
Quartz	S,R	1.2 – 3.0
Albite	S,R	2
Chlorite	S,R	9.5
Chrysotile	S	>8
Vermiculite	S	2.9 (PZNPC)
(Magnesio)Chromite	S	7.2 – 7.7
Magnetite	S	5.2 – 6.8
Hematite	R	4.5 – 9.5 (mainly at 7.5 – 8.5)
Goethite	S	7.5 – 9.5

S: soil, R: rock

As presented in chapter 4 (Table 4.6) the mass balance as determined by XRF and via quantitative XRD analysis of the -0.5 mm fraction of the soil sample, showed that the amorphous fraction of soil consists mainly of Fe, Si and Mg and its concentration is equal to 101.2 g/kg. The low content of iron in the well crystallized minerals (as observed by XRD analysis) indicated the occurrence of amorphous oxides in the ophiolitic soil. Iron oxides such as goethite (a-FeOOH), ferrihydrite ($Fe_2O_3 \cdot H_2O$), and hematite (Fe_2O_3) are considered as important natural adsorbents for heavy metals and inorganic contaminants. The partially crystallized goethite is possibly the predominant amorphous oxide of iron since it is usually presented in serpentinitic soils (Chardot et al., 2007) without excluding the presence of other iron oxides. In addition, silicon amorphous oxides and amorphous magnesite may also occur in the tested soil as products of disintegration of ultramafic rocks (Peterson, 1984; Zachmann & Johannes, 1989).

Although the aluminum content in the tested samples was low and seems that aluminum is almost exclusively presented in the structure of the crystalline minerals, XRF analysis of the collected samples from other soil horizons exhibited occasionally higher contents in aluminum, up to 30 g/Kg. This indicates the presence of aluminum amorphous oxides (Al_2O_3) in the soil sample. Taking into account that aluminum amorphous oxides can also contribute to the adsorption of Cr(VI) and other anions, a re-calculation of the mass balance was performed in order to determine the concentration of aluminum amorphous oxides.

Thus the adsorption simulation will be performed taking into account the contribution of iron and aluminum concentrations. However, since the adsorption simulation in this study is based on the assumptions of the GC approach of modeling, the estimation of the oxides contribution is based only on the quantitative contribution of the iron and aluminum oxides and the

contribution of each type of surface is not distinguished. The importance of hydrous ferric oxides as predominant adsorbents in cases of adsorption modeling has also been mentioned by Mengistu et al. (2015). Table 6.2 presents the concentration of iron and aluminum oxides in the tested soil and the soil samples used in the batch experiments.

Table 6.2 Concentration of Fe- and Al- amorphous oxides used in the batch experiments.

Element	Fe	Al
XRD (g/kg)	38	19
XRF (g/kg)	74	30
Amorphous (g/kg)	38	11
% XRD/XRF	49	63
% Amorphous	51	37
Amorphous (g/kg)	38.0	11.0
Amorphous Oxides (g/kg)	54.3	20.8
Amorphous Oxides Batch (g/L)	1.1	0.4

In addition, the content of amorphous iron oxides at the ophiolitic soil was determined by applying the Chao and Zhou (1983) method at the -0.5 mm soil fraction. The iron concentration in the extraction was equal to 180 mg/L. This concentration corresponds to the concentration of amorphous iron in the soil sample. Thus iron concentration is calculated as following:

$$180\frac{\text{mg amor. Fe}}{\text{L}}\ \text{x}\ 20\frac{\text{L}}{\text{kg soil}} = 3600\ \frac{\text{mg amor. Fe}}{\text{kg soil}}$$

In batch experiments 1 gr of soil added in 50 mL of solution and so the concentration of amorphous iron is:

$$3600\frac{\text{mg amor. Fe}}{\text{kg soil}}\text{x}\frac{1\ \text{gr soil}}{50\ \text{mL}} = 0.072\ \frac{\text{gr amor. Fe}}{\text{L}}$$

Assuming that amorphous iron is presented as Fe_2O_3 amorphous oxides, the concentration of amorphous oxides in the soil is equal to:

$$0.072\frac{\text{gr amor. Fe}}{\text{L}}\text{x}\frac{\text{MW Fe}_2\text{O}_3}{2 * \text{AW Fe}} = 0.072\ \text{x}\frac{160}{112} = 0.103\ \frac{\text{gr amor. Fe}_2\text{O}_3}{\text{L}}$$

Concluding, the three scenarios of solid concentration used for adsorption simulation in this study are as follows:

I. Solid concentration = 1.5 g/L, including the iron and aluminum amorphous oxides as calculated by the XRD and XRF analysis (Table 6.2)
II. Solid concentration = 1.1 g/L, including the iron amorphous oxides as calculated by the XRD and XRF analysis (Table 6.2)
III. Solid concentration = 0.103 g/L, including the iron amorphous oxides as determined by the Chao and Zhou (1983) method.

6.1.2 Determination of other parameters used at the surface complexation models

Apart from the solid concentration, several parameters are required for adsorption simulation using the surface complexation models. All the parameters used in this study are presented at Table 6.3. The SSA of the ophiolitic soil is equal to 55.95 m^2/g. The values of inner (C_1) and outer (C_2) capacitances were obtained from literature, since their experimental determination for heterogeneous systems like soils includes high uncertainty and is very difficult to be calculated. Thus the values presented in Table 6.3 have been generally accepted by the literature as common values for real soils. Similarly, the site density value used in this study, equal to 2.3 sites/nm^2, is thought as representative for modeling at real soils (Zachara et al., 1987; Davis & Kent, 1990; Villalobos et al., 2001; Goldberg, 2014).

Table 6.3 Parameters obtained by literature data and used for adsorption simulation.

Parameter	Value	Reference
Site density (sites/nm^2)	2.3	**Goldberg, 2014**
Inner capacitance, C_1 (F/m^2)	1.4	**Villalobos et al., 2001**
Outer capacitance, C_2 (F/m^2)	0.2	**Goldberg, 2014**

The next step was to create the reactions database at the Visual MINTEQ software, which will include all those surface complexation reactions able to contribute to the adsorption of the tested ions presented in the batch experiments. Simulation was performed by adjusting the constant of the surface complexation reaction that optimum fits the experimental data. Thus, for the creation of the adsorption database the following parameters were introduced:

i. The surface complexation reaction (reactants and products), the Rossendorf Expert System For Surface and Sorption Thermodynamics (RES^3T) database was used for obtaining all the kind of reactions that possibly occur in each case according batch experiments conditions (http://www.hzdr.de/db/RES3T.queryData),
ii. The surface complexation constant (K),
iii. The Boltzmann factor, which consider the electrostatic contribution (which in turn will be determined by the change in surface charge that occurs because of the reaction). For the inner and outer layers the Boltzmann factor is defined as PSI_o and PSI_b, respectively.

At the following paragraphs the results of the application of the aforementioned surface complexation models, the Triple Layer Model (TLM), the Diffuse Layer Model (DLM) and the Constant Capacitance Model (CCM) are presented.

6.1.3 Application of the Triple Layer Model

The TLM model was chosen for adsorption simulation for the following reasons:

i. It can simulate adsorption based on the formation of both inner and outer sphere complexes. Inner sphere complexes can be either monodentate (one bond occurs between the surface functional group and the adsorbed contaminant) or bidentate (the adsorbed contaminant is bonded with two functional groups of the soil surface).

ii. TLM can simulate the effect of electrolyte, metal and ligand adsorption constants in addition to protonation and deprotonation equilibrium constants and to equilibrium constants for adsorption of other species of the solution.
iii. TLM model has been applied in several studies for adsorption of contaminants and specifically for Cr(VI) adsorption and, thus, it is more efficient to evaluate the data obtained from literature and used for simulation in this study and also to compare our results with that of other studies.

Table 6.4 presents the reactions used for adsorption simulation, the optimum logK values for each reaction and for each solid concentration tested, and the PSI values as calculated by the equations described in Goldberg (2007). A literature review (Table A3.2., Appendix III) verified that the logK values obtained in this study are similar with those presented by other studies for the case of applying the TLM model in order to simulate the adsorption of the tested contaminants. More specifically, reactions No. 1 and 2 describe the dissociation and protonation reactions, respectively. Reactions No. 3 and 4 regard to the presence of background electrolyte NaCl in the soil solution, considering that chlorides form outer sphere complexes. Phosphates (Reactions No. 5 - 7) are thought to be bounded in several ways, able to form bidentate non-protonated (Reaction No. 5), bidentate non-protonated (Reaction No. 7) and monodentate protonated (Reaction No. 6) complexes. Nitrates are represented by reaction No. 8, which describes the formation of outer sphere complexes with the soil surface. In the case of Cr(VI) two scenarios of surface complexation were investigated taking into account the formation of either both monodentate and bidentate (Reactions No. 9 - 11) or only monodentate (Reactions No. 12 - 14) complexes (Table 6.4). The difference of these two scenarios is the formation of inner sphere bidentate or monodentate complexes as shown by reactions 9 and 12. Reactions No. 10 - 11 and No. 13 - 14 represent the outer sphere complexes and are kept the same in all cases tested regarding Cr(VI) modeling. In the case of outer sphere complexes the hydration sphere is retained during adsorption, whereas in the case of inner sphere complexes at the surface, part or all of the hydration sphere is lost in the adsorption reaction. Such complexes are often identified based on evidence from bulk solution experiments, which are used in the present study, since decreased adsorption with increasing ionic strength of the background electrolyte has been taken as evidence of non-specific adsorption and, thus, formation of outer sphere complexes. The question of whether a species is adsorbed as inner-sphere or as outer-sphere complex is important due to the influence that the type of adsorption has on the structure and reactivity of the adsorbed species. It is considered that outer-sphere complexation causes minimal changes in the electron density distribution of the adsorbed species as compared to the aqueous complex (Koretsky, 2000).

Table 6.4 Reactions and their corresponding values of adsorption constants applied at the TLM.

Reactions							logK (per solid concentration)			PSI_o	PSI_b	Reference regarding the type of reaction used
No.	Reactants				Products							
	Soil	Ligand 1	Ligand 2		Product 1	Product 2	1.5 g/L	1.1 g/L	0.103 g/L			
1	SOH			↔	SO^-	H^+	-9.0			-1		Goldberg et al., 2007
2	SOH	H^+		↔	SOH_2^+		4.2			1		
3	SOH	Na^+		↔	SONa	H^+	-9.29			-1	1	Villalobos and Leckie, 2001
4	SOH	Cl^-	H^+	↔	SOH_2Cl		8.43			1	-1	
5	SOH	PO_4^{3-}	H^+	↔	$SOPO_3^{2-}$	H_2O	19.0	20.5	30.0	-2		Antelo et al., 2005
6	2SOH	PO_4^{3-}	$2H^+$	↔	$S_2O_2PO_2^-$	$2H_2O$	25.2	25.0	30.0	-1		
7	2SOH	PO_4^{3-}	$3H^+$	↔	S_2O_2POOH	$2H_2O$	29.2	30.0	37.0	0		
8	SOH	NO_3^-	H^+	↔	SOH_2NO_3		9.0	9.2	10.3	1	-1	Villalobos et al., 2001
Reactions at the Bidentate Minteq Database												
9	2SOH	CrO_4^{2-}	$2H^+$	↔	S_2CrO_4	$2H_2O$	14.5	14.5	15.8	0		Villalobos et al., 2001
10	SOH	CrO_4^{2-}	$2H^+$	↔	SOH_2-$HCrO_4$		16.0	16.4	17.2	1	-1	
11	SOH	CrO_4^{2-}	H^+	↔	$SOH_2CrO_4^-$		11.2	11.4	13.5	1	-2	Rai et al., 1988
Reactions at the Monodentate Minteq Database												
12	SOH	CrO_4^{2-}	H^+	↔	$SCrO_4^-$	H_2O	8.0	8.0	15.1	-1		Villalobos et al., 2001
13	SOH	CrO_4^{2-}	$2H^+$	↔	SOH_2-$HCrO_4$		16.0	16.4	17.2	1	-1	
14	SOH	CrO_4^{2-}	H^+	↔	$SOH_2CrO_4^-$		11.2	11.4	13.8	1	-2	Rai et al., 1988

The three scenarios of solid concentrations that tested using the TLM model are presented below.

6.1.3.1 Solid concentration equal to 1.5 g/L

As mentioned in paragraph 6.1.1, solid concentration equal to 1.5 g/L represents the concentration of iron (Fe_2O_3=1.1 g/L) and aluminum (Al_2O_3=0.4 g/L) oxides as calculated by the mass balance of XRD and XRF analysis. The effect of several parameters on Cr(VI) adsorption is presented below.

Effect of pH and ionic strength of the soil solution on Cr(VI) adsorption

The adsorption mechanism can be affected by pH values when surface complexation occurs or by ionic strength when the ion exchange is the adsorption mechanism, without excluding the simultaneous occurrence of both adsorption mechanisms. The ionic strength can influence the anion binding by two ways affecting a) the thickness of double layer and b) the interface potential. The determination of ionic strength effects on adsorption has been extensively used as a tool for distinguishing macroscopically between inner and outer sphere complexation of ions. Outer sphere complexes exhibit remarkable effects on adsorption efficiency due to the alteration of ionic strength, while inner sphere complexes are usually not susceptible to ionic strength alterations. More specifically, adsorption decreases with increasing ionic strength value since the background electrolyte ions are located in the same plane with the outer-sphere complexes. On the contrary, inner sphere complexes exhibit low dependence from ionic strength or exhibit increasing adsorption with increasing ionic strength. Higher ion adsorption with increasing ionic strength is attributed to the higher activity of the counter ions available to offset the surface charge created by specific ion adsorption (McBride, 1997; Weerasooriya and Tobschall, 2000; Ajouyed et al., 2010; Goldberg 2013). In addition, the increase of ionic strength can lead to the alteration of the adsorption mechanism from outer-sphere to inner-sphere complexation (Goldberg et al., 2001).

The results of Cr(VI) adsorption simulation as a function of pH and ionic strength of the soil solution are presented at Figure 6.1. In both cases of ionic strength Cr(VI) adsorption decreases with increasing pH, irrespectively of the ionic strength of the solution. This fact indicates that Cr(VI) adsorption on the ophiolitic soil is strongly affected by the formation of the “weaker” outer sphere complexes, instead of the “stronger” inner sphere complexes without excluding the simultaneous formation of both types of complexes (Goldberg 2007; Goldberg, 2014). Concerning the effect of ionic strength on Cr(VI) adsorption, the TLM model indicates noticeable decrease in Cr(VI) adsorption with increasing ionic strength, using a 10-fold concentration of electrolyte (0.01 M and 0.1 M NaCl). In both cases it is perceived that adsorption is maximized at acidic pH values reaching 60% and 30% for ionic strength equal to 0.01 M and 0.1 m, respectively. In addition, for pH values about 8, which are typically found in groundwater, Cr(VI) adsorption is approximately 3% using 0.1 M NaCl, while in the case of 0.01 M NaCl, adsorption is estimated at about 12%. The effect of ionic strength via the formation of outer sphere complexes is represented by the equations No. 10 and 11 (or correspondingly by No. 13 and 14 which are the same) of Table 6.4. Thus the TLM model can efficiently simulate

the effect of outer sphere surface complexation for the tested ophiolitic soil. The strong correlation between experimental and modeling data regarding Cr(VI) adsorption is presented at Figure A1.5. Despite all cases exhibited high R^2 values the slope of the linear equation in the case of monodentate complexes at high ionic strength values is higher than 1.

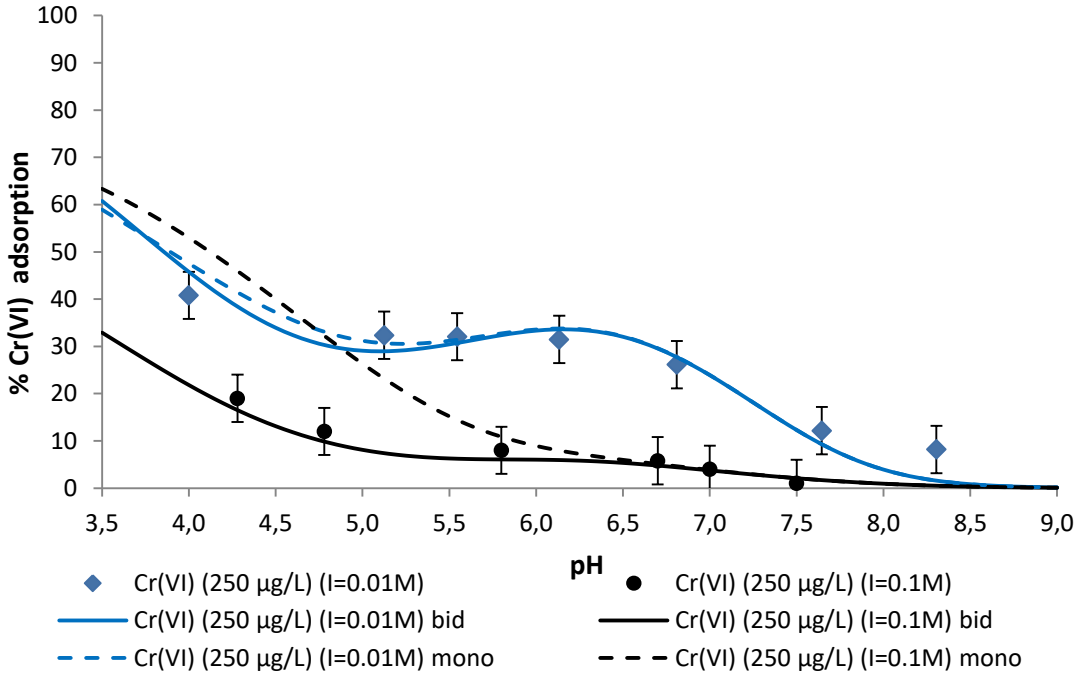

Figure 6.1 Simulation of the effect of pH and ionic strength on Cr(VI) adsorption (250 µg/L) using the TLM.

The effect of ionic strength on Cr(VI) adsorption using NaCl as electrolyte was investigated by Azizian (1993) mentioning that higher ionic strength resulted in lower Cr(VI) adsorption. The adsorption decrease can be attributed to either direct competition of chromates with chlorides for the soil's oxides surface sites or to the decrease in the electrostatic potential close to the surface sites. The adsorption of chlorides reduces the site density of the adsorption sites and thus reduces adsorption of chromates. Ionic strength also affects the activity coefficient ratios which are directly related to the 0-plane or the β-plane potential or both of them and therefore affects the surface complexes. Since the outer sphere surface reactions have a direct dependence on the plane potential, their activity coefficient ratios are more directly influenced by ionic strength changes. Thus, the effect on electrostatic potential is related to the surface potential (ψ_β), which occurs in the outer sphere complexes as shown by reactions 10 and 11 (Table 6.4). More specifically, the increase of chlorides concentration decreases the ψ_β surface potential and increases the $\exp(F(\psi_0 - \psi_\beta)/RT)$ factor. Consequently, the $[SOH_2\text{-}HCrO_4^-]$ and $[SOH_2\text{-}CrO_4^{2-}]$ concentrations decrease, since the corresponding K values remain constant (Azizian, 1993). Similar results were reported by Zachara et al. (1989) using soil samples from subsurface horizons as adsorbents for Cr(VI). The effect of ionic strength was tested using sodium nitrate (0.01 - 0.1 M $NaNO_3$) as background electrolyte. Cr(VI) adsorption decreased with increasing ionic strength indicating the presence of outer sphere complexes. The decrease is attributed to the effect of ionic strength on either a) the surface charge and aqueous activity coefficient of chromates, or b) to the increase of nitrates concentration with increasing ionic

strength which cause competitive adsorption effects between nitrates and chromates. In general, inorganic ligands that occur in soil solutions, are differently adsorbed on variable charge minerals and soils. Anions such as NO_3^-, Cl^-, Br^-, I^- and ClO_4^- are mainly adsorbed forming outer-sphere complexes and rarely on surfaces that exhibit a positive charge (Violante et al., 2002).

Apart from the formation of inner and outer sphere complexes the adsorption simulation using the TLM model revealed information about the formation of monodentate or bidentate complexes between chromates and the solid surface. Bidentate or monodentate complexes are thought to be formed in the case of inner sphere complexes and are described by equations 9 and 12, respectively. The approach of forming bidentate complexes between chromates and the soil surface describes adsorption with high accuracy for both cases of ionic strength tested. On the contrary, the monodentate complexation is efficient only in the case of low ionic strength (0.01 M) of the solution. For ionic strength equal to 0.1 M, the scenario of forming exclusively monodentate complexes verifies experimental data only at almost neutral and acidic pH values (greater than 6.0), overestimating Cr(VI) adsorption efficiency at lower pH values. Specifically, at pH equal to 4.3 the deviation is almost 26%. Thus, we can conclude that at increased concentrations of electrolyte (0.1 M NaCl), the predominant adsorption mechanism of Cr(VI) in the ophiolitic soil is the formation of bidentate rather than monodentate complexes. The formation of bidentate complexes of chromates has also been suggested by Hiemstra et al. (2004).

Effect of pH and Cr(VI) on phosphates adsorption

The effect of pH and Cr(VI) presence on phosphates adsorption was also investigated. Three surface complexation reactions were taken into account for phosphates simulation as shown at Table 6.4 (reactions 5-7). All of the used reactions consider that phosphates form inner sphere complexes with the soil oxides surface. Adsorption simulation using the TLM model was in very good agreement with the experimental data as can be observed from Figures 6.2 and A1.6. The TLM model predicted the decrease of phosphates adsorption with increasing pH and verified that the presence of Cr(VI) in the soil solution did not affect their adsorption. The effect of Cr(VI) presence on phosphates adsorption was negligible independently of the type of Cr(VI) complexation (monodentate or bidentate) with the soil surface, which could affect the available soil surface sites for phosphates. In fact, the results of the two models are identical; suggesting that the type of chromium complex created does not affect the adsorption of phosphates. The absence of any competitive effects between chromates and phosphates is probably attributed to the high difference in the concentrations of the two ions or also due to the preference of the ophiolitic soil to adsorb phosphate anions rather than chromates. This preference can be explained by the formation of inner sphere complexes between phosphates and the soil surface, which are based on stronger bonds like ionic or covalent, contrary to outer sphere complexes that are based mainly on electrostatic forces (Antelo et al., 2005).

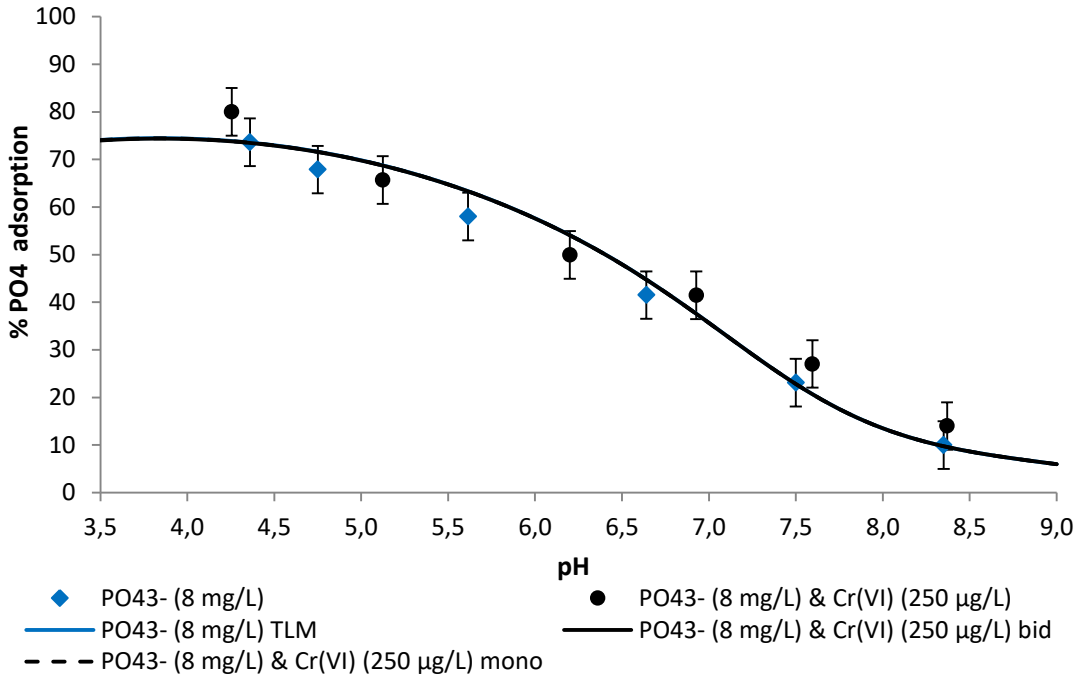

Figure 6.2 Adsorption simulation of PO_4^{3-} (8 mg/L) in the presence (250 µg/L) and absence of Cr(VI) using the TLM.

Phosphates adsorption on the oxide surfaces was firstly investigated by Parfitt (1978) reporting the formation of binuclear bridging complexes by replacing two singly coordinated hydroxyl groups per phosphate molecule. The ligand exchange mechanism and the formation of bidentate complexes of phosphates with the iron oxides surface were also confirmed by Torrent et al. (1990) using infrared spectroscopy. A recent study performed by Fink et al (2016) showed that phosphates are adsorbed on iron oxides via inner sphere surface complexation. More specifically P is preferentially adsorbed by hydroxyl surface groups in iron oxides (hydroxylation), which are protonated below pH_{PZC} value. Iron hydroxylation occurs, since Fe ions on mineral surfaces are exposed to water and complete its coordination with hydroxyl groups. Hydroxyls can be coordinated by one (type A), two (type C) or three (type B) iron atoms, corresponding to hydroxyls of simple, double or triple coordination, respectively. Among these types, Type A are the most easily protonated hydroxyls due to the charge balance in Fe—O bonds. At such bonds the electron cloud of oxygen exhibits higher electronegativity than in doubly or triply coordinated hydroxyls. The reactivity of these sites is attributed to the positively charged and very unstable water molecule, which can be easily exchanged with an organic or inorganic anion in solution. During protonation the Fe—OH bond becomes weaker and the electron cloud of oxygen is displaced to the hydrogen side. As a result, hydroxyl protonation triggers the two following processes in phosphates adsorption: (*a*) protonated surfaces create a positive electric field that attracts phosphate anions; and (*b*) a replacement between phosphates and protonated hydroxyl groups occurs. Thus phosphates may be absorbed in monodentate or bidentate form depending on the number of OH groups in the phosphate that are bonded to the iron atoms (Fink et al., 2016). Thus the reactions used in this study (Table 6.4, reactions 5-7) is considered that can sufficiently describe the adsorption of phosphates on the ophiolitic soil.

In addition, the insignificant effect of chromates and chlorides (background electrolyte) on phosphates adsorption can be explained by the different adsorption mechanisms among these ions on the variable charge minerals and soils. Anions such as NO_3^-, Br^-, Cl^-, I^- and ClO_4^- are adsorbed as outer-sphere complexes and thus are weakly adsorbed on positively charged surfaces. Thus the adsorption of these anions is sensitive to ionic strength alterations and do not compete with phosphates for adsorption on clay minerals, which are adsorbed by replacing the coordinated $-OH_2$ and -OH groups. On the contrary, inorganic ligands like chromates that can form both inner and outer sphere complexes may compete for phosphates adsorption (Violante et al., 2002 and refs. therein). Thus the presence of chromates and the formation of outer sphere complexes as observed in above paragraphs in combination with their relative lower concentration than phosphates can support the absence of any competitive effects with phosphates.

Effect of pH and Cr(VI) on nitrates adsorption

Subsequently, the simulation results of nitrates adsorption as a function of pH and Cr(VI) anions are presented at Figure 6.3. Simulation was performed for the two concentrations (5 and 50 mg/L) of nitrates used in the batch experiments.

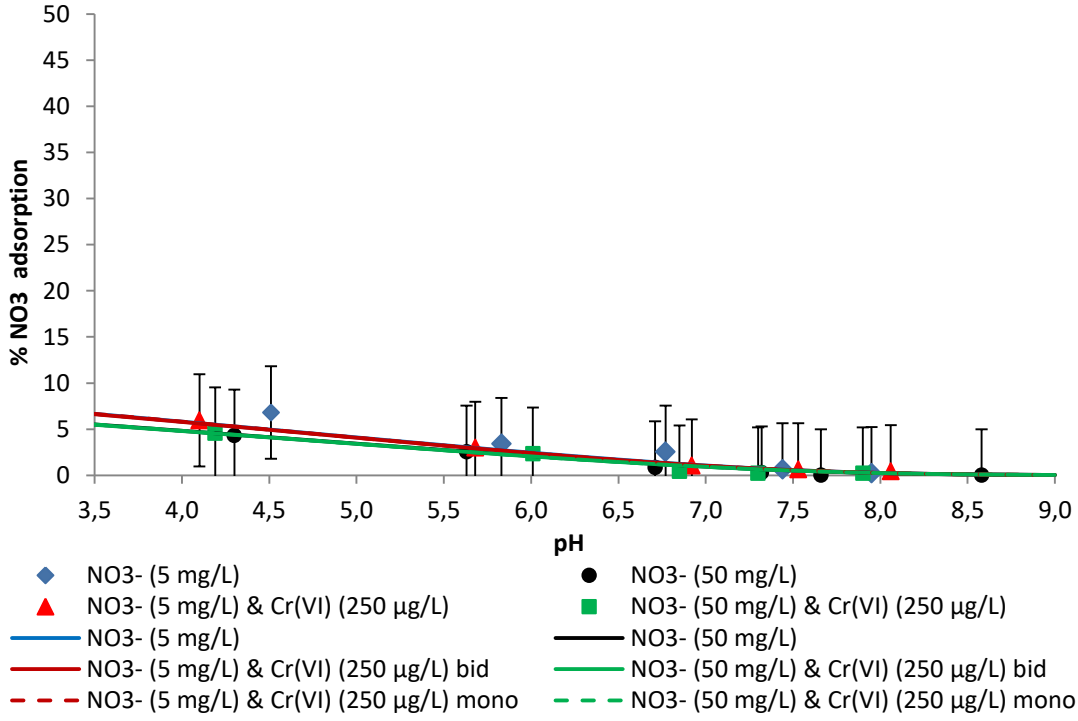

Figure 6.3 Adsorption simulation of nitrates (5 and 50 mg/L) in the presence (250 µg/L) and absence of Cr(VI) using the TLM.

The application of TLM model predicted well the adsorption behavior of nitrates for all the cases tested as can be further observed by Figure A1.7. In addition, the minimal effect of Cr(VI) presence on nitrate adsorption is easily ascertained and confirmed. The minimal effect of Cr(VI) on nitrates adsorption is presented regardless the type of Cr(VI) complexation (monodentate or bidentate) with the soil surface. However, nitrates are supposed to form only

outer sphere complexes and thus the absence of any competitive effect of Cr(VI) on their adsorption efficiency can be attributed to their superior concentration in the soil solution. The formation of outer sphere complexes of nitrates was also reported by Sposito (1989) who mentioned that nitrates are adsorbed on the diffusion layer, forming surface complexes in the outer layer (outer sphere complexes). The formation of outer sphere complexes of nitrates with variable charged minerals and soils has also been mentioned by Violante et al. (2002).

The very low adsorption efficiency of nitrates can also be related to the presence of chlorides in the soil solution. Chlorides are also adsorbed mainly by electrostatic attractions without excluding the formation of covalent bonds with the soil surface. Even in the presence of Coulomb forces chlorides are thought to be stronger adsorbed on soils exhibiting higher affinity with the soil surface (Wang et al., 1987).

Effect of pH and inorganic ions on Cr(VI) adsorption

In the above paragraphs the effect of Cr(VI) presence on the inorganic contaminants adsorption was tested. Figure 6.4 presents the effect of the tested inorganic contaminants on Cr(VI) adsorption as a function of pH.

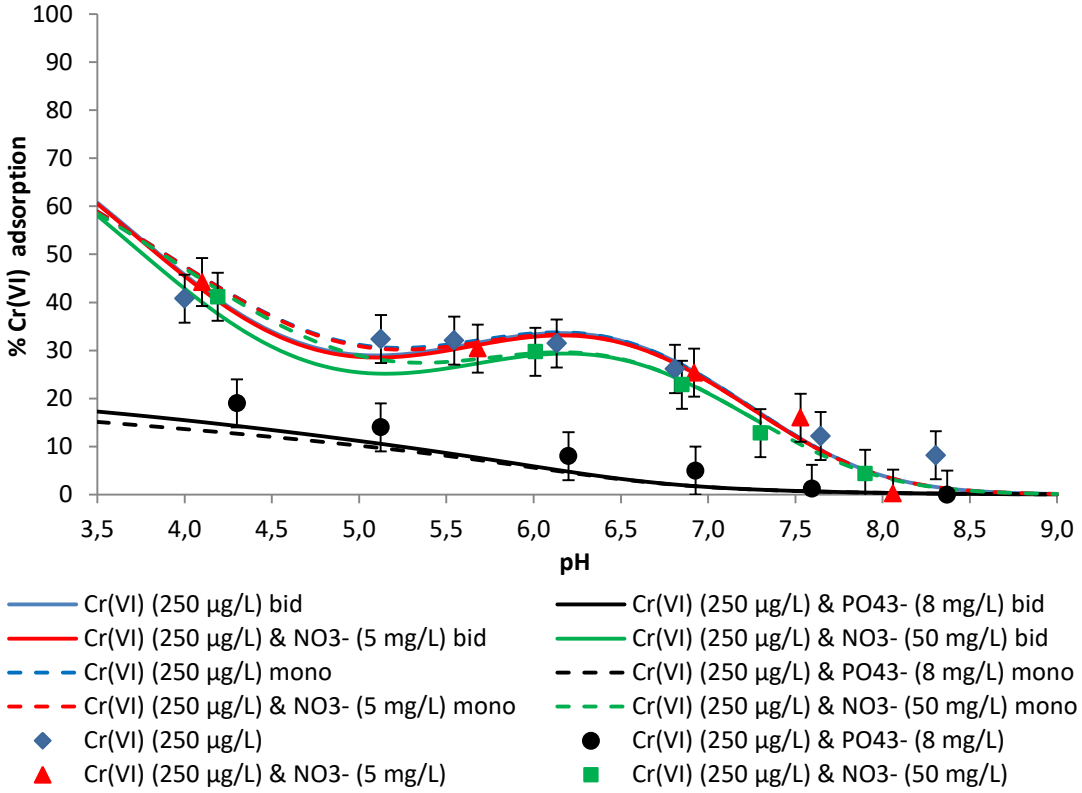

Figure 6.4 Simulation of competitive adsorption of Cr(VI) with inorganic contaminants using the TLM.

Firstly, the TLM model verified with very good accuracy the decrease caused at Cr(VI) adsorption efficiency due to the presence of phosphates. The verification observed either in the case of using bidentate or monodentate type of complexes for simulating Cr(VI) adsorption. The type of complexation, monodentate or bidentate, for Cr(VI) seems not to be affected by the presence of phosphates in the solution. Thus, phosphates can be considered as

an important contaminant able to act competitively with chromates regarding their adsorption on soils.

Concerning any competitive adsorption between Cr(VI) and NO_3^-, the Cr(VI) curve follows the expected trend with increasing pH. The presence of nitrates at low concentration (5 mg/L) exerts a very small to negligible effect on the adsorption of Cr(VI), despite their different concentrations and their possible competition for surface functional groups. This fact verifies the preference of soil for adsorption of chromates. Higher concentration of nitrates (50 mg/L) causes more significant decrease at chromates adsorption. In addition, the fact that nitrates are adsorbed in very small amounts, even in the absence of Cr(VI), indicates that their presence does not alter the availability of adsorption sites. Moreover, the higher valence of chromates (divalent) than nitrates (monovalent), can support the preference of soil surface for chromates (Sposito, 1989). In all cases, simulation shows that adsorption is zeroing for pH values higher than 8.

Finally, we can conclude that the TLM model simulates with very good accuracy the adsorption of Cr(VI), either by assuming monodentate or bidentate complexes, and during the presence of the tested inorganic contaminants (Figure A1.8).

Sensitivity analysis of inner capacitance

The inner (C_1) and outer (C_2) capacitances in the triple-layer model are parameters consistent with physically reasonable distances and interfacial dielectric constants for water. In the case of TLM the capacitances do not depend on anion radius. One of the most important parameters during surface complexation modeling is the determination of the C_1 parameter, since the value of C_2 is mostly taken as constant to 0.2 F/m^2. The C_1 value directly affects the proton surface charge and relates the charge at the inner plane of adsorption (σ_0) with (ψ_0) to the drop in potential at a distance β, with ψ_β potential. The experimental determination of inner capacitance values involves great uncertainty and presents important difficulties as has been referred in many studies. This is why only few studies have determined the values of inner or outer capacitances (Sverjensky, 2001; Goldberg, 2014).

In the present study, the value of inner capacitance C_1 is considered as 1.4 F/m^2, while that of outer capacitance C_2 equal to 0.2 F/m^2. These values have been referred in the literature as representative values for surface complexation modeling when using as adsorbent real soil. In order to quantify the model's sensitivity on Cr(VI) adsorption due to inner capacitance parameter, C_1 values between 0.1 and 2.0 F/m^2 were used. These two values correspond to the minimum and maximum values, which are found in the literature. It should be noted, that the minimum value used is equal to 0.8 F/m^2 for chromium adsorption on goethite (Hayes et al., 1991; Sverjensky, 2001; Villalobos et al., 2001). Figure 6.5 presents the results of sensitivity analysis of inner capacitance (C_1) on Cr(VI) adsorption as obtained by applying the TLM model. The simulation was performed using 250 μg/L at a soil solution of 0.01 M ionic strength.

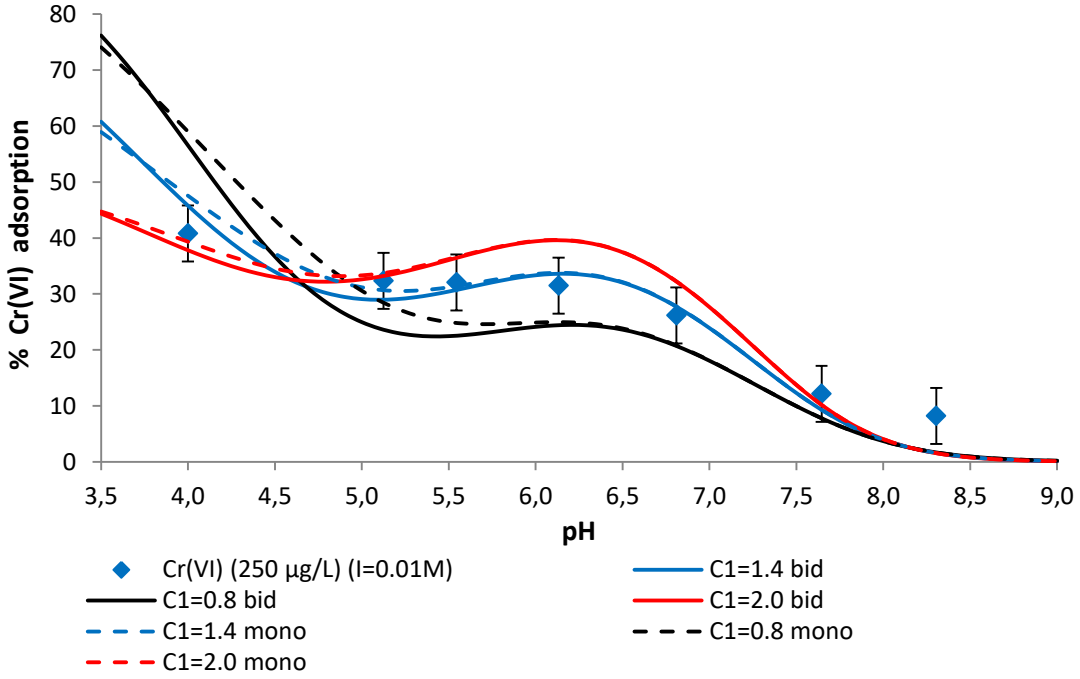

Figure 6.5 Sensitivity analysis of the inner capacitance parameter on Cr(VI) adsorption using the TLM.

As observed from Figure 6.5, for pH values higher than 7.5, which is the pH that predominantly occurs in groundwater related to ophiolitic materials, the TLM model does not exhibit high sensitivity to Cr(VI) adsorption during the alteration of inner capacitance in the range 0.8 to 2 F/m^2. In particular, the maximum deviation was lower than 6% for pH values higher than 7, independently of the kind of complexes, mono- or bi- dentate, considered. The maximum deviation observed, compared to the 1.4 F/m^2 used for adsorption simulation, was not higher than 17% for assuming either monodentate or bidentate complexes (Table 6.5). Thus the importance of the inner capacitance during simulation is higher at acidic values. Therefore we can conclude that inner capacitance does not play a dominant role on adsorption simulation during the application of TLM model for the description of Cr(VI) adsorption on the ophiolitic soil.

Table 6.5 Deviation on adsorption efficiency for C_1 values 0.8 and 2 F/m^2 compared with the results of obtained for C_1 equal to 1.4 F/m^2 used for adsorption simulation with the TLM.

C_1 (F/m^2)	Bidentate			Monodentate		
	pH = 3.5	pH = 7.0	pH = 9.0	pH = 3.5	pH = 7.0	pH = 9.0
0.8	15.4%	5.8%	0.0%	15.1%	5.8%	0.0%
2.0	16.4%	3.7%	0.0%	14.2%	3.7%	0.0%

6.1.3.2 Solid concentration equal to 1.1 g/L

In this series of experiments solid concentration equal to 1.1 g/L was used representing quantitatively only the concentration of iron amorphous oxides (Fe_2O_3) as calculated by the mass balance of XRD and XRF analysis (paragraph 6.1.1) excluding the contribution of aluminum oxides in the total solid concentration. Table 6.4 presents the logK values that best fitted the experimental data regarding the adsorption of Cr(VI) and inorganic contaminants. As

expected the decrease of solid concentration would led to the increase of logK values in order to achieve the same adsorption efficiency, keeping the other parameters constant. This is an advantage of the GC models since they can approach the heterogeneous soil surface as a unique surface. Thus the decrease of solid concentration can be interpreted as a decrease of the available adsorption sites.

Effect of pH and ionic strength of the soil solution on Cr(VI) adsorption

Figure 6.6 presents the results of Cr(VI) adsorption simulation as a function of pH and ionic strength. In both cases of ionic strength tested Cr(VI) adsorption decreases with increasing pH, irrespective of the ionic strength of the solution. Similar results obtained in the case of using 1.5 g/L as solid concentration. In addition, the increase of ionic strength leads to different results regarding simulation through monodentate or bidentate complexes. The increase of ionic strength to 0.1 M indicates the formation of both bidentate complexes of Cr(VI) with the solid surface. As in the case of using 1.5 g/L, the TLM application describes with very good accuracy Cr(VI) adsorption (Figure A1.9). Efficient Cr(VI) adsorption simulation was achieved by elevating the logK value of the reactions representing the formation of outer sphere complexes either assuming monodentate or bidentate complexes. This indicates that the decrease of solid concentration firstly affects the formation of outer sphere complexes. Thus in the solid concentration range from 1.1 to 1.5 g/L the TLM can be efficiently used for Cr(VI) adsorption simulation.

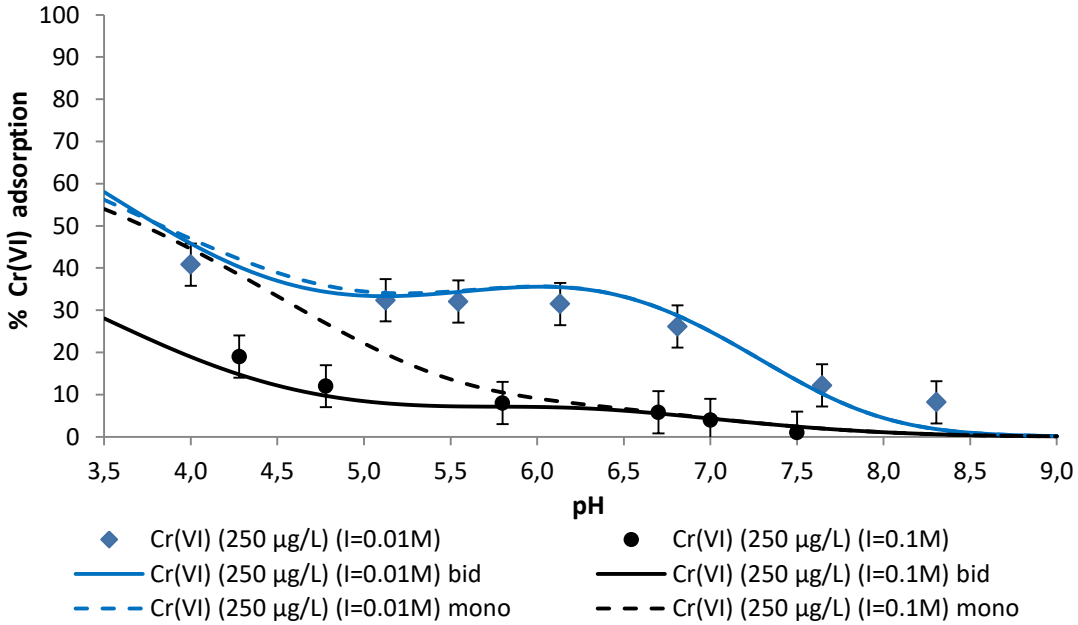

Figure 6.6 Simulation of the effect of pH and ionic strength on Cr(VI) adsorption (250 µg/L) using the TLM model for solid concentration equal to 1.1 g/L.

Effect of pH and Cr(VI) on phosphates adsorption

In Figure 6.7 the effect of pH and Cr(VI) presence on phosphates adsorption is presented. In order to simulate phosphates adsorption the higher increase of logK value performed for the reaction describing the formation of monodentate ($SOPO_3^{2-}$) complexes (reaction 6). In

addition, increase slightly lower than one unit of the logK value, that corresponds to the bidentate complex S_2O_2POOH was performed. Adsorption simulation using the TLM model was in very good agreement with the experimental data (Figure A1.10). Thus for the solid concentration range 1.1 to 1.5 g/L phosphates adsorption can be efficiently simulated.

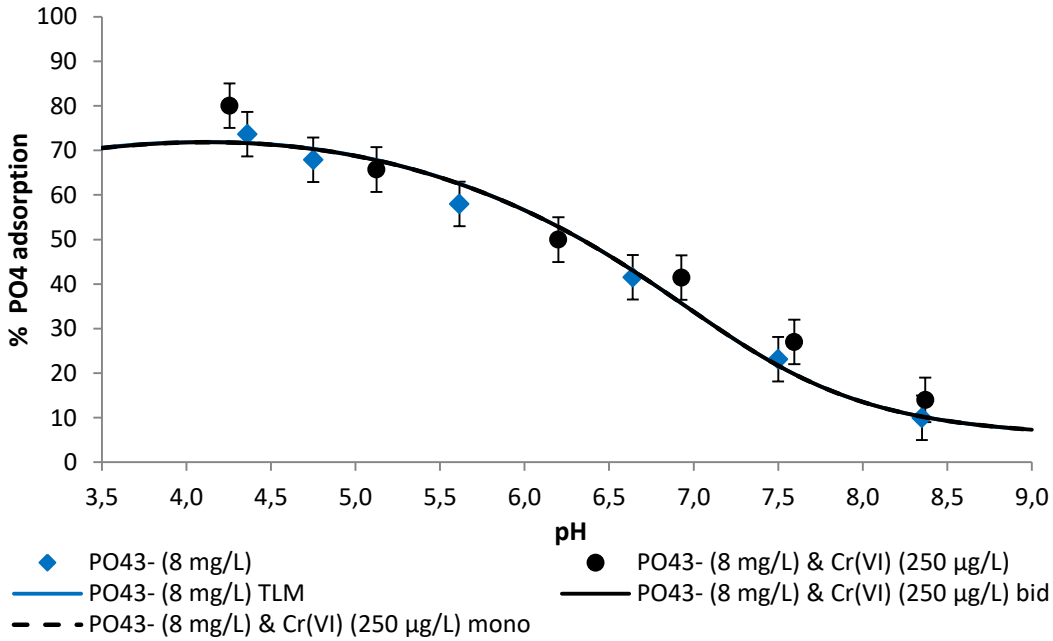

Figure 6.7 Adsorption simulation of PO_4^{3-} (8 mg/L) in the presence (250 µg/L) and absence of Cr(VI) using the TLM model for solid concentration equal to 1.1 g/L.

Effect of pH and Cr(VI) on nitrates adsorption

Figure 6.8 presents the simulation results of nitrates adsorption as a function of pH and Cr(VI) presence. Simulation was performed for the two concentrations (5 and 50 mg/L) of nitrates used in the batch experiments. Efficient simulation of the experimental data (Figure A1.11) achieved by slightly elevating the logK value of the reaction that forms the SOH_2-NO_3 outer sphere complex, from 9 to 9.2.

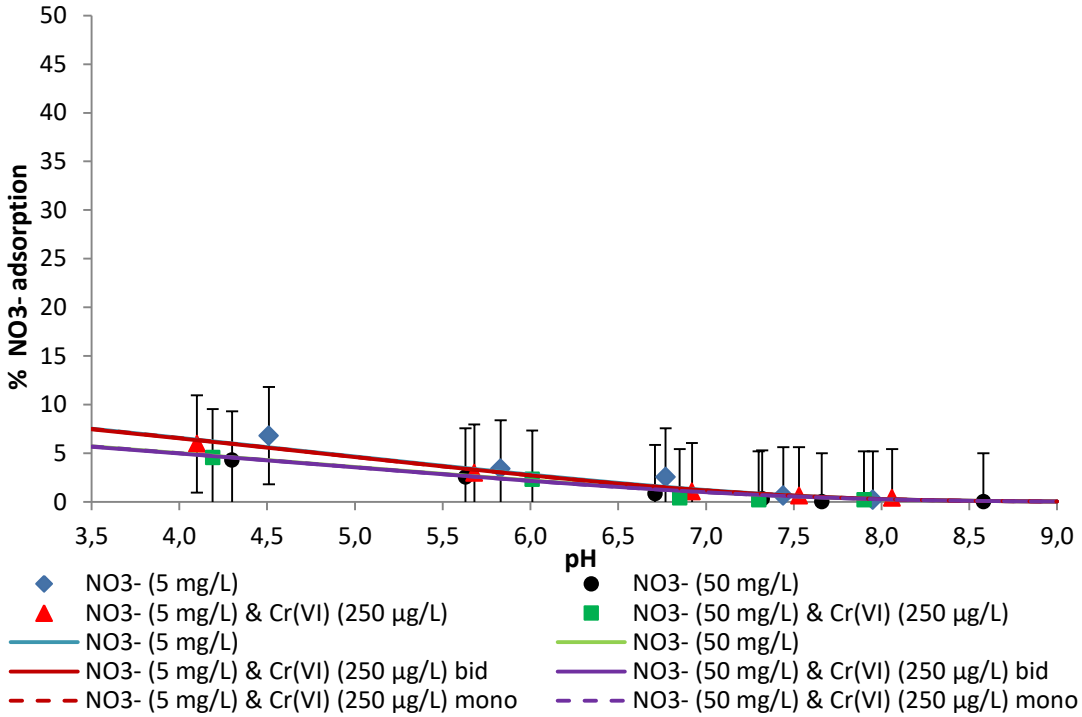

Figure 6.8 Adsorption simulation of nitrates (5 and 50 mg/L) in the presence (250 µg/L) and absence of Cr(VI) using the TLM model for solid concentration equal to 1.1 g/L.

Effect of pH and inorganic ions on Cr(VI) adsorption

In this paragraph the effect of the above tested inorganic contaminants on Cr(VI) adsorption as a function of pH is presented (Figure 6.9). The possible competitive effects of other contaminants on Cr(VI) adsorption was described with high accuracy (Figure A1.12) using the logK values obtained during the adsorption of each contaminant separately as mentioned in the above cases. In all cases, the formation of bidentate complexes describes better Cr(VI) adsorption.

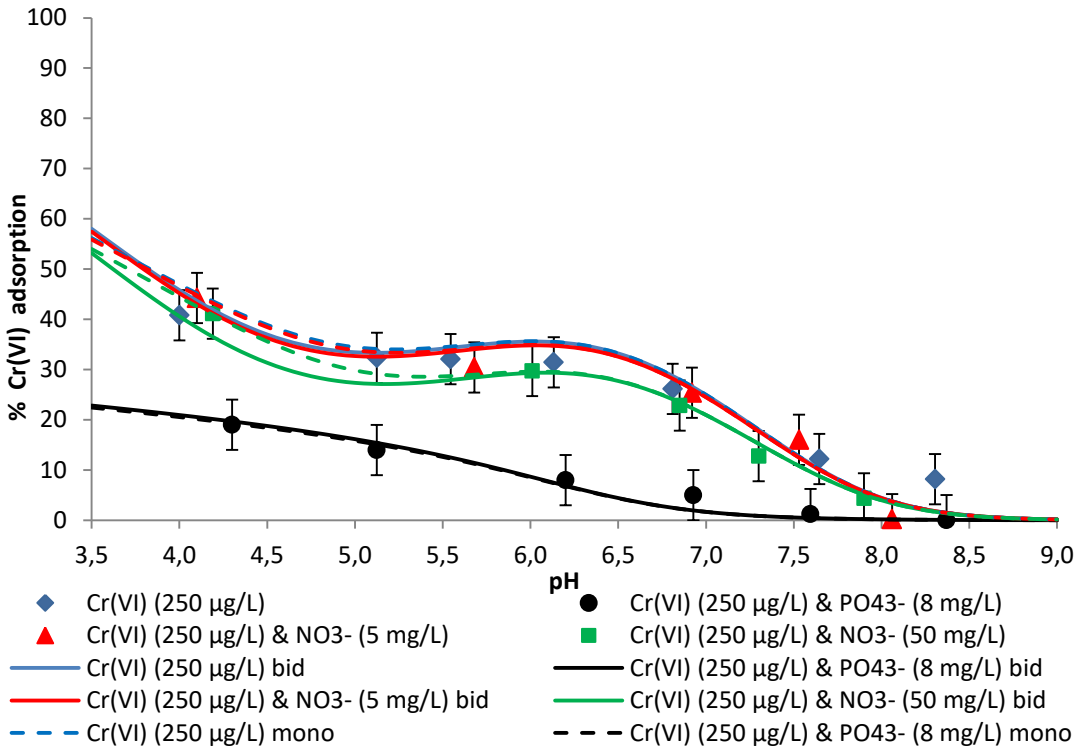

Figure 6.9 Simulation of competitive adsorption of Cr(VI) with inorganic contaminants using the TLM model for solid concentration equal to 1.1 g/L.

Sensitivity analysis of inner capacitance

Figure 6.10 presents the results of sensitivity analysis of inner capacitance (C_1) on Cr(VI) adsorption as obtained by applying the TLM model. The simulation was performed using 250 µg/L at a soil solution of 0.01 M ionic strength.

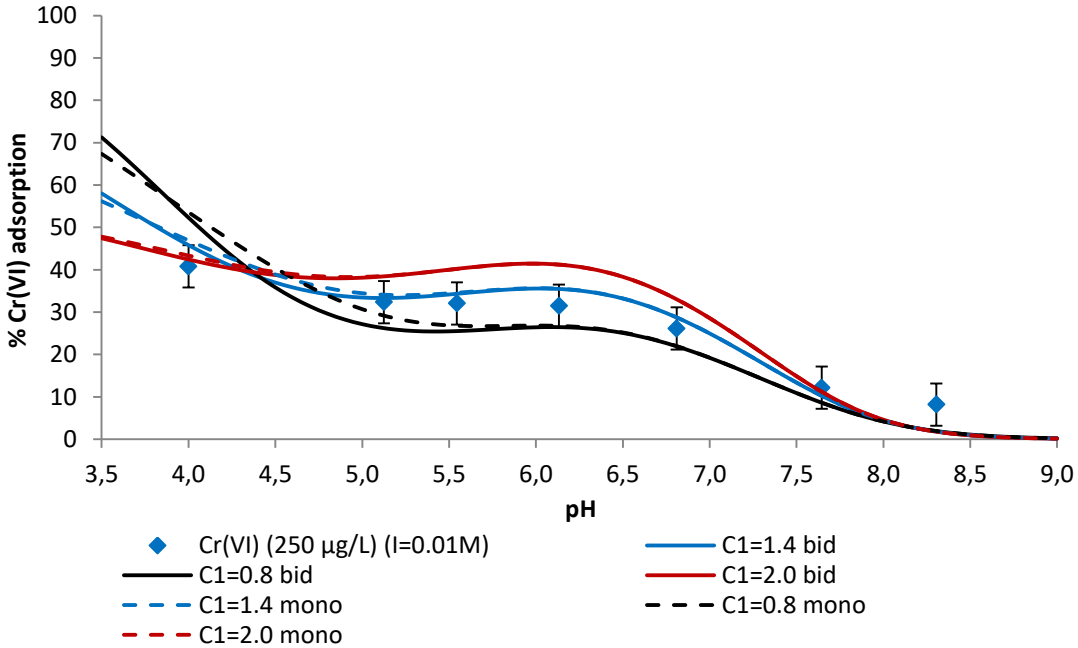

Figure 6.10 Sensitivity analysis of the inner capacitance parameter on Cr(VI) adsorption using the TLM model for solid concentration equal to 1.1 g/L.

As observed, the TLM model did not exhibit high sensitivity to Cr(VI) adsorption due to the alteration of inner capacitance in the range from 0.8 to 2 F/m^2 for pH values higher than 7.5 since the deviation is lower than 6% and almost zeroed at pH 9. The maximum deviation observed compared to the 1.4 F/m^2 value used for adsorption simulation was about 13% for either assuming monodentate or bidentate complexes (Table 6.6). The highest deviations observed for acidic pH values lower than 4 and in the pH range 5.5 – 7. Therefore, the application of TLM model can efficiently describe Cr(VI) adsorption on the ophiolitic soil as a function of inner capacitance value since the pH values of groundwater measured as higher than 7.5.

Table 6.6 Deviation on adsorption efficiency for C_1 values 0.8 and 2 F/m^2 compared with the results obtained for C_1 equal to 1.4 F/m^2 using the TLM model for solid concentration equal to 1.1 g/L.

C_1 (F/m^2)	Bidentate			Monodentate		
	pH = 3.5	pH = 7.0	pH = 9.0	pH = 3.5	pH = 7.0	pH = 9.0
0.8	13.2%	5.7%	0.1%	11.2%	5.7%	0.1%
2.0	10.6%	3.6%	0.0%	8.4%	3.6%	0.0%

6.1.3.3 Solid concentration equal to 0.103 g/L

The last scenario of solid concentration used (0.103 g/L) was that of taking into account only the concentration of iron oxides as determined by the Chao and Zhou (1983) method. In this scenario the contribution of the crystallized or not well crystallized iron oxides was excluded and thus adsorption is considered to be based only on the "real" amorphous iron phase. As shown at Table 6.4 the decrease of solid concentration one order of magnitude led to the increase of the logK values in order to best fit the experimental data. However, as it will be shown at the following paragraphs, adsorption simulation was not effective since important deviations observed between the experimental data and the results of the TLM model. Thus the application of TLM model using as solid concentration the amorphous iron oxides concentration is not capable of simulating the effect of pH and ionic strength on Cr(VI) adsorption (Figure 6.11), nor the adsorption of phosphates (Figure 6.12) and nitrates (Figure 6.13) on ophiolitic soil, nor the competition between these contaminants (Figure 6.14). Thus it can be concluded that the concentration of amorphous iron oxides does not correspond to the concentration of the oxides of the tested soil that exclusively contribute to the adsorption process.

Effect of pH and ionic strength of the soil solution on Cr(VI) adsorption

Simulation of Cr(VI) adsorption as a function of pH and ionic strength using 0.103 g/L solid concentration, an order of magnitude, is presented at Figure 6.11. Using this solid concentration the experimental data of using 0.1 M NaCl were not verified assuming the formation of either monodentate or bidentate complexes despite using significantly elevated logK values for all the surface complexation reactions. This fact indicates that the solid concentration used is not enough in order to simulate the adsorption capacity of the tested soil.

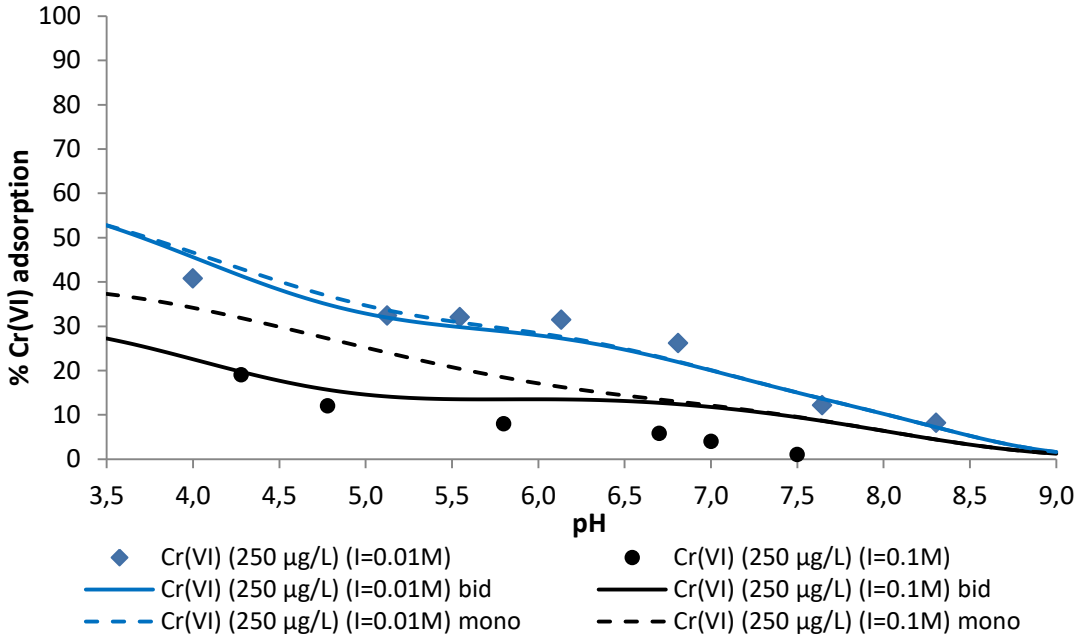

Figure 6.11 Simulation of the effect of pH and ionic strength on Cr(VI) adsorption (250 µg/L) using the TLM model for solid concentration equal to 0.103 g/L.

Effect of pH and Cr(VI) on phosphates adsorption

Inefficient simulation of phosphates adsorption was also occurred when using solid concentration equal to 0.103 g/L. The simulation showed that adsorption capacity was almost constant independently the pH values indicating that the solid surface was saturated and no active sites were available for phosphates adsorption. Thus the TLM model cannot predict phosphates adsorption using such a low value of solid concentration.

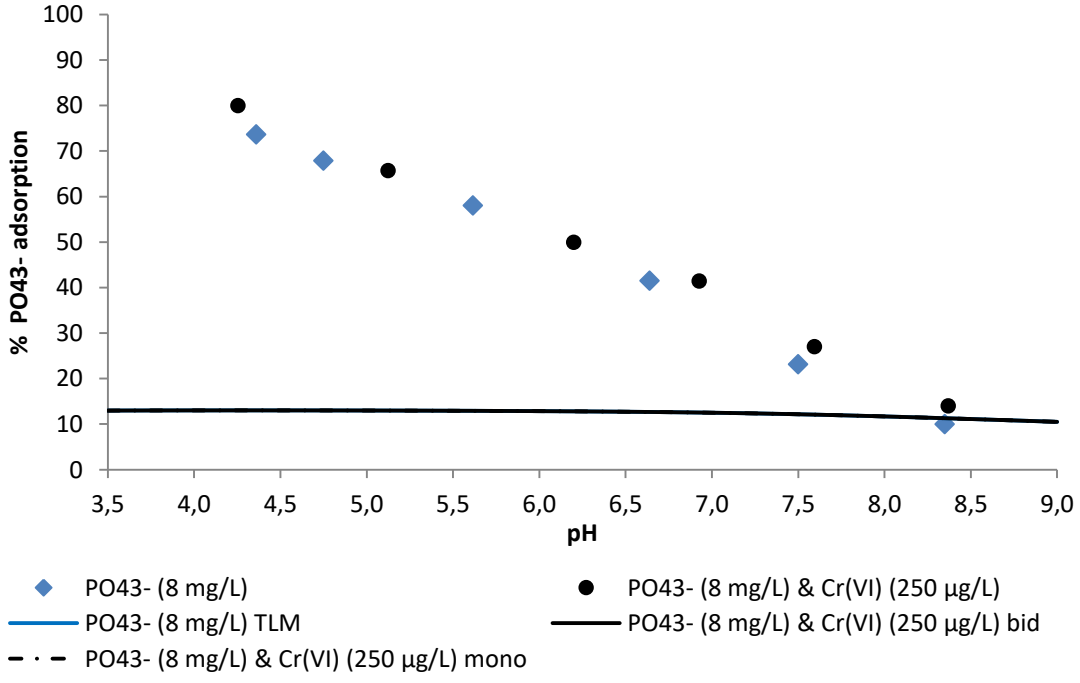

Figure 6.12 Adsorption simulation of PO_4^{3-} (8 mg/L) in the presence (250 µg/L) and absence of Cr(VI) using the TLM model for solid concentration equal to 0.103 g/L.

Effect of pH and Cr(VI) on nitrates adsorption

In the case of nitrates adsorption simulation results were much better since the high increase of the logK value (Table 6.4) for the formation of SOH_2-NO_3 complex could describe the low experimental values of nitrates adsorption, except for the case of using the high concentration of nitrates equal to 50 mg/L. This indicates that the solid concentration used is not enough for simulating the adsorption of nitrates due to surface saturation.

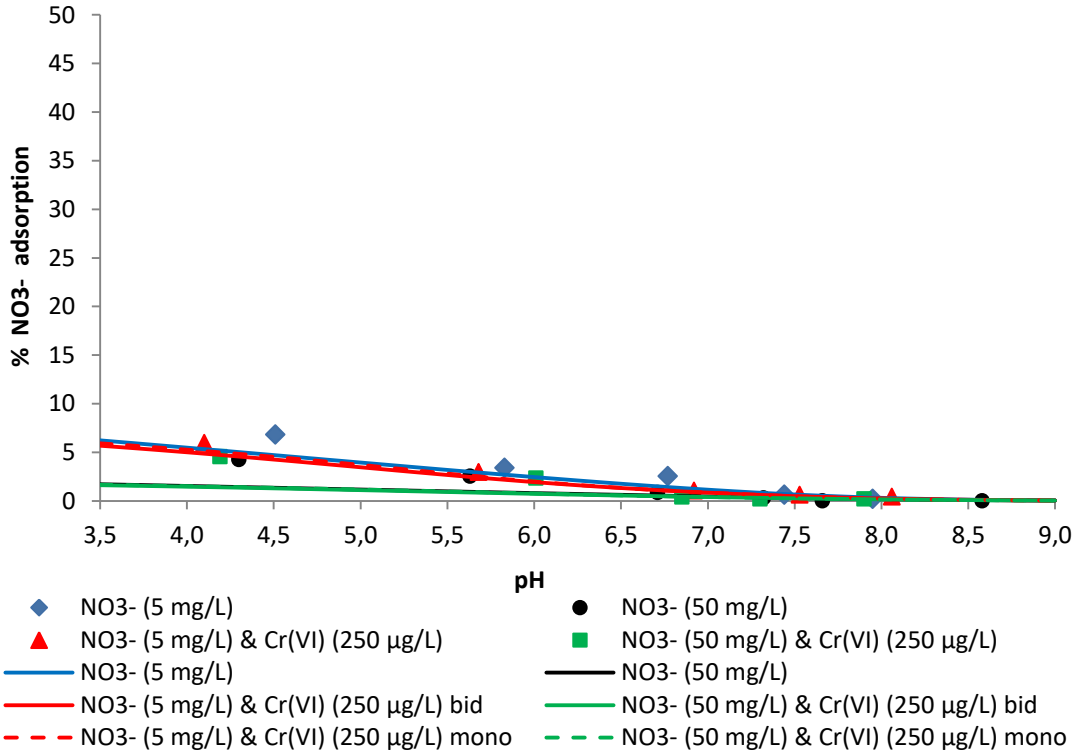

Figure 6.13 Adsorption simulation of nitrates (5 and 50 mg/L) in the presence (250 µg/L) and absence of Cr(VI) using the TLM model for solid concentration equal to 0.103 g/L.

Effect of pH and inorganic ions on Cr(VI) adsorption

Finally, similar results with those mentioned above for each contaminant were observed for the case of Cr(VI) adsorption and its possible competition with the other contaminants. The adsorption percentage obtained using the TLM model was significantly lower than the experimental removal, indicating that the low value of solid concentration used could not simulate the experimental data. Cr(VI) adsorption was slightly lower in the case that nitrates (5 mg/L) presented in the soil solution, significantly lower in the presence of 50 mg/L nitrates, while was almost zeroed in the presence of phosphates. Thus, it can be concluded that this solid concentration is not sufficient for describing the competitive adsorption phenomena between chromates and the inorganic contaminants.

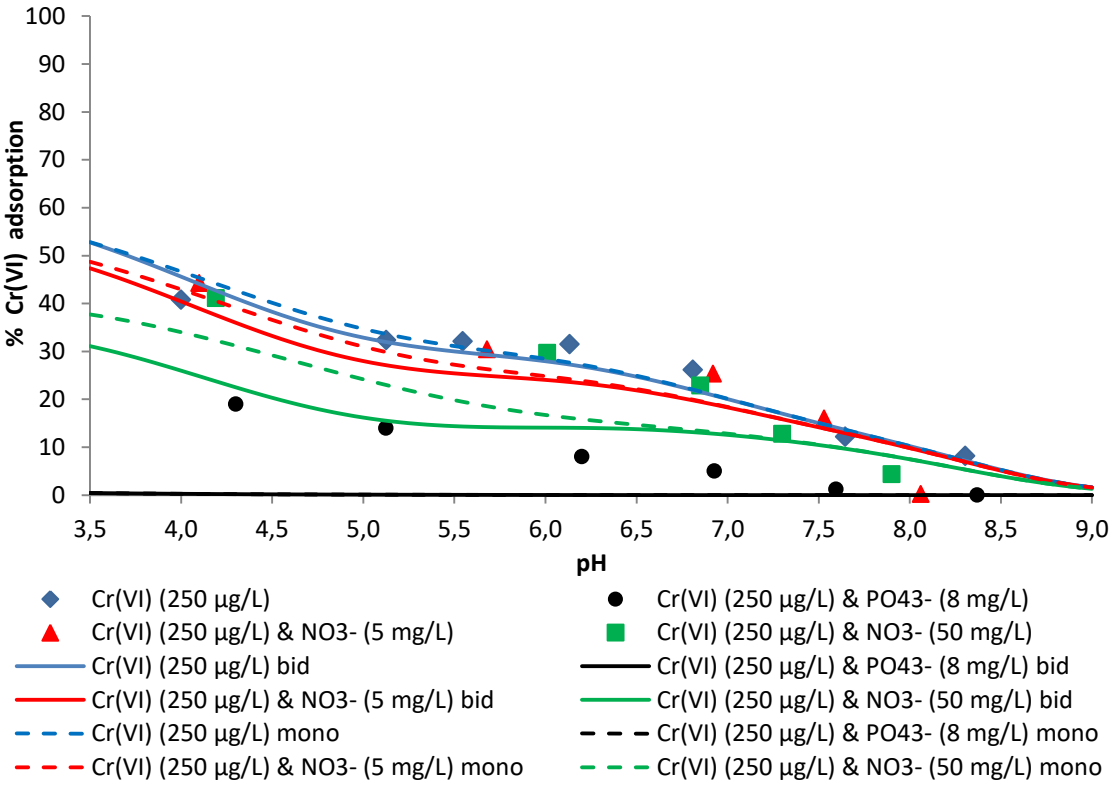

Figure 6.14 Simulation of competitive adsorption of Cr(VI) with inorganic contaminants using the TLM for solid concentration equal to 0.103 g/L.

6.1.4 Application of the Diffuse Layer Model

Diffuse Layer Model (DLM) is based on the formation of inner sphere monodentate complexes and at the presence of a diffusion layer in which ions with opposite charge of that of the soil surface exist. However these ions remain in the aqueous phase (Goldberg et al., 2007). In the DLM specific adsorption at the solid surface plane is balanced by a diffuse ion "swarm", rather than a plane of counterions, contrary to TLM at which adsorption takes place at two separate planes with a diffuse ion "swarm" providing the charge balance. The general advantage of DLM, is that it requires fewer parameters for adsorption modeling compared with TLM. However, the logK of protonation-dissociation values are affected by the background electrolyte (Koretsky, 2000). Table 6.7 presents the reactions and their corresponding logK values, which exhibited the optimum results for adsorption simulation on the ophiolitic soil as it will be shown at the next paragraphs. A literature review (Table A3.3, Appendix III) verified that the logK values obtained in this study are similar with those presented by other studies for the case of applying the DLM model in order to simulate the adsorption of the tested contaminants.

Table 6.7 Reactions and their corresponding values of adsorption constants (logK) applied at the DLM.

Reactions							logK	PSI_o	Reference
No.	Reactants				Products				
	Soil	Ligand 1	Ligand 2		Product 1	Product 2			
1	SOH			↔	SO^-	H^+	-9	-1	Goldberg et al., 2007
2	SOH	H^+		↔	SOH_2^+		4.2	1	
3	SOH	Na^+		↔	SONa	H^+	-9.29	0	Ermakova et al., 2001
4	SOH	Cl^-	H^+	↔	SCl	H_2O	8.43	0	
5	SOH	PO_4^{3-}	H^+	↔	SPO_4^{2-}	H_2O	18	-2	Mathur & Dzombak, 2006
6	SOH	PO_4^{3-}	$2H^+$	↔	$SHPO_4^-$	H_2O	22	-1	
7	SOH	PO_4^{3-}	$3H^+$	↔	SH_2PO4	H_2O	30	0	
8	SOH	NO_3^-	H^+	↔	SNO_3	H_2O	8.8	0	Goldberg et al., 2007
Inner sphere & Monodentate Complexation									
9	SOH	CrO_4^{2-}	$2H^+$	↔	$SHCrO_4$	H_2O	16.2	0	Mathur & Dzombak, 2006
10	SOH	CrO_4^{2-}	H^+	↔	$SCrO_4^-$	H_2O	10.25	-1	

Adsorption simulation using the 2pk-DLM model included the simulation of experimental data obtained by the batch series experiments investigating the effect of ionic strength and pH on Cr(VI) adsorption and the effect of pH on inorganic contaminants adsorption. In general, the 2pk approach is expected to provide better fitting compared to 1pk approach, which gives poorer fitting to experimental results (Lutzenkirchen, 1998). The following diagrams represent the best results obtained during simulation results using the 2pk-DLM model and are referred to solid concentration equal to 1.5 g/L. It is obvious that the 2pk-DLM model cannot predict with good accuracy neither the adsorption of Cr(VI) (Figure 6.15) nor of phosphates (Figure 6.16), and consequently not the competitive adsorption effects between these contaminants, on the ophiolitic soil (Figures 6.16 and 6.18).

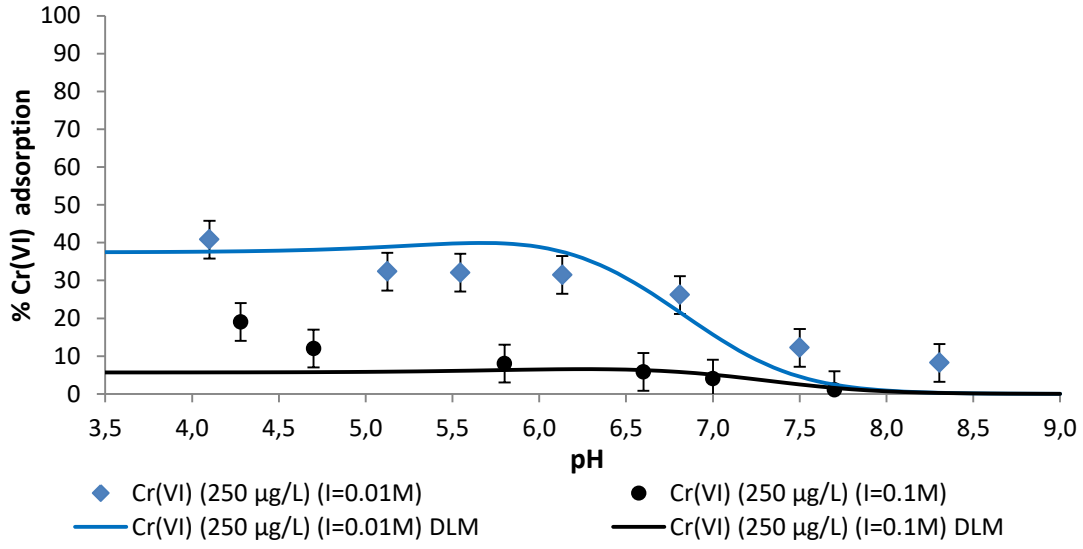

Figure 6.15 Simulation of the effect of pH and ionic strength on Cr(VI) adsorption (250 µg/L) using the DLM model for solid concentration equal to 1.5 g/L.

These observations are in accordance with the findings of other studies regarding Cr(VI) adsorption mechanisms on amorphous soil oxides (Zachara et al., 1987; Ainsworth et al., 1989; Mesuere & Fish, 1992; Villalobos et al., 2001; Xie et al., 2015). The inability of 2pk-DLM to simulate Cr(VI) adsorption process (Figure 6.15), both in terms of pH and ionic strength, can be attributed to the fact that Cr(VI) probably forms both inner and outer sphere complexes (as observed by applying the TLM) upon adsorption on the ophiolitic soil and not exclusively inner sphere, as assumed applying the DLM model. This assumption was verified by Veselská et al. (2016) mentioning that despite EXAFS analyses verified the formation of inner sphere complexes (in higher percentage monodentate complexes and less as bidentate) the application of DLM could not simulate Cr(VI) adsorption since the contribution of outer sphere complexes should be taken into account. In addition, as mentioned above, the DLM is affected by the background electrolyte and, thus, by the ionic strength of the solution. Dzombak and Morel (1990) reported an approach for applying the DLM to higher concentrations up to 0.1M since its fitness to higher ionic strengths was not satisfied. Hayes et al (1991) also mentioned that in the DLM model only one parameter can significantly affect the shape of the curve and this is the $\log K^{+}$ and $\log K^{-}$, for pH values lower and higher than the pH_{PZC}, respectively. Thus, it is expected that the fitting to experimental values is poorer in a wide range of ionic strengths.

As regarding phosphates, the formation of inner-sphere complexes of phosphate with the hydrous ferric oxides surface has been reported by several studies (Torrent et al., 1990; Persson et al., 1996; Torrent and Delgado, 2000; Saha and Streat, 2005; Mengistu et al., 2015). Persson et al (1996) based on spectroscopic evidence reported that orthophosphates are adsorbed on hydrous ferric oxide surface by forming monodentate complexes like, >FeO-H_2PO_4, >FeO-HPO_4^{-} and >FeO-PO_4^{2-}, where phosphates are bound to a low-energy proton-exchangeable surface site. Hoell and Kalinichev (2004) further verified this fact by mentioning the little contribution of bidentate or bridging complexes. However, as shown at Figure 6.16, the application of 2pk-DLM, using surface complexation reactions which correspond to only monodentate complexes, for describing the adsorption of phosphates on the ophiolitic soil is inadequate. Similar results have been published by Mengistu et al. (2015) showing that the DLM based on the above mentioned monodentate complexes fairly describes the adsorption of phosphates in a wide pH range. On the other hand Mao et al. (2016) showed that DLM could simulate with good accuracy the adsorption of phosphates on hydrous ferric oxides. The application of DLM for simulating phosphate adsorption on modified clays with NaCl, $CaCl_2$ and $FeCl_3$ was also investigated by Moharami and Jalali (2015).

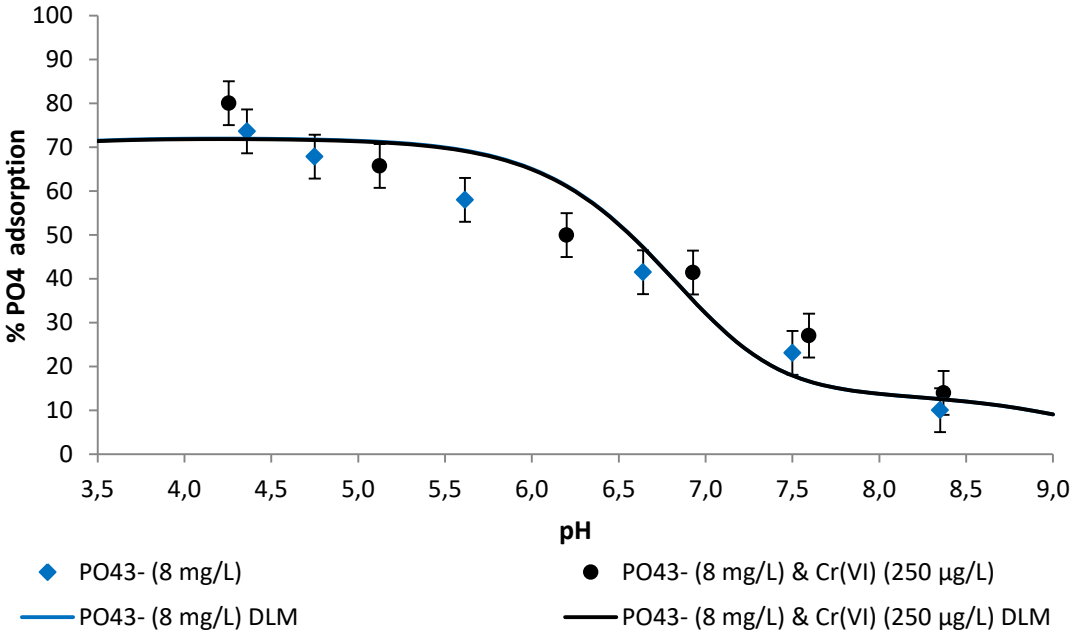

Figure 6.16 Adsorption simulation of PO_4^{3-} (8 mg/L) in the presence (250 µg/L) and absence of Cr(VI) using the DLM model for solid concentration equal to 1.5 g/L.

As previously discussed, nitrates adsorption is thought to be based on the formation of outer sphere complexes. Although, the 2pk-DLM did not expect to simulate the adsorption phenomenon since it considers all complexes to be formed in the inner layer, the results showed very good accuracy. Adsorption simulation was performed using equation No. 8 **(Table 6.7)**, which was created assuming inner sphere complexation and the logK value used was equal to 8.8. This value is similar to that referred in the literature for nitrates adsorption. As observed from **Figure 6.17,** simulation was performed with satisfactory results. Thus, further research maybe required in order to identify the types of surface complexes that nitrates form with the surface of amorphous oxides and about the ability of 2pk-DLM to predict their adsorption.

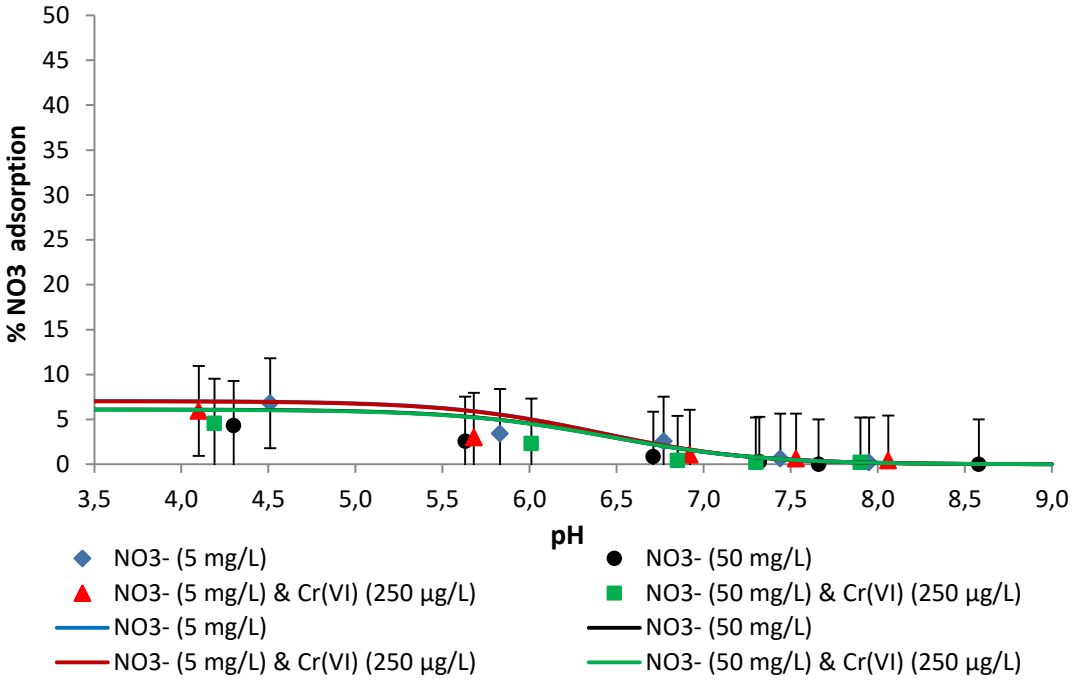

Figure 6.17 Adsorption simulation of nitrates (5 and 50 mg/L) in the presence (250 µg/L) and absence of Cr(VI) using the DLM model for solid concentration equal to 1.5 g/L.

Finally, the application of the 2pk-DLM for predicting the competitive adsorption effects between Cr(VI) and the inorganic contaminants is shown at Figure 6.18. Experimental data were poorly simulated applying this model, especially in the case of binary systems with chromates and phosphates in the aqueous solution.

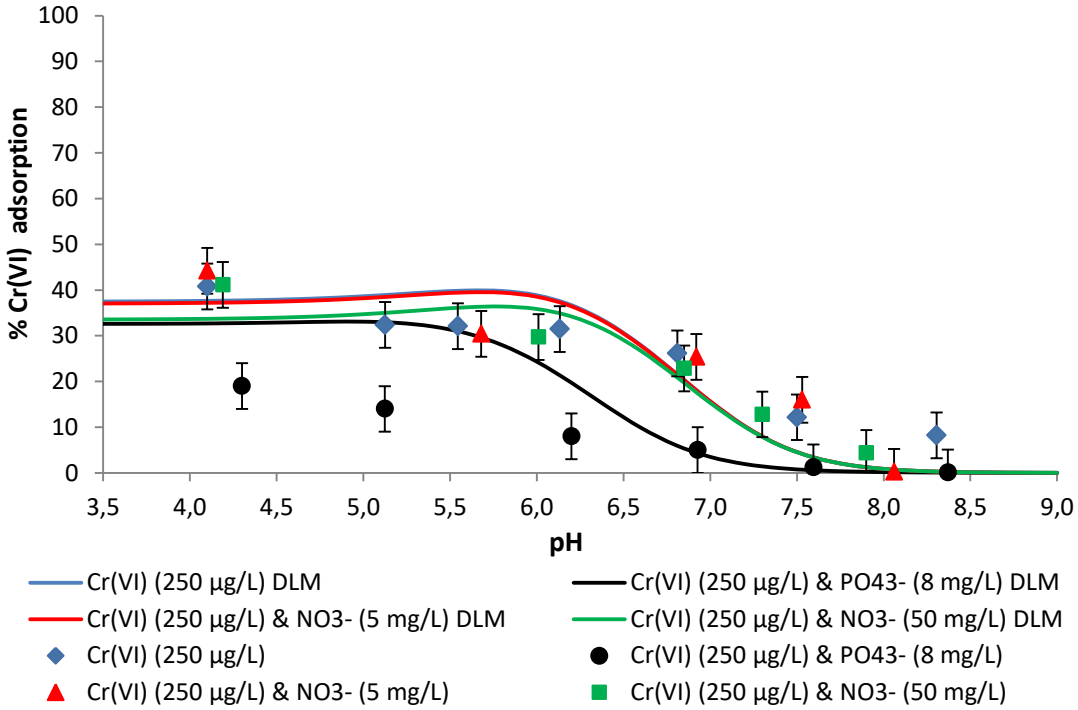

Figure 6.18 Simulation of competitive adsorption of Cr(VI) with inorganic contaminants using the DLM.

6.1.5 Application of the Constant Capacitance Model

The Constant Capacitance Model (CCM) is based on the formation of inner sphere complexes either monodentate or bidentate. Thus, using the CCM model, is possible to regulate/optimize fewer parameters than in TLM, since fewer surface complexation reactions are introduced into the database. Table 6.8 presents the reactions used for the adsorption database set up and their corresponding logK values which exhibited the optimum results applying the 2pk-CCM model, as it will be shown in the following paragraphs. A literature review (Table A3.4, Appendix III) verified that the logK values obtained in this study are similar with those presented by other studies for the case of applying the CCM model in order to simulate the adsorption of the tested contaminants. As shown at Table 6.8 surface complexation of chromates is based on the formation of both monodentate and bidentate inner sphere complexes. This scenario gave the best results during simulation. In addition, the following three cases were tested regarding the surface complexes able to be formed:

1. Formation of exclusively monodentate (mono-protonated) complexes (Reaction 10)
2. Formation of exclusively bidentate complexes (Reaction 11)
3. Formation of both monodentate (mono-protonated) and bidentate complexes (Reactions 10 & 11)

All these scenarios were tested for each case of solid concentration mentioned above, but none of them verified the experimental data.

Table 6.8 Reactions and their corresponding values of adsorption constants (logK) applied at the CCM.

Reactions							logK	PSIo	Reference
No.	Reactants				Products				
	Soil	Ligand 1	Ligand 2		Product 1	Product 2			
1	SOH			↔	SO-	H^+	-9	-1	Goldberg et al., 2007
2	SOH	H^+		↔	SOH_2^+		4.2	1	
3	SOH	Na^+		↔	SONa	H^+	-9.29	0	Grossl et al., 1997
4	SOH	Cl^-	H^+	↔	SCl	H_2O	8.43	0	
5	SOH	PO_4^{3-}	H^+	↔	SPO_4^{2-}	H_2O	16	-2	Goldberg, 1985
6	SOH	PO_4^{3-}	$2H^+$	↔	$SHPO_4^-$	H_2O	23.1	-1	
7	SOH	PO_4^{3-}	$3H^+$	↔	SH_2PO_4	H_2O	29.8	0	
8	SOH	NO_3^-	H^+	↔	SNO_3	H_2O	8.7	0	Goldberg et al., 2007
Inner sphere & Bidentate or Monodentate Complexation									
9	SOH	CrO_4^{2-}	$2H^+$	↔	$SHCrO_4$	H_2O	16.2	0	Grossl et al., 1997
10	SOH	CrO_4^{2-}	H^+	↔	$SCrO_4^-$	H_2O	10.2	-1	
11	2SOH	CrO_4^{2-}	$2H^+$	↔	S_2CrO_4	$2H_2O$	10	0	

Adsorption simulation using the 2pk-CCM model included the simulation of experimental data obtained by the batch series experiments investigating the effect of ionic strength and pH on Cr(VI) adsorption and the effect of pH on inorganic contaminants adsorption. As in the case of using the 2pk-DLM, simulation was performed using the highest solid concentration equal to

1.5 g/L without verifying satisfactorily the experimental data. The following diagrams represent the best modeling results obtained using the 2pk-CCM model.

Contrary to DLM, the application of the CCM is restricted to constant ionic strength values due to the formation of charge-potential relationship. The interfacial potential is not dependent on ionic strength alterations and as a result the CCM surface equilibrium constants must be changed by changing ionic strength during simulation. In addition, CCM application is limited to high ionic strength values as mentioned by Hayes et al. (1991). As regarding the weakness of CCM over TLM to simulate Cr(VI) adsorption process it can be attributed to the fact that Cr(VI) probably forms both inner and outer sphere complexes when adsorbed and not just inner sphere, as considered applying the CCM model (Goldberg, 2014). However, in our case CCM predicted with relatively good accuracy Cr(VI) adsorption on the ophiolitic soil in the case of using the low ionic strength value (I=0.01M). Using the same logK values, while increasing the ionic strength value, adsorption simulation was not efficient for pH values lower than 5.

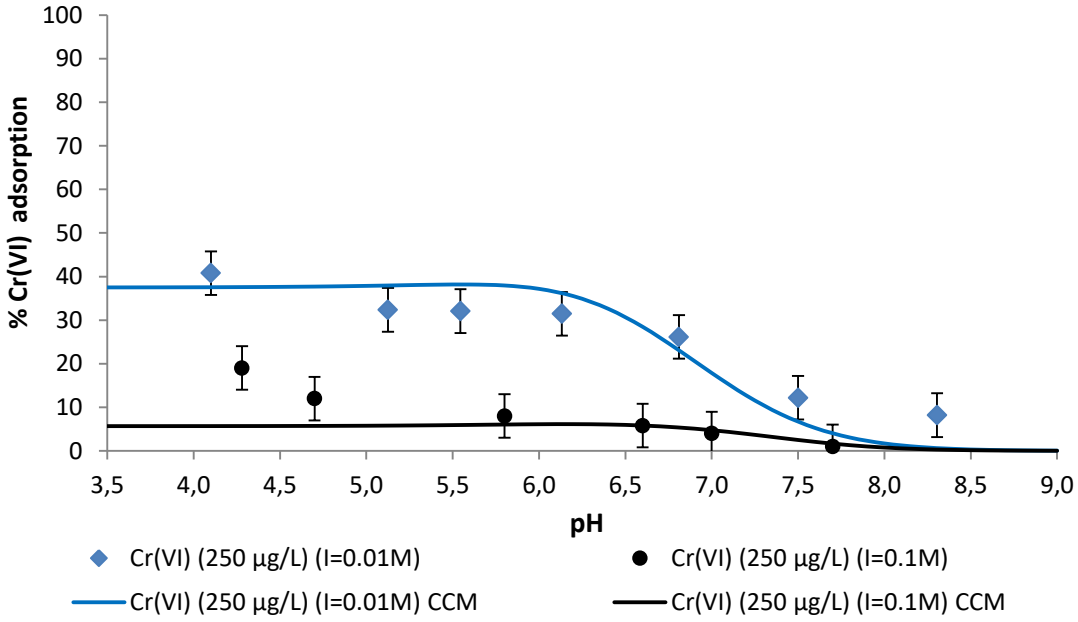

Figure 6.19 Simulation of the effect of pH and ionic strength on Cr(VI) adsorption (250 µg/L) using the CCM model for solid concentration equal to 1.5 g/L.

As regarding adsorption of phosphate Goldberg was the first researcher used the CCM for describing adsorption of orthophosphates by non calcareous mineral soils. The results showed that CCM simulated with accuracy the orthophosphate adsorption taking into account the effect of pH. At another study Goldberg and Sposito (1984) showed that CCM was qualitatively able to predict phosphate adsorption on soil using an average set of anion surface complexation constants obtained from numerous soils. In the case of ophiolitic soil adsorption of phosphates is not sufficiently predicted applying the 2pk-CCM especially at acidic pH values (Figure 6.20).

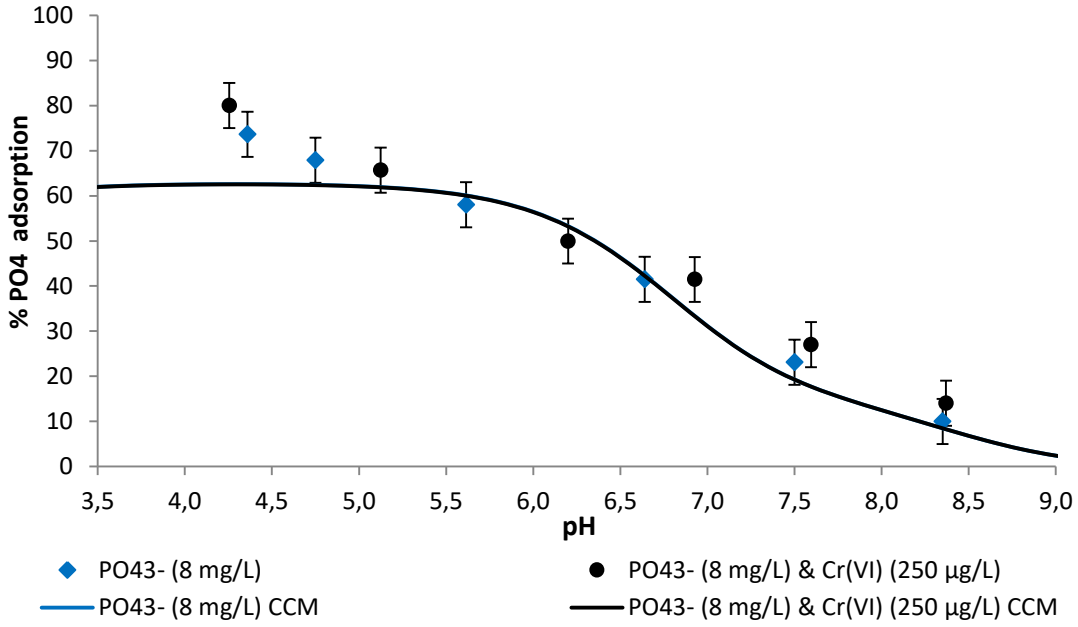

Figure 6.20 Adsorption simulation of PO_4^{3-} (8 mg/L) in the presence (250 µg/L) and absence of Cr(VI) using the CCM model for solid concentration equal to 1.5 g/L.

Regarding nitrate adsorption simulation, similarly to the case of using the DLM model, the CCM supports only the formation of inner sphere complexes. The addition of equation No. 8 (Table 6.8), in order to describe the adsorption behavior of nitrates, with logK value equal to 8.7, verified with high accuracy nitrate ions adsorption on the ophiolitic soil (Figure 6.21).

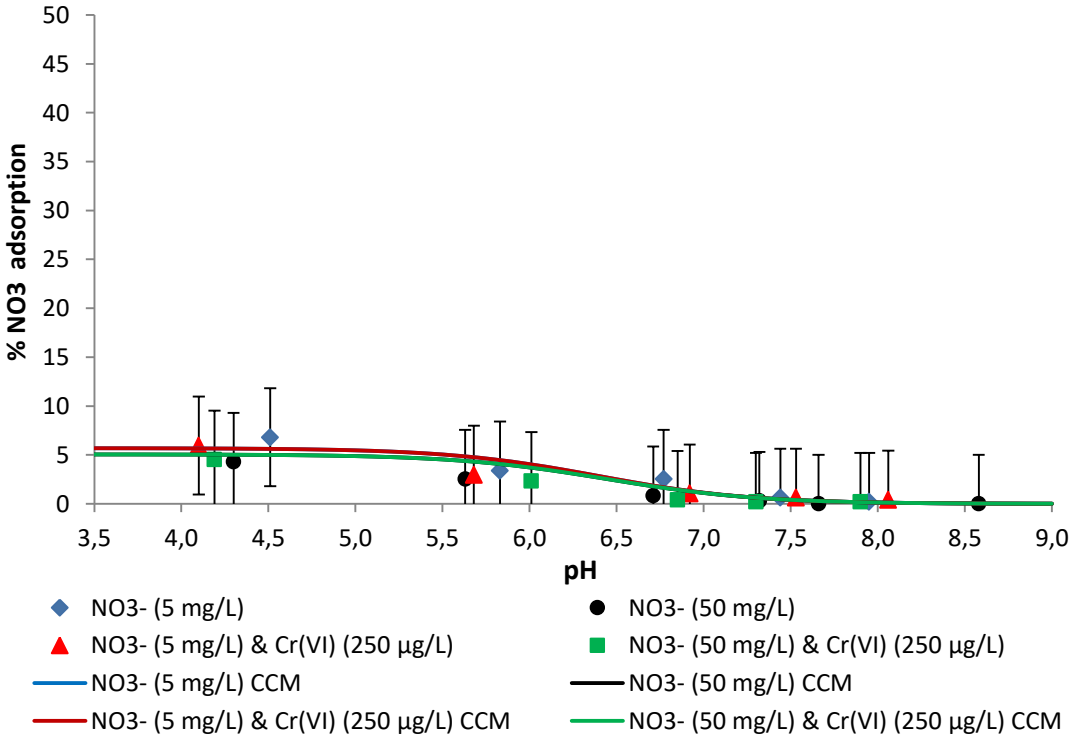

Figure 6.21 Adsorption simulation of nitrates (5 and 50 mg/L) in the presence (250 µg/L) and absence of Cr(VI) using the CCM model for solid concentration equal to 1.5 g/L.

Despite the application of 2pk-CCM predicted with good accuracy the adsorption of contaminants in single anion solutions, this was not verified in the case of using binary contaminants solution. The 2pk-CCM was not capable of predicting the adsorption behavior of Cr(VI) especially in the presence of phosphates in the soil solution (Figure 6.22).

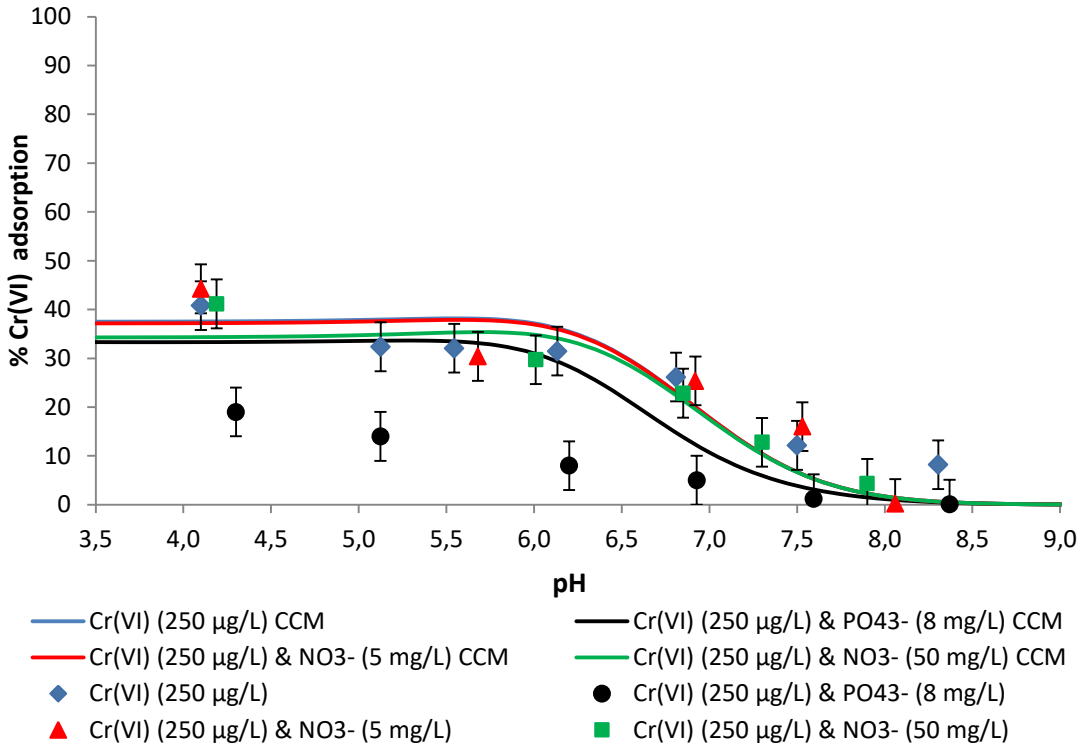

Figure 6.22 Simulation of competitive adsorption of Cr(VI) with inorganic contaminants using the 2pk-CCM.

6.2 Adsorption simulation of Cr(VI) on goethite

Adsorption modeling of the experimental data of Cr(VI) adsorption on goethite was performed using Visual Minteq v.3.1 software (Gustafsson, 2013). The three adsorption models based on surface complexation reactions, the TLM, the DLM and the CCM models were used for simulation of the experimental data as in the case of using the ophiolitic soil. The acceptable deviation between the experimental data and the modeling results was determined to ±5%, in order to evaluate simulation as satisfactory and thus to accept the values of surface complexation constants.

The parameters used for simulation of experimental data by applying the aforementioned models are provided at Table 6.9. The total SSA determined by the N_2/BET adsorption method and was equal to 9.09 m^2/g. The relatively low SSA measured in the tested goethite can be a result of the synthesis process since factors such as aggregation caused by ageing and freezing–thawing temperatures as well as the presence of CO_2 during synthesis can affect the surface area value (Mengistu et al., 2015).

Table 6.9 Parameters used for simulating adsorption on goethite applying the TLM model

Adsorption model	2-pk TLM
SSA (m^2/g)	9.09
Inner capacitance (F/m^2)	1.4
Outer capacitance (F/m^2)	0.2
Site density (nm^{-2})	2.3
Solid concentration (g/L)	10

The chemical and physical properties of soil iron oxides, like goethite, are thought to be more a function of their surface area than of their mineralogical form. A possible factor able to determine the low value of surface area of the tested goethite is its degree of crystallinity (Borggaard, 1983). The interpretation of term “crystallinity” regards the crystal size distribution and the structural perfections. The crystallinity is reflected by the surface area value with the better crystallized solids exhibiting lower SSA (Strauss et al, 1997). In addition, low degree of crystallinity facilitates the incorporation of foreign elements in the crystal lattice due to structural imperfections. Thus, "high defect materials" behave like "poorly crystalline materials". Poorly crystalline goethite is considered to incorporate several elements in its structure such as nickel, chromium and especially aluminum.

In the geoenvironment crystallinity is affected by a number of factors and, thus, can vary vertically as well as laterally at soil profiles. More specifically, goethite that occurs in laterites exhibits decreasing crystallinity with increasing depth. On the other hand serpentinitic minerals exhibit the lowest crystallinity at topsoils, which present higher degree of weathering. Specifically for serpentine minerals the decreasing crystallinity depends also on the degree of decomposition but in general its determination is more complicated due to different genetic types, different polymorphs and changes during progressive weathering (Kuhnel, 1975). Taking into account these data the presence of goethite or generally iron oxides in deep serpentinitic profiles can be considered of high crystallinity due to low weathering. Thus, the low surface area goethite selected for this study aimed at a) simulating the goethite that may occurs in ophiolitic complexes or/and b) simulating the low surface area serpentinitic minerals that may contribute to anions adsorption. In addition, high crystallinity and low surface area of goethite affects the time needed for accomplishing the adsorption process, since well crystallized solid minerals is thought to need about one day to adsorb anions like chromates and phosphates (Torrent et al., 1990; Strauss et al, 1997). This range of time is similar to that used in the batch experiments of this study.

6.2.1 Application of the Triple Layer Model

Firstly, adsorption simulation was performed applying the TLM surface complexation model. The parameters used for applying the TLM model are provided at Table 6.9. The reactions used for data simulation are presented at Table 6.10. A literature review (Table A3.2., Appendix III) verified that the logK values obtained in this study are similar with those presented by other studies for the case of applying the TLM model in order to simulate the adsorption of the tested contaminants on goethite. The PSI_o and PSI_b parameters represent the Boltzman’s

factor and referred to the o- and β- surface planes, respectively. Their values were calculated according to the equations provided by Goldberg et al. (2007) regarding the TLM model and the formation of outer and inner sphere complexes.

Table 6.10 Reactions used at the TLM model for simulating adsorption on goethite.

Reactions							Log K	PSI_o	PSI_b
No.	Reactants				Products				
	Solid	Ligand 1	Ligand 2		Product 1	Product 2			
1	FeOH			↔		H^+	-9	-1	
2	FeOH	H^+		↔	$FeOH_2^+$		4.2	1	
3	FeOH	Na^+		↔	FeONa	H^+	-9.29	-1	1
4	FeOH	Cl^-	H^+	↔	$FeOH_2Cl$		8.43	1	-1
5	FeOH	PO_4^{3-}	H^+	↔	$FeOPO_3^{2-}$	H_2O	15.5	-2	
6	2FeOH	PO_4^{3-}	$2H^+$	↔	$Fe_2O_2PO_2^-$	$2H_2O$	20	-1	
7	2FeOH	PO_4^{3-}	$3H^+$	↔	Fe_2O_2POOH	$2H_2O$	33	0	
8	FeOH	NO_3^-	H^+	↔	$FeOH_2NO_3$		9.8	1	-1
1st scenario for bidentate modeling									
9	2FeOH	CrO_4^{2-}	$2H^+$	↔	Fe_2CrO_4	$2H_2O$	14	0	
10	FeOH	CrO_4^{2-}	$2H^+$	↔	$FeOH_2$-$HCrO_4$		19.9	1	-1
11	FeOH	CrO_4^{2-}	H^+	↔	$FeOH_2CrO_4^-$		10	1	-2
2nd scenario for monodentate modeling									
12	FeOH	CrO_4^{2-}	H^+	↔	$FeCrO_4^-$	H_2O	12.1	-1	
13	FeOH	CrO_4^{2-}	$2H^+$	↔	$FeOH_2$-$HCrO_4$		19.9	1	-1
14	FeOH	CrO_4^{2-}	H^+	↔	$FeOH_2CrO_4^-$		10	1	-2

Effect of pH and ionic strength of the soil solution on Cr(VI) adsorption

Two different scenarios were investigated in this study regarding the formation of inner sphere complexes of chromates on the goethite surface. At the first scenario the formation of bidentate complexes was assumed (reactions No. 9 - 11), while at the second one only monodentate complexes (reactions No. 12 - 14) were taken into account. The rest of the reactions were kept constant in both cases.

The strong pH dependence (Figure 6.23) suggests that Cr(VI) adsorption is based on the formation of inner sphere complexes. On the other hand, the decrease of adsorption efficiency with increasing ionic strength indicates the formation of outer sphere complexes of chromates with the goethite surface. The effect of ionic strength is used for determining the formation of outer sphere complexes, since it can affect the thickness of the double layer and thus the anions binding. In this study the decrase is probably attributed to the fact that chromates are placed in the same plane with clorides of the background electrolyte (Goldberg et al., 2007; Ajouyed et al., 2010). Taking into account the experimental data the formation of both inner

and outer sphere complexes is possible. The formation of both inner and outer sphere complexes of chromates with surface sites of goethite has also been mentioned by Weerasooriya and Tobschall (2000). The difference between inner- and outer-sphere complexes can be distinguished by the effects of ionic strengths on the adsorption edges (Hayes and Leckie, 1987). In this study, the application of TLM simulated with very good accuracy (Figure A1.13) the experimental data when considering that chromates form bidentate complexes with the goethite surface. In addition, these results indicate that the increase of the ionic strength affects the formation of bi- or mono- dentate complexes.

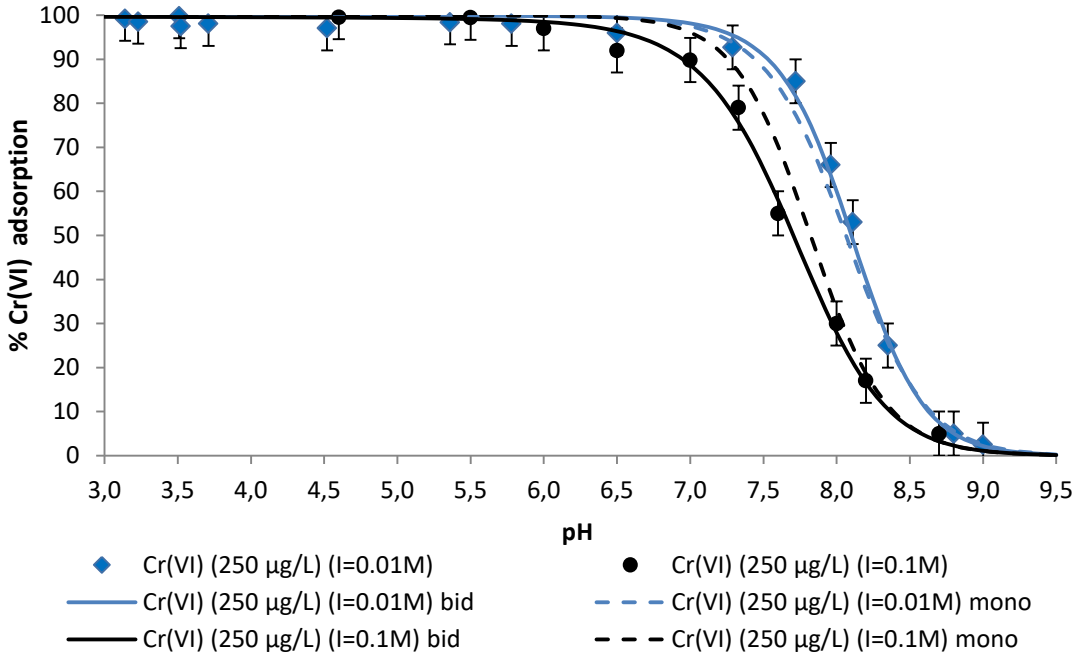

Figure 6.23 Simulation of the effect of pH and ionic strength on Cr(VI) adsorption (250 µg/L) by goethie using the TLM.

Similar results regarding adsorption of chromates on goethite have been reported by several studies (Hayes and Leckie, 1987; Mesuere and Fish, 1992; Fendorf et al., 1997; Weerasooriya and Tobschall, 2000; Xie et al., 2015). Hayes and Leckie (1987) reported that the pH_{50} (pH corresponding to 50% adsorption) value of Cr(VI) adsorption was slightly shifted by 0.4 units lower for increasing the concentration of background electrolyte 2 orders of magnitude. In addition, Xie et al. (2015) recently reported EXAFS data proving the formation of inner sphere mono- or bi- dentate complexes with the goethite surface. Determining the Fe – Cr distance they concluded that chromate occurs via the formation of three different surface complexes, a monodentate complex, a bidentate binuclear complex, and a bidentate – mononuclear complex. They also suggested that each complex was favorably formed depending on the initial concentration of chromate and thus the surface coverage of the oxide. However, they assumed only inner sphere complexes monodentate or bidentate in order to simulate chromate adsorption (Figure 6.24).

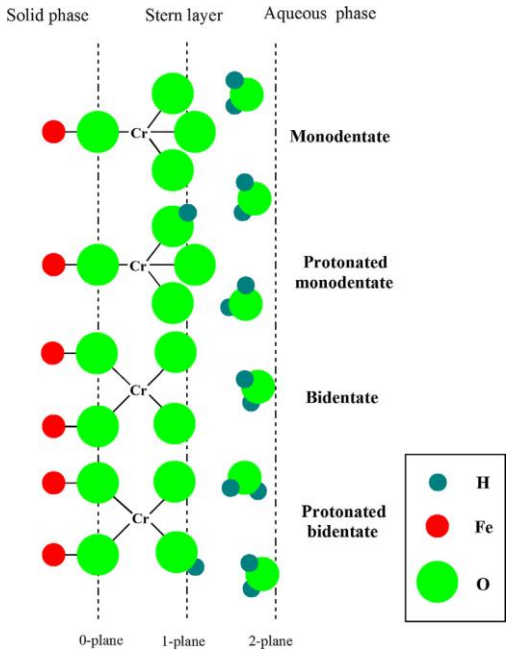

Source: (Xie et al., 2015)

Figure 6.24 Scheme of the formation of inner sphere complexes on the goethite/water interface.

Effect of pH and Cr(VI) concentration on phosphates adsorption

As mentioned above, phosphates adsorption on goethite is based on ligand exchange mechanism and thus inner sphere monodentate (reaction No. 5, Table 6.10) and bidentate (reactions No. 6 and 7, Table 6.10) complexes are considered to be formed on the goethite surface.

Spectroscopic evidence have shown that phopshates form mainly bidentate and monodentate complexes for pH < 8 and pH > 8, respectively (Antelo et al., 2005; Chitrakar et al., 2006). These evidence were supported by the present study since the effect of the reactions No. 6 and 7 during simulation of the experimental results was more signficant. In addition, phosphates adsorption was not affected by the formation of either monodentate or bidentate complexes of chromates (Figure A1.14). Only a very slight decrease when using 8 mg/L phosphates and considering that chromates form exclusively monodentate complexes was observed (Figure 6.25). This is possibly an indication that the adsorption sites are limited and possible competition between chromates and phosphates occurs. Boukemara and Boukhalfa (2012) mentioned that the presence of chromates in the goethite solution caused the formation of inner sphere complexes of phosphates instead of some outer sphere complexes formed during the absence of chromates. In addition, regarding the effect of different structural properties as discussed previously, Torrent et al. (1990) reported that the amount of phosphate adsorbed at different types of goethite, was similar and not affected by the crystal faces of goethite, since different crystal faces exhibited similar adsorption capacities.

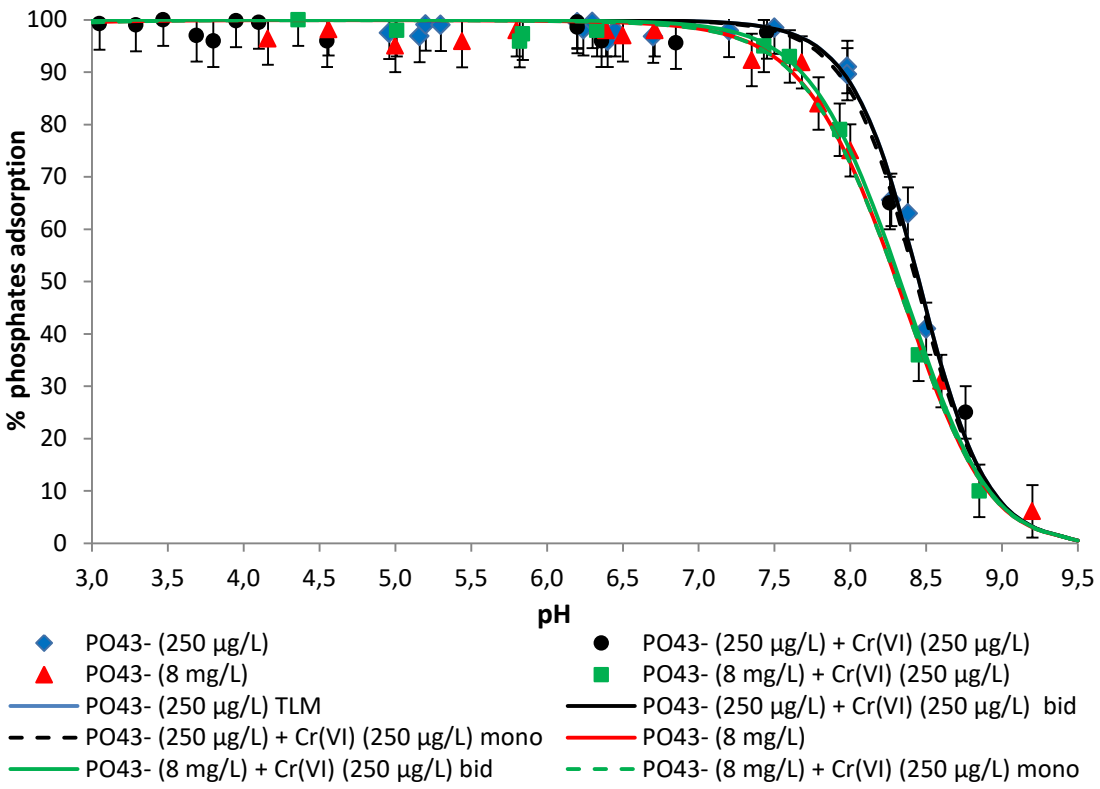

Figure 6.25 Adsorption simulation of PO_4^{3-} (8 mg/L) in the presence (250 µg/L) and absence of Cr(VI) using the TLM.

Adsorption of orthophosphates on hydrous iron oxides like goethite has been widely studied and used for the development of surface complexation models for anions. However, the reactions that used during simulation with a surface complexation model (SCM) are actually less complicated than those that occur during adsorption of phosphate on the goethite surface (Hongshao and Stanforth, 2001). Tejedor-Tejedor and Anderson (1990) were of the first studies using CIR-FTIR spectroscopy for investigating the phosphate adsorption on goethite and concluded that phosphate form three different inner-sphere surface complexes, a monodentate non protonated complex, and two bidentate complexes, one protonated and one non protonated. Antelo et al., (2005) studied the combined effects of pH and ionic strength on phosphate adsorption. The results showed higher adsorption efficiency in acidic media at most ionic strengths tested, and lower phosphate adsorption in alkali pH values and low ionic strengths. Simulation of the experimental data using the CD-MUSIC model, which exhibits similarities with the TLM, showed good fitting with the experimental data. Simulation showed the presence of three inner-sphere surface complexes (monodentate non-protonated, bidentate non-protonated, and bidentate protonated). Figure 6.26 represents the structure of the protonated monodentate (upper) and bidentate (lower) phosphate surface species.

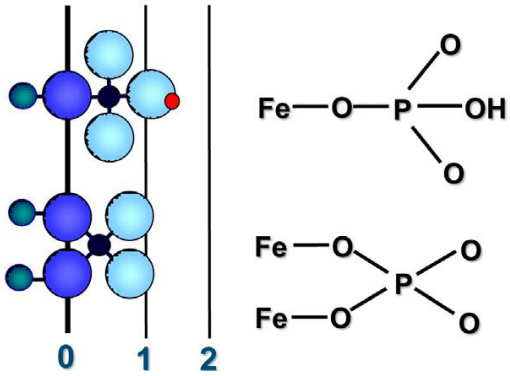

Source: (Weng et al., 2012).

Figure 6.26 Representation of the structure of the protonated monodentate (upper) and bidentate (lower) phosphate surface species on goethite.

The formation of inner sphere complexes of phosphates was further verified by other studies. Luengo et al. (2006) performed ATR-IR experiments in order to identify the surface complexation species formed between phosphate and the goethite surface. The results showed that at acidic pH values two complexes were formed the bidentate non protonated $(FeO)_2PO_2$ and the bidentate protonated $(FeO)_2(OH)PO$. At higher pH values and specifically at the pH range 7.5 to 9 the dominating complex is $(FeO)_2PO_2$. Rahnemaie et al. (2007) observed the presence of two dominant surface species related to the pH values and the concentration of phosphate using in situ IR spectroscopy. A non-protonated bidentate complex which is dominant over a broad pH range. More specifically, for low pH and high loading, a strong contribution of a singly protonated monodentate complex is observed. At higher pH values a non-protonated bidentate complex ($Fe_2O_2PO_2$) is considered to be the main complex in the neutral pH range. Finally, Wang et al., (2013) using spectroscopic evidence reported that phosphates are adsorbed on iron (hydr)oxides mainly as bidentate complexes. More specifically protonated $[(FeO)_2(OH)PO]$ and unprotonated $[(FeO)_2PO_2]$ binuclear bidentate complexes are thought to be the main surface species, with few monodentate complexes existing at high pH values. All these complexes referred above as potentially formed complexes, have been used for the simulation of the results of this study.

Effect of pH and Cr(VI) on nitrates adsorption

In the case of nitrates it is expected that they form outer sphere complexes (reaction No. 8) since the adsorption mechanism is based on electrostatic attractions. As shown at Figure 6.27 and verified by Figure A1.15, the TLM simulated with good accuracy the low adsorption percentage of nitrates. The absence of any competitive effect of nitrate with chromates was also verified during simulation.

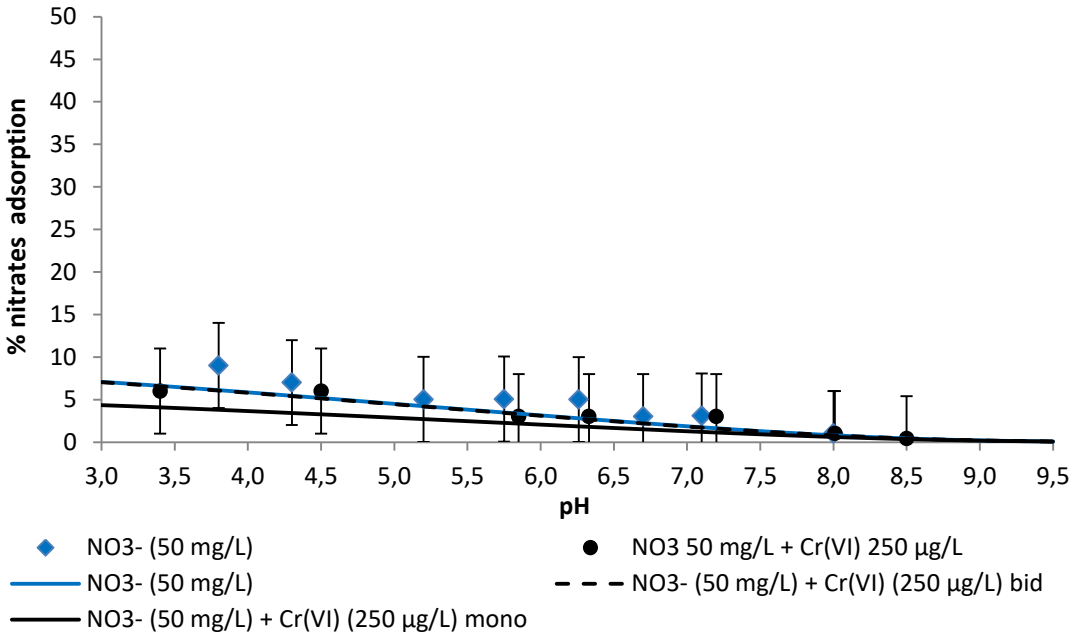

Figure 6.27 Adsorption simulation of nitrates (50 mg/L) in the presence (250 µg/L) and absence of Cr(VI) using the TLM.

Despite nitrates are common groundwater contaminants there are only few studies that have tried to model adsorption of nitrates on goethite using surface complexation models. One of them performed by Zachara et al. (1987) used the TLM model in order to simulate adsorption of nitrates. The nitrate complex was assumed to be the $FeOH_2NO_3$ and the results showed that adsorption of nitrates could be efficiently simulated through TLM. The high concentration of nitrate (0.1M) was thought to be the driving force of adsorption taking into account that the adsorption constant was relatively low ($logK_{NO3}$-=7.5). On the contrary the concentration of nitrates used in this study was very low (50 mg/L) compared to that mention in Zachara et al work.

Effect of pH and inorganic ions on Cr(VI) adsorption

The effect of inorganic contaminants on Cr(VI) adsorption was simulated using the TLM as shown at Figure 6.28. The effect of both phosphate and nitrates was efficiently simulated using the TLM model keeping constant the values of surface complexation constants for each contaminant as presented in Table 6.10. Best verification of experimental data observed in the case of using bidentate complexes for simulating Cr(VI) adsorption (Figure A1.16). The effect of initial concentration in the case of phosphate was also verified by the TLM, since no competitive effects were observed in the case of low concentration of phosphate. In the case of nitrates significant competitive effects were observed probably due to the relative high concentration of nitrates compared to chromates.

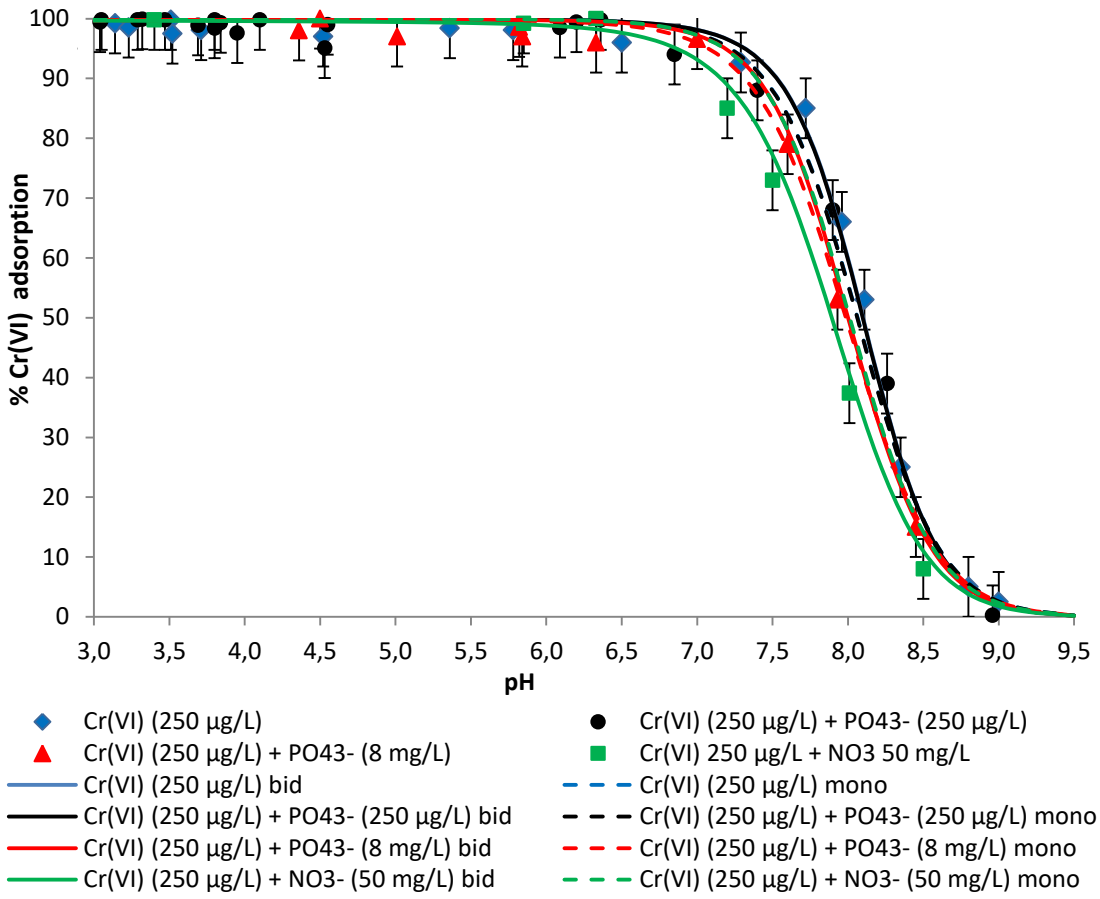

Figure 6.28 Simulation of competitive adsorption of Cr(VI) with inorganic contaminants using the TLM.

The competitive effects of phosphates on adsorption of chromates have been reported by several studies. Phosphates exhibit higher specific affinity for goethite than chromates. The less significant effect of other contaminants such as chlorides and nitrates compared to that of phosphate is attributed to the decrease of electrostatic potential near the surface of a particle, which further leads to weaker adsorption via nonspecific processes (Schroth 1990). There are not any studies regarding the application of TLM for predicting the possible competition between phosphate and chromate. Only a recent study by Xie et al (2015), who applied the CD-MUSIC model, predicted with good accuracy the inhibition caused by phosphates on chromates adsorption. However, in that study chromates were assumed to form exclusively inner sphere complexes and not both inner and outer sphere as in the present study.

Sensitivity analysis of inner capacitance

In the present study the value of inner capacitance C_1 is considered as 1.4 F/m^2, while that of outer capacitance C_2 equal to 0.2 F/m^2. These values have been mostly referred in the literature for surface complexation modeling when using goethite as adsorbent. In order to quantify the model's sensitivity on Cr(VI) adsorption due to inner capacitance parameter, C_1 values between 0.8 and 2.0 F/m^2 were used. According to the literature, the minimum and maximum values that have been used during adsorption of chromates on goethite are in the range 0.8 and 2.0 F/m^2 (Hayes et al., 1991; Sverjensky, 2001; Villalobos et al., 2001). Figure 6.29 presents the results of sensitivity analysis of inner capacitance (C_1) on Cr(VI) adsorption as

obtained by applying the TLM model. The simulation was performed using 250 μg/L Cr(VI) at a soil solution of 0.01 M ionic strength, assuming the formation of bidentate complexes between chromates and the goethite surface. The selection of only bidentate complexes was due to fact that the best simulation results were observed as mentioned above. As shown at Figure 6.27, the TLM model does not exhibit high sensitivity to Cr(VI) adsorption during the alteration of inner capacitance in the range 0.8 to 2 F/m^2. Therefore we can conclude that inner capacitance does not play a dominant role on adsorption simulation during the application of TLM model for the description of Cr(VI) adsorption on goethite.

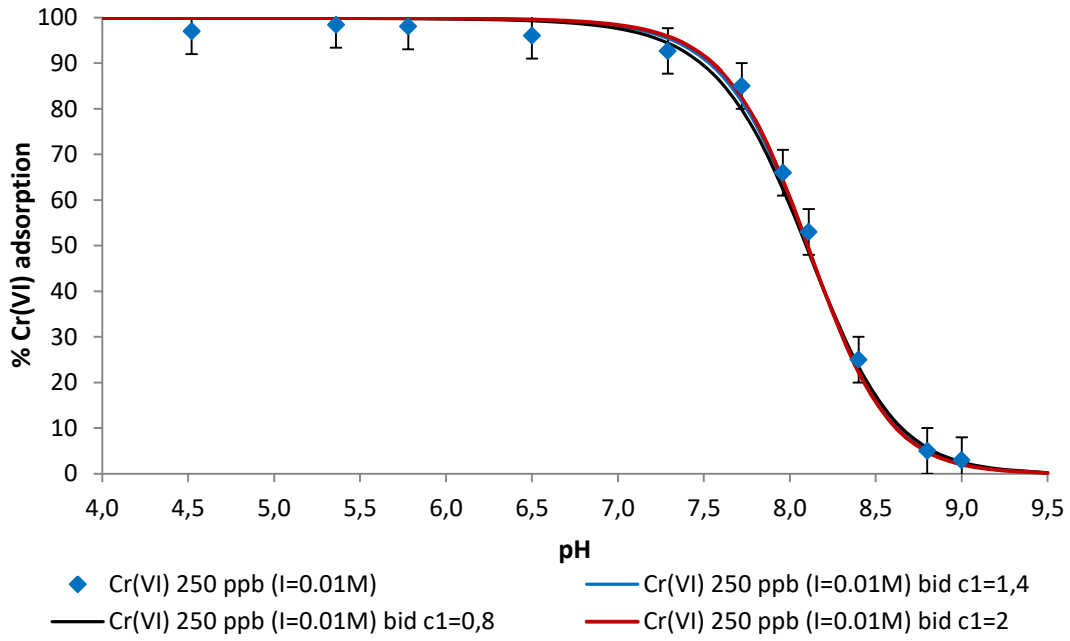

Figure 6.29 Sensitivity analysis of the inner capacitance parameter on Cr(VI) adsorption by goethite using the TLM.

The effect of C_1 capacitance on Cr(VI) adsorption was also tested by Sverjenksy (2001) using goethites with low surface area, below 50 m^2/g. The results showed that goethites with BET surface areas lower than 50 m^2/g, do not present significant variations on adsorption due to alteration of C_1 value since they do not seem to have anomalously high surface charge and capacitance characteristics. Similar results have been reported by Hiemstra and van Riemsdijk (1991).

6.2.2 Application of the Diffuse Layer Model

The DLM surface complexation model was also applied in order to simulate the results of batch experiments. Table 6.11 presents the necessary parameters for applying the DLM model.

Table 6.11 Parameters used for simulating adsorption on goethite applying the DLM.

Adsorption model	2-pk DLM
SSA (m^2/g)	9.09
Site density (nm^{-2})	2.3
Solid concentration (g/L)	10

Table 6.12 presents the reactions used for data simulation. A literature review (Table A3.3, Appendix III) verified that the logK values obtained in this study are similar with those presented by other studies for the case of applying the DLM model in order to simulate the adsorption of the tested contaminants on goethite. The PSI_o parameter represents the Boltzman's factor and refers to the o- surface plane. The PSI_o value was calculated according to the equations provided by Goldberg et al. (2007) regarding the DLM model and the formation of inner sphere monodentate complexes.

Table 6.12 Reactions used at the DLM model for simulating adsorption on goethite.

Reactions							**logK**	**PSI_o**
No.	**Reactants**				**Products**			
	Solid	**Ligand 1**	**Ligand 2**		**Product 1**	**Product 2**		
1	FeOH			↔	FeO^-	H^+	-9	-1
2	FeOH	H^+		↔	$FeOH_2^+$		4.2	1
3	FeOH	Na^+		↔	FeONa	H^+	-9.29	0
4	FeOH	Cl^-	H^+	↔	FeCl	H_2O	8.43	0
5	FeOH	PO_4^{3-}	H^+	↔	$FePO_4^{2-}$	H_2O	18	-2
6	FeOH	PO_4^{3-}	$2H^+$	↔	$Fe_2O_2PO_2^-$	H_2O	26	-1
7	FeOH	PO_4^{3-}	$3H^+$	↔	Fe_2O_2POOH	H_2O	32	0
8	FeOH	NO_3^-	H^+	↔	$FeNO_3$	H_2O	9	0
9	FeOH	CrO_4^{2-}	$2H^+$	↔	$FeHCrO_4$	H_2O	19.5	0
10	FeOH	CrO_4^{2-}	H^+	↔	$FeCrO_4^-$	H_2O	12	-1

Effect of pH and ionic strength of the soil solution on Cr(VI) adsorption

The effect of pH and ionic strength on Cr(VI) adsorption was not well simulated using the DLM, as shown at Figure 6.30. The highest deviations occur in the pH range 7.5 to 8 for both values of ionic strength tested. Better simulation results but not sufficient were observed for the case of using ionic strength equal to 0.01M.

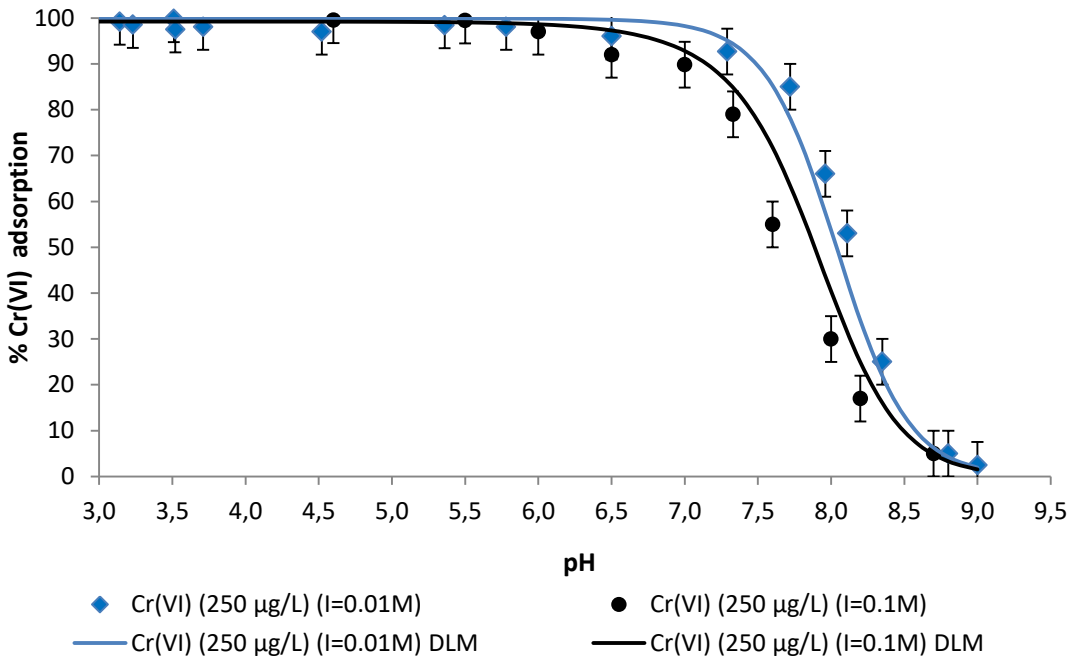

Figure 6.30 Simulation of the effect of pH and ionic strength on Cr(VI) adsorption (250 µg/L) using the DLM.

Contrary to the results of this study, the effective application of DLM for describing Cr(VI) adsorption has been reported by Mesuere and Fish (1992). However, the effective simulation was performed for Cr(VI) concentration in the range of some mg/L. For concentrations lower than 2 mg/L the model prediction was very poor.

Effect of pH and Cr(VI) on phosphates adsorption

The effect of pH and chromates on phosphates adsorption simulated by DLM is presented in Figure 6.31. The application of DLM showed that no competitive effects were created on phosphate adsorption due to the presence of chromates. In the case of using 8 mg/L concentration of phosphate, the deviation was significant for pH values higher than 8.5. In the case of the lower concentration (250 µg/L) the deviation between experimental and modeling results was significantly greater for pH values higher 8.

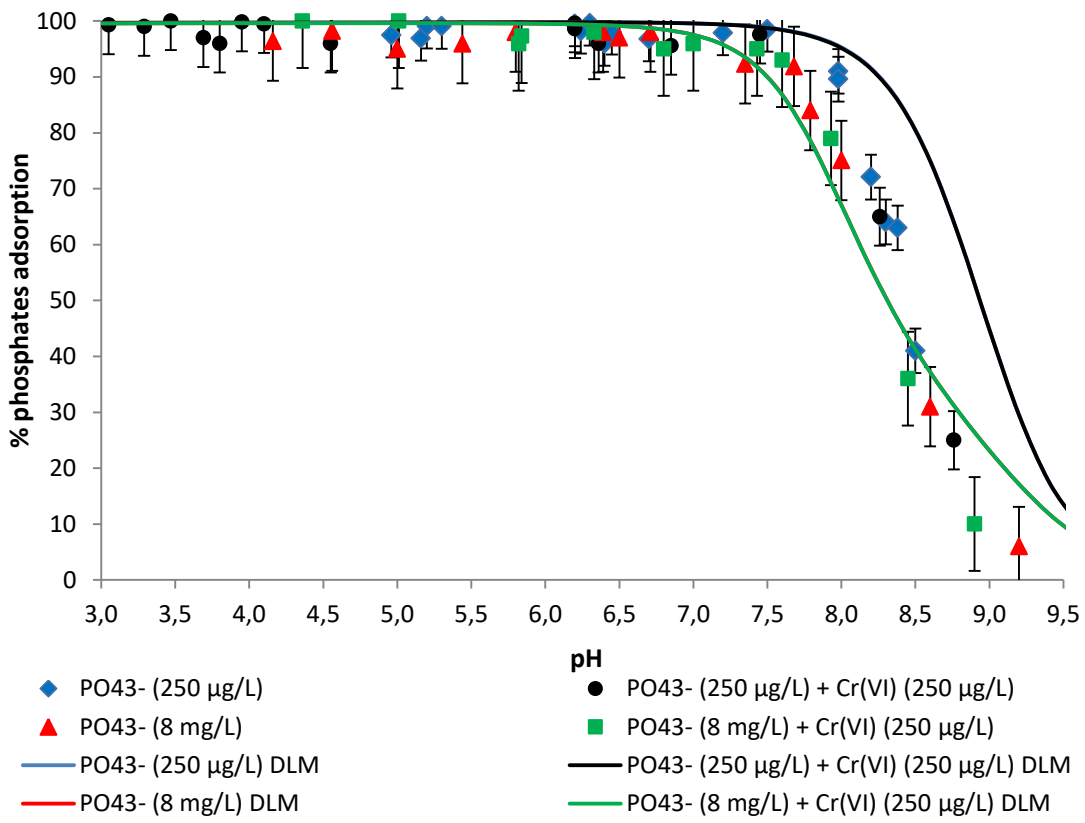

Figure 6.31 Adsorption simulation of PO_4^{3-} in the presence (250 µg/L) and absence of Cr(VI) using the TLM.

The application of DLM for simulating the adsorption of phosphate was also performed by two other studies (Mengistu et al., 2015; Mao et al., 2016). Mengistu et al. (2015) using hydrous ferric oxides as adsorbent used 2pk-DLM model in order to simulate phosphate adsorption. Considering the formation of inner sphere monodentate complexes, poor simulation was observed using a concentration of phosphates about 5 mg/L. On the other hand, better results were reported by Mao et al (2016) using lower concentration of phosphate in the range of 0.3 – 1.2 mg/L phosphate.

Effect of pH and Cr(VI) on nitrates adsorption

The effect of pH and chromates on nitrate adsorption was simulated by DLM and the results are presented in Figure 6.32. As has been discussed in previous sections nitrates adsorption is thought to be based on the formation of outer sphere complexes. Although, the 2pk-DLM did not expect to simulate the adsorption phenomenon since it considers all complexes to be formed in the inner layer, the results showed very good accuracy. This is obviously the reason for why no other studies have used the DLM for simulating the adsorption of nitrates on goethite but is interesting to investigate why the DLM can accusatively predict the adsorption of nitrates. The same observation was made in the case of using the ophiolitic soil as adsorbent (Section 6.1.4).

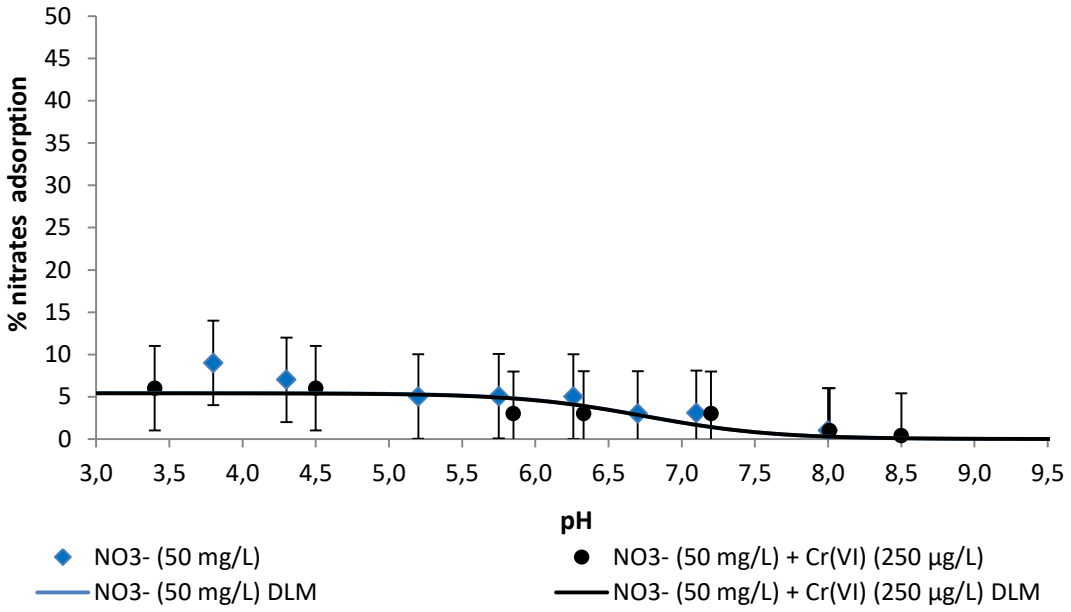

Figure 6.32 Adsorption simulation of nitrates (50 mg/L) in the presence (250 µg/L) and absence of Cr(VI) using the DLM.

Effect of pH and inorganic ions on Cr(VI) adsorption

The effect of the above mentioned inorganic contaminants on Cr(VI) adsorption simulation using the DLM is presented at Figure 6.33. The DLM simulated with poor accuracy the adsorption of chromates in the simultaneous presence of either phosphates or nitrates in the aqueous phase. In this point it must be mentioned that no other studies occur in the literature regarding the application of DLM for simulating any competitive effects for the adsorption of chromates with phosphates or nitrates.

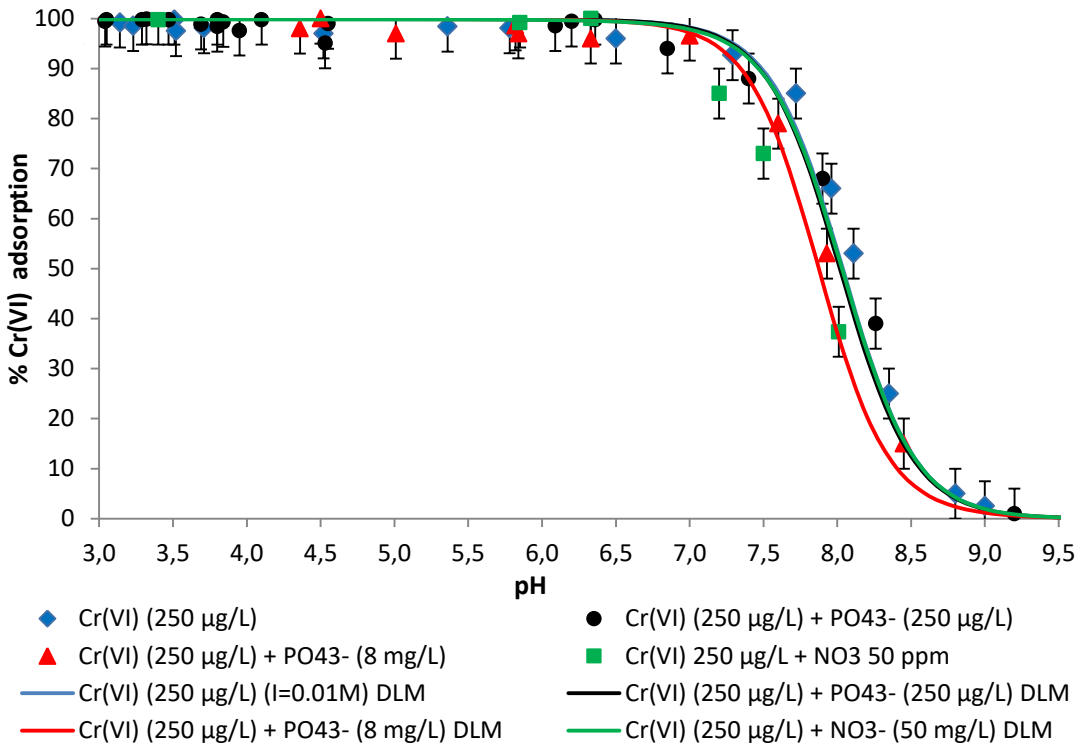

Figure 6.33 Simulation of competitive adsorption of Cr(VI) with inorganic contaminants using the DLM.

Overall the application of DLM did not simulate efficiently the adsorption of chromates or of the other inorganic contaminants or any possible competitive adsorption effects among them.

6.2.3 Application of the Constant Capacitance Model

The CCM surface complexation model was also applied in order to simulate the results of batch experiments. Table 6.13 presents the necessary parameters for applying the CCM model.

Table 6.13 Parameters used for simulating adsorption on goethite applying the CCM.

Adsorption model	2-pk CCM
SSA (m^2/g)	9.09
Inner capacitance (F/m^2)	1.4
Site density (nm^{-2})	2.3
Solid concentration (g/L)	10

Table 6.14 presents the reactions used for data simulation. A literature review (Table A3.4, Appendix III) verified that the logK values obtained in this study are similar with those presented by other studies for the case of applying the TLM model in order to simulate the adsorption of the tested contaminants on goethite. The PSI_o parameter represents the Boltzman's factor and refers to the o- surface plane. The PSI_o value was calculated according to the equations provided by Goldberg et al. (2007) regarding the CCM model and the formation of inner sphere, both monodentate (Reactions 9 & 10) and bidentate (Reaction 11) complexes. As shown at Table 6.14 surface complexation of chromates is based on the formation of both

monodentate and bidentate inner sphere complexes. This scenario was that giving the best results during simulation compared to the three cases of complexation listed below:

1. Formation of exclusively monodentate (mono-protonated) complexes (Reaction 10)
2. Formation of exclusively bidentate complexes (Reaction 11)
3. Formation of both monodentate (mono-protonated) and bidentate complexes (Reactions 10 & 11).

Table 6.14 Reactions used at the CCM model for simulating adsorption on goethite.

Reactions							logK	PSI_o
No.	Reactants				Products			
	Solid	Ligand 1	Ligand 2		Product 1	Product 2		
1	FeOH			↔	FeO^-	H^+	-9	-1
2	FeOH	H^+		↔	$FeOH_2^+$		4.2	1
3	FeOH	Na^+		↔	FeONa	H^+	-9.29	0
4	FeOH	Cl^-	H^+	↔	FeCl	H_2O	8.43	0
5	FeOH	PO_4^{3-}	H^+	↔	$FePO_4^{2-}$	H_2O	15	-2
6	FeOH	PO_4^{3-}	$2H^+$	↔	$Fe_2O_2PO_2^-$	H_2O	25	-1
7	FeOH	PO_4^{3-}	$3H^+$	↔	Fe_2O_2POOH	H_2O	32	0
8	FeOH	NO_3^-	H^+	↔	$FeNO_3$	H_2O	9	0
9	FeOH	CrO_4^{2-}	$2H^+$	↔	$FeHCrO_4$	H_2O	20	0
10	FeOH	CrO_4^{2-}	H^+	↔	$FeCrO_4^-$	H_2O	9	-1
11	2FeOH	CrO_4^{2-}	$2H^+$	↔	Fe_2CrO_4	$2H_2O$	10	0

Effect of pH and ionic strength of the soil solution on Cr(VI) adsorption

Adsorption simulation of chromates on goethite was performed using the CCM model and the results are presented at Figure 6.34. The application of CCM simulated with good accuracy the adsorption of chromate in the case of using 0.01 M ionic strength for the tested pH range. On the contrary less accuracy, observed in the case of using 0.1 M ionic strength. Taking into account that the decrease of adsorption efficiency is attributed to the formation of outer sphere complexes which cannot be simulated by the CCM model it is considered as normal the fact that CCM cannot predict the adsorption in the case of higher ionic strength.

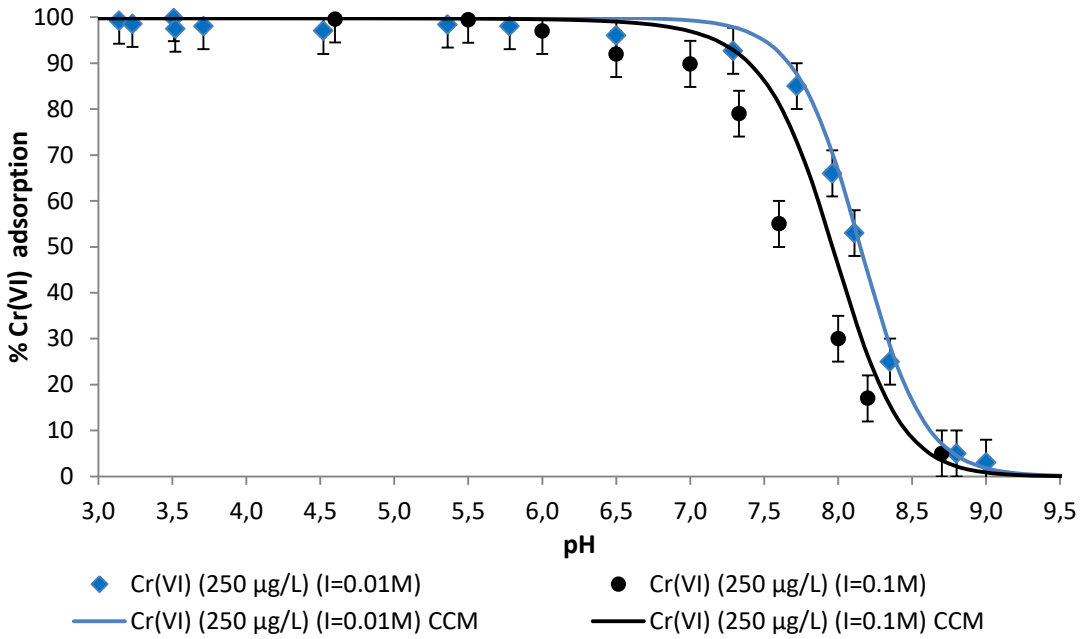

Figure 6.34 Simulation of the effect of pH and ionic strength on Cr(VI) adsorption (250 µg/L) using the CCM.

The application of CCM for simulating the adsorption of chromate as inner sphere bidentate surface complex was performed by Grossl et al. (1997) with the results not exhibiting significant accuracy for neither of the two ionic strengths (0.01 and 0.1 M as $NaNO_3$) used in their study.

Effect of pH and Cr(VI) on phosphates adsorption

Figure 6.35 presents the results of phosphate adsorption simulation using the CCM model. The results showed that CCM can predict the adsorption of phosphate assuming the formation of inner sphere monodentate complexes. The simulation was performed with very good accuracy either with the presence or not of chromates. The absence of any competitive effects was also verified with the CCM model.

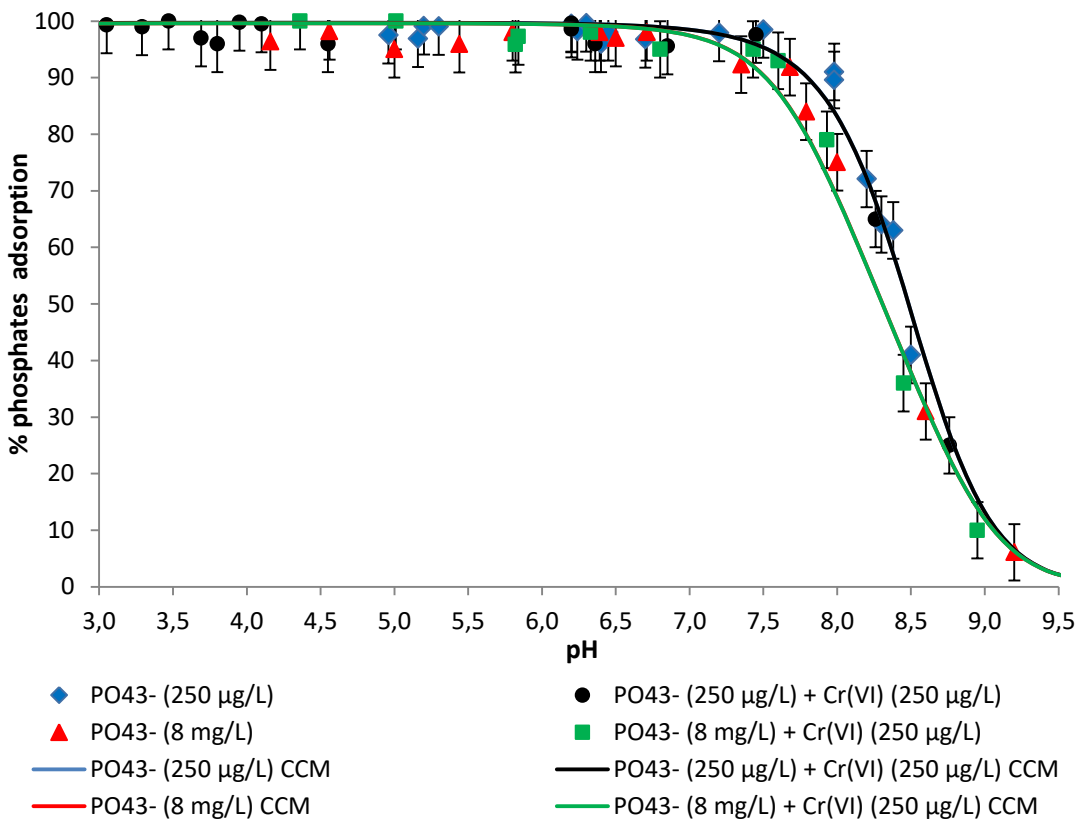

Figure 6.35 Adsorption simulation of PO_4^{3-} in the presence (250 μg/L) and absence of Cr(VI) using the CCM.

Two main studies have reported the application of CCM for simulating the adsorption of phosphate on goethite using different approaches regarding the type of surface complexes formed achieving both of them good accuracy of experimental data simulation. Manning and Goldberg (1996) mentioned the simultaneous formation of bidentate and monodentate surface complexes when simulating the adsorption of phosphates using the CCM. Later, Gao and Mucci (2001) reported the formation of three monodentate surface complexes on the goethite surface. In the present study, the usage of only monodentate complexes simulation was efficient.

Effect of pH and Cr(VI) on nitrates adsorption

Figure 6.36 presents the results of nitrate adsorption simulation using the CCM model. The results showed that CCM can simulate the low adsorption efficiency of nitrates on goethite. No other studies occur in the literature presenting the surface complexation of nitrates on goethite using CCM model. This is probably due to the inability of CCM to simulate the formation of outer sphere complexes which are typically considered to be formed between nitrates and the goethite surface. However, more research is needed in order to determine the exact adsorption mechanism of nitrates and why their adsorption can be simulated by the DLM.

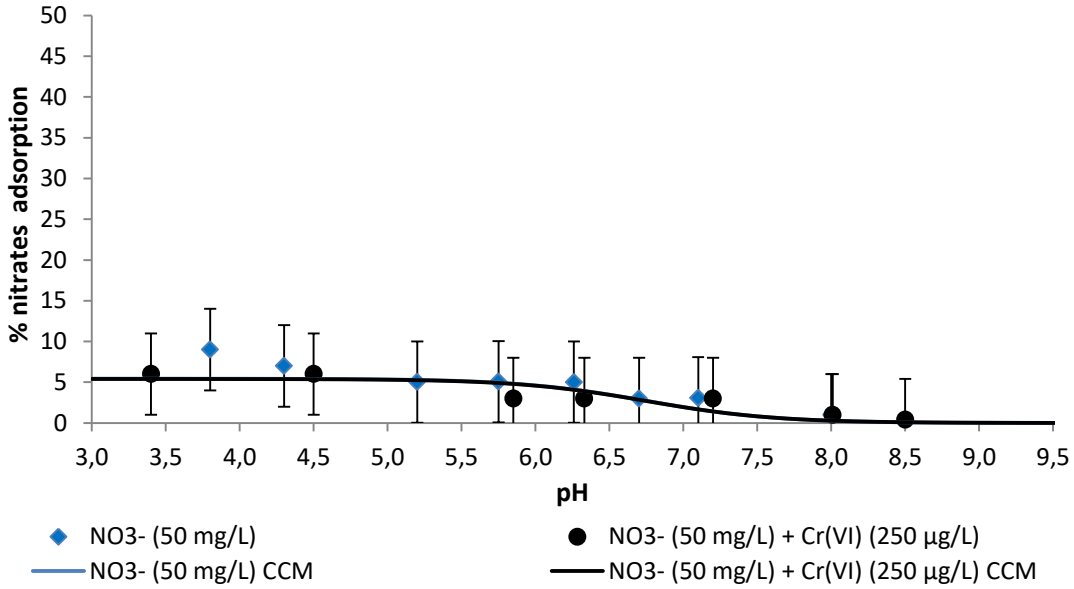

Figure 6.36 Adsorption simulation of nitrates (50 mg/L) in the presence (250 µg/L) and absence of Cr(VI) using the CCM.

Effect of pH and inorganic ions on Cr(VI) adsorption

Despite the fact that CCM simulated the adsorption of chromates during their presence in single solution this was not the case in the presence of the inorganic contaminants. More specifically, the CCM overestimates the adsorption of chromates in the presence of phosphates (8 mg/L) and nitrates (50 mg/L) (Figure 6.37). In both cases it seems that the inorganic contaminants do not cause any competition to chromates for adsorption on the goethite active surface groups.

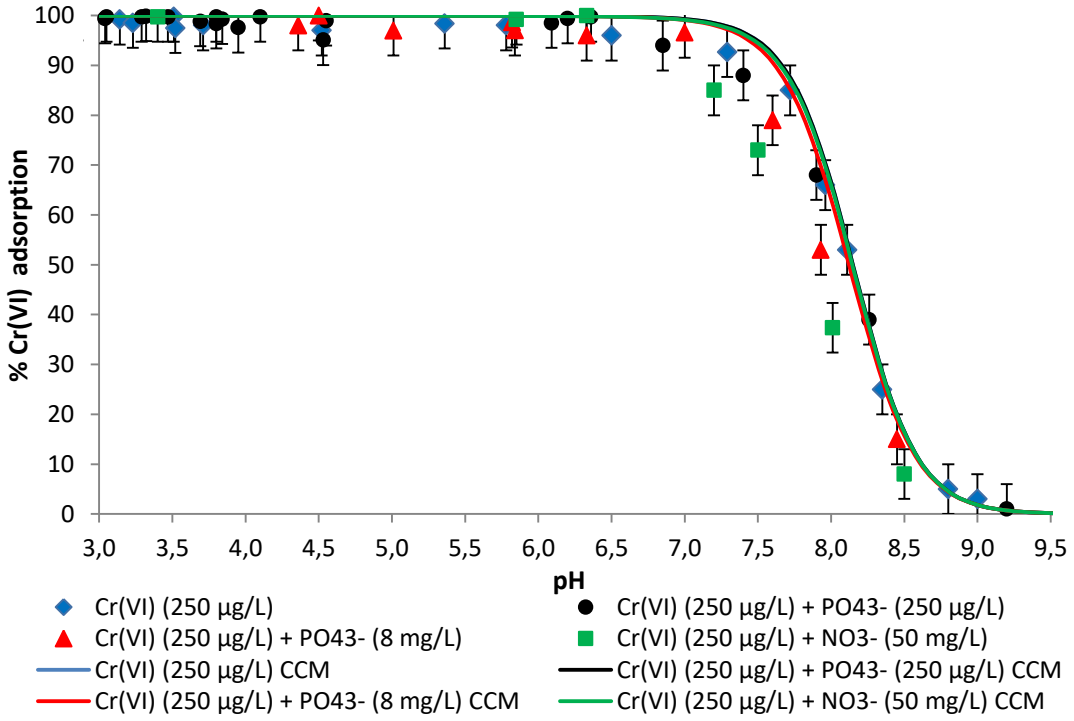

Figure 6.37 Simulation of competitive adsorption of Cr(VI) with inorganic contaminants using the CCM.

Closing this sixth chapter an evaluation of the SCMs applied can lead to the conclusion that the TLM simulates with the highest accuracy the experimental data obtained from both ophiolitic soil and goethite (Table 6.15). This is probably due to the fact that TLM can predict the formation of both inner, monodentate and bidentate, and outer sphere complexes.

Table 6.15 Evaluation of the SCMs applied in this thesis.

Adsorbent	Model	Cr(VI)	Cr(VI)/ PO_4^{3-}	Cr(VI)/NO_3^-	PO_4^{3-}	PO_4^{3-}/Cr(VI)	NO_3^-	NO_3^-/Cr(VI)
Soil	TLM	Yes	Yes	Yes	Yes	Yes	Yes	Yes
	DLM	Yes	No	Yes	No	No	Yes	Yes
	CCM	Yes	No	No	No	No	Yes	Yes
Goethite	TLM	Yes	Yes	Yes	Yes	Yes	Yes	Yes
	DLM	No	No	No	No	No	Yes	Yes
	CCM	No	No	No	Yes	Yes	Yes	Yes

6.2.4 Comparison of adsorption capacity of goethite and ophiolitic soil

The comparison of the adsorption capacity between goethite and ophiolitic soil is shown at Figure 6.38. At this figure the adsorption capacity of soil is calculated assuming that adsorption is attributed exclusively to the mass of iron and aluminum oxides. As it is observed goethite presents higher adsorption capacity than soil, indicating the higher affinity of goethite than soil for Cr(VI). More specifically, the adsorption capacity of goethite is about 2.5 times higher in the pH range 3 – 7 and then gradually decreases and almost zeroes at pH higher than 8.5.

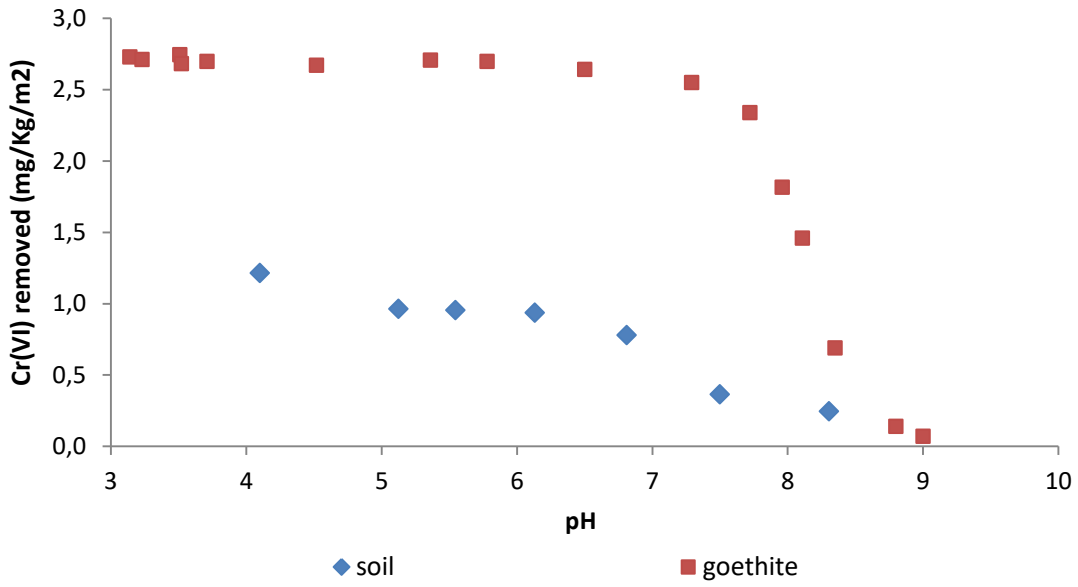

Figure 6.38 Comparison of the adsorption capacity of goethite and ophiolitic soil.

This stronger affinity of goethite for Cr(VI) is also represented by the logK values at every surface complexation model applied. Adsorption simulation in the case of goethite required in general not much higher logK values than those used for soil (Tables A3.5 – A3.7, Appendix III).

7 CONCLUSIONS AND RECOMMENDATIONS

7.1 Conclusions

The present thesis aimed at investigating the geochemical fate of hexavalent chromium in ophiolitic soils and quantifying those processes, and especially adsorption, able to retard its transport in the aquifer. Adsorption quantification was further simulated applying surface complexation modeling. For achieving this goal three general stages were followed, the most important results of which are mentioned below.

The first stage of the thesis investigated the origin and concentration profile of chromium in soil and groundwater in a ~100 m deep soil column of a Greek ophiolitic aquifer. Geotechnical and mineralogical analysis of soil samples and physicochemical analysis of soil and groundwater samples were carried out and led to the following conclusions:

- The grain size distribution curve of the ophiolitic soil indicated that the soil is classified as a coarse grained soil. A more detailed analysis showed that according to ASTM 2487-06 unified soil classification system the ophiolitic soil can be characterized as poorly graded sand with silty clay and gravel.

- The ophiolitic geological background was directly identified by the visual observation of rock fragments with the characteristic green color of serpentinites. X-ray diffraction analysis of rock fragments and soil samples indicated that the soil column was a mixture of ultramafic and mafic rocks and their weathering products. Serpentine minerals such as antigorite, chrysotile and lizardite, as well as talc, olivines, Mg-rich pyroxenes and amphiboles were the predominant phases in the solid fractions. In addition, the presence of chromite/magnetite was observed by the X-ray diffraction analysis. SEM-EDS analysis further verified the occurrence of a spinel mainly covered by bulk serpentinized mass.

- Physicochemical analysis of soil samples showed that pH increased with depth. pH is probably affected by organic matter and nitrification process in the top soil layers and by weathering processes in greater depths.

- Elemental analysis showed that the tested soil was poorer in iron and aluminum, richer in silicon and about average in magnesium, compared with serpentine soils of other areas worldwide. Soil samples collected exclusively from the identified aquifers exhibited high concentrations of aluminum and calcium and low magnesium content, indicating that non-ophiolitic materials occur predominantly at the aquifers.

- The relative abundance of magnesium versus aluminum strongly indicated the relative contribution of ultramafic versus mafic materials in the soil sample. The mafic fraction was coarser grained and more likely to conduct water.

- Total chromium concentration did not exhibit a uniform trend with depth. Initially, it was decreased down to 5 m depth followed by a slight increase for depths between 5 and 10.5 m. This is consistent with the literature and is a result of weathering processes in the shallow unsaturated zone that favor leaching of magnesium and accumulation of iron, aluminum and chromium. In greater depths in the saturated zone (>43 m) total chromium concentration increased with increasing depth. This is probably attributed to the greater contribution of unweathered serpentinitic phases.

- Contrary to total chromium, hexavalent chromium concentration exhibits an almost continuous decrease with increasing depth, with the maximum concentration (7.5 mg/Kg) being measured in a topsoil sample and the minimum (0.7 mg/Kg) in 92.4 m depth. XANES analyses indicated that Mn(III)-Mn(IV) oxides, which are responsible for oxidation of trivalent chromium, occurred in all layers. The only plausible explanation for the decreased hexavalent chromium levels in deeper soil layers is the decrease of weathering in higher depths that render trivalent chromium less available for oxidation.

- The concentrations of total (up to 91 μg/L) and hexavalent (up to 64 μg/L) chromium detected in groundwater are among the highest reported globally in aquifers with similar geological background.

- Both total and hexavalent chromium concentrations in groundwater decreased almost linearly with depth. The dissolved total chromium is highly correlated with hexavalent chromium with the ratio of hexavalent/total chromium being higher than 83%. Such high ratios have also been observed in groundwater related to the presence of ophiolitic/ultramafic geological background.

- The intense agricultural activities in the area resulted in high nitrate concentrations.

The second stage of the thesis focused on investigating the sorption behavior of hexavalent chromium in serpentine soils and goethite by carrying out batch experiments. The most important conclusions are listed below for each solid material:

<u>Ophiolitic soil</u>

- Two main processes were responsible for hexavalent chromium removal, adsorption and reduction. The efficiency of both processes increased as pH decreased from 8.5 to 3. More specifically for low pH values the adsorption capacity of the tested soil is 9.7 mg/kg (pH 3.0), while for higher pH values the adsorbed hexavalent chromium decreases at about 80% (1.0 mg/kg για pH 8.0). This process is attributed to the presence of amorphous iron oxy-hydroxides in the soil. Reduction process was most pronounced for pH values lower than 5, contributing 50% of the removal in the pH range 3-7. Reduction was attributed to the presence of a magnetic fraction in the soil sample which includes magnetite and magnesio-chromite as primary minerals.

- Both processes are surface-driven with reduction being influenced by adsorption since partitioning of hexavalent chromium onto the solid surface is required before reduction takes place.

- Desorption experiments revealed that hexavalent chromium adsorption is not completely reversible due to (a) reduction of hexavalent chromium from divalent iron; or/and (b) the formation of inner sphere complexes which are sufficiently stable, including exclusively ionic and/or covalent bonds.

- Evaluation of sorption as a function of particle size showed that the finer fraction, with grain size less than 0.075 mm, dominated the adsorption behavior of the soil. Coarser fractions were also found to possess substantial adsorption capacity, related to the high surface area, which is uncharacteristic of most coarse soils. Thus, serpentine soils are found to have substantial surface porosity even in coarser fractions.

- Langmuir and Freundlich isotherms fit very well the experimental data, indicating thus the simultaneous heterogenity of the surface sites on the serpentinitic soils and possibly the formation of a monolayer for hexavalent chromium adsorption. The resulting distribution factors may be used to describe hexavalent chromium retardation in transport models, either for removal (adsorption plus reduction) or adsorption alone, by selecting the respective datasets obtained.

- Increasing the ionic strength of the solution an order of magnitude, results in decreasing adsorption of hexavalent chromium on soil. Specifically, for pH values in the range 7 - 8.5, which usually occurs in groundwater, the decrease is 77%. This decrease suggests that hexavalent chromium adsorption on soil is dominated by outer sphere complexes, which involve weak electrostatic interactions, rather than by strong inner sphere complexes, without excluding the simultaneous formation of both types of complexes.

- The increase of pH decreases the adsorption of phosphates. More specifically, phosphate adsorption is maximized (420 mg/kg or 90% adsorption) at acidic pH values and minimized at pH 8.5 (60 mg/kg or 10% adsorption)

- The effect of the presence of hexavalent chromium on the adsorption of phosphates is almost negligible. This can be either due to the high concentration of phosphate ions compared to the concentration of chromates, or/and due to the formation of inner sphere complexes of phosphate. The formation of inner sphere causes the formation of strong ionic and/or covalent bonds, while chromates adsorption is based on the formation of both inner and outer sphere complexes.

- The presence of phosphates reduces significantly the adsorption of hexavalent chromium on soil. Adsorption efficiency decreases to 60% at pH 5, and at 93% at pH 7.5. This is probably attributed to the competition between chromates and phosphates for the available surface functional groups of the soil and to the fact that adsorption of

phosphate reduces the positive potential of the surface and thus the electrostatic attraction between the surface and the negatively charged chromate anions.

- Nitrates adsorption on the ophiolitic soil is very low up to 7%, while for pH values greater than 8 adsorption is zeroed. The increase of pH causes a small decrease at nitrate adsorption to the soil. The effect of hexavalent chromium on nitrate adsorption is almost negligible. This is possibly due to the high concentration of nitrates relatively to chromate.

- The presence of nitrates did not affect the adsorption of hexavalent chromium, despite their competition for the available surface functional groups of the soil. This is probably due to the soil preference for adsorption of higher valence than monovalent ions, and to the fact that hexavalent chromium is retained more strongly than nitrate, forming inner sphere complexes, contrary to weak outer sphere complexes of nitrates.

<u>Goethite</u>

- The pH increase causes decrease of the adsorption capacity of goethite for hexavalent chromium, phosphates and nitrate ions. In particular, for pH values greater than 7, the adsorption efficiency decreases sharply, due to the increase of the negatively charged surface of goethite. This is probably due to the repulsions of chromates and other anions with the negatively charged surface as well as due to the competition of hydroxyls and other anions for the goethite surface.

- Goethite is an efficient adsorbent for chromate and phosphate ions but not for nitrates. More specifically, the experimental results showed that goethite in acidic pH values adsorbs chromate and phosphate with more than 90% efficiency while in the case of nitrate ions in the same pH range adsorption does not exceed 10%. This is a result of the adsorption mechanisms of these three anions to the goethite surface.

- The increase of ionic strength resulted in noticeable decrease of the adsorption of hexavalent chromium. This phenomenon suggests that hexavalent chromium adsorption to goethite consists in the formation of outer sphere complexes, which are based on weak electrostatic forces.

- The investigation of any competitive effects between chromate and phosphate for adsorption to goethite showed that phosphates adsorption is not affected by the presence of chromates. On the contrary, an important effect on the adsorption of chromates, was observed in the simultaneous presence of phosphates. This is probably attributed to the fact that chromates, during the presence of phosphates, are mainly adsorbed via outer sphere complexes since phosphate are adsorbed only via inner sphere complexation.

- The investigation of any competitive effects between chromate and nitrate during their adsorption on goethite showed that adsorption of chromates decreased under

the presence of nitrates. This is probably due to the significant difference on their concentrations. The significant higher concentration of nitrate probably creates electrostatic repulsions which may affect the complexation of chromates, especially the formation of outer sphere complexes. Regarding nitrates the already low adsorption efficiency was not affected by the presence of chromate in the solution.

The third and last stage of the present thesis aimed at simulating the adsorption capacity of the tested soil and goethite for the aforementioned anions. Simulation was performed using three different surface complexation models the Triple Layer Model, the Diffuse Layer Model and the Constant Capacitance Model. The main conclusions obtained by simulation of the experimental data are the following:

Ophiolitic soil - Triple Layer Model

The application of Triple Layer Model leads to satisfactory description of the adsorption process for all the anions tested. For adsorption simulation three different approaches of solid concentration were used taking into account the contribution of either a) iron and aluminum oxides, b) only iron oxides and c) only the amorphous iron oxides. The adsorption simulation was effective for any parameters tested like effect of pH, ionic strength and competitive effects in the case of using the first two solid concentrations. The concentration of only amorphous iron oxides in the soil sample does not correspond to the concentration of the solid phase that contributes to adsorption. Simulating the effect of ionic strength it was revealed that at low ionic strength values adsorption of chromates can be described by the formation of either monodentate or bidentate complexes. However, the increase of ionic strength showed that adsorption chromate can be efficiently described only by the formation of bidentate complexes. The formation of bidentate complexes of chromates with the soil surface can also describe the competitive effects under the presence of phosphates and nitrates. In addition, satisfactory simulation was achieved for phosphate and nitrate adsorption and their competition with chromates in the soil solution. Finally, regarding the sensitivity of the model to the alterations of the inner capacitance no significant changes were observed. Thus, Triple Layer Model can in general describe efficiently the adsorption of chromates and the inorganic contaminants on the ophiolitic soil.

Ophiolitic soil - Diffuse Layer Model

Simulation of adsorption experimental data using the DLM showed that the application of this model is not suitable for describing the adsorption process of the tested contaminants on the ophiolitic soil. Despite, the DLM was capable to simulate the adsorption of chromates and nitrates adsorption poor accuracy was observed in the case of simulating adsorption of phosphates. In addition, the DLM could not predict the competitive effects occurred on Cr(VI) adsorption during the presence of the inorganic contaminants in the solution. A possible explanation is the assumption of monodentate complexes of chromates and phosphates by applying the DLM and the absence of any outer sphere complexes in the case of chromates and nitrates. This further verifies the results obtained by applying the TLM which involves the formation of outer sphere complexes demonstrating their importance on Cr(VI) adsorption.

Ophiolitic soil - Constant Capacitance Model

The CCM is capable of simulating the adsorption of Cr(VI) phosphates and nitrates but exhibited very poor accuracy in the case of competitive adsorption between Cr(VI) and phosphates. The better simulation of Cr(VI) adsorption compared to the DLM is probably the formation of bidentate inner sphere complexes indicating their importance on Cr(VI) adsorption.

Goethite - Triple Layer Model

The Triple Layer Model described satisfactorily the adsorption of hexavalent chromium and inorganic contaminants, as well as their competition on the goethite surface. Simulation showed that chromates are adsorbed via inner and outer sphere complexation. This fact was verified by the decrease of the adsorption efficiency due to ionic strength increase. Chromates complexation is considered to be governed by the formation of bidentate complexes with the solid surface. The adsorption of phosphate and nitrate was also satisfactorily simulated. The competitive effects occurred between chromates and each inorganic contaminant, were also simulated with high accuracy. The sensitivity of the model to the alterations of the inner capacitance was not significant indicating that the Triple Layer Model can overall describe efficiently the adsorption of chromates and the inorganic contaminants on goethite.

Goethite - Diffuse Layer Model

Simulation of the adsorption of chromates and inorganic contaminants using the DLM exhibited poor accuracy. As mentioned above, a possible explanation is the formation of exclusively inner sphere monodentate complexes and the absence of any outer sphere complexes or bidentate inner sphere. As in the case of using ophiolitic soil as adsorbent this model is thought to be less effective than TLM for adsorption simulation of Cr(VI).

Goethite - Constant Capacitance Model

The application of CCM for simulating adsorption of Cr(VI) and inorganic contaminants at single anion solutions could efficiently describe their adsorption. However, CCM could not describe the competitive effects created between chromate and inorganic contaminants. As in the case of DLM this is probably a strong evidence about the formation of outer sphere complexes between Cr(VI) and goethite surface.

Overall, the adsorption of the tested contaminants can be described effectively and with very good accuracy applying the TLM for both cases of adsorbents. This is probably attributed to the ability of TLM to involve both mono- and bi- dentate inner sphere complexes, as well as outer sphere. Regarding the adsorption capacity of goethite and ophiolitic soil, goethite presents higher adsorption capacity than soil, indicating its higher affinity for Cr(VI). This stronger affinity of goethite for Cr(VI) is represented by the logK values at every surface

complexation model applied the required logK values were in general not much higher than those used for the ophiolitic soil.

7.2 Recommendations for future work

The results of the present thesis showed that ophiolitic soil can remove from groundwater contaminants like Cr(VI) and phosphate, via adsorption and reduction processes. Further experimental data can be obtained by performing column experiments in order to further verify the removal capacity of the ophiolitic soil. In addition, the effectiveness of the tested soil can be further verified using ophiolitic soil from other areas.

Regarding the application of the surface complexation models, and especially the TLM model, for describing the adsorption behavior of the ophiolitic soil, the obtained logK values can be verified using ophiolitic soil from other areas. Keeping constant the experimental conditions and the way of calculating the solid concentration used in this thesis the accuracy of the obtained logK values can be determined. This could create a general framework for logK values that can be used in the case of ophiolitic type of soils. Finally, the application of the data obtained in this thesis can be used during transport modeling of Cr(VI) and the tested contaminants in order to take into account the geochemical contribution at their transport in aquifers.

REFERENCES

Abraham P. and Hanson C. (2008). Annual groundwater quality survey, Spring 2008, Environment Canterbury technical report R09/46.

Agency for Toxic Substances and Disease Registry. (2012). Toxicological profile for chromium, Department of health and human services, September 2012.

Ainsworth C.C., Girvin D.C., Zachara J.M., Smith S.C. (1989). Chromate adsorption on goethite: Effects of aluminum substitutions, *Soil Sci. Soc. Am. J.*, 53, pp. 411-418.

Ajouyed O., Hurel C., Ammari M., Ben Allal L., Marmier N. (2010). Sorption of Cr(VI) onto natural iron and aluminum (oxy)hydroxides: Effects of pH, ionic strength and initial concentration, *J Hazard Mater,* 174, pp. 616-622.

Ajouyed O., Hurel C., Marmier N. (2011). Evaluation of the Adsorption of Hexavalent Chromium on Kaolinite and Illite. *J. Environ. Protect.,* 2, pp. 1347-1352.

Al-Anber M.A. (2011). Thermodynamics Approach in the Adsorption of Heavy Metals, Thermodynamics - Interaction Studies - Solids, Liquids and Gases, Dr. Juan Carlos Moreno PirajÃ¡n (Ed.)

Al-Boghdady A. and Economou M. (2005). Fluid inclusions in chromite from a pyroxenite dike of the Pindos ophiolite complex. *Chemie der Erde*, 65, pp. 191–202.

Alessi D.S. and Fein J.B. (2010). Cadmium adsorption to mixtures of soil components: Testing the component additivity approach. *Chem Geol.,* 270, pp. 186–195.

Alloway B.J. (2013). Heavy metals in soils, 3rd ed., trace metals and metalloids in soils and their bioavailability. *Environ Pollut*, 22.

Amacher M.C. and Baker D.E. (1982). Redox reactions involving chromium, plutonium, and manganese in soils, Institute for Research on Land and Water Research, Pennsylvania State University, University Park, PA

Amir H. and Pineau R. (2003). Relationships between extractable Ni, Co, and other metals and some microbiological characteristics of different ultramafic soils from New Caledonia. *Aust J Soil Res*, 41, pp. 215–228.

Anderson R.A. (1989). Essentiality of chromium in humans. *Sci Total Environ.,* 86, pp. 75-81.

Antelo J., Arce F., Avena M., Fiol S., López R., Macías F., (2007). Adsorption of a soil humic acid at the surface of goethite and its competitive interaction with phosphate. *Geoderma*, 138; pp. 12–19.

Antelo J., Avena M., Fiol S., López R. and Arce F. (2005). Effects of pH and ionic strength on the adsorption of phosphate and arsenate at the goethite–water interface. *J. Colloid Interface Sci,* 285, pp. 476-486.

Antibachi D., Kelepertzis E., Kelepertzis A., (2012). Heavy Metals in Agricultural Soils of the Mouriki-Thiva Area (Central Greece) and Environmental Impact Implications. *Soil Sediment Contam*, 21, pp. 434–450.

Apollaro C., Marini L., Critelli T., Barca D., Bloise A., De Rosa R., Liberi F., Miriello D. (2011). Investigation of rock-to-water release and fate of major, minor, and trace elements in the metabasalt–serpentinite shallow aquifer of Mt. Reventino (CZ, Italy) by reaction path modeling. *Appl Geochem.,* 26, pp. 1722–1740.

Apollaro C., Fuoco I., Brozzo G., De Rosa R. (2019). Release and fate of Cr(VI) in the ophiolitic aquifers of Italy: the role of Fe(III) as a potential oxidant of Cr(III) supported by reaction path modelling. *Sci. Total Environ.*, 660, pp. 1459–1471.

Apte A., Tare V., Bose P. (2006). Extent of oxidation of Cr(III) to Cr(VI) under various conditions

pertaining to natural environment. *J Hazard Mater*, 128, pp. 164-174.

Aravanakumar K.S. and Umar A.K. (2011). Removal of Hexavalent Chromium from Aqueous Solution using Vigna Radiata Husk (Green Gram). *Asian J. Chem.,* 23, pp. 2635-2638.

ASTM Committee, 2006, ASTM D2487-06 Standard Practice for Classification of Soils for Engineering Purposes (Unified Soil Classification System), ASTM International, 100 Barr Harbor Drive, PO Box C700, West Conshohocken, PA 19428-2959, United States.

Azizian M.A. (1993). Experimental evaluation and chemical modeling of hexavalent chromium adsorption, desorption, and reduction in a natural soil, Oregon state university.

Bache B.W. (1964). Aluminum and iron phosphate studies relating to soils reactions between phosphate and hydrous oxides. *J. Soil Sci.,* 15; pp. 110.

Balistrieri L. and Murray J.W. (1979). Surface of goethite (α-FeOOH) in seawater. In Chemical Modeling in Aqueous Systems, 93, pp. 275.

Balistrieri L.S. and Murray J.W., (1981). The surface chemistry of goethite (alpha FeOOH) in major ion seawater. *Am. J. Sci.*, 281, pp. 788-806.

Ball J.W. and Izbicki J.A. (2004). Occurrence of hexavalent chromium in ground water in the western Mojave Desert, California. *Appl. Geochem*., 19, pp. 1123–1135.

Ball J.W. and Nordstrom D.K. (1998). Critical evaluation and selection of standard state thermodynamic properties for chromium metal and its aqueous ions, hydrolysis species, oxides and hydroxides. *J. Chem. Eng. Data*, 43, pp. 895-918.

Barberis E., Marsan F.A., Scalenghe R., Lammers A., Schwertmann U., Edwards A.C., Maguire R., Wilson M.J., Delgado A., Torrent J. (1996). European soils over fertilized with phosphorus: 1. Basic properties. *Fert. Res.,* 45, pp. 199–207.

Barnes S.J. and Roeder P.L. (2001). The range of spinel compositions in terrestrial mafic and ultramafic rocks. *J. Petrol.,* 42, pp. 2279–2302.

Baron D. and Palmer C.D. (1996). Solubility of KFe3(CrO4)2(OH)6 at 4-35 °C. *Geochim. Cosmochim. Acta*, 60, pp. 3815-3824.

Baron D. and Palmer C.D. (1998). Solubility of KFe(CrO4)2•2H2O at 4-75 °C. *Appl. Geochem.*, 13, pp. 961-973.

Baron D., Palmer C.D., Stanley J.T. (1996). Identification of two iron chromate precipitates in a Cr(VI)-contaminated soil. *Environ. Sci. Technol.*, 30, pp. 964-968.

Barrow N.J. (1985). Reactions of anions and cations with variable charge soils. *Adv Agron*, 38, pp. 183-230.

Bartlett R.J. (1991). Chromium cycling in soils and water: links, gaps and methods. *Environ. Health Perspect.*, 92, pp. 31-34.

Bartlett R.J. and James B. (1979). Behavior of chromium in soils: III. Oxidation. J*. Environ. Qual.,* 8, pp. 31–35.

Bartlett R.J. and James B.R. (1983). Behavior of chromium in soils, Part VI: interactions between oxidation-reduction and organic complexation. *J. Environ. Qual.*, 12, pp. 173–176.

Bartlett, R.J. and Kimble, J.M.. (1976). Behavior of Chromium in Soils: II. Hexavalent Forms. *J. Environ. Qual.*, 4, pp. 383-386.

Becquer T., Quantin C., Rotte-Capet S., Ghanbaja J., Mustin C., Herbillon A.J. (2006). Sources of trace metals in Ferralsols in New Caledonia. *Eur J Soil Sci.*, 57, pp. 200-213.

Becquer T., Quantin C., Sicot M., Boudot J.P. (2003). Chromium availability in ultramafic soils from New Caledonia. *Sci. Total Environ.*, 301, pp. 251–261.

Behm D. (1989). Ill Waters: The Fouling of Wisconsin's Lakes and Streams (Special Report). *The*

Milwaukee Journal, pp. 2.

Bethke C.M. and Brady P.V., (2000). How the K-d approach undermines ground water cleanup. *Ground Water*, 38, 435–443.

Bhatnagar A. and Sillanpaa M. (2011). A review of emerging adsorbents for nitrate removal from water. *Chem. Eng. J*, 168, 493-504.

Bonifacio E., Falsone G., Piazza S. (2010). Linking Ni and Cr concentrations to soil mineralogy: does it help to assess metal contamination when the natural background is high?. *J Soils Sediments*, 10, pp. 1475–1486.

Bonifacio E., Zanini E., Boero V., Franchini-Angela M. (1997). Pedogenesis in a soil catena on serpentinite in North-Western Italy. *Geoderma*, 75, 33-51.

Borggaard O.K. (1983). Effect of surface area and mineralogy of iron oxides on their surface charge and anion-adsorption properties. *Clays Clay Miner.,* 31, pp. 230-232.

Bortoluzzi E.C., Pérez C.A.S., Ardisson J.D., Tiecher T., Caner L. (2015). Occurrence of iron and aluminum sesquioxides and their implications for the P sorption in subtropical soils. *Appl Clay Sci,* 104; pp. 196–204.

Bouyoucos G.J. (1936). Directions for making mechanical analysis of soils by the hydrometer method. *Soil Sci.,* 42, pp. 225-230.

Brennan R.F., Bolland M.D., Jeffery R.C., Allen D.G. (1994). Phosphorus adsorption by a range of western Australian soils related to soil properties. *Commun. Soil Sci. Plant Anal.*, 25, pp. 2785-2795.

Brigatti M.F., Franchini G., Lugli C., Medici L., Poppi L., Turci, E. (2000). Interaction between aqueous chromium solutions and layer silicates. *Appl. Geochem.,* 15, pp. 1307-1316.

Brookins D.G., (1987). Eh-pH Diagrams for Geochemistry, Springer-Verlag, New York, pp. 176.

Brooks R.R., (1987). Serpentine and its Vegetation, Dioscorides, Portland.

Brousseau P.A., (2012). Nitrate Sorption in the Soils of the Coweeta Hydrologic Laboratory, Virginia Polytechnic Institute and State University.

Bulmer C.E. and Lavkulich L.M. (1994). Pedogenic and geochemical processes of ultramafic soils along a climatic gradient in southwestern British-Columbia, Can J Soil Sci., 74, pp. 165-177.

Burden D.S., (1989). Kinetics of Chromate and Phosphate Sorption by Oxide Minerals and Soils, LSU Historical Dissertations and Theses, 4833.

Burkart M.R. and Kolpin D.W. (1993). Hydrologic and Land-Use Factors Associated with Herbicides and Nitrate in Near-Surface Aquifers. *J Environ. Qual.,* 22, pp. 646-656.

Burkart M.R., Simpkins W., Morrow A.J., Gannon J.M. (2004). Occurrence of TDP in unconsolidated aquifers and aquitards in Iowa. *J Am Water Resour Assoc*, 40, pp. 827-834.

Buurman P., Meijer E.L., van Wijck J.H. (1988). Weathering of chlorite and vermiculite in ultramafic rocks of cabo ortegal, northwestern Spain. *Clays Clay Miner.*, 36, pp. 263-269.

Caillaud J., Proust D., Philippe S., Fontaine C., Fialin M. (2009). Trace metals distribution from a serpentinite weathering at the scales of the weathering profile and its related weathering microsystems and clay minerals. *Geoderma*, 149, pp. 199-208.

CalEPA OEHHA, 2011, Public health goal for hexavalent chromium (Cr(VI)) in drinking water, California Environmental Protection Agency, Office of Environmental Health Hazard Assessment, (http://www.oehha.org/water/phg/072911Cr6PHG.html).

Camargo F.A.O., Bento F.M., Okeke B.C., Frankenberger W.T. (2003). Chromate reduction by chromium-resistant bacteria isolated from soils contaminated with dichromate. *J Environ. Qual.*, 32, pp. 1228-1233.

Carlyle G.C. and Hill A.R. (2001). Groundwater phosphate dynamics in a river riparian zone: effects of hydrologic flow paths, lithology and redox chemistry. *J Hydrol*, 247, pp. 151-168.

Carroll S.A., Roberts S.K., Criscenti L.J., O'Day P.A. (2008). Surface complexation model for strontium sorption to amorphous silica and goethite. *Geochem. Trans.,* 9, pp. 2.

Chaney R.L., Ryan J.A., Brown S.L., (1997). Development of the US-EPA Limits for Chromium in Land-Applied Biosolids and Applicability of these Limits to Tannery By-Product Derived Fertilizers and Other Cr-Rich Soil Amendments, In: Chromium Environmental Issues, Eds. Canali S., Tittarelli F. and Sequi P., (Eds.), Franco-Angeli Editore, Bologna.

Chao T.T. and Zhou L. (1983). Extraction Techniques for Selective Dissolution of Amorphous Iron Oxides from Soils and Sediments. *Soil Sci Soc Am J.*, 47, pp. 225-232.

Chardot V., Echevarria G., Gury M., Massoura S., Morel J.L. (2007). Nickel bioavailability in an ultramafic toposequence in the Vosges Mountains (France). *Plant Soil*, 293, pp. 7–21.

Chen Y.X., Chen Y.Y., Lin Q., Hu Z.Q., Hu H., Wu J.Y. (1997). Factors affecting Cr(III) oxidation by manganese oxides. *Pedosphere*, 7, pp. 185-192.

Cheng C.H., Jien S.H., Lizuka Y., Tsai H., Chang Y.H., Hseu Z.Y. (2011). Pedogenic chromium and nickel partitioning in serpentine soils along a toposequence. *Soil Sci. Soc. Am.,* 75, pp. 659-668.

Chiha M., Samar M.H., Hamdaoui O., (2006). Extraction of chromium (VI) from sulphuric acid aqueous solutions by a liquid surfactant membrane (LSM). *Desalination*, 194, pp. 69–80.

Chitrakar R., Tezuka S., Sonoda A., Sakane K., Ooi K., Hirotsu T. (2006). Phosphate adsorption on synthetic goethite and akaganeite. *J. Colloid Interface Sci,* 298, pp. 602-608.

Cho D.W., Song H., Schwartz F.W., Kim B., Jeon B.H. (2015). The role of magnetite nanoparticles in the reduction of nitrate in groundwater by zero-valent iron. *Chemosphere*, 125, pp. 41-49.

Choi J., Jung Y., Lee W. (2008). Fe(II)-initiated reduction of hexavalent chromium in heterogeneous iron oxide suspension. *Korean J. Chem. Eng.*, 25, pp. 764-769.

Choudhury T.R., Amin M.N., Quraishi S.B, Mustafa A.I. (2014). Adsorption, desorption and kinetic study on hexavalent chromium removal from aqueous solution using groundnut shell. *Res. J. Eng. Appl. Sci.*, 3, pp. 1-6.

Chrysochoou M., Theologou E., Dermatas D. and Panagiotakis I. (2016). Occurrence, origin and transformation processes of geogenic chromium: a review. *Curr Pollution Rep*, 2, pp. 224–235.

Ciavatta C. and Sequi P. (1989). Evaluation of chromium release during the decomposition of leather meal fertilizers applied to the soil. *Fertil Res*, 19, pp. 7-11.

Ciavatta C., Manoli C., Cavani L., Franceschi C., Sequi P. (2012). Chromium-Containing Organic Fertilizers from Tanned Hides and Skins: A Review on Chemical, Environmental, Agronomical and Legislative Aspects. *J Environ Prot*, 3, pp. 1532-1541.

Coleman R.G. and Jove C. (1992). Geological origin of serpentinites, in: The Vegetation of Ultramafic (Serpentine) Soils, A.J.M. Baker, J. Proctor, R.D. Reeves, (Eds.), Intercept, Andover, 1–17.

Cooper G.R.C. (2002). Oxidation and toxicity of chromium in ultramafic soils in Zimbabwe. *Appl Geochem.*, 17, pp. 981–986.

Cornell R.M. and Schwertmann U. (2006). The Iron Oxides: Structure, Properties, Reactions, Occurrences and Uses, 2nd, Completely Revised and Extended Edition, Wiley VCH.

Correll D.L. (1998). The role of phosphorus in the eutrophication of receiving waters: a review. *J Environ. Qual.*, 27, pp. 261-266.

Covelo E.F., Vega F.A., Andrade M.L. (2007). Heavy metal sorption and desorption capacity of soils containing endogenous contaminants, *J Hazard Mater*, 143, pp. 419-430.

Criscenti L.J. and Sverjensky D.A. (2002). A single-site model for divalent transition and heavy metal

adsorption over a range of metal concentrations. *J. Colloid Interface Sci.,* 253, pp. 329-352.

D' Amico M., Julitta F., Previtali F., Cantelli D. (2008). Podzolization over ophiolitic materials in the western alps (Natural Park of Mont Avic, Aosta Valley, Italy). *Geoderma*, 146, pp. 129-137.

Dai R., Liu J., Yu C., Sun R., Lan Y., Mao D. (2009). A comparative study of oxidation of Cr(III) in aqueous ions, complex ions and insoluble compounds by manganese-bearing mineral (birnessite). *Chemosphere*, 76, pp. 536-541.

Daval D., Hellmann R., Schrothez I., Gangloff S., Guyot F. (2013). Lizardite serpentine dissolution kinetics as a function of pH and temperature including effects of elevated pCO_2. *Chem Geol*, 351, pp. 245-256.

Davis J. (1978). Adsorption of trace metals and complexing ligands at the oxide/water interface. Stanford University

Davis J.A. and Kent D.B. (1990). Surface Complexation Modeling, in Aqueous Geochemistry, Eds. Hochella M.F. and White A.F., Mineral-Water Interface Geochemistry. *Min. Soc. Am. Reviews in Mineralogy*, 23, pp. 177-260.

Davis J.A., Coston J.A., Kent D.B., Fuller C.C. (1998). Application of the Surface Complexation Concept to Complex Mineral Assemblages. *Environ. Sci. Technol.*, 32, pp. 2820-2828.

Davis J.A., Fuller C.C., Cook A.D. (1987). Mechanisms of trace metal sorption by calcite: adsorption of Cd2+ and subsequent solid solution formation. *Geochim. Cosmochim. Acta*, 51, pp. 1477-1490.

de Jonge L.W., Moldrup P., Rubæk G.H., Schelde K., Djurhuus J. (2004). Particle leaching and particle-facilitated transport of phosphorus at field scale. *Vadose Zone J.*, 3, pp. 462-470.

De la Torre A.G., Bruque S., Aranda M.A.G., (2001). Rietveld Quantitative Amorphous Content Analysis. *J. Appl. Crystallogr.*, 34, pp. 196-202.

Deng B. and Stone A.T. (1996). Surface-Catalyzed Chromium(VI) Reduction: Reactivity Comparisons of Different Organic Reductants and Different Oxide Surfaces. *Environ. Sci. Tech.*, 30, pp. 2484-2494.

Dermatas D., Vatseris C., Panagiotakis I., Chrysochoou M. (2012). Potential contribution of geogenic chromium in groundwater contamination of a Greek heavily industrialized area. *Chem Eng Trans*, 28, pp. 217-222.

Deschamps F., Godard M., Guillot S., Hattori K. (2013). Geochemistry of subduction zone serpentinites: a review. *Lithos*, 178, pp. 96-127.

Desjardin V., Bayard R., Huck N., Manceau A., Gourdon A. (2002). Effect of microbial activity on the mobility of chromium in soils. *Waste Manag.*, 22, pp. 195-200.

Dhakal P. (2013). Abiotic Nitrate and Nitrite Reactivity with Iron Oxide Minerals, pp. 1-117, College of Agriculture at the University of Kentucky.

Dionex (1996). Determination of Cr(VI) in water, wastewater and solid waste extracts, Technical Note 26 LPN 34398-01 1M 7/96, Dionex Corporation.

Donn M.J. and Menzies N.W. (2005). Simulated rainwater effects on anion exchange capacity and nitrate retention in Ferrosols. *Aust J Soil Res*, 43, pp. 33-42.

Dynia J.F. (2000). Nitrate retention and leaching in variable charge soils of a watershed in Sao Paulo state, Brazil. *Commun Soil Sci Plant Anal.*, 31, pp. 777–791.

Dzemua G.L., Mees F., Stoops G., Van Ranst E. (2011). Micromorphology, mineralogy and geochemistry of lateritic weathering over serpentinites in south-east Cameroon. *J Afr Earth Sci.*, 60, pp. 38-48.

Dzombak D. and Morel F. (1990). Surface Complexation Modeling: Hydrous Ferric Oxide, Wiley Company, New York. pp. 393.

Eary L.E. and Rai D. (1987). Kinetics of Cr(III) oxidation by manganese dioxide. *Environ. Sci. Technol.*, 21, pp. 1187-1193.

Eary L.E. and Rai D. (1988). Chromate removal from aqueous wastes by reduction with ferrous iron. *Environ. Sci. Technol.*, 22, pp. 972-977.

Eary L.E. and Rai D. (1989). Kinetics of chromate reduction by ferrous ions derived from hematite and biotite at 25°C, Am. J. Sci., 289, pp. 180-213.

EC (Commission Regulation) (2010). Laying Down Detailed Rules for the Implementation of Council Regulation (EC) No. 834/2007 on Organic Production and Labelling of Organic Products with Regard to Organic Production, Labelling and Control, Commission Regulation (EU) No. 271/201.

EC (European Council), (2003). Draft-WG Fertilizers, Regulation (EC) 2003/2003 of the European Parliament and of the Council of 13 October 2003 Referred to Fertilizers.

Economou-Eliopoulos M. (2003). Apatite and Mn, Zn, Co-enriched chromite in Ni-laterites of northern Greece and their genetic significance, *J Geochem Explor.*, 80, pp. 41-54.

Economou-Eliopoulos M., Megremi I., Vasilatos C. (2011). Factors controlling the heterogeneous distribution of Cr(VI) in soil, plants and groundwater: evidence from the Assopos basin, Greece, *Chemie der Erde*, 71, pp. 39-52.

Eick M.J., Brady W.D., Lynch C.K. (1999). Charge properties and nitrate adsorption of some acid Southeastern soils. *J. Environ. Qual*, 28, pp. 138–144.

Eliopoulos D.G., Economou-Eliopoulos M., Apostolikas A., Golightly J.P. (2012). Geochemical features of nickel-laterite deposits from the Balkan Peninsula and Gordes, Turkey: the genetic and environmental significance of arsenic. *Ore Geol. Rev.,* 48, pp. 413-427.

EPA Ohio (2005). Technical guidance for ground water investigations, Use of Direct Push Technologies for Soil and Groundwater Sampling (Chapter15), USA.

Ermakova L., Sidorova M., Bogdanova N., Klebanov A. (2001). Electrokinetic and adsorption characteristics of (hydr)oxides and oxide nanostructures in 1:1 electrolytes. *Colloid Surface A.*, 192, pp. 337-348.

EU (European Union), (2009). Fertiliser, New Approach discussion document, 15-09-2009, European Commission, D.G. Enterprise and Industry.

European Environmental Agency, (1999). Ground water quality and quantity in Europe, June 1999.

Fadiran A.O., Dlamini S.C., Mavuso A. (2008). A comparative study of the phosphate levels in some surface and ground water bodies of Swaziland. *Bull. Chem. Soc. Ethiop.*, 22, pp. 197-206.

Fandeur D., Juillot F., Morin G., Olivi L., Cognigni A., Ambrosi J.P., Guyot F., Fritsch E. (2009). Synchrotron-based speciation of chromium in an Oxisol from New Caledonia: importance of secondary Fe-oxyhydroxides. *Am Mineral.*, 94, pp. 710-719.

Fandeur D., Juillot F., Morin G., Olivi L., Cognigni A., Webb S.M., Ambrosi J.P., Fritsch E., Guyot F., Brown Jr G.E. (2009). XANES evidence for oxidation of Cr(III) to Cr(VI) by Mn-oxides in a lateritic regolith developed on serpentinized ultramafic rocks of New Caledonia. *Environ. Sci. Technol.,* 43, pp. 7384-7390.

Fantoni D., Brozzo G., Canepa M., Cipolli F., Marini L., Ottonello G., Zuccolini M.V. (2002). Natural hexavalent chromium in groundwaters interacting with ophiolitic rocks. *Environ Geo.*, 42, pp. 871-882.

Farahat E.S. (2008). Chrome-spinels in serpentinites and talc carbonates of the El Ideid-El Sodmein District, central Eastern Desert, Egypt: their metamorphism and petrogenetic implications. *Chemie der Erde*, 68, pp. 193-205.

Faybishenko B., Hazen T.C., Long P.E., Brodie E., Conrad M.E., Hubbard S.S., Christensen J.N., Joyner

D., Borglin S.E., Chakraborty R., Williams K.H., Peterson J.E., Chen J., Brown S.T., Tokunaga T.K., Wan J., Firestone M., Newcomer D.R., Resch C.T., Cantrell K.J., Willett A., Koenigsberg S. (2008). In Situ Long-Term Reductive Bioimmobilization of Cr(VI) in Groundwater Using Hydrogen Release Compound. *Environ. Sci. Tech.*, 42, pp. 8478-8485.

Feder F. and Findeling A. (2007). Retention and leaching of nitrate and chloride in andic soil after pig manure amendment. *European J. Soil Sci.*, 58, pp. 393-404.

Fendorf S. (1995). Surface reactions of chromium in soils and waters, Geoderma, 67, pp. 55-71.

Fendorf S. and Zasoski R. (1992). Chromium(III) Oxidation by δ-MnOs. *Environ. Sci. Technol.*, 26, pp. 79-85.

Fendorf S., Eick M.J., Grossl P., Sparks D.L. (1997). Arsenate and Chromate Retention Mechanisms on Goethite. 1. Surface Structure. *Environ. Sci. Technol.*, 31, pp. 315-320.

Fink J.R., Inda A.V., Bayer C., Torrent J. and Barrón V. (2014). Mineralogy and phosphorus adsorption in soils of south and central-west Brazil under conventional and no-tillage systems, Acta Scientiarum. *Agronomy Maringá*, 36, pp. 379-387.

Fink J.R., Inda A.V., Tiecher T., Barrón V. (2016). Iron oxides and organic matter on soil phosphorus availability. *Ciência e Agrotecnologia*, 40, pp. 369-379.

Fontes M.P.F. and Weed S.B. (1996). Phosphate adsorption by clays from Brazilian Oxisols: relationships with specific surface area and mineralogy. *Geoderma*, 72, pp. 37-51.

Fordham A.W. and Norrish K. (1979). Electron microprobe and electron microscope studies of soil clay particles. *Aust J Soil Res*, 17, pp. 283 – 306.

Fourcade S., Trotignon l., Boulvais P., Techer I., Elie M., Vandamme D., Salameh E., Khoury H. (2007). Cementation of kerogen-rich marls by alkaline fluids released during weathering of thermally metamorphosed marly sediments. Part I: Isotopic (C, O) study of the Khushaym Matruk natural analogue (Central Jordan). *Appl Geochem*, 22, pp. 1293-1310.

Freedman D.L., Lehmicke L., Verce M.F. (2005). Reductive dechlorination of tetrachloroethene following abiotic versus biotic reduction of hexavalent chromium. *Bioremediation J.*, 9, pp. 87-97.

Fujita T. and Tsukamoto M. (1996). Influence of carbonate ions on europium sorption onto iron-oxides. MRS Online Proceedings Library Archive, 465.

Fuller C.C. and Davis J.A. (1989). Influence of coupling of sorption and photosynthetic processes on trace element cycles in natural waters. *Nature*, 340, pp. 52-54.

Gao Y. and Mucci A. (2001). Acid base reactions, phosphate and arsenate complexation, and their competitive adsorption at the surface of goethite in 0.7 M NaCl solution. *Geochim. Cosmochim Acta*, 65, pp. 2361–2378.

Garnier J., Quantin C., Schroths E.S., Becquer T. (2006). Solid speciation and availability of chromium in ultramafic soils from Niquelândia, Brazil. *J Geochem Explor.*, 88, pp. 206-209.

Gasser U., Juchlerl S., Hobson W., Sticher H. (1995). The fate of chromium and nickel in subalpine soils derived from serpentinite, *Can. J. Soil Sci.*, 75, pp. 187-195.

Geelhoed J.S., Hiemstra T., Van Riemsdijk W.H. (1997). Phosphate and sulfate adsorption on goethite: Single anion and competitive adsorption. *Geochim. Cosmochim Acta*, 61, pp. 2389-2396.

Geotechnical engineering bureau of New York, (2007). Geotechnical test method: Test method for liquid limit, plastic limit, and plasticity index (GTM-7), Revision #1, New York state department of transportation.

Ghilardi M., Kunesch S., Styllas M., Fouache E., (2008). Reconstruction of Mid-Holocene sedimentary

environments in the central part of the Thessaloniki Plain (Greece), based on microfaunal identification, magnetic susceptibility and grain-size analyses, *Geomorphology*, 97, pp. 617-630.

Goldberg S. (1985). Chemical Modeling of Anion Competition on Goethite Using the Constant Capacitance Model 1. *SSSA*J, 49, pp. 851-856.

Goldberg S. (2004). Surface complexation modeling, USDA–ARS, Riverside, CA, USA, Elsevier Ltd.

Goldberg S. (2013). Surface complexation modeling, Reference module in earth systems and environmental sciences, pp 1-14.

Goldberg S. (2014). Application of surface complexation models to anion adsorption by natural materials. *Environ Toxicol Chem.*, 33, pp. 2172–2180.

Goldberg S. and Johnston C.T. (2001). Mechanisms of Arsenic Adsorption on Amorphous Oxides Evaluated Using Macroscopic Measurements, Vibrational Spectroscopy, and Surface Complexation Modeling. *J. Colloid Interface Sci*, 234, pp. 204–216.

Goldberg S. and Sposito G. (1984). A chemical model of phosphate adsorption by soils: I. Reference oxide minerals. *Soil Sci. Soc. Am. J.*, 48, pp. 772-778.

Goldberg S., Criscenti L.J., Turner D.R., Davis J.A., Cantrell K.J. (2007). Adsorption–desorption processes in subsurface reactive transport modeling. *Vadose Zone J.*, 6, pp. 407-435.

Goldberg S., Su C., Forster H.S. (1998). Sorption of molybdenum on oxides, clay minerals, and soils. Adsorption of Metals by Geomedia, Academic Press, San Diego, 401-426.

Gonzalez A.R., Ndung'u K., Flegal A.R. (2005). Natural occurrence of hexavalent chromium in the aromas Red Sands aquifer, California. *Environ. Sci. Technol.*, 39, pp. 5505-5511.

Gorshkov A.I., Tikov S.V., Bershov L.V., Marfunin A.S. (1996). The first finds of native Cr, Ni, and Fe in carbonato from the diamond deposits of Yakutia. *Geochem. Int.,* 33, pp. 59–63.

Gray C.W., Pang L., Dodd R., McDowell R.W., Close M.E. (2015). Transport of phosphorus in an alluvial gravel aquifer, New Zealand. *J. Agric. Res.,* 58, pp. 490-501.

Grossl P.R., Eick M., Sparks D.L., Goldberg S., Ainsworth C.C. (1997). Arsenate and Chromate Retention Mechanisms on Goethite. 2. Kinetic Evaluation Using a Pressure-Jump Relaxation Technique. *Environ. Sci. Technol.*, 31, pp. 321-326.

Grubinger V.P., Gutenmann W.H., Doss G.J., Rutzke M., Lisk D.J. (1994). Chromium in Swiss chard grown on soil amended with tannery meal fertilizer. *Chemosphere*, 28, pp. 717-720.

Guisewite, A. (2001). Mineral Collection Images, http://www2.cscmu.edu/~adg/adgpeimages html, pp. 5.

Gunia P. (2000). The petrology and geochemistry of mantle-derived basic and ultrabasic rocks from the Szklary massif in the fore-Sudeticblock (SW Poland). *Geol Sudetica*, 33, pp. 71-83.

Gustafsson J.P. (2013). Visual MINTEQ version 3.1. Available at: http://www.lwr.kth.se [verified: January 2018].

Hamdi W., Gamaoun F., Pelster D.E., Seffen M. (2013). Nitrate Sorption in an Agricultural Soil Profile, *Appl Environ Soil Sci.*, pp. 1-7.

Han F.X., Kingery W.L., Selim H.M., Gerald P. (2000). Accumulation of heavy metals in a long-term poultry waste-amended soil. *Soil Sci.*, 165, pp. 260-268.

Harris W. and White G.N. (2008). Chapter 4: X-ray Diffraction Techniques for Soil Mineral Identification, In: Methods of Soil Analysis. Part 5. Mineralogical Methods, Soil Science Society of America, 677 S. Segoe Road, Madison, WI 53711, USA.

Harrison J.B. and Berkheiser V.E. (1982). Anion interactions with freshly prepared hydrous iron oxides. *Clays Clay Miner.*, 30, pp. 97-102.

Hawley L.E., Deeb A.R., Kavanaugh C.M., Jacobs R.GJ. (2004). Handbook of Cr(VI), Treatment Technologies for Chromium(VI), pp 273-308, CRC press.

Hayes K.F. (1987). Equilibrium, spectroscopic, and kinetic studies of ion adsorption at the oxide-aqueous interface, Stanford University.

Hayes K.F. and Leckie J.O. (1986). Mechanism of lead ion adsorption at the goethite—water interface. ACS Symposium Series, 323, pp. 115-141

Hayes K.F., Papelis C., Leckie J.O. (1988). Modeling ionic strength effects on anion adsorption at hydrous oxide/solution interface. *J. Colloid Interface Sci.*, 125, pp. 717-726.

Hayes K.F., Redden G., Ela W., Leckie J.O. (1991). Surface complexation models: an evaluation of model parameter estimation using FITEQL and oxide mineral titration data. *J. Colloid Interface Sci.*, 142, pp. 448-469.

He Y.T. and Traina J.S. (2005). Cr(VI) Reduction and Immobilization by Magnetite under Alkaline pH Conditions: The Role of Passivation. *Environ. Sci. Technol.*, 39, pp. 4499–4504.

Heeren D.M., Fox G.A., Miller R.B., Storm D.E., Fox A.K., Penn C.J., Halihan T., Mittelstet A.R. (2011). Stage-dependent transient storage of phosphorus in alluvial floodplains. *Hydrol. Process.*, 25, pp. 3230-3243.

Henderson T. (1994). Geochemical reduction of hexavalent chromium in the Trinity sand aquifer. *Groundwater*, 32, pp. 477-486.

Hiemstra T. and Van Riemsdijk W.H. (1996). A Surface Structural Approach to Ion Adsorption: The Charge Distribution (CD) Model. *J. Colloid Interface Sci.*, 179, pp. 488 –508.

Hiemstra T. and Van Riemsdijk W.H. (1999). Surface Structural Ion Adsorption Modeling of Competitive Binding of Oxyanions by Metal (Hydr)oxides. *J. Colloid Interface Sci.,* 210, pp. 182–193.

Hiemstra T., Rahnemaie R., van Riemsdijk W.H. (2004). Surface complexation of carbonate on goethite: IR spectroscopy, structure and charge distribution. *J. Colloid Interface Sci.*, 278, pp. 282–290.

Hingston F.J. (1981). A review of anion adsorption. In: Adsorption of inorganics at solid-liquid interfaces. M.A. Anderson and A.J. Rubin (eds), Ann Arbor science, Ann Arbor, Mich, pp. 51-90.

Hinsinger P. (2001). Bioavailability of soil inorganic P in the rhizosphere as affected by root-induced chemical changes: a review. *Plant Soil,* 237, pp. 173-195.

Ho C.P., Hseu Z.Y., Iizuka Y., Jien S.H. (2013). Chromium Speciation Associated with Iron and Manganese Oxides in Serpentine Mine Tailings. *Environ. Eng. sci.,* 30, pp. 241-247.

Hoell W. and Kalinichev A. (2004.) The theory of formation of surface complexes and its application to the description of multi-component dynamic sorption systems. *Russ. Chem. Rev.,* 73, pp. 351–370.

Hoins U., Charlet L., Sticher H. (1993). Ligand effect on the adsorption of heavy metals: The sulfate—Cadmium—Goethite case. *Water Air Soil Pollut*., 68, pp. 241-255.

Holman I.P., Howden N.H.K., Ballamy P., Willby N., Whelan M.J., Rivas-Casado M. (2010). An assessment of the risk to surface water ecosystems of groundwater P in the UK and Ireland. *Sci Total Environ.*, 408, pp. 1847-1857.

Hongshao Z. and Stanforth R. (2001). Competitive Adsorption of Phosphate and Arsenate on Goethite. *Environ. Sci. Technol*., 35, pp. 4753-4757.

Hseu Z.Y. (2006). Concentration and distribution of chromium and nickel fractions along a serpentinitic toposequence. *Soil Sci.,* 171, pp. 341-353.

Hseu Z.Y., Tsai H., Hsi H.C., Chen Y.C. (2007). Weathering sequences of clay minerals in soils along a

serpentinitic toposequence. *Clays Clay Miner.*, 55, pp. 389-401.

Hsi C.K.D. and Langmuir D. (1985). Adsorption of uranyl onto ferric oxyhydroxides: Application of the surface complexation site-binding model. *Geochim. Cosmochim. Acta*, 49, pp. 1931-1941.

Issa M., Abdul Azim A.A. and Issa R.M. (1955). Oxidation with alkaline permanganate using formic acid for the back-titration: Potentiometric determination of chromium. *Analytica Chimica Acta*, 12, pp. 92-100.

Izbicki J.A., Ball J.W., Bullen T.D., Sutley S.J. (2008). Chromium, chromium isotopes and selected trace elements, western Mojave Desert, USA. *Appl. Geochem.*, 23, pp. 1325-1352.

Jacobs J.A. and Testa S.M. (2005). Overview of Chromium(VI) in the Environment: Background and History, Chapter 1 In: "Cr(VI)-Handbook" edited by Guertin J., Jacobs J.A. and Avakian C.P., CRC press.

James B.R. and Bartlett R.J. (1983). Behavior of chromium in soils: V. Fate of organically complexed Cr(III) added to soil; VI. Interaction between oxidation-reduction and organic complexation; VII. Adsorption and reduction of hexavalent forms. *J. Environ. Qual.*, 12, pp. 169-181.

James R.O. and Parks G.A. (1982) Characterization of aqueous colloids by their electrical double-layer and intrinsic surface chemical properties, In: Surface and Colloid Science, Eds: Matijevic E., Good R.J., 12, pp. 119-216, Plenum Press, New York.

Jeyasingh J. and Philip L. (2005). Bioremediation of chromium contaminated soil: optimization of operating parameters under laboratory conditions. *J. Hazard. Materials*, 118, pp. 113-120.

Jiang H., Liao L-B., Wang J-L., Long M., Chen L-P. (2004). Competitive adsorption of phosphate and chromate on hydroxy-Fe-montmorillonite complex. *Mineral. Petr*.

Johnson C. and Xyla A. (1991). The oxidation of chromium(III) to chromium(VI) on the surface of manganite (γ-MnOOH). *Geochim. Cosmochim. Acta*, 55, pp. 2861-2866.

Jones R.C., Babcock C.J., Knowlton W.B., (2000). Estimation of the Total Amorphous Content of Hawai'i Soils by the Rietveld Method. *SSSAJ*, 64, pp. 1100-1108.

Jung J.H., Cho Y.H., Hahn P. (1998). Comparative Study of Cu^{2+} adsorption on Goethite, Hematite and Kaolinite: Mechanistic Modeling Approach. *Bull. Korean Chem. Soc.,* 19, pp. 324-327.

Jung Y., Choi J., Lee W. (2007). Spectroscopic investigation of magnetite surface for the reduction of hexavalent chromium. *Chemosphere*, 68, pp. 1968-1975.

Kabata-Pendias A. and Pendias H., (2011). "Chromium," In: Trace Elements in Soils and Plants, A. Kabata-Pendias and H. Pendias (Eds.), 3rd Edn, CRC Press, Boca Raton.

Kaprara E., Kazakis N., Simeonidis K., Coles S., Zouboulis A.I., Samaras P., Mitrakas M. (2015). Occurrence of Cr(VI) in drinking water of Greece and relation to the geological background. *J Hazard Mater*, 281, pp. 2–11.

Kaupenjohann M. and Wilcke W. (1995). Heavy Metal Release from a Serpentine Soil Using a pH-Stat Technique. *Soil Sci Soc Am J*, 59, pp. 1027-1031.

Kelepertsis A., Alexakis D., Kita I. (2001). Environmental geochemistry of soils and waters of susaki area, Korinthos, Greece, Environ. *Geochem. Health*, 23, pp. 117–135.

Kelepertzis E., Galanos E., Mitsis I. (2013). Origin, mineral speciation and geochemical baseline mapping of Ni and Cr in agricultural topsoils of Thiva Valley (central Greece). *J. Geochem. Explor.*, 125, pp. 56-68.

Kendelewicz T., Liu P., Doyle C.S., Brown Jr. G.E. (2000). Spectroscopic study of the reaction of aqueous Cr(VI) with Fe_3O_4 (111) surfaces. *Surf. Sci.*, 469, pp. 144–163.

Kendelewicz T., Liu P., Doyle C.S., Brown Jr. G.E., Nelson E.J., Chambers S.A. (1999). X-ray absorption and photoemission study of the adsorption of aqueous Cr(VI) on single crystal hematite and

magnetite surfaces. *Surf. Sci.,* 424, 219-231.

Kierczak J., Neel C., Bril H., Puziewicz J. (2007). Effect of mineralogy and pedoclimatic variations on Ni and Cr distribution in serpentine soils under temperate climate. *Geoderma*, 142, pp. 165-177.

Kilic E., Font J., Puig R., Colak S., Celik D. (2011). Chromium recovery from tannery sludge with saponin and oxidative remediation. *J Hazard Mater*, 185, pp. 456-462.

Kinjo T., Pratt P.F. (1971). Nitrate adsorption: I. some acid soils of Mexico and South America, Soil Science Society of America Proceedings, 35, pp. 722–725.

Komárek M., Koretsky C.M., Krishna J.S., Alessi D.S., Chrastny V. (2015). Competitive Adsorption of Cd(II), Cr(VI), and Pb(II) onto Nanomaghemite: A Spectroscopic and Modeling Approach. *Environ. Sci. Technol.*, 49, pp. 12851−12859.

Koopmans G.F., Chardon W.J., McDowell R.W. (2007). Phosphorus movement and speciation in a sandy soil profile after long-term animal manure applications*. J. Environ. Qual*, 36, pp. 305-315.

Koretsky C. (2000). The significance of surface complexation reactions in hydrologic systems: a geochemist's perspective. *J. Hydrol.*, 230, pp. 127–171.

Kotas J. and Stasicka Z. (2000). Chromium occurrence in the environment and methods)of its speciation. *Environ. Poll.,* 107, pp. 263-283.

Kovačević D., Pohlmeier A., Özbaş G., Narres H.D., Kallay M.J.N. (2000). The adsorption of lead species on goethite. *Colloid Surface A.*, 166, pp. 225-233.

Krishna R.H. and Swamy A.V.V.S. (2012). Investigation on the effect of particle size and adsorption kinetics for the removal of Cr(VI) from the aqueous solutions using low cost sorbent. *Eur. Chem. Bull.*, 7, pp. 258-262.

Krüger O., Fiedler F., Adam C., Vogel C., Senz R. (2017). Determination of chromium(VI) in primary and secondary fertilizer and their respective precursors. *Chemosphere*, 182, pp. 48-53.

Kuhnel R.A., Roorda H.J., Steensma J.J. (1975). The crystallinity of minerals - A new variable in pedogenetic processes: A study of goethite and associated silicates in laterites. *Clays Clay Miner.,* 23, pp. 349-354.

Kwikima M.M. and Lema M.W. (2017). Sorption Characteristics of Hexavalent Chromium in the Soil Based on Batch Experiment and Their Implications to the Environment. *GEP*, 5, pp. 152-164.

La Flamme B.D. and Murray J.W. (1987). Solidsolution interaction: The effect of carbonate alkalinity on adsorbed thorium. *Geochim. Cosmochim. Acta*, 51, pp. 243-250.

Latsoudas C. and Sonis C. (1991). Geological Map of Greece, Sheet Kolindros, Scale1:50,000, Institute of Geology and Mineral Exploration, Athens.

Lee B.D., Graham R.C., Laurent T.E., Amrhein C., Creasy R.M. (2001). Spatial Distributions of Soil Chemical Conditions in a Serpentinitic Wetland and Surrounding Landscape. *Soil Sci. Soc. Am. J.*, 65, pp. 1183–1196.

Lee G. and Hering J.G. (2005). Oxidative Dissolution of Chromium(III) Hydroxide at pH 9, 3, and 2 with Product Inhibition at pH 2. *Environ. Sci. Technol.*, 39, pp. 4921–4928.

Lelli M., Grassi S., Amadori M., Francescini F. (2014). Natural Cr(VI) contamination of groundwater in the Cecina coastal area and its inner sectors (Tuscany, Italy). *Environ Earth Sci.*, 71, pp. 3907-3919.

Li L. and Stanforth R. (2000). Distinguishing adsorption and surface precipitation of phosphate on goethite (a-FeOOH). *J. Colloid Interface Sci.*, 230, pp. 12-21.

Loyaux-Lawniczak S., Lecomte P., Ehrhardt J. (2001). Behavior of hexavalent chromium in a polluted groundwater: redox processes and immobilization in soils. *Environ. Sci. Technol.,* 35, pp. 1350-1357.

Luengo C., Brigante M., Antelo J, Avena M. (2006). Kinetics of phosphate adsorption on goethite: Comparing batch adsorption and ATR-IR measurements. *J. Colloid Interface Sci.*, 300, pp. 511–518.

Lumsdon D.O. and Evans L.J. (1994). Surface complexation model parameters for goethite (α-FeOOH). *J. Colloid Interface Sci.*, 164, pp. 119-125.

Lutzenkirchen J. (1998). Comparison of 1-pK and 2-pK Versions of Surface Complexation Theory by the Goodness of Fit in Describing Surface Charge Data of (Hydr)oxides. *Environ. Sci. Technol.,* 32, pp. 3149-3154.

Mahler R.L., Colter A., Hirnyck R. (2007). Nitrate and groundwater, Quality water for Idaho, University of Idaho, College of agricultural and life sciences.

Manceau A. and Charier L. (1992). X-ray absorption spectroscopic study of the sorption of Cr(III) at the oxide/water interface. I Molecular mechanism of Cr(Ill) oxidation on Mn oxides, *J. Colloid Interface Sci.*, 148, pp. 425-442.

Manning A.H., Mills C.T., Morrison J.M., Ball L.B. (2015). Insights into controls on hexavalent chromium in groundwater provided by environmental tracers, Sacramento Valley, California, USA, *Appl. Geochem.*, 62, pp. 186-199.

Manning B.A. and Goldberg S. (1996). Modeling Competitive Adsorption of Arsenate with Phosphate and Molybdate on Oxide Minerals, *Soil Sci. Soc. Am. J.*, 60, pp. 121-131.

Mao Y., Wang W., Ma C. (2016). Study on the effects of soluble microbial product on phosphate adsorption onto fresh hydrous ferric oxides by surface complexation models, *Wat. Sci. Tech.,* 74, pp. 2446-2453.

Margiotta S., Mongelli G., Summa V., Paternoster M., Fiore S. (2012). Trace element distribution and Cr(VI) speciation in Ca-HCO3 and Mg-HCO_3 spring waters from the northern sector of the Pollino massif, southern Italy. *J Geochem Explor.*, 115, pp. 1-12.

Mathur S.S. and Dzombak D.A. (2006). Surface complexation modeling: goethite. In Interface Science and Technology, 11, pp. 443-468.

McBride M.B. (1997). A critique of diffuse double layer models applied to colloid and surface chemistry, *Clays Clay Miner.*, 45, pp. 598-608.

McClain C.N. and Maher K. (2016). Chromium fluxes and speciation in ultramafic catchments and global rivers, *Chem Geol.,* 426, pp. 135-157.

McDowell R.W., Cox N., Daughney C.J., Wheeler D., Moreau M. (2015). A national assessment of the potential linkage between soil and ground and surface water concentrations of phosphorus. *J Am Water Resour Assoc.*

McGrath S.P. and Smith. S. (1990). In Chromium and Nickel, B.J. Alloway (Ed.), pp. 125–146, Blackie and Sons, London.

Megremi I. (2010). Distribution and bioavailability of Cr in central Euboea, Greece. *Cent Eur J Geosci.*, 2, pp. 103-123.

Megremi I., Vasilatos Ch., Atsarou A., Theodoratou Ch., Economou-Eliopoulos M., Mitsis I., (2013). Geochemical evidences for the sources of the Cr(VI) contamination in groundwater in central Euboea and Assopos-Thiva basins, Greece: Natural versus anthropogenic origin. *European Water*, 41, pp. 23-34.

Meloni P., Carcangiu F., Delogu F. (2012). Specific surface area and chemical reactivity of quartz powders during mechanical processing. *Mater Res Bull*, 47, pp. 146-151.

Mengistu H.A., Tessema A., Demlie M.B., Abiye T.A, Roeyset O. (2015). Surface-complexation modelling for describing adsorption of phosphate on hydrous ferric oxide surface. *Water SA*,

41.

Mesuere K. and Fish W. (1992). Chromate and oxalate adsorption on goethite. 2. Surface complexatlon modeling of competitive adsorption. *Environ Sci Technol*, 26, pp. 2365-2370.

Mikutta C., Lang F., Kaupenjohann M. (2006). Citrate impairs the micropore diffusion of phosphate into pure and C-coated goethite. *Geochim. Cosmochim Acta*, 70, pp. 595-607.

Mills C.T. and Goldhaber M.B. (2012). Laboratory investigations of the effects of nitrification-induced acidification on Cr cycling in vadose zone material partially derived from ultramafic rocks. *Sci. Total Environ.*, 435–436, pp. 363–373.

Mills C.T., Morrison J.M., Goldhaber M.B., Ellefsen K.J. (2011). Chromium(VI) generation in vadose zone soils and alluvial sediments of the southwestern Sacramento Valley, California: a potential source of geogenic Cr(VI) to groundwater. *Appl. Geochem.*, 26, pp. 1488-1501.

Mise S.R. and Bashetty R., (2013). Study of nitrate adsorption characteristics on red soil, *IJRET*.

Mitchell J.K. (1993). Fundamentals of Soil Behavior, 2nd Edn., University of California, Berkley, Wiley.

Mittelstet A.R., Heeren D.M., Fox G.A., Storm D.E., White M.J., Miller R.B. (2011). Comparison of subsurface and surface runoff phosphorus transport rates in alluvial floodplains. *Agriculture, Ecosyst. Environ.,* 141, pp. 417-425.

Mizuno N. (1979). Studies on chemical characteristics of serpentine soils and mineral deficiencies and toxicities of crops, Report Hokkaido Prefect. *Agric. Exp. Stn.,* 29, pp. 1–79.

Moharami S. and Jalali M. (2015). Use of modified clays for removal of phosphorus from aqueous Solutions. *Environ Monit Assess*, 187.

Mohsenipour M., Shahid S., Ebrahimi K. (2015). Nitrate adsorption on clay kaolin: batch tests. *J. Chem.*, pp. 1-7.

Moraetis D., Nikolaidis N.P., Karatzas G.P., Dokou Z., Kalogerakis N., Winkel L.H.E., Palaiogianni-Bellou A. (2012). Origin and mobility of hexavalent chromium in north-eastern Attica, Greece. *Appl Geochem.*, 27, pp. 1170-1178.

Morrison J.M., Goldhaber M.B., Lee L., Holloway J.M., Wanty R.B., Wolf R.E., Ranville J.F. (2009). A regional-scale study of chromium and nickel in soils of northern California, USA. *Appl. Geochem.*, 24, pp. 1500-1511.

Motzer W.E. and Engineers Todd, (2004). Handbook of Cr(VI), Chemistry, Geochemistry, and Geology of Chromium and Chromium Compounds, p 23-88, CRC PRESS.

Motzer W.E., (2005). Chemistry, Geochemistry and Geology of Chromium and Chromium Compounds, Chapter 2 In: "Cr(VI)-Handbook" edited by Guertin J., Jacobs J.A. and Avakian C.P., CRC press.

Mouvet C. and Bourg A.C.M. (1983). Speciation (including adsorbed species) of copper, lead, nickel and zinc in the Meuse River: Observed results compared to values calculated with a chemical equilibrium computer program. *Water Res.*, 17, pp. 641-649.

MPCA (Minnesota Pollution Control Agency) (1999). Phosphorus in Minnesota's Ground Water.

Murphy S. (2005). USGS Water Quality Monitoring, available at http://www.water.usgs.gov/nawqa/circ-1136.html.

Nielsen M.D. (2005). Handbook of Environmental Site Characterization and Ground-Water Monitoring, Multilevel Ground-Water Monitoring, CRC Press.

Nilsson N., Lövgren L., and Sjöberg S. (1992). Phosphate complexation at the surface of goethite. *Chem. Spec. Bioavailab.*, 4, pp. 121-130.

Nriagu J.O. and Dell C.I. (1974). Diagenetic formation of iron phosphates in recent lake sediments. *Am. Mineral.*, 59, pp. 934-946.

Nriagu J.O. and Moore P.B. (1984). Phosphate Minerals. Springer-Verlag, Berlin. Pp. 442.

Olazabal M.A., Etxebarria N., Fernandez L.A., Madariaga J.M. (1994). Study of the complexation and precipitation equilibria in the system Cr(VI)-Fe(III)-H_2O. *J. Solution Chem.*, 23, pp. 1111-1123.

Olazabal M.A., Nikolaidis N.P., Suib S.A., Madariaga J.M. (1997). Precipitation equilibria of the chromium(VI)/iron(III) system and spectroscopic characterization of the precipitates. *Environ. Sci. Technol.*, 31, pp. 2898-2902.

Oliver D.S., Brockman F.J., Bowman R.S., Kieft T.L. (2003). Microbial reduction of hexavalent chromium under vadose zone conditions. *J. Environ. Qual.*, 32, pp. 317-324.

Oram B. (2005). What are Phosphates? University Center for Environmental Quality, Geoenvironmental Sciences and Engineering Department: Phosphate and Water Quality.

Oram B. (2014). Phosphate in Surface Water Streams Lakes, Water Research Center.

Oze C., Bird K.D., Fendorf S. (2007). Genesis of hexavalent chromium from natural sources in soil and groundwater, Proc Natl Acad Sci U.S.A., 104, pp. 6544–6549.

Oze C., Fendorf S., Bird D.K., Coleman R.G. (2004). Chromium geochemistry in serpentinized ultramafic rocks and serpentine soils from the Franciscan Complex of California. *Am. J. Sci.,* 304, pp. 67-101.

Oze C., Fendorf S., Bird K.D. (2004). Coleman GR. Chromium geochemistry of serpentine soils. *Int Geol Rev.*, 46, pp. 97-126.

Padmanabham M. (1983b). Comparative study of the adsorption-desorption behavior of copper(II), zinc(II), cobalt(II) and lead(II) at the goethite-solution interface. *Aust. J. Soil Res.*, 21, pp. 515-525.

Palmer C.D. and Puls R.W. (1994). Natural attenuation of hexavalent chromium in groundwater and soils, EPA Ground Water Issue, EPA/540/5–94/505.

Panagiotakis I., Dermatas D., Vatseris C., Chrysochoou M., Papassiopi N., Xenidis A., Vaxevanidou K. (2015). Forensic investigation of a chromium (VI) groundwater plume in Thiva, Greece. *J Hazard Mater*, 281, pp. 27-34.

Panagiotakis I., Tettas K., Dermatas D., Mamais D., Gavalaki E., Papasiopi N., Xenidis A., Vatseris C. (2012). Investigation of geogenic chromium in groundwater of Greece using available and new data, in 1st Thessaly Environmental Conference, Skiathos, Greece (in Greek).

Pang L., Lafogler M., Knorr B., McGill E., Saunders D., Baumann T., Abraham P., Close M. (2016). Influence of colloids on the attenuation and transport of phosphorus in alluvial gravel aquifer and vadose zone media. *Sci Total Environ.,* 550, pp. 60-68.

Panuccio M.R., Muscolo A., Nardi S. (2001). Effect of humic substances on N uptake and assimilation in two species of pinus. *J. Plant Nutr.*, 24, pp. 693-704.

Papanikolaou D. (2009). Timing of tectonic emplacement of the ophiolites and terrane paleogeography in the Hellenides. *Lithos,* 108, pp. 262-280.

Papassiopi N., Kontoyianni A., Vaxevanidou K., Xenidis A. (2009). Assessment of chromium biostabilization in contaminated soils using standard leaching and sequential extraction techniques. *Sci. of the Tot. Environ.*, 407, pp. 925-936.

Parfitt R.L. (1978). Anion adsorption by soils and soil materials. *Adv. Agron.*, 30, pp. 1-49.

Parfitt R.L. (1989). Phosphate reactions with natural allophane, ferrihydrate and goethite. *J. Soil Sci.*, 40, pp. 359-369.

Parker L.V. and Clark C.H. (2004). Study of five discrete-interval-type ground water sampling devices. *Ground Water Monit. Rem.*, 24, pp. 111-112.

Paz-Gonzalez A., Taboada-Castro T., Taboada-Castro M. (2000). Levels of Heavy metals (Co, Cu, Cr, Ni,

Pb, and Zn) in agricultural soils of Northwest Spain, *Commun Soil Sci Plant Anal.*, 31, pp. 1773-1783.

Peacock C.L. and Sherman D.M. (2004). Copper (II) sorption onto goethite, hematite and lepidocrocite: a surface complexation model based on ab initio molecular geometries and EXAFS spectroscopy. *Geochim. Cosmochim. Acta*, 68, pp. 2623-2637.

Persson P., Nilsson N., Sjoberg S. (1996). Structure and bonding of orthophosphate ions at the iron oxide–aqueous interface. *J. Colloid Interface Sci.*, 177, pp. 263–275.

Peterson J.A. (1984). Metallogenetic Maps Of The Ophiolite Belts Of The Western United States, USGS Miscellaneous Investigations Series, Map Publications, U.S. Geological Survey.

Peterson M.L., White A.F, Brown Jr G.E., Parks G.A. (1997). Surface Passivation of Magnetite by Reaction with Aqueous Cr(VI): XAFS and TEM Results. *Environ. Sci. Technol.*, 31, pp. 1573-1576.

Pettine M., D'Ottone L., Campanella L., Millero F.J., Passino R. (1998). The reduction of chromium(VI) by iron(II) in aqueous solutions. *Geochim. Cosmochim. Acta*, 62, pp. 1509-1519.

Pettine M., Gennari F., Campanella L., Millero F. (2008). The effect of organic compounds in the oxidation kinetics of Cr(III) by H_2O_2. *Geochim. Cosmochim Acta*, 72, 5692-5707.

Pinto F.A, de Souza E.D., Paulino H.B., Curi N., Carneiro M.A.C. (2013). P-sorption and desorption in savanna Brazilian soils as a support for phosphorus fertilizer management. *Ciênc. agrotec. Lavras,* 37, pp. 521-530.

Proenza J. (1999). Uvarovitien podiformc hromitite: the moa-baracoa ophiolitic massif Cuba. *Can. Mineral.*, 37, pp. 679-690.

Qafoku N.P., Sumner M.E., Radcliffe D.E. (2000). Anion transport in columns of variable charge subsoils: nitrate and chloride. *J. Environ. Qual.*, 29, pp. 484-493.

Quantin C., Ettler V., Garnier J., Šebek O. (2008). Sources and extractability of chromium and nickel in soil profiles developed on Czech serpentinites. *CR Geosci*, 340, pp. 872-882.

Rabenhorst M.C., Foss J.E., Fanning D.S. (1982). Genesis of Maryland soils formed from serpentinite. *Soil Sci. Soc. Am. J.*, 46, pp. 607-616.

Rahnemaie R., Hiemstra T., van Riemsdi W.H. (2007). Geometry, Charge Distribution, and Surface Speciation of Phosphate on Goethite. *Langmuir*, 23, pp. 3680-3689.

Rai D., Eary L.E., Zachara J.M. (1989). Environmental chemistry of chromium. *Sci Total Environ.*, 86, pp. 15-23.

Rai D., Zachara J.M., Eary L.E., Ainsworth C.C., Amonette J.E., Cowan C.E., Szelmeczka R.W., Resch C.T., Schmidt R.L., Girvin D.C., Smith S.C. (1988). Chromium Reactions in Geologic Materials, EA-5741, Electric Power Research Institute, Palo Alto, California.

Rai D., Zachara J.M., Eary L.E., Girvin D.C., Moore D.A., Resch C.T., Sass B.M., Schmidt R.L. (1986). Geochemical behavior of chromium species, Interim Report Electric Power Research Institute (EPRI) EA EA–4544, EPRI, Palo Alto, California.

Rai E., Sass B.M., Moore D.A. (1987). Cr(III) hydrolysis constants and solubility of Cr(III) hydroxide. *Inorg. Chem.*, 26, pp. 345-349.

Rajapashka A.U., Vithanage M., Oze C., Bandara W.M.A.T., Weerasooriya R. (2012). Nickel and manganese release in serpentine soil from the Ussangoda ultramafic complex, Sri Lanka. *Geoderma*, 189-190, pp. 1-9.

Ravel B. and Newville M. (2005). ATHENA, ARTEMIS, HEPHAESTUS: data analysis for X-ray absorption spectroscopy using IFEFFIT. *J. Synchrotron Radiat.*, 12, pp. 537–541.

Razaq I.B.A. (1989). Effect of pH and exchangeable metals on phosphate adsorption by soils.

Retrospective Theses and Dissertations. 9170.

Reynolds-Vargas J.S., Richter D.D., Bornemisza E. (1994). Environmental impacts of nitrification and nitrate adsorption in fertilized and isols in the Valle Central of Costa Rica. *Soil Sci.*, 157, pp. 289-299.

Richard F.C. and Bourg A.C.M. (1991). Aqueous geochemistry of chromium: a review. *Wat. Res.*, 25, pp. 807–816.

Rietra R.P.J.J., Hiemstra T., Van Riemsdijk W.H. (2000). Electrolyte anion affinity and its effect on oxyanion adsorption on goethite, J. Colloid Interface Sci, 229, pp. 199-206.

Rietra R.P.J.J., Hiemstra T., Van Riemsdijk W.H. (2001). Interaction between calcium and phosphate adsorption on goethite. *Environ Sci Technol*, 35, pp. 3369-3374.

Roberts B.A. and Proctor J. (1992). The ecology of areas with serpentinized rocks, Kluwer Academic Publishers.

Robertson A.P. and Leckie J.O. (1997). Cation binding predictions of surface complexation models: effects of pH, ionic strength, cation loading, surface complex, and model fit. *J. Colloid Interface Sci*, 188, pp. 444-472.

Robertson W.D. (2003). Enhanced attenuation of septic system phosphate in noncalcareous sediments. *Ground Water*, 40, pp. 48-56.

Robles-Camacho J. and Armienta M.A. (2000). Natural chromium contamination of groundwater at León Valley, México. *J Geochem Explor.*, 68, pp. 167-181.

Rundberg R.S., Albinsson Y., Vannerberg K. (1994). Sodium adsorption onto goethite as a function of pH and ionic strength. *Radiochim. Acta*, 66, pp. 333-340.

Sager M. (2005). About Chromium(VI) Extraction from Fertilizers and Soils. *Econ. Environ. Geol.,* 38, pp. 657-662.

Saha B. and Streat M. (2005). Adsorption of trace heavy metals: Application of surface complexation theory to a macroporous polymer and a weakly acidic ion-exchange resin. *Ind. Chem. Res.,* 44, pp. 8671–8681.

Saha R., Nandi R., Saha B. (2011). Sources and toxicity of hexavalent chromium, J. Coord. Chem., 64, pp. 1782-1806.

Sahai N. and Sverjensky D.A. (1997). Evaluation of internally consistent parameters for the triple-layer model by the systematic analysis of oxide surface titration data. *Geochim. Cosmochim. Acta*, 61, pp. 2801-2826.

Salunkhe O.B., Dhakephalkar P.K., Paknikar K.M. (1998). Bioremediation of hexavalent chromium in soil microcosms. *Biotechnol. Letters*, 20, pp. 749-751.

Sass B.M. and Rai D. (1987). Volubility of amorphous chromium(III)-Iron(III) hydroxide solid solutions. *Inorg. Chem.,* 26, pp. 2228-2232.

Schelde K., de Jonge L.W., Kjaergaard C., Laegdsmand M., Rubæk G.H. (2006). Effects of manure application and plowing on transport of colloids and phosphorus to tile drains. *Vadose Zone J.,* 5, pp. 455-458.

Schroeder D.C. and Lee G.F. (1975). Potential transformations of chromium in natural waters. *Water, Air, Soil Pollut.*, 4, pp. 355-365.

Schroth M.H. (1990). Chromium(VI) Sorption in Soils: Chemical Behavior and Solute Transport Modeling, Oregon State University.

Schrothez-Villegas N., Flores-Velez L.M., Dominguez O. (2004). Sorption of lead in soil as a function of pH: a study case in Mexico. *Chemosphere*, 57, pp. 1537-1542.

Schwertmann U., Cambier P., Murad E. (1985). Properties of goethites of varying crystallinity. *Clays*

Clay Miner., 33, pp. 369-378.

Sei J., Jumas J.C., Olivier-Fourcade J., Quiquampoix H., Staunton S. (2002). Role of iron oxides in the phosphate adsorption properties of kaolinites from the Ivory Coast, *Clays Clay Miner.*, 50, pp. 217–222.

Sequi P., Benedetti A., Canali S., Tittarelli F. (1997). Aboliti negli Usa i Limiti di Cromo nei Fertilizzanti. *L'Informatore Agrario*, 53, pp. 35-37.

Shallari S., Schwartz C., Hasko A., Morel J.L. (1998). Heavy metals in soils and plants of serpentine and industrial sites of Albania, *Sci. Total Environ.*, 209, pp. 133-142.

Sharpley A.N., Chapra S.C., Wedepohl R., Sims J.T., Daniel T.C., Reddy K.R. (1994). Managing agricultural phosphorus for protection of surface waters: Issues and options, *J. Environ. Qual.,* 23, pp. 437-451.

Shitza A., Swennen R., Tashko A. (2005). Chromium and nickel distribution in soils, active river, overbank sediments and dust around the Burrel chromium smelter (Albania), *J Geochem Explor.*, 87, pp. 92– 108.

Sibanda H.M. and Young S.D. (1986). Competitive adsorption of humus acids and phosphate on goethite, gibbsite and two tropical soils, *J. Soil Sci.*, 37, pp. 197-204.

Siemos N. (2010). Groundwater Monitoring Network of Greece, IGME, Athens.

Singh A., Ulrich K.U., Giammar D.E. (2010). Impact of phosphate on U (VI) immobilization in the presence of goethite. *Geochim. Cosmochim. Acta*, 74, pp. 6324-6343.

Singh D.B., Gupta G.S., Prasad G., Rupainwar D.C. (1993). The Use of Hematite for Chromium(VI) Removal, J. Environ. Sci. Health, 28, pp. 1813-1826.

Sivakugan N. (2000). Chapter 3: Soil classification, In: Geotechnical Engineering: A practical problem solving approach. Ed. by Sivakugan N. and Das B.M., James Cook University.

Skordas K. and Kelepertzis A. (2005). Soil contamination by toxic metals in the cultivated region of Agia, Thessaly, Greece. Identification of sources of contamination, *Environ Geol.*, 48, pp. 615–624.

Slomp C.P., Malschaert J.F.P., Van Raaphorst W. (1998). The role of adsorption in sediment-water exchange of phosphate in North Sea continental margin sediments, *Limnol Oceanogr.,* 43, pp. 832-846.

Smith R.M., Martell A.E., Motekaitis R.J. (2003). NIST crititically selected stability constants of metal complexes database. NIST standard reference database 46, version 7.0. NIST, Gaithersburg, MD, USA.

Smith R.W. and Jenne E.A. (1991). Recalculation, evaluation, and prediction of surface complexation constants for metal adsorption on iron and manganese oxides. *Environ. Sci. Technol.*, 25, pp. 525-531.

Sokol E.V., Gaskova O.L., Kokh S.N., Kozmenko O.A., Seryotkin Y.V., Vapnik Y., Murashko M.N. (2011). Chromatite and its Cr3+- and Cr6+- bearing precursor minerals from the Nabi Musa mottled zone complex, Judean Desert. *Am Mineral.*, 96, pp. 659–674.

Sørensen P., Jensen J., Scott-Fordsmand J., Christensen B.T. (2011). Ecotoxicological evaluation of As, Cd, Cr, Pb, Hg and Ni applied with fertilisers in Denmark, Internal report nr. 111, Aarhus University.

Sparks D.L. (2003). Environmental Soil Chemistry, 2nd Edition, Academic Press.

Spiteri C., Slomp C.P., Regnier P., Meile C., Van Cappellen P. (2007). Modelling the geochemical fate and transport of wastewater-derived phosphorus in contrasting groundwater systems, *J Contam Hydrol*, 92, pp. 87-108.

Spiteri C., Van Cappellen P., Regnier P. (2008). Surface complexation effects on phosphate adsorption to ferric iron oxyhydroxides along pH and salinity gradients in estuaries and coastal aquifers, *Geochim. Cosmochim Acta*, 72, pp. 3431–3445.

Sposito G. (1989). The Chemistry of Soils, Oxford, New York, University Press.

Sposito G. (2008). The Chemistry of Soils, 2nd ed., pp. 174-214, Oxford, University Press.

Srivastava S. and Thakur I.S. (2006). Evaluation of bioremediation and detoxification potentiality of Aspergillus niger for removal of hexavalent chromium in soil microcosm, *Soil Biol. Biochem.*, 38, pp. 1904-1911.

Standard Methods for the Examination of Water and Wastewater, (2012). 22nd Edition.

Stanin F. and Pirnie M. (2004). Handbook of Cr(VI), The Transport and Fate of Cr(VI) in the Environment, pp 161-212, CRC PRESS

Strahm B.D. and Harrison R.B., (2006). Nitrate sorption in a variable-charge forest soil of the Pacific Northwest, *Soil Sci.*, 171, pp. 313-321.

Strauss R., Brümmer G.W., Barrow N.J. (1997). Effects of crystallinity of goethite: II. Rates of sorption and desorption of phosphate, *Eur. J. Soil Sci.*, 48, pp. 101-114.

Sverjensky D.A. (2001). Interpretation and prediction of triple-layer model capacitances and the structure of the oxide– electrolyte–water interface, *Geochim. Cosmochim Acta*, 21, pp. 3643–3655.

Sverjensky D.A. (2005). Prediction of surface charge on oxides in salt solutions: revisions for 1: 1 (M+ L−) electrolytes. *Geochim. Cosmochim. Acta*, 69, pp. 225-257.

Sverjensky D.A. (2006). Prediction of the speciation of alkaline earths adsorbed on mineral surfaces in salt solutions. *Geochim. Cosmochim. Acta*, 70, pp. 2427-2453.

Sverjensky D.A. and Fukushi K. (2006). Anion adsorption on oxide surfaces: Inclusion of the water dipole in modeling the electrostatics of ligand exchange. *Environ. Sci. Technol.*, 40, pp. 263-271.

Tani M., Okuten T., Koike M., Kuramochi K., Kondo R. (2004). Nitrate adsorption in some andisols developed under different moisture conditions, *J. Soil Sci. Plant Nutr.*, 50, pp. 439-446.

Tebo B.M. and Obraztsova A.Y. (1998). Sulfate-reducing bacterium grows with Cr(VI), U(VI), Mn(IV), and Fe(III) as electron acceptors, *FEMS Microbiol. Letters*, 162, pp. 193-198.

Tejedor-Tejedor M.I. and Anderson M.A., (1990). Protonation of phosphate on the surface of goethite as studied by CIR-FTIR and electrophoretic mobility, *Langmuir*, 6, pp. 602-611.

Tokunaga T.K., Wan J., Firestone M.K., Hazen T.C., Olson K.R., Herman D.J., Sutton S.R., Lanzirotti A. (2003a). In Situ reduction of chromium(VI) in heavily contaminated soils through organic carbon amendment, *J. Environ. Qual.*, 32, pp. 1641-1649.

Torrent J. and Delgado A. (2001). Using phosphorus concentration in the soil solution to predict phosphorus desorption to water, *J. Environ. Qual.*, 30, pp. 1829–1835.

Torrent J., Barron V., Schwertmann U. (1990). Phosphate Adsorption and Desorption by Goethites Differing in Crystal Morphology, *Soil Sci. Soc. Am. J.*, 54, pp. 1007-1012.

Torrent J., Schwertmann U., Barrón V. (1992). Fast and slow phosphate sorption by goethite-rich natural materials, *Clays Clay Miner.*, 40, pp. 14-21.

Tredoux G., Engelbrecht P., Israel S. (2009). Nitrate in groundwater, Why is it a hazard and how to control it?, WRC Report No. TT 410/09, Report to the Water Research Commission by CSIR, Natural Resources and the Environment, Stellenbosch.

Trolard F., Bourrie G., Jeanroy E., Herbillon A.J., Schroth H. (1995). Trace metals in natural iron oxides from laterites: a study using selective kinetic extraction, *Geochim. Cosmochim. Acta*, 59, pp.

1285-1297.

Tseng J.K. and Bielefeldt A.R. (2002). Low-temperature Cr(VI) biotransformation in soil with varying electron acceptors, *J. Environ. Qual.,* 31, pp. 1831-1841.

Turick C.E., Apel W.A., Carmiol N.S. (1996). Isolation of hexavalent chromium-reducing anaerobes from hexavalent-chromium-contaminated and non contaminated environments, *Appl. Microbiol. Biotechnol.*, 44, pp. 683-688.

Turner D.R. and Sassman S.A. (1996). Approaches to sorption modeling for high-level waste performance assessment. *J. Contam. Hydrol.*, 21, pp. 311-332.

Tziritis, E., Kelepertzis, E., Korres, G., Perivolaris, D. and Repani, S. (2012). Hexavalent chromium contamination in groundwaters of Thiva basin, Central Greece, *Bull Environ Contam Toxicol.*, 89, 1073-1077.

Tzou Y.M., Chen Y.R., Wang M.K. (1998). Chromate sorption by acidic and alkaline soils, *J. Environ. Sci. Health A*, 33, pp. 1607-1630.

Tzou Y.M., Wang M.K., Loeppert R.H. (2003). Effects of Phosphate, HEDTA, and Light Sources on Cr(VI) Retention by Goethite, *Soil Sediment Contam*, 12, pp. 69-84.

U.S.G.S (U.S. Geological Survey), (2012). Phosphorus and Groundwater: Establishing Links Between Agricultural Use and Transport to Streams, by Joseph L Domagalski and Henry Johnson, California Water Science Center, 6000 J Street, Placer Hall, Sacramento, CA 95819.

USEPA (1998), Toxicological review of hexavalent chromium (CAS No. 18540-29-9), In Support of Summary Information on the Integrated Risk Information System (IRIS), August 1998, U.S. Environmental Protection Agency, Washington, DC.

USEPA (2005). N and Phosphorus in Agricultural Streams, Report on the Environment

USEPA (2010). Code of Federal Regulations (CFR), "Standards for the Use or Disposal of Sewage Sludge," Title 40 (Protection of Environment), Part 503.

USEPA (U.S. Environmental Protection Agency), (1984). Ambient Water Quality- Criteria for Chromium, Federal Register 440/5-84-029.

van Geen A., Robertson A.P., Leckie J.O. (1994). Complexation of carbonate species at the goethite surface: Implications for adsorption of metal ions in natural waters. *Geochim. Cosmochim. Acta*, 58, pp. 2073-2086.

Van Riemsdijk W.H., Boumans L.J.M., De Haan F.A.M. (1984). Phosphate sorption by soils: I. A model for phosphate reaction with metal-oxides in soils, *SSSA Journal*, 48, pp. 537-541.

Vázquez G., González-Álvarez J., Garcia A.I., Freire M.S., Antorrena G. (2007). Adsorption of Phenol on Formalde-Hyde-Pretreated Pinus Pinaster Bark: Equilibrium and Kinetics, *Bioresource Technol.*, 98, pp. 1535-1540.

Venema P., Hiemstra T., van Riemsduk W.H. (1996). Comparison of different site binding models for cation sorption: description of pH dependency, salt dependency, and cation proton exchange. *J. Colloid Interface Sci.*, 181, pp. 45-59.

Veselská V., Fajgar R., Číhalová S., Bolanz R.M., Göttlicher J., Steininger R., Siddique J.A., Komárek M. (2016). Chromate adsorption on selected soil minerals: Surface complexation modeling coupled with spectroscopic investigation*, J Hazard Mater*, 318, pp. 433–442.

Vilardi G., Verdone N., Di Palma L. (2017). The influence of nitrate on the reduction of hexavalent chromium by zero-valent iron nanoparticles in polluted wastewater, Desalin. *Water Treat.*, 86, pp. 252-258.

Villalobos M. and Pérez-Gallegos A. (2008). Goethite surface reactivity: a macroscopic investigation unifying proton, chromate, carbonate, and lead(II) adsorption, *J Colloid Interface Sci.*, 2, pp.

307-323.

Villalobos M., Trotz M.A., Leckie J.O. (2001). Surface Complexation Modeling of Carbonate Effects on the Adsorption of Cr(VI), Pb(II), and U(VI) on Goethite, *Environ. Sci. Technol.*, 35, pp. 3849-3856.

Violante A., Pigna M., Ricciardella M., Gianfred L. (2002). Adsorption of phosphate on variable charge minerals and soils as affected by organic and inorganic ligands, *Dev. Soil Sci.*, 28A, pp. 279-295.

Vithanage M., Rajapaksha A.U., Oze C., Rajakaruna N., Dissanayake C.B. (2014). Metal release from serpentine soils in Sri Lanka, *Environ Monit Assess.*, 186, pp. 3415-3429.

Walshe G.E., Pang L., Flury M., Close M.E., Flintoft M. (2010). The effects of pH, ionic strength, dissolved organic matter, and flowrate on the co-transport of MS2 bacteriophages with kaolinite in gravel aquifer media, *Water Res.*, 44, pp. 1255-1269.

Wang X., Liu F., Tan W., Li W., Feng X., Sparks D.L. (2013). Characteristics of phosphate adsorption-desorption onto ferrihydrite: comparison with well-crystalline Fe (hydr)oxides, *Soil Sci.*, 178, pp. 1–11.

Watanabe H. (1984). Accumulation of chromium from fertilizers in cultivated soils, *Soil Sci. Plant Nutr.*, 30, pp. 543-554.

Weerasooriya R. and Tobschall H.J. (2000). Mechanistic modeling of chromate adsorption onto goethite, *Colloids Surf A Physicochem Eng Asp.*, 162, pp. 167-175.

Wen X., Du Q., Tang H. (1998). Heavy Metal Adsorption on Natural Sediment, *Environ. Sci. Technol.*, 32, pp. 870-875.

Weng L., Van Riemsdijk W.H., Hiemstra T. (2012). Factors Controlling Phosphate Interaction with Iron Oxides, *J. Environ. Qual.*, 41, pp. 628-635.

Weng L., Vega F.A., Van Riemsdijk W.H. (2011). Competitive and Synergistic Effects in pH Dependent Phosphate Adsorption in Soils: LCD Modeling, *Environ. Sci. Technol.*, 45, pp. 8420–8428.

Whitfield P.S. and Mitchell L.D., (2003). Quantitative Rietveld analysis of the amorphous content in cements and clinkers, *J. Mat. Sci.*, 38, pp 4415–4421.

WHO (World Health Organization) (1993). Guidelines for Drinking-Water Quality. Second ed. (vol. 1-Recommendations, Geneva).

Wielinga B., Mizub M.M., Hansel C.M., Fendorf S. (2001). Iron Promoted Reduction of Chromate by Dissimilatory Iron-Reducing Bacteria, *Environ. Sci. Tech.*, 35, pp. 522-527.

Withers P.J.A., Davidson I.A., Foy R.H. (2000). Prospects for controlling nonpoint phosphorus loss to water: A UK perspective, *J. Environ. Qual.*, 29, pp. 167-175.

Wittbrodt R.P. and Palmer D.C. (1995). Reduction of Cr(VI) in the presence of excess soil fulvic acid, *Environ. Sci. Techn.*, 29, pp. 255-263.

Wittbrodt R.P. and Palmer D.C. (1996). Reduction of Cr(VI) by soil humic acids, *European J. Soil Sci.*, 47, pp. 151-162.

Wong M.T.F. and Wittwer K. (2009). Positive charge discovered across Western Australian wheatbelt soils challenges key soil and N management assumptions, *Aust J Soil Res*, 47, pp. 127-135.

Xie J., Gu X., Tong F., Zhao Y., Tan Y. (2015). Surface complexation modeling of Cr(VI) adsorption at the goethite–water interface, *J. Colloid Interface Sci.*, 455, pp. 55–62.

Yongue-Fouateu R., Yemefack M., Wouatong A.S.L., Ndjigui P.D., Bilong P. (2009). Contrasted mineralogical composition of the laterite cover on serpentinites of Nkamouna-Kongo, Southeast Cameroon, *Clay Miner.*, 44, pp. 221–237.

Zachara J.M., Girvin D.C., Schmidt R.L., Resch C.T. (1987). Chromate adsorption on amorphous iron oxyhydroxide in presence of major ground water ions, *Environ. Sci. Technol.*, 21, pp. 589-594.

Zachmann D.W. and Johannes W. (1989). Cryptocrystalline magnesite, *Monograph series on Mineral Deposits*, 28, pp. 15-28.

Zanini L., Robertson W.D., Ptacek C.J., Schiff S.L., Mayer T. (1998). Phosphorus characterization in sediments impacted by septic effluent at four sites in central Canada, *J Contam. Hydrol.*, 33, pp. 405-429.

Zazo J.A., Paull J.S., Jaffe P.R. (2008). Influence of plants on the reduction of hexavalent chromium in wetland sediments, *Environ. Pollut.*, 156, pp. 29-35.

Zhang J.S., Stanforth R., and Pehkonen S.O. (2007). Proton–arsenic adsorption ratios and zeta potential measurements: Implications for protonation of hydroxyls on the goethite surface. *J. Colloid Interface Sci.*, 315, pp. 13-20.

Zhang M.K. (2008). Effects of soil properties on phosphorus subsurface migration in sandy soils, *Pedosphere*, 18, pp. 599-610.

Zhang P. and Sparks D.L. (1990). Kinetics of selenate and selenite adsorption/desorption at the goethite/water interface. *Environ. Sci. Technol.*, 24, pp. 1848-1856.

Zhang P.C. and Sparks D.L. (1989). Kinetics and mechanisms of molybdate adsorption/ desorption at the goethite/water interface using pressure-jump relaxation. *SSSA*, 53, pp. 1028-1034.

Zhu I. and Getting T. (2012). A review of nitrate reduction using inorganic materials, *Environ. Technol. Rev.*, 1, pp. 46-58.

Internet sources

https://www.eea.europa.eu/themes/water/status-and-monitoring/state-of-groundwater/water-quality-and-pollution-by-nutrients

http://www.britannica.com/EBchecked/topic/377777/metamorphic-rock/80338/Greenschist-facies (verified: May 2014).

http://www.lenntech.com/groundwater/nitrates.htm#ixzz4hWzL8IKY

https://www.eea.europa.eu/themes/water/status-and-monitoring/state-of-groundwater/water-quality-and-pollution-by-nutrients

RES^{3}T, Rossendorf Expert System for Surface and Sorption Thermodynamics, http://www.hzdr.de/db/RES3T.queryData (last accessed September 18th, 2018).

APPENDIX I - FIGURES

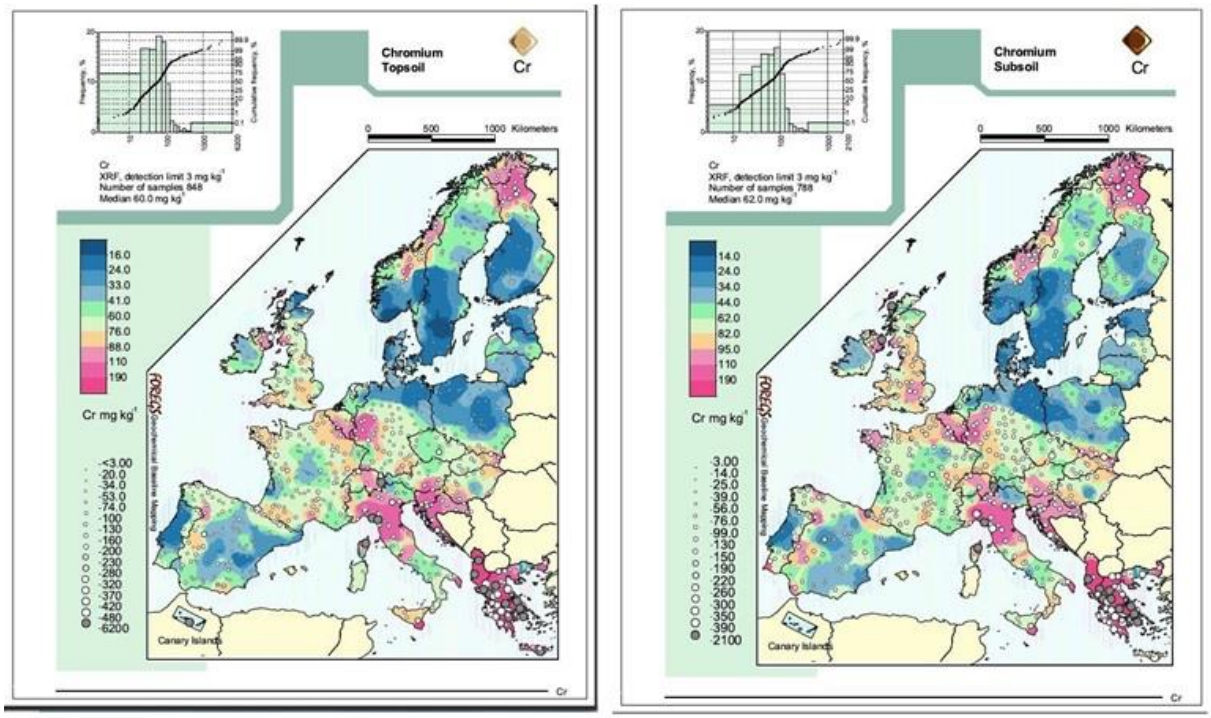

Figure A1.1 Spatial distribution of chromium in the topsoil and subsoil in Europe **(source: http://www.gsf.fi/publ/foregsatlas/).**

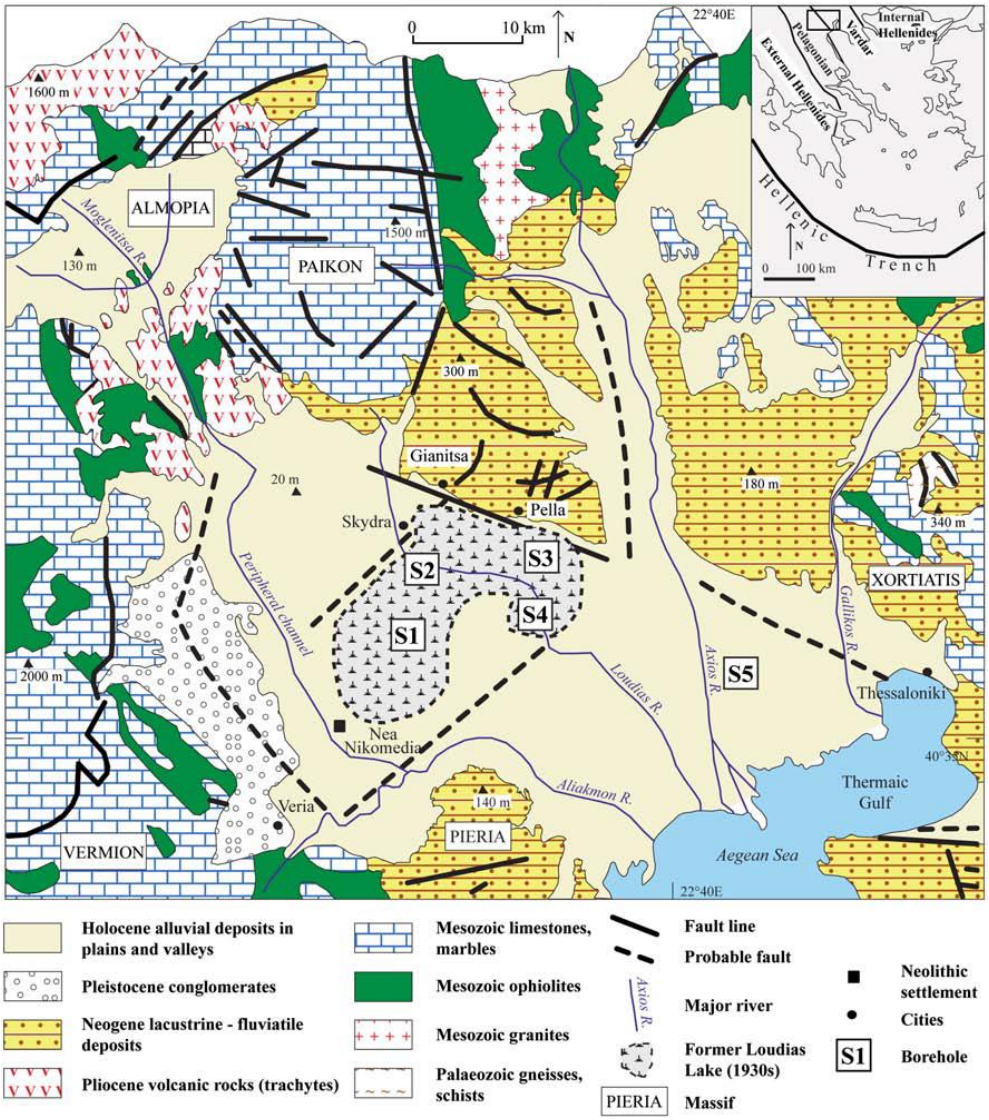

Source: (Ghilardi et al., 2008)

Figure A1.2 Geological background of the Thessaloniki Plain and borehole locations.

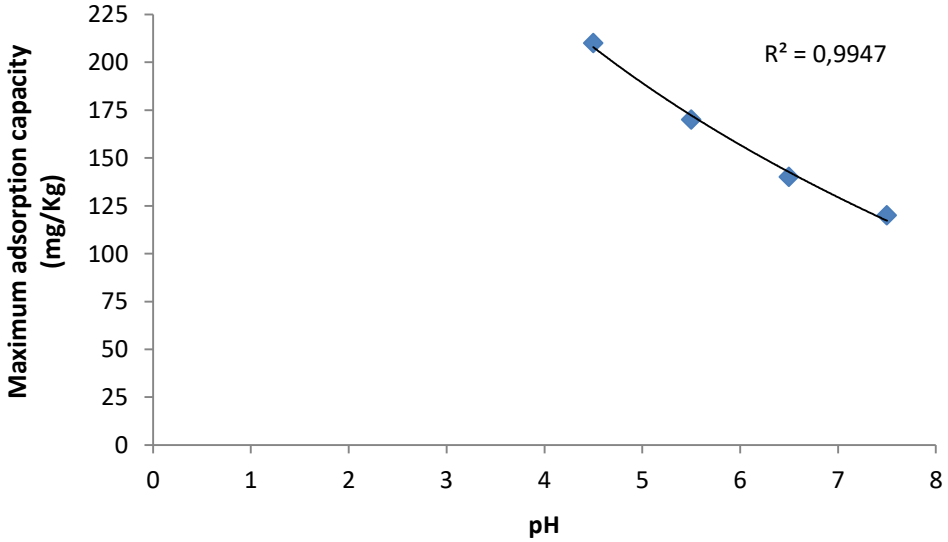

Figure A1.3 Trend of maximum adsorption capacity of the ophiolitic soil versus pH.

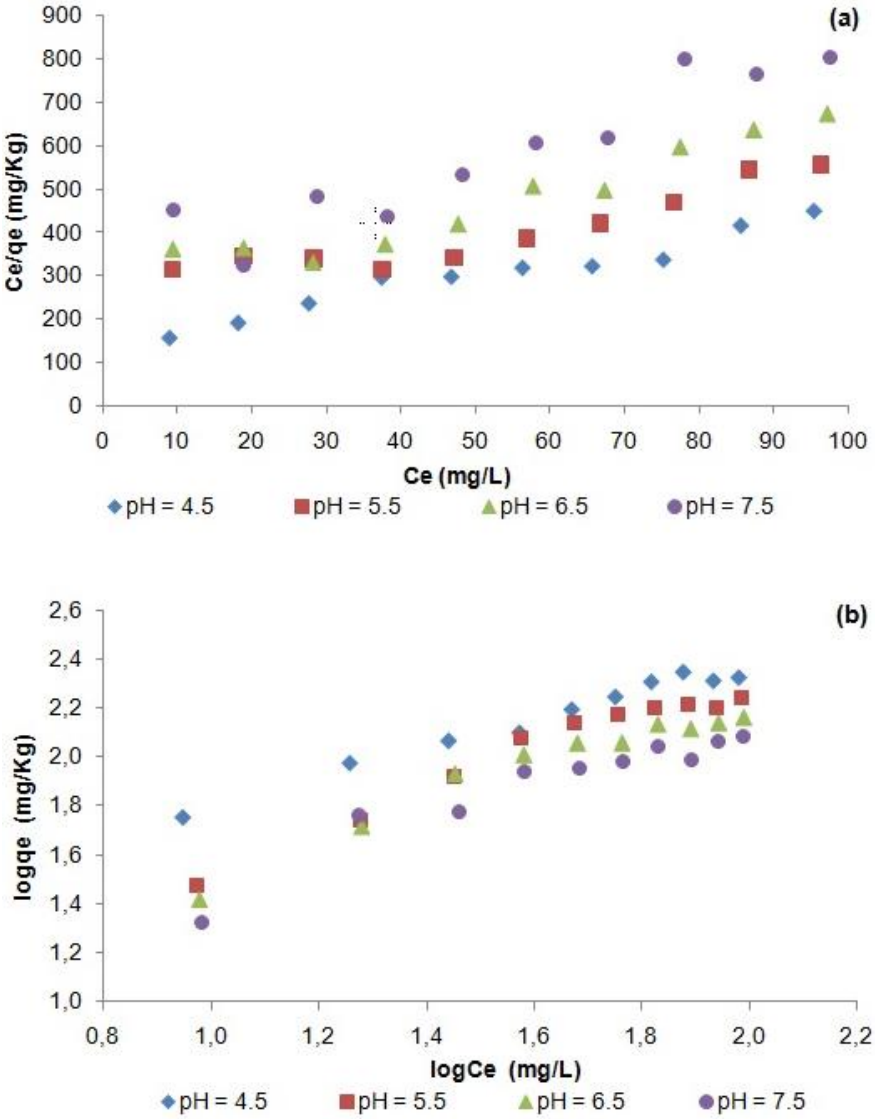

Figure A1.4 a) Langmuir and b) Freundlich adsorption isotherms for Cr(VI) adsorption for four different pH values (4.5, 5.5, 6.5 and 7.5) at room temperature (25^0C).

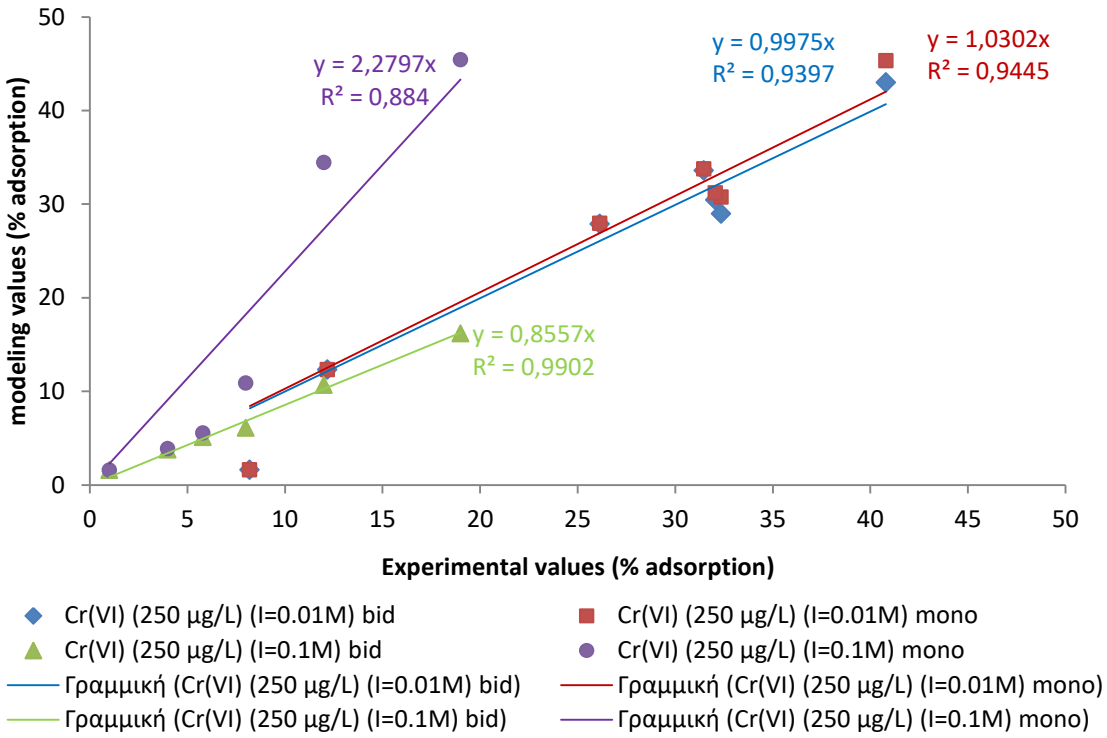

Figure A1.5 Values of correlation factors (R^2) during simulation of Cr(VI) adsorption by ophiolitic soil (solid concentration = 1.5 g/L) as a function of ionic strength.

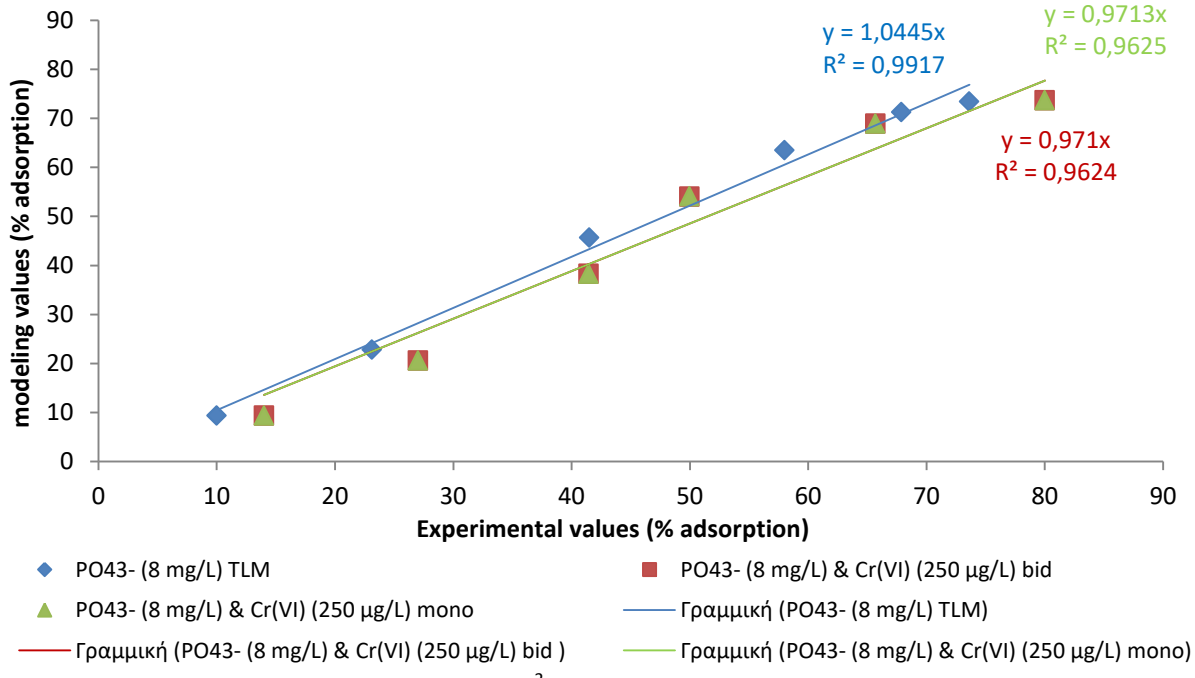

Figure A1.6 Values of correlation factors (R^2) during simulation of phosphate adsorption by ophiolitic soil (solid concentration = 1.5 g/L) and competitive effects with chromates.

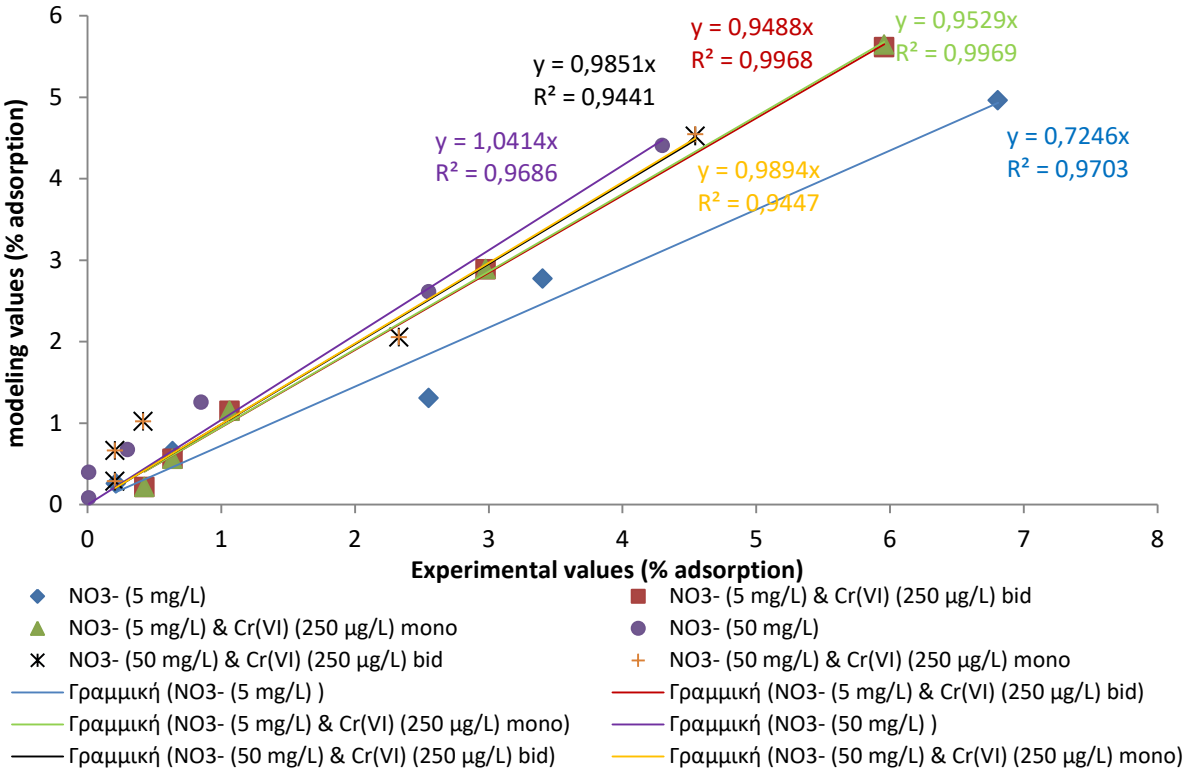

Figure A1.7 Values of correlation factors (R^2) during simulation of nitrates adsorption by ophiolitic soil (solid concentration = 1.5 g/L) and competitive effects with chromates.

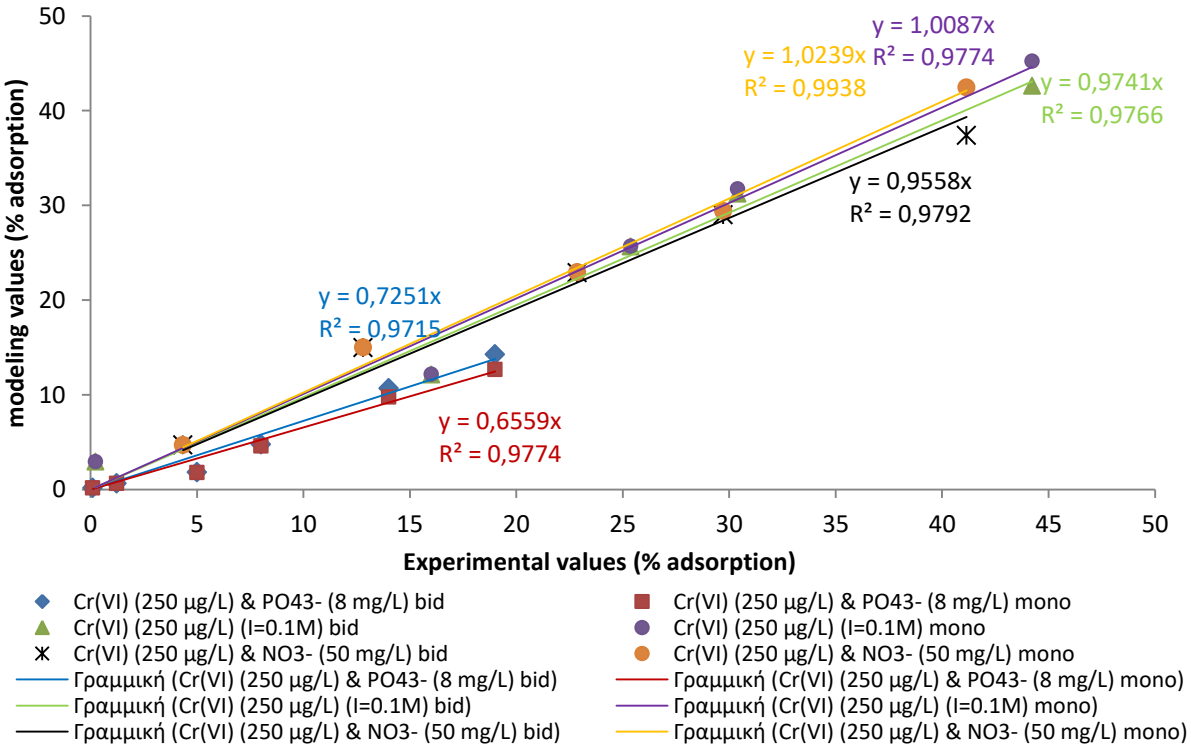

Figure A1.8 Values of correlation factors (R^2) during simulation of Cr(VI) adsorption by ophiolitic soil (solid concentration = 1.5 g/L) and competitive effects with inorganic contaminants.

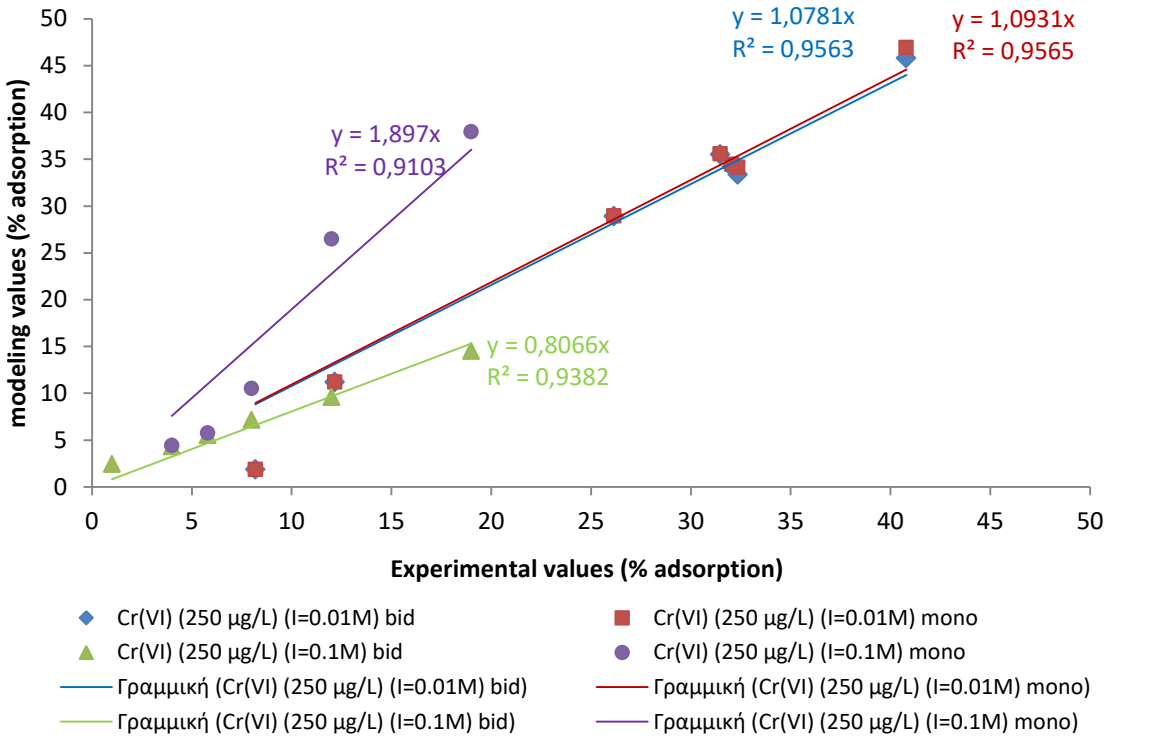

Figure A1.9 Values of correlation factors (R^2) during simulation of Cr(VI) adsorption by ophiolitic soil (solid concentration = 1.1 g/L) as a function of ionic strength.

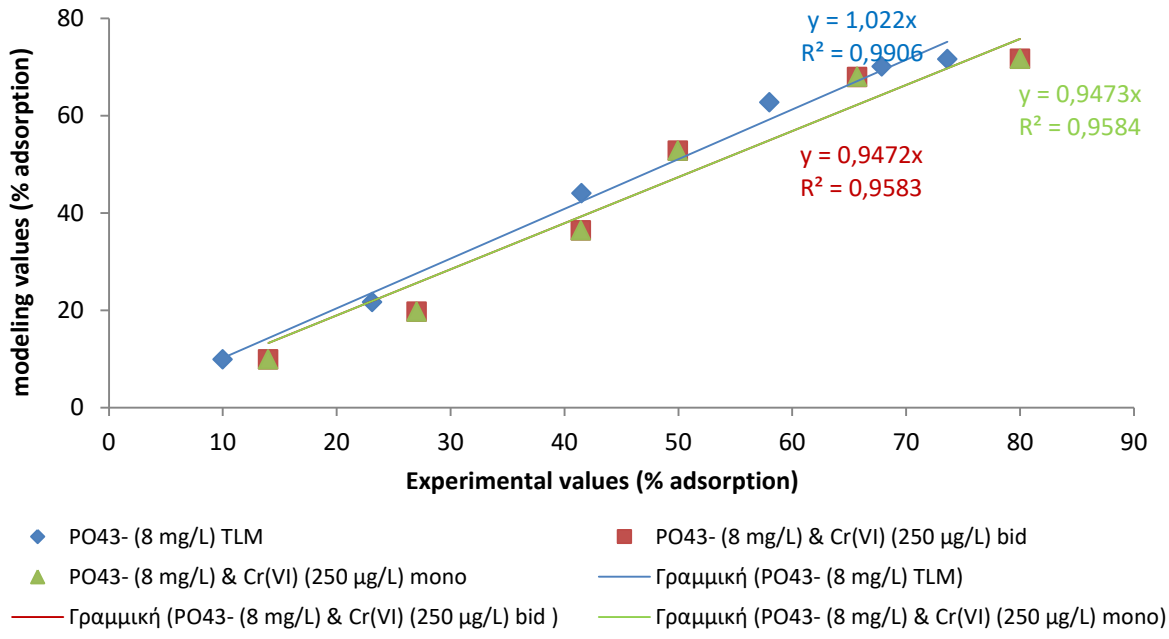

Figure A1.10 Values of correlation factors (R^2) during simulation of phosphate adsorption by ophiolitic soil (solid concentration = 1.1 g/L) and competitive effects with chromates.

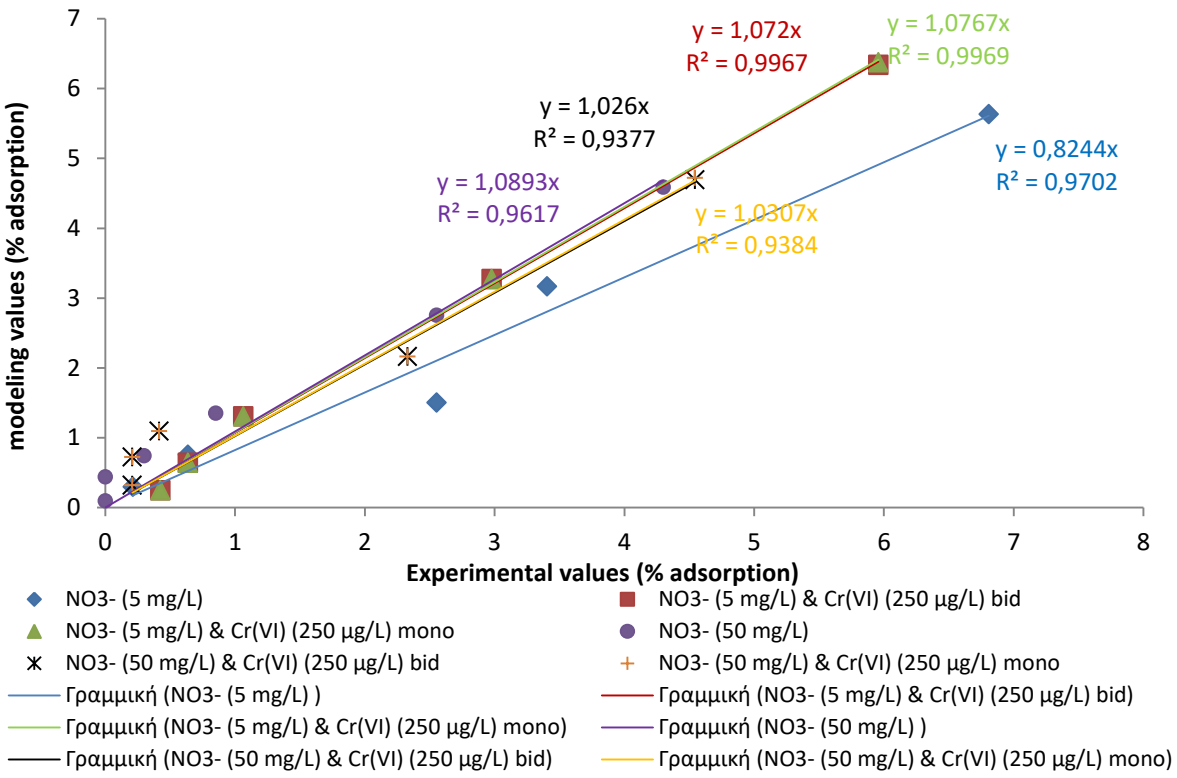

Figure A1.11 Values of correlation factors (R^2) during simulation of nitrates adsorption by ophiolitic soil (solid concentration = 1.1 g/L) and competitive effects with chromates.

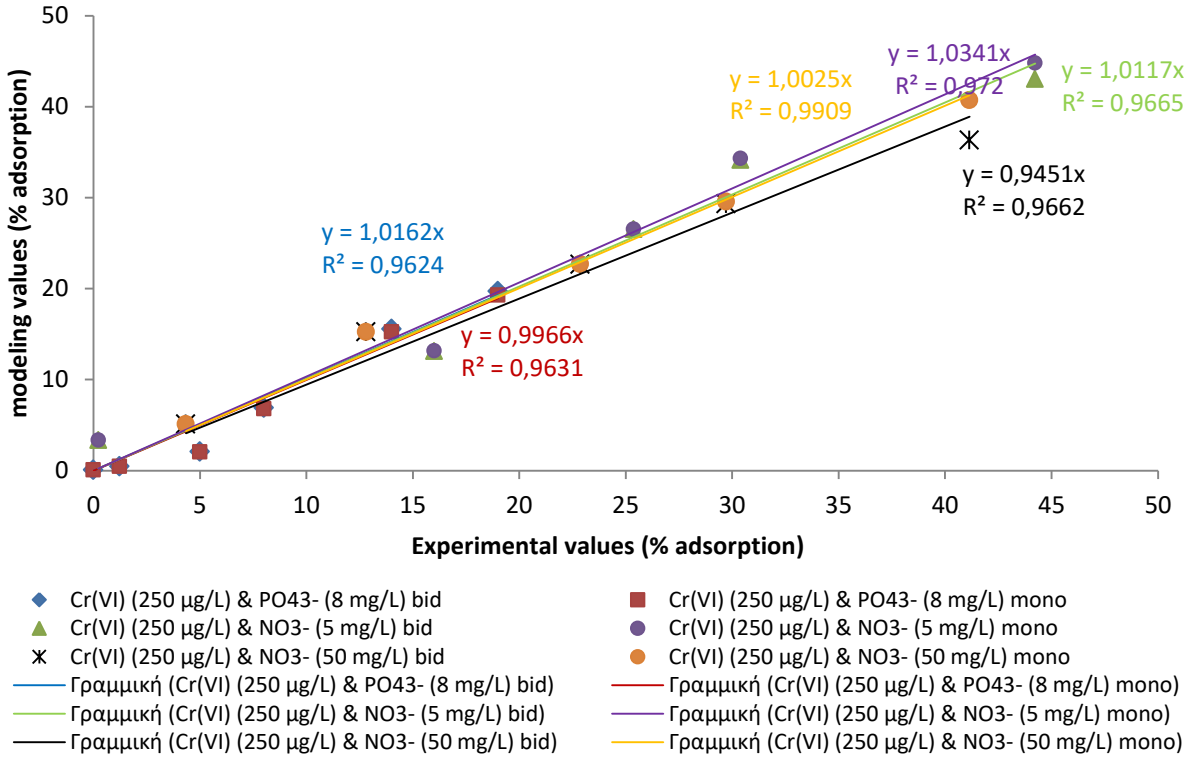

Figure A1.12 Values of correlation factors (R^2) during simulation of Cr(VI) adsorption by ophiolitic soil (solid concentration = 1.1 g/L) and competitive effects with inorganic contaminants.

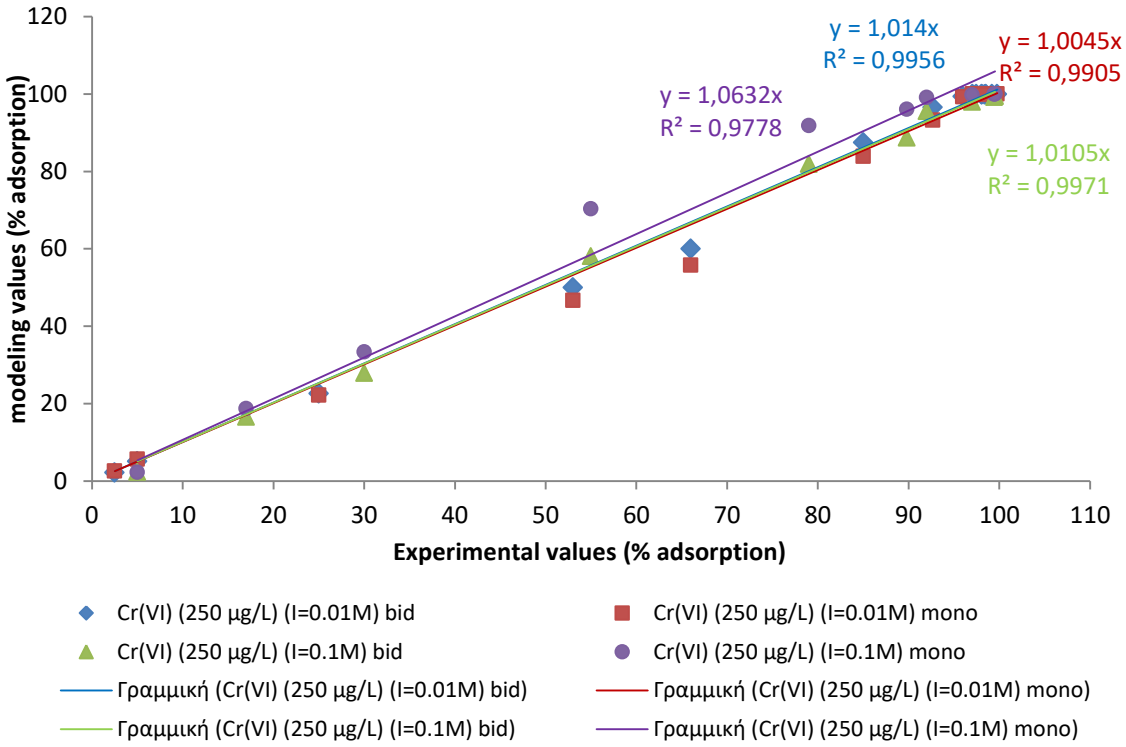

Figure A1.13 Values of correlation factors (R^2) during simulation of Cr(VI) adsorption by goethite as a function of ionic strength.

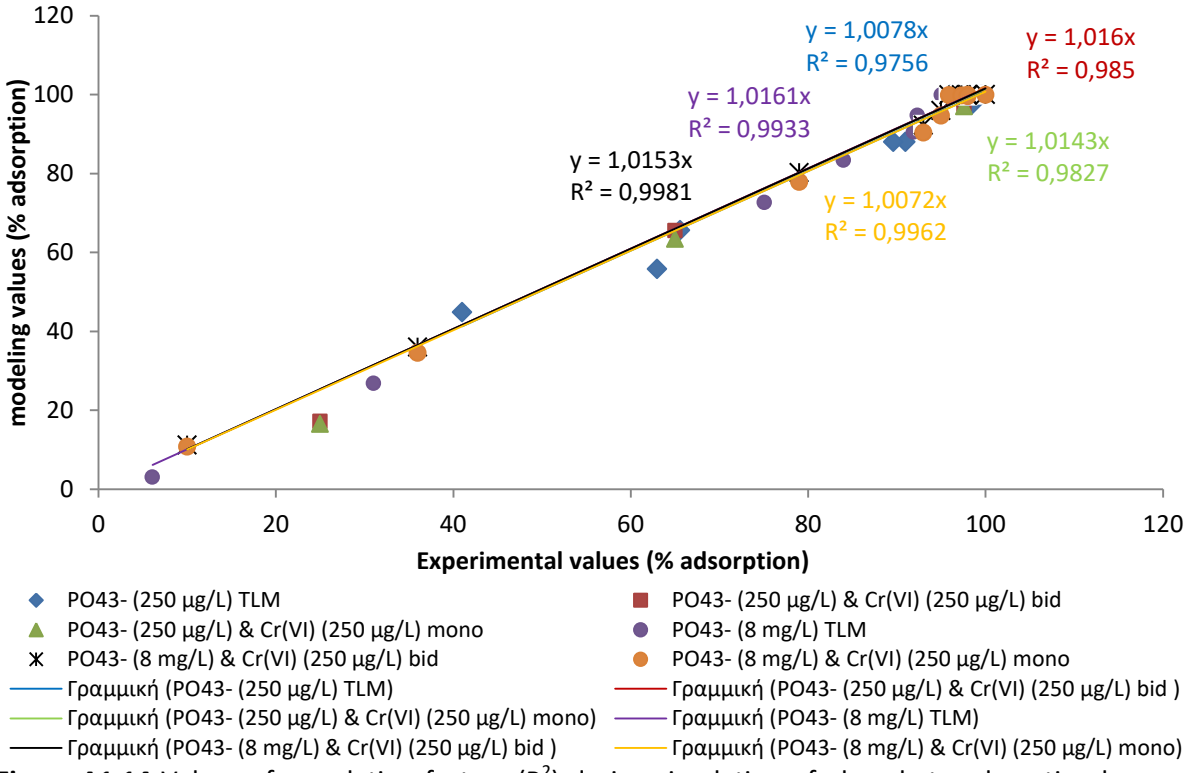

Figure A1.14 Values of correlation factors (R^2) during simulation of phosphate adsorption by goethite and competitive effects with chromates.

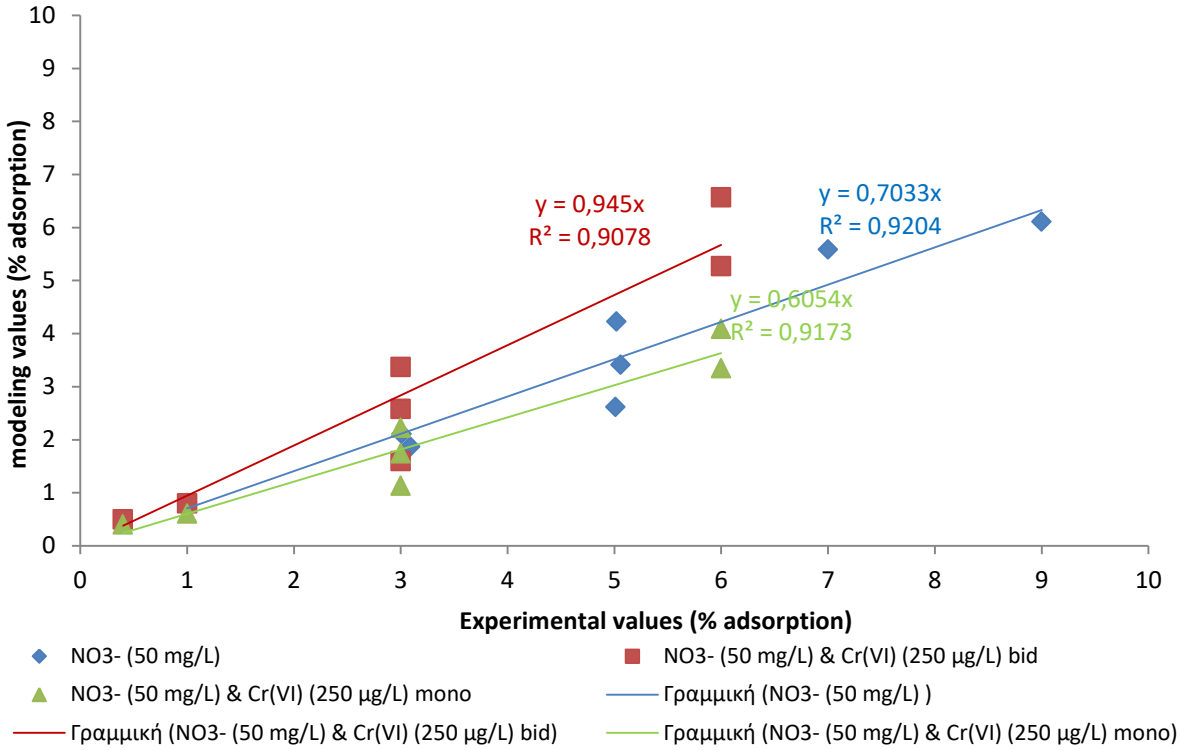

Figure A1.15 Values of correlation factors (R^2) during simulation of nitrates adsorption by goethite and competitive effects with chromates.

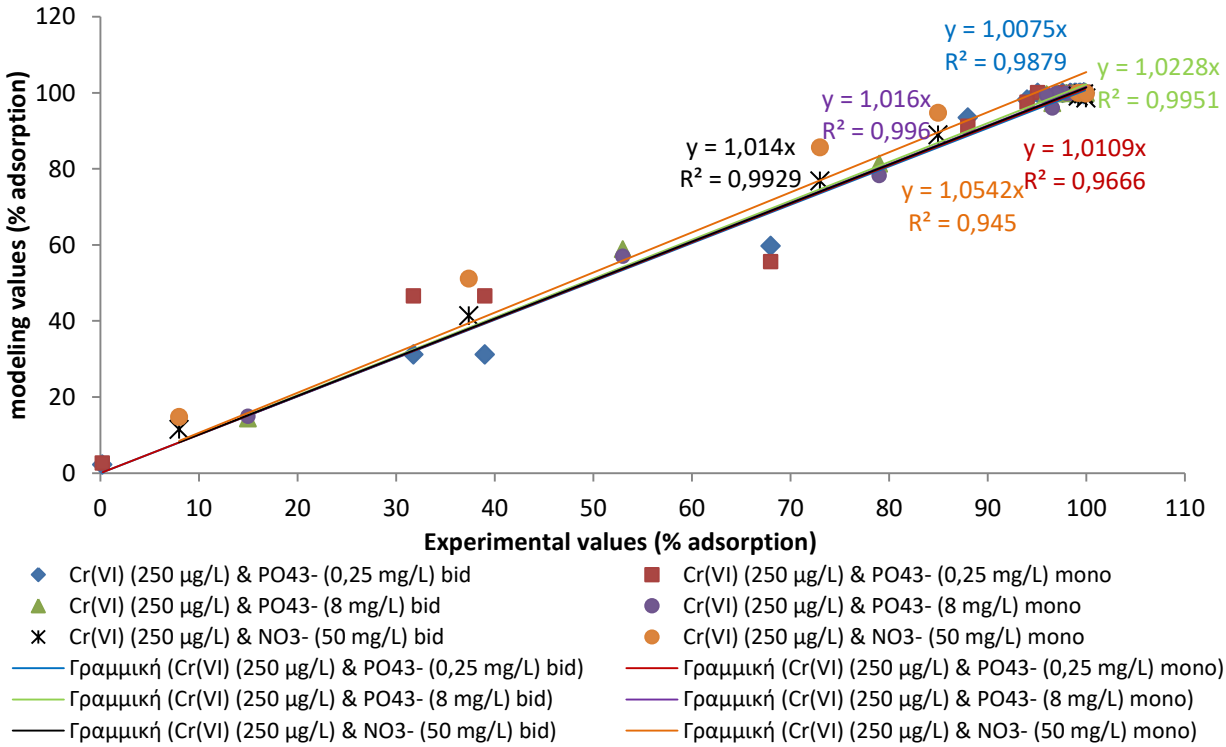

Figure A1.16 Values of correlation factors (R^2) during simulation of Cr(VI) adsorption by goethite and competitive effects with inorganic contaminants.

APPENDIX II – EXPERIMENTAL PROTOCOLS

1. Procedure for the determination of particle size distribution of the finer fraction

- Place 50 - 100 g of dry soil into a soil dispersing cup. Record the weight to at least 0.1g.
- Fill cup to within two inches of the top with tap water. If local tap water is hard, use distilled water. Water should be at room temperature, not directly out of tap.
- Add 5 ml of 1N sodium hexameta-phosphate $Na(PO_3)_6$. Allow to slake (soak) for 15 minutes (high-clay soils only).
- Attach cup to mixer; mix 5 minutes for sandy soils, 15 minutes for fine-textured soils.
- Transfer suspension to sedimentation cylinder; use tap water from squirt bottle to get all of sample from mixing cup.
- Fill cylinder to 1000-mL mark with tap water.
- Carefully mix suspension with plunger. After removing plunger, begin timing. Carefully place hydrometer into suspension; note reading at 40 seconds. This 40-second reading should be repeated several times to improve accuracy. Because the suspension is opaque, read the hydrometer at the top of the meniscus rather than at the bottom.
- After final 40-second reading, remove hydrometer, carefully lower a thermometer into the suspension and record the temperature. Mixing raises temperature by 3-5°C, so it is important to record the temperature for both hydrometer readings (40 s and 2 h).
- Mix suspension again and begin timing for the two-hour reading. Be sure that the cylinder is back from the edge of the counter and in a location where it won't be disturbed.
- Make up a blank cylinder with water and sodium hexameta=phosphate. Record the blank hydrometer reading. If the reading is above 0 (zero) on the hydrometer scale (in other words, if the zero mark is below the surface), record the blank correction as a negative number. Read at the top of the meniscus as before.
- Take a hydrometer reading at 2 hours, followed by a temperature reading.

Calculations

The calculation of the fractions is shown below:

1. (Clay + Silt) g % = n (X_1+X_{T1})
2. Clay g % = n (X_2+X_{T2})
3. Sand g % = 100 - n(X_1+X_{T1})
4. Silt g % = 100 - (Clay + Sand)

where:

X_1= hydrometer's indication after 40 s

X_{T1}= hydrometer's temperature correction at first time

X_2= hydrometer's indication after 2 h

X_{T2} = hydrometer's temperature correction at second time

n = constant parameter equal to 2.

2. Procedure for the determination of Cr(VI)

Reagents

- Reagent water: Reagent water should be monitored for impurities.
- Potassium dichromate stock solution: Dissolve 141.4 mg of dried potassium dichromate, $K_2Cr_2O_7$ (analytical reagent grade), in reagent water and dilute to 1 liter (1 mL = 50 µg Cr).
- Potassium dichromate standard solution: Dilute 10.00 mL potassium dichromate stock solution to 100 mL (1 mL = 5 µg Cr).
- Sulfuric acid, 10% (v/v): Dilute 10 mL of distilled reagent grade or spectrograde quality sulfuric acid, H_2SO_4, to 100 mL with reagent water.
- Diphenylcarbazide solution: Dissolve 250 mg 1,5-diphenylcarbazide in 50 mL acetone. Store in a brown bottle. Discard when the solution becomes discolored.
- Acetone (analytical reagent grade): Avoid or redistill material that comes in containers with metal or metal-lined caps.

Procedure

Transfer 95 mL of the extract to be tested to a 100-mL volumetric flask. Add 2.0 mL diphenylcarbazide solution and mix. Add H_2SO_4 solution to give a pH of 2±0.5, dilute to 100 mL with reagent water, and let stand 5 to 10 min for full color development. Transfer an appropriate portion of the solution to a 1-cm absorption cell and measure its absorbance at 540 nm. Use reagent water as a reference. Correct the absorbance reading of the sample by subtracting the absorbance of a blank carried through the method (see Note below). An aliquot of the sample containing all reagents except diphenylcarbazide should be prepared and used to correct the sample for turbidity (i.e., a turbidity blank). From the corrected absorbance, determine the mg/L of chromium present by reference to the calibration curve.
NOTE: If the solution is turbid after dilution to 100 mL take an absorbance reading before adding the carbazide reagent and correct the absorbance reading of the final colored solution by subtracting the absorbance measured previously.

Interferences

The chromium reaction with diphenylcarbazide is usually free from interferences. However, certain substances may interfere if the chromium concentration is relatively low. Hexavalent molybdenum and mercury salts also react to form color with the reagent; however, the red-violet intensities produced are much lower than those for chromium at the specified pH. Concentrations of up to 200 mg/L of molybdenum and mercury can be tolerated. Vanadium interferes strongly, but concentrations up to 10 times that of chromium will not cause trouble. Iron in concentrations greater than 1 mg/L may produce a yellow color, but the ferric iron color is not strong and difficulty is not normally encountered if the absorbance is measured photometrically at the appropriate wavelength.

3. Procedure for the determination of phosphates

Reagents

- Sulfuric acid (H_2SO_4) 5N: Dilute 70 mL concentrated H_2SO_4 to 500 mL with distilled water.
- Antimony potassium tartrate solution: Dissolve 1.3715 g $K(SbO)C_4H_4O_6$ *½H_2O in 400 mL distilled water in a 500 mL volumetric flask and dilute to volume. Store in a glass stoppered bottle.
- Ammonium molybdate solution: Dissolve 20 g $(NH_4)6Mo_7O_{24}$ *4H_2O in 500 mL distilled water. Store in a glass-stoppered bottle.
- Ascorbic acid, 0.1M: Dissolve 1.76g ascorbic acid in 100 mL distilled water. The solution is stable for about 1 week at 4^{o}C.
- Combined reagent: Mix the above reagents in the following proportions for 100 mL of the combined reagent: 50 mL 5N H_2SO_4 .5mL antimony potassium tartrate solution, 15 mL ammonium molybdate solution, and 30 mL ascorbic acid solution. Mix after addition of each reagent. Let all reagents reach room temperature before they are mixed and mix in the order given. If turbidity forms in the combined reagent, shake and let stand for a few minutes until turbidity disappears before proceeding. The reagent is stable for 4 h.

Procedure

Add, using pipette, 50.0 mL sample into a clean, dry test tube or 125 mL Erlenmeyer flask. Add 0.05 mL (1 drop) phenolphthalein indicator. If a red color develops add 5N H_2SO_4 solution dropwise to just discharge the color. Add 8.0 mL combined reagent and mix thoroughly. After at least 10 min but no more than 30 min, measure absorbance of each sample at 880 nm, using reagent blank as the reference solution. Natural color of water generally does not interfere at the high wavelength used. For highly colored or turbid waters, prepare a blank by adding all reagents except ascorbic acid and antimony potassium tartrate to the sample. Subtract blank absorbance from absorbance of each sample.

Interferences

Arsenates react with the molybdate reagent to produce a blue color similar to that formed with phosphate. Concentrations as low as 0.1 mg As/L interfere with the phosphate determination. Cr(VI) and NO_2^- interfere to give results about 3% low at concentrations of 1 mg/L and 10 to 15% low at 10 mg/L. Sulfide (Na_2S) and silicate do not interfere at concentrations of 1.0 and 10 mg/L.

4. Procedure for the determination of nitrates

Interferences

The K^+, Na^+, Cl^-, Ag^+, Pb^{2+}, Zn^{2+}, Ni^{2+}, Fe^{3+}, $Cd^{2+,}$ Sn^{2+}, Ca^{2+}, Cu^{2+}, Co^{2+}, Fe^{2+}, Cr^{6+} ions have been individually checked up to the given concentrations and do not cause interference. No cumulative effects and influence of other ions has been determined. High loads of oxidizable organic substances (COD) cause the reagent to change colour and to give high-bias results. The test can thus only be used for waste water analyses if the COD is less than 200 mg/L. The results must be subjected to plausibility checks (dilute and/or spike the sample).

5. Procedure for the determination of chlorides

Interferences

The ions SO_4^{2-}, NO_3^-, Pb^{2+}, Zn^{2+}, Ni^{2+}, Cu^{2+}, Cr^{3+}, Cr^{6+}, Cd^{2+}, CN^-, S^{2-} have been individually checked up to the given concentrations and do not cause interference. There have not been determined cumulative effects and the influence of other ions. Silver interferes due to the precipitation of silver chloride (low-bias results). Mercury hinders the reaction (low-bias results). Bromides and iodides, which are found in particular in many mineral waters, undergo the same reaction (high-bias results). Substances which form colored complexes with iron(III) salts interfere with the determination.

APPENDIX III – TABLES

Table A3.1. SEM-EDS results of a soil sample with grain size -0.5 mm.

Circular red point of Fig. 4.8: Cr-magnetite ($Fe^{2+}F^{3+}{}_2O_4$)						
Elmt	Spect. Type	%Element	% Atomic	Compound	%	Nos. of ions
Si K	ED	0.16	0.20	SiO2	0.35	0.02
Cr K	ED	0.94	0.62	Cr2O3	1.37	0.06
Fe K	ED	63.44	39.14	Fe2O3	90.70	3.91
O		27.88	60.04			6.00
Total		92.42	100.00		92.42	
Cation sum						3.99
Rectangular red point of Fig. 4.8: Chromite ($Fe^{2+}Cr_2O_4$)						
Elmt	Spect. Type	% Element	% Atomic	Compound	%	Nos. of ions
Mg K	ED	7.22	8.56	MgO	11.97	0.88
Al K	ED	13.51	14.44	Al2O3	25.53	1.49
Cr K	ED	23.50	13.03	Cr2O3	34.35	1.34
Fe K	ED	11.00	5.68	Fe2O3	15.72	0.58
O		32.34	58.29			6.00
Total		87.57	100.00		87.57	
Cation sum						4.29

Table A3.2. logK values used for adsorption simulation by other studies using goethite as adsorbent and applying the TLM.

No. of Equation at Tables 6.4 & 6.10	logK value	Reference
9	14.05	Villalobos et al., 2001
9	12.76	Villalobos et al., 2001
9	12.82	Van Geen et al., 1994
10	18.1	Rai et al., 1988
10	19.4	Rai et al., 1988
10	20.41	Villalobos et al., 2001
10	20.7 ± 0.3	Mesuere and Fish, 1992a
10	20.98	Villalobos et al., 2001
11	9.8	Rai et al., 1988
8	3.3	Carroll et al., 2008
8	8	Criscenti and Sverjensky, 2002
8	8.5	Criscenti and Sverjensky, 2002
8	8	Criscenti and Sverjensky, 2002
8	6.1	Davis, 1978
8	8.69	Hoins et al., 1993
8	7	Hsi and Langmuir, 1985
8	6.2	Hsi and Langmuir, 1985
8	7.6	Hayes and Leckie, 1986a
8	8.74	Hayes et al., 1991
8	7.7	Hayes KF 1987
8	6.2	Jung et al., 1998

8	6.2 ± 0.3	James and Parks, 1982
8	7.5	Kovacevic et al., 2000
8	7	La Flamme and Murray, 1987
8	9.2	Mesuere, 1992
8	8.31	Peacock and Sherman, 2004c
8	7.5 ± 0.3	Smith and Jenne, 1991
8	9.5	Sverjensky, 2005
8	8.78 ± 0.13	Turner and Sassman, 1996
8	1	Venema et al., 1996a
8	1.7	Venema et al., 1996a
8	0.1	Venema et al., 1996a
8	-0.5	Venema et al., 1996a
8	8.088	Villalobos and Leckie, 2001
8	8.826	Villalobos and Leckie, 2001
8	8.35	Villalobos et al., 2001
8	9.1	Villalobos et al., 2001
8	8.38	Villalobos et al., 2001
8	8.93	Villalobos et al., 2001
8	1.61	Zhang et al., 2007
8	7.6	Zhang and Sparks, 1989
4	5.5	Balistrieri and Murray, 1979
4	7	Balistrieri and Murray, 1981
4	6.6	Davis, 1978
4	5.4	Goldberg et al., 1998
4	9.3	Sverjensky and Fukushi, 2006a
4	8	Sverjensky and Fukushi, 2006a
4	-6.2 ± 0.6	Smith and Jenne, 1991
4	8.7	Sahai and Sverjensky, 1977a
4	9.6	Sverjensky, 2005
4	9.036	Villalobos and Leckie, 2001
4	8.432	Villalobos and Leckie, 2001
4	5.4	Zhang and Sparks, 1990a
3	-9.6	Balistrieri and Murray, 1979
3	-8.4	Balistrieri and Murray, 1981
3	-3.1	Carroll et al., 2008
3	-2.9	Carroll et al., 2008
3	-9	Criscenti and Sverjensky, 2002
3	-9.2	Criscenti and Sverjensky, 2002
3	-9.8	Criscenti and Sverjensky, 2002
3	-9	Criscenti and Sverjensky, 2002
3	-8.76	Fujita and Tsukamoto, 1997
3	-9.3	Goldberg et al., 1998
3	-6.87	Hoins et al., 1993
3	-10.1	Hsi and Langmuir, 1985
3	-6.6	Hsi and Langmuir, 1985
3	-8.8	Hayes and Leckie, 1986a
3	-8.33	Hayes et al., 1991
3	-9.4	Kovacevic et al., 2000
3	-9.648	Lumsdon and Evans, 1994
3	-8.083	Lumsdon and Evans, 1994

3	-8.926	Lumsdon and Evans, 1994
3	-8.4	La Flamme and Murray, 1987
3	-9.07	Peacock and Sherman, 2004c
3	-7.2 ± 0.1	Rundberg et al., 1994
3	-2.477	Robertson and Leckie, 1997
3	-9.332	Robertson and Leckie, 1997
3	-9.9	Rai et al., 1988
3	-8.9	Sverjensky and Fukushi, 2006a
3	-7.8	Sverjensky and Fukushi, 2006a
3	-9.3 ± 0.5	Smith and Jenne, 1991
3	-9.5	Sahai and Sverjensky, 1997a
3	-8.6	Sverjensky, 2005
3	-8.6	Sverjensky, 2006c
3	-8.8	Sverjensky, 2006c
3	-7.2	Sigg, 1979
3	-7.64 ± 0.07	Turner and Sassman, 1996
3	1	Venema et al., 1996a
3	-0.5	Venema et al., 1996a
3	4	Venema et al., 1996a
3	0.1	Venema et al., 1996a
3	2.3	Venema et al., 1996a
3	-9.287	Villalobos and Leckie, 2001
3	-9.912	Villalobos and Leckie, 2001
3	-10.01	Villalobos and Leckie, 2001
3	-9.295	Villalobos and Leckie, 2001
3	-8.76	Van Geen et al., 1994
3	-9.61	Villalobos et al., 2001
3	-10.37	Villalobos et al., 2001
3	-8.73	Villalobos et al., 2001
3	-9.29	Villalobos et al., 2001
3	-1.93	Zhang et al., 2007
3	-8.8	Zhang and Sparks, 1989
3	-9.3	Zhang and Sparks, 1990a

Table A3.3. logK values used for adsorption simulation by other studies using goethite as adsorbent and applying the DLM.

No. of Equation at Tables 6.4 & 6.10	logK value	Reference
9	17.11 ± 0.47	Mathur and Dzombak, 2006
9	18.7 ± 0.2	Mesuere and Fish, 1992a
10	11.17 ± 0.19	Mathur and Dzombak, 2006
10	11.6 ± 0.1	Mesuere and Fish, 1992a
5	19.65 ± 0.39	Mathur and Dzombak, 2006
6	24.91 ± 0.62	Mathur and Dzombak, 2006
7	30.72 ± 0.14	Mathur and Dzombak, 2006
4	0.9	Ermakova et al., 2001
3	0.3	Ermakova et al., 2001

Table A3.4. logK values used for adsorption simulation by other studies using goethite as adsorbent and applying the CCM.

No. of Equation at Tables 6.4 & 6.10	logK value	Reference
9	9.8	Grossl et al., 1997
9	4.2	Grossl et al., 1997
9	15.3	Grossl et al., 1997
7	30.5 ± 0.2	Gao and Mucci, 2001
7	32.192	Goldberg, 1985
7	32.132	Goldberg, 1985
7	32.922	Goldberg, 1985
7	30.602	Manning and Goldberg, 1996b
7	19.402	Manning and Goldberg, 1996b
7	29.752	Manning and Goldberg, 1996b
7	31.13 ± 0.05	Nilsson et al., 1992
7	32.27	Singh et al., 2010
7	30.202	Sigg, 1979
7	31.202	Sigg, 1979
6	25.86 ± 0.06	Gao and Mucci, 2001
6	28.762	Goldberg, 1985
6	27.972	Goldberg, 1985
6	27.952	Goldberg, 1985
6	25.102	Manning and Goldberg, 1996b
6	24.802	Manning and Goldberg, 1996b
6	26.38 ± 0.09	Nilsson et al., 1992
6	26.83	Singh et al., 2010
5	18.73 ± 0.46	Gao and Mucci, 2001
5	21.872	Goldberg, 1985
5	22.692	Goldberg, 1985
5	19.502	Manning and Goldberg, 1996b
5	20.61 ± 0.1	Nilsson et al., 1992
5	19.64	Singh et al., 2010
5	20.202	Sigg, 1979

Table A3.5. Comparison of the logK values used in the case of soil and goethite as adsorbents, applying the TLM.

Reactions							PSI_o	PSI_b	logK (per solid concentration)			LogK goethite
No.	Reactants				Products							
	Solid	Ligand 1	Ligand 2		Product 1	Product 2			1.5 g/L	1.1 g/L	0.103 g/L	10 g/L
1	SOH			↔	SO^-	H^+	-1		-9.0			-9.0
2	SOH	H^+		↔	SOH_2^+		1		4.2			4.2
3	SOH	Na^+		↔	SONa	H^+	-1	1	-9.29			-9.29
4	SOH	Cl^-	H^+	↔	SOH_2Cl		1	-1	8.43			8.43
5	SOH	PO_4^{3-}	H^+	↔	$SOPO_3^{2-}$	H_2O	-2		19.0	20.5	30.0	15.5
6	2SOH	PO_4^{3-}	$2H^+$	↔	$S_2O_2PO_2^-$	$2H_2O$	-1		25.2	25.0	30.0	20
7	2SOH	PO_4^{3-}	$3H^+$	↔	S_2O_2POOH	$2H_2O$	0		29.2	30.0	37.0	33
8	SOH	NO_3^-	H^+	↔	SOH_2NO_3		1	-1	9.0	9.2	10.3	9.8
Reactions at the Bidentate Minteq Database												
9	2SOH	CrO_4^{2-}	$2H^+$	↔	S_2CrO_4	$2H_2O$	0		14.5	14.5	15.8	14
10	SOH	CrO_4^{2-}	$2H^+$	↔	SOH_2-$HCrO_4$		1	-1	16.0	16.4	17.2	19.9
11	SOH	CrO_4^{2-}	H^+	↔	$SOH_2CrO_4^-$		1	-2	11.2	11.4	13.5	10
Reactions at the Monodentate Minteq Database												
12	SOH	CrO_4^{2-}	H^+	↔	$SCrO_4^-$	H_2O	-1		8.0	8.0	15.1	12.1
13	SOH	CrO_4^{2-}	$2H^+$	↔	SOH_2-$HCrO_4$		1	-1	16.0	16.4	17.2	19.9
14	SOH	CrO_4^{2-}	H^+	↔	$SOH_2CrO_4^-$		1	-2	11.2	11.4	13.8	10

Table A3.6. Comparison of the logK values used in the case of soil and goethite as adsorbents, applying the DLM.

Reactions							PSI_o	logK soil	logK goethite
No.	Reactants				Products				
	Solid	Ligand 1	Ligand 2		Product 1	Product 2			
1	SOH			↔	SO^-	H^+	-1	-9	-9
2	SOH	H^+		↔	SOH_2^+		1	4.2	4.2
3	SOH	Na^+		↔	SONa	H^+	0	-9.29	-9.29
4	SOH	Cl^-	H^+	↔	SCl	H_2O	0	8.43	8.43
5	SOH	PO_4^{3-}	H^+	↔	SPO_4^{2-}	H_2O	-2	18	18
6	SOH	PO_4^{3-}	$2H^+$	↔	$SHPO_4^-$	H_2O	-1	22	26
7	SOH	PO_4^{3-}	$3H^+$	↔	SH_2PO4	H_2O	0	30	32
8	SOH	NO_3^-	H^+	↔	SNO_3	H_2O	0	8.8	9
9	SOH	CrO_4^{2-}	$2H^+$	↔	$SHCrO_4$	H_2O	0	16.2	19.5
10	SOH	CrO_4^{2-}	H^+	↔	$SCrO_4^-$	H_2O	-1	10.25	12

Table A3.7. Comparison of the logK values used in the case of soil and goethite as adsorbents, applying the CCM.

Reactions							PSIo	LogK soil	logK goethite
No.	Reactants				Products				
	Solid	Ligand 1	Ligand 2		Product 1	Product 2			
1	SOH			↔	SO^-	H^+	-1	-9	-9
2	SOH	H^+		↔	SOH_2^+		1	4.2	4.2
3	SOH	Na^+		↔	SONa	H^+	0	-9.29	-9.29
4	SOH	Cl^-	H^+	↔	SCl	H_2O	0	8.43	8.43
5	SOH	PO_4^{3-}	H^+	↔	$SOPO_3^{2-}$	H_2O	-2	16	15
6	SOH	PO_4^{3-}	$2H^+$	↔	$S_2O_2PO_2^-$	H_2O	-1	23.1	25
7	SOH	PO_4^{3-}	$3H^+$	↔	S_2O_2POOH	H_2O	0	29.8	32
8	SOH	NO_3^-	H^+	↔	SNO_3	H_2O	0	8.7	9
9	SOH	CrO_4^{2-}	$2H^+$	↔	$SHCrO_4$	H_2O	0	16.2	20
10	SOH	CrO_4^{2-}	H^+	↔	$SCrO_4^-$	H_2O	-1	10.2	9
11	2SOH	CrO_4^{2-}	$2H^+$	↔	S_2CrO_4	$2H_2O$	0	10	10

APPENDIX IV – PUBLICATIONS

Publications related to PhD thesis

In journals

1. Mpouras T., Chrysochoou M., Dermatas D., (2017). Investigation of hexavalent chromium sorption in serpentine sediments, *Journal of Contaminant Hydrology*, vol. 197, pp. 29-38.
2. Dermatas D., Mpouras T., Chyrsochoou M., Panagiotakis I., Vatseris C., Linardos N., Theologou E., Xenidis A., Papasiopi N., Sakellariou L., (2015). Origin and concentration profile of chromium in a Greek aquifer, *J Hazard Mater*, 281, 35–46.

In conferences

1. Mpouras T., Lagkouvardos K., Vyrini A., Dermatas D. and Chrysochoou M., (2017) Competitive adsorption of hexavalent chromium and inorganic pollutants on goethite, 15th International Conference on Environmental Science and Technology, Rhodes, Greece, September 2017.
2. Mpouras T., Lagkouvardos K., Dermatas D., Chrysochoou M., (2016). Adsorption of hexavalent chromium on ophiolitic sediment, hematite and goethite in the presence of phosphates, 13th International Conference "Protection & Restoration of the Environment - PRE12", Mykonos Island, Greece, July 2016.
3. Mpouras T., Dermatas D., Chrysochoou M., (2014). Evaluation of the adsorption of hexavalent chromium on ophiolitic soils, 12th International Conference "Protection & Restoration of the Environment - PRE12", Skiathos, Greece, July 2014.
4. Dermatas D., Panagiotakis I., Vatseris C., Xenidis A., Papasiopi N., Mpouras T., Theologou E., Vaxevanidou K., Chyrsochoou M., (2013). Investigation of the origin of hexavalent chromium in a Greek ophiolitic aquifer, 13th International Conference on Environmental Science and Technology, Athens, Greece, September 2013.

Other publications during the period of PhD thesis

In books

1. Dermatas D., Mpouras T., Papasiopi N., Mystrioti C., Toli K., (2018). Iron nanomaterials for water and soil treatment, Chapter 3 "Adsorption of groundwater pollutants by iron nanomaterials", Pan Stanford, May 2018.

In journals

1. Dermatas D., Mpouras T., Panagiotakis I., (2018). Application of Nanotechnology for waste management: Challenges and limitations, *Waste Management & Research*, Vol. 36 (3), pp. 197–199.
2. Vilardi G., Mpouras T., Dermatas D., Verdone N., Polydera A., Di Palma L., (2018). Nanomaterials application for heavy metals recovery from polluted water: the combination of nano zero-valent iron and carbon nanotubes. Competitive adsorption non-linear modeling, *Chemosphere*, Vol. 201, pp. 716-729.
3. Lagiopoulos I., Binteris A., Mpouras T., Panagiotakis I., Chrysochoou M., Dermatas D., (2017). Potential biosorbents for treatment of chromium(VI) contaminated water discharged into

Asopos River, *International Journal of Environmental Science and Technology*, 14 (7), pp 1481–1488.

4. Dermatas D., Panagiotakis I., Mpouras T., Tettas K., (2017). The origin of hexavalent chromium as a critical parameter for remediation of contaminated aquifers, *Bulletin of Environmental Contamination and Toxicology*, 98 (3), pp. 331-337.
5. Mpouras T., Panagiotakis I., Dermatas D. and Chrysochoou M., (2014) Nano-zero valent iron: An emerging technology for Cr(VI)-contaminated site remediation, American Society of Civil Engineers, *Geotechnical Special Publication*.

In conferences

1. Mpouras T., Papadaki S., Dermatas D. and Papassiopi N., (2019). Adsorption of heavy metals (hexavalent chromium, lead, manganese and cadmium) on multiwall carbon nanotubes, 16th International Conference on Environmental Science and Technology, Rhodes, Greece, September 2019.
2. Mpouras T., Papassiopi N., Lagkouvardos K., Mystrioti C. and Dermatas D., (2019). Evaluation of calcium polysulfide as a reducing agent for the restoration of a Cr(VI)-contaminated aquifer, 16th International Conference on Environmental Science and Technology, Rhodes, Greece, September 2019.
3. Pyrgaki K., Argyraki A, Kelepertzis S., Botsou F. , Megremi I., Karavoltsos S., Mpouras T., Dassenakis E., Hatzaki M. and Dermatas D., (2019). A DPSIR Approach To Selected Cr(VI) Impacted Groundwater Bodies Within Attica and Eastern Sterea Ellada River Basin Districts, 16th International Conference on Environmental Science and Technology, Rhodes, Greece, September 2019.
4. Mystrioti C., Mpouras A., Papassiopi N., and Dermatas D., (2019). Evaluation of soil loaded with green iron nanoparticles for hexavalent chromium reduction, 16th International Conference on Environmental Science and Technology, Rhodes, Greece, September 2019.
5. Mpouras T., Polydera A., Dermatas D., (2018). Carbon nanotubes application for hexavalent chromium adsorption from contaminated groundwater, 14th International Conference "Protection & Restoration of the Environment – PRE XIV", Thessaloniki, Greece, July 2018.
6. Lagiopoulos I., Binteris A., Mpouras T., Panagiotakis I., Chrysochoou M., Dermatas D., (2016). Potential biosorbents for treatment of Cr(VI) contaminated water discharged into Asopos river, 13th International Conference "Protection & Restoration of the Environment – PRE XIII", Mykonos Island, Greece, June 2016.
7. Panagiotakis I., Dermatas D., Vatseris C., Merkos P., Chrysochoou M., Linardos N., Mpouras T., Theologou E., Papassiopi N., Xenidis A., (2016), Assessment of a Cr(VI)-contaminated industrial site in Greece, 13th International Conference "Protection & Restoration of the Environment – PRE XIII", Mykonos Island, Greece, June 2016.
8. Mpouras T. and Dermatas D., (2016). Nanostructured materials for advanced remediation processes, International conference on nanotechnology based innovative applications for the environment (NINE), Rome, Italy, March 2016.
9. Mpouras T., Panagiotakis I., Dermatas D. and Chrysochoou M., Nano-zero valent iron: An emerging technology for Cr(VI)-contaminated site remediation, Geo-Congress conference, Atlanta, Georgia, February 2014.

10. Dermatas D., Panagiotakis I., Mpouras T., (2015). Origin of hexavalent chromium found in groundwater: a critical decision-making parameter, Conference on Environmental Science and Technology, Rhodes, Greece, September 2015.
11. Binteris A., Mpouras T., Panagiotakis I., Dermatas D., Chrysochoou M., (2015). Reed material – A potential biosorbent for the treatment of Cr(VI)-contaminated water discharged into Asopos river, Conference on Environmental Science and Technology, Rhodes, Greece, September 2015.
12. Panagiotakis I., Dermatas D., Vatseris C., Merkos P., Chrysochoou M., Linardos N., Mpouras T., Theologou E., Papassiopi N. and Xenidis A., (2014). Assessment of a Cr(VI)-contaminated industrial site in Greece, 12th International Conference "Protection & Restoration of the Environment – PRE XII", Skiathos Island, Greece, July 2014.
13. Panagiotakis I., Dermatas D,. Vatseris C., Chyrsochoou M., Papasiopi N., Xenidis A., Theologou E., Mpouras T., Sakellariou L., (2013). Investigation of chromium sources in the groundwater of Thiva industrialized area, 13th International Conference on Environmental Science and Technology, Athens, Greece, September 2013.
14. Παναγιωτάκης Ηρ., Δερματάς Δ., Βατσέρης Χρ., Μέρκος Π., Χρυσοχόου Μ., Λινάρδος Ν., Μπούρας Θ., Θεολόγου Ε., Παπασιώπη Ν., Ξενίδης Α., (2015). Προκαταρκτική διερεύνηση υδροφορέα ρυπασμένου με εξασθενές χρώμιο στα Οινόφυτα Βοιωτίας, 3ο Κοινό Συνέδριο: Ολοκληρωμένη διαχείριση υδατικών πόρων στη νέα εποχή, Αθήνα, Δεκέμβριος 2015.
15. Λαγιόπουλος Ι., Μπίντερης Α., Μπούρας Θ., Παναγιωτάκης Ηρ., Χρυσοχόου Μ., Δερματάς Δ., (2015). Επεξεργασία νερού ρυπασμένου με εξασθενές χρώμιο με τη χρήση οργανικών υλικών, 2ο Περιβαλλοντικό Συνέδριο Θεσσαλίας, Σκιάθος, Σεπτέμβριος 2015.